Laboratory and Modelling Studies on the Effects of Injection Gas Composition on CO_2-Rich Flooding in Cooper Basin, South Australia

By

Johannes Bon

A thesis submitted for the degree of

Doctor of Philosophy
in
Petroleum Engineering

February, 2009

Australian School of Petroleum
Faculty of Engineering, Computer and Mathematical Sciences
The University of Adelaide, Australia

For my wife Erika and our daughter Isabella

ABSTRACT

This Ph.D. research project targets Cooper Basin oil reservoirs of very low permeability (approximately 1mD) where injectivities required for water flooding are not achievable. However, the use of injection gases such as CO_2 would not have injectivity problems. CO_2 is abundant in the region and available for EOR use. CO_2 was compared to other CO_2-rich injection gases with a hydrocarbon content including pentane plus components. While the effect of hydrocarbon components up to butane have been investigated in the past, the effect of n-pentane has on impure CO_2 gas streams has not.

One particular field of the Cooper Basin was investigated in detail (Field A). However, since similar reservoir and fluid characteristics of Field A are common to the region it is expected that the data measured and developed has applications to many other oil reservoirs of the region and similar reservoirs else where.

The aim of this Ph.D. project is to determine the applicability of CO_2 as an injection gas for Enhanced Oil Recovery (EOR) in the Cooper Basin oil reservoirs and to compare CO_2 with other possible CO_2-rich injection gases.

The summarised goals of this research are to:

- Determine the compatibility of Field A reservoir fluid with CO_2 as an injection gas.
- Compare CO_2 to other injection gas options for Field A.
- Development of a correlation to predict the effect of nC_5 on MMP for a CO_2-rich injection gas stream.

These goals were achieved through the following work:

- Extensive experimental studies of the reservoir properties and the effects of interaction between CO_2-rich injection gas streams and Field A reservoir fluid measuring properties related to:
  - Miscibility of the injection gas with Field A reservoir fluid

  - Solubility and swelling properties of the injection gas with Field A reservoir fluid
  - Change in viscosity-pressure relationship of Field A reservoir fluid due to addition of injection gas
- A reservoir condition core flood experiment
- Compositional simulation of the reservoir condition core flood to compare expected recoveries from different injection gases
- Development of a set of Minimum Miscibility Pressure (MMP) measurements targeted at correlating the effect of nC_5 on CO_2 MMP.

The key findings of this research are as follows:

- Miscibility is achievable at practical pressures for Field A and similar reservoir fluids with pure CO_2 or CO_2-rich injection gases.
- For Field A reservoir fluid, viscosity of the remaining flashed liquid will increase at pressures below ~2500psi due to mixing the reservoir fluid with a CO_2-rich injection gas stream.
- Comparison of injection gases showed that methane rich gases are miscible with Field A so long as a significant quantity of C_3+ components is also present in the gas stream.
- There is a defined trend for effect of nC_5 on MMP of impure CO_2. This trend was correlated with an error of less than 4%.
- Even though oil composition is taken into account with the base gas MMP, it still affects the trend for effect of nC_5 on MMP of a CO_2-rich gas stream.
- An oil characterisation factor was developed to account for this effect, significantly improving the results, reducing the error of the correlation to only 1.6%.

The significance of these findings is as follows:

- An injection pressure above ~3000psi should be targeted. At these pressures miscibility is achieved and the viscosity of the reservoir fluid-injection gas mix is reduced.

- CO_2 should be compared to gases such as Tim Gas should after considering the cost of compression, pipeline costs and distance from source to destination will need to be considered.
- The addition of nC_5 will reduce the MMP and increase the recovery factor, however the cost of the nC_5 used would be more than the value of increased oil recovered.
- The developed correlation for the effect of nC_5 on impure CO_2 MMP can be used broadly within the limits of the correlation.
- Further research using more oils is necessary to validate the developed oil characterisation factor and if successful, using the same or similar method used to improve other correlations.

STATEMENT OF ORIGINALITY

This work contains no material which has been accepted for the award of any other degree or diploma in any university or other tertiary institution and, to the best of my knowledge and belief, contains no material previously published or written by another person, except where due reference has been made in the text.

I give consent to this copy of my thesis when deposited at the University Library, being made available for loan and photocopying, subject to the provisions of the Copyright Act 1968.

Johannes Bon

February 2009

ACKNOWLEDGEMENTS

First, I am very grateful to my supervisor **Professor Hemanta Sarma** for his support and guidance throughout my time as his student and thereafter. I am also very grateful to my co-supervisor **Dr. Seung Ihl Kam** and I also thank everybody at the Australian School of Petroleum for their help, in particular Mohammed Emera, Maureen Sutton, Prashant Jadhawar, Rahul Shrivastava and Ric Daniel.

Two companies gave strong support to the project without which nothing could have been done. I am very grateful to **Santos Limited** who not only provided me with the data and funding for this project but, when I needed samples organised all logistics around my sampling trips including flights, liaising with field engineers and well test companies. Many people within Santos Limited provided technical support; these include Lou Dello, Teof Rodrigues, Andrew Theophilos, Kylie Beatty, Jamie Burgess, Patrick McCarthy, Carl Greenstreet, Gary Reid, Ed Pugh, Gavin Munn and Nick Lemon.

I am also very grateful to **Petrolab Australia Pty. Ltd.** who provided me with the laboratory facilities for much of the analyses performed. While continuing as an actively running commercial PVT laboratory, Petrolab scheduled in my needs for cylinders, pumps, cells, ovens and gas chromatographs and opened up a comfortable area for me to do my lab work with minimal disturbances. A big thank you goes to my father **Jan G. Bon** for his technical and moral support.

I am greatly appreciative to several of my close friends and family who on several occasions spent large amounts of time discussing ideas and providing moral, technical and editorial support, these include Gavin Munn, Jerry Meyer, Paul Bon, Ramon Bon, Nubia Meyer and my parents Jan G. Bon and Nubia Bon.

And last but not least, to help get me over the line in the final stages, I thank my wife **Erika** and our baby daughter **Isabella**. They provided me with the last push of motivation that I needed to get me over the line.

DISCLAIMER

This Ph.D. thesis reflects the opinions of the author and does not necessarily reflect the opinions of the Cooper Basin Joint Venture parties.

PUBLISHED PAPERS FROM THIS WORK

1. Bon, J. and Sarma, H.K.: "**Investigation of the Effect of Injection Gas Composition on CO_2-rich MMP and its Implications in Flooding in an Onshore Australia Oil Field**", paper to be presented at the Canadian International Petroleum Conference 60th Annual Technical Meeting of the Petroleum Society, Calgary, Alberta, Canada, June 16-18 2009
2. Bon, J., Sarma, H.K., Rodrigues, T. and Bon, J.G.: "**Reservoir Fluid Sampling Revisited - A Practical Perspective**", *SPE Reservoir Evaluation & Engineering*, Vol. 10, No. 6 (December 2007) 589-596
3. Bon, J., Emera, M.K and Sarma, H.K.: "**An Experimental Study and Genetic Algorithm (GA) Correlation to Explore the Effect of nC_5 on Impure CO_2 Minimum Miscibility Pressure (MMP)**", paper SPE 101036 presented at the SPE Asia Pacific Oil & Gas Conference and Exhibition (APOGCE), Adelaide, Australia, 11–13 September 2006
4. Bon, J., Sarma, H.K., Rodrigues, T. and Bon, J.G.: "**Reservoir Fluid Sampling Revisited - A Practical Perspective**", paper SPE 101037 presented at the SPE Asia Pacific Oil & Gas Conference and Exhibition (APOGCE), Adelaide, Australia, 11–13 September 2006
5. Bon, J., Sarma, H.K. and Theophilos, A. M.: "**An Investigation of Minimum Miscibility Pressure for CO_2-Rich Injection Gases with Pentanes-Plus Fraction**", paper SPE 97536 presented at the International Improved Oil Recovery Conference (IIORC) in Asia Pacific, Kuala Lumpur, Malaysia, December 5-6 2005
6. Bon, J. and Sarma, H.K.: "**A Technical Evaluation of a CO_2 Flood for EOR Benefits in the Cooper Basin, South Australia**", paper SPE 88451 presented at the SPE Asia Pacific Oil and Gas Conference and Exhibition (APOGCE), Perth, Australia, October 18-20 2004

TABLE OF CONTENTS

Abstract ..... **i**
Statement of Originality ..... **iv**
Acknowledgements ..... **v**
Published papers from this work ..... **vii**
Table of Contents ..... **viii**
List of Figures ..... **xi**
List of Tables ..... **xv**
Nomenclature ..... **xvii**
1 Introduction **1**
1.1 Regional Geology 3
1.2 Data 6
1.3 Project Aim 6
1.4 Motivation (A): Why should we investigate the potential for a CO_2 flood at Field A or other fields in the Cooper Basin? 7
1.5 Motivation (B): How does pure CO_2 compare to other proposed injection gases? 9
1.6 Motivation (C): The effect of C_5+ and nC_5 on CO_2-Oil miscibility 10
1.7 Summarised Conclusions from this Work 11
2 Literature Review **13**
2.1 Introduction 13
2.2 Enhanced Oil Recovery 13
2.3 Recovery Efficiency and the Factors that Affect It 15
2.4 Carbon Dioxide Flooding 17
2.5 CO_2-Oil Interaction 23
2.6 Corrosive/Scaling Effects of CO_2 24
2.7 Minimum Miscibility Pressure 24
2.8 Methods to Determine the MMP 26
2.9 Correlations for Determining the MMP 29
2.10 Asphaltenes – Their Role in CO_2 Flooding 41

3 Reservoir Fluid Sampling 50
3.1 Summary of Samples Taken for This Project 50
3.2 Review of Literature on Sampling and Different Sampling Techniques 51
3.3 Understanding our Reservoir Processes 54
3.4 Well Conditioning 56
3.5 Reservoir Fluid Sampling Methods 58
3.6 Other Components of Interest 64
3.7 Chapter Summary 67
4 Methodology and Procedures of Reservoir Fluid Analyses Performed 69
4.1 Determination of Asphaltene Content 69
4.2 Quality Checks and Compositional Analyses 71
4.3 PVT Analysis 78
5 Discussion and Results of Reservoir Fluid Studies 93
5.1 Asphaltene Precipitation Analysis 93
5.2 Reservoir Fluid Analyses 94
5.3 Chapter Summary 116
6 Tests with Reservoir Cores 117
6.1 Porosity Measurement by Liquid Saturation 118
6.2 Permeability 119
6.3 Reservoir Condition Core Flood 119
6.4 Discussion of Results 121
6.5 Chapter Summary 123
7 Simulation Studies 124
7.1 Comparison of Injection Gases 126
7.2 Comparison of Base Case to Experimental Core Flood 132
7.3 Comparison of Different Injection Gases 134
7.4 Economic Benefit of Different Injection Gases 138
7.5 Chapter Summary 140
8 Miscibility Studies 141
8.1 Slim Tube Method 141
8.2 Rising Bubble Apparatus 145
8.3 Comparison of Slim Tube and RBA 147
8.4 Results of MMP Measured by Slim Tube Tests 148
8.5 MMP Measured by Rising Bubble Apparatus 162

8.6 Chapter Summary....170
9 Development of Correlation for the Effect of nC_5 on Impure CO_2 MMP 171
9.1 Genetic Algorithm 171
9.2 Linear Regression Correlations 177
9.3 Chapter Summary....182
9.4 Recommendations for Use of Correlations 186
10 Conclusions and Recommendations 188
10.1 Recommendations for Use of Correlations to Predict nC_5 Effect on CO_2-rich MMP 190
References....193

LIST OF FIGURES

Figure 1-1: Location of the Cooper Basin and overlying basins 2
Figure 1-2: Map of Cooper Basin 3
Figure 1-3: Location and structure of the southern Cooper Basin 4
Figure 1-4: Lithology and age of Cooper Basin formations and surrounding basins 5
Figure 2-1: Suitability of CO_2 processes.....17
Figure 2-2: Pseudo-ternary diagram for a hypothetical hydrocarbon system diagram showing ranges of miscibility with a solvent. 20
Figure 2-3: MMP as a function of reservoir temperature and mole weight of the C_5+ component in the reservoir fluid. 30
Figure 2-4: Asphaltene precipitation and potential locations of clogging.....42
Figure 2-5: Example of effect of n-paraffin solvent carbon number on insolubles. 43
Figure 2-6: Illustrating asphaltene micelle agglomeration due to reduction in resin concentration and asphaltene micelle suspended by resin molecules 44
Figure 2-7: Asphaltene percent by volume in solution versus pressure. 45
Figure 2-8: de Boer plot for screening reservoirs with possible asphaltene precipitation problems 46
Figure 2-9: SARA stability screening.....47
Figure 2-10: Asphaltene depositional envelope (ADE), superimposed upon a reservoir fluid phase envelope 48
Figure 3-1: Flow chart of sampling process based on fluid saturation.....58
Figure 3-2: Surface sampling methods 59
Figure 4-1: Determination of bubble point pressure from pressure – volume relationship.....72
Figure 4-2: Typical TCD chromatogram of gas sample.....73
Figure 4-3: Typical FID chromatogram of gas sample. 73
Figure 4-4: Typical FID liquid chromatogram 77
Figure 4-5: Schematic representation of the CMS experiment and relative volume plot 80
Figure 4-6: Pressure – relative volume relationship from constant mass study 81
Figure 4-7: The CVD experiment 84

Figure 4-8: Separator test schematic. 89
Figure 4-9: Viscosity of a crude oil at elevated pressures. 90
Figure 4-10: Schematic representation of the solubility-swelling test 91
Figure 5-1: Oil A relative volume plot (P-V Relationship) 98
Figure 5-2: Oil A compressibility and thermal expansion 98
Figure 5-3: Oil A formation volume factor and solution GOR after correction with separator test data 101
Figure 5-4: Oil A data for produced gas streams during CVD test 102
Figure 5-5: Oil A data for produced gas streams during CVD test 102
Figure 5-6 Oil A - data for produced gas streams during CVD test 103
Figure 5-7: Oil A separator test data 107
Figure 5-8: Solubility-Swelling Test for Oil A with CO_2 – Relative Volume increase with increase in gas....108
Figure 5-9: Solubility-Swelling Test for Oil A with SG#1 – Relative Volume increase with increase in gas 109
Figure 5-10: Solubility-Swelling Test for Oil A with CO_2 and SG#1 – Increase in Swelling Factor with respect to the increase in Saturation Pressure....110
Figure 5-11: Solubility-Swelling Test for Oil A with CO_2 SG#1 – Change in saturation pressure with addition of injection gas....110
Figure 5-12: Typical viscosity relationship of a reservoir fluid compared to that of a reservoir fluid and injection gas mix 113
Figure 5-13: High pressure viscosity of Oil A and effect of injection gas on oil viscosity 115
Figure 5-14: High pressure viscosity of Oil A and effect of injection gas on single-phase oil viscosity 115
Figure 6-1: Field A core plug samples....117
Figure 6-2: Schematic of Slim Tube experimental set-up....121
Figure 7-1: 3D diagram and cross section of core flood model. 124
Figure 7-2: Comparison of simulated and measured formation volume factor and produced gas from CVD test. 130
Figure 7-3: Comparison of simulated and measured relative oil volume plot. 130
Figure 7-4: Comparison of simulated and measured Z-factor. 131
Figure 7-5: Comparison of simulated to measured oil viscosity as a function of pressure. 131

Figure 7-6: Oil A phase diagram produced from fluid model with gas-liquid ratios curves. 132
Figure 7-7: Comparison of simulated and experimental core flood of Oil A with Field A plugs using SG#1 as the injection gas at 3000psig and 279°F 134
Figure 7-8: Cumulative oil recovery of Ray Gas, SG#1, CO_2 and C_1 135
Figure 7-9: Cumulative oil recovery of Sam Gas, Bob Gas, Tim Gas and Ben Gas 135
Figure 7-10: Cumulative oil recovery of Sam Gas, Tim gas and SG#1 with injection after depletion to 2200 psia....136
Figure 7-11: Cumulative oil recovery of Gas #1, Gas #2, Gas #3 and Gas #4....137
Figure 7-12: Comparison of cumulative oil recovery of all injection gases injected at 3000psia....137
Figure 7-13: Comparison of AUD produced minus injected for Sam Gas, Bob Gas, Tim Gas, SG#1 and CO_2....139
Figure 7-14: Comparison of AUD produced minus injected for CO_2, Gas #1, Gas #2, Gas #3 and Gas #4 140
Figure 8-1: MMP determination from break-over point on recovery versus injection pressure plot 142
Figure 8-2: Slim tube experimental set-up. 144
Figure 8-3: Schematic of RBA experimental set-up 146
Figure 8-4: Slim tube results – CO_2 at 3000psig 152
Figure 8-5: Slim tube results – CO_2 at 2850psig 153
Figure 8-6: Slim tube results – CO_2 at 2700psig 154
Figure 8-7: Slim tube results – CO_2 at 2550psig 155
Figure 8-8: MMP plot for CO_2....156
Figure 8-9: Slim tube results – SG#1 at 3200psig....157
Figure 8-10: Slim tube results – SG#1 at 3000psig....158
Figure 8-11: Slim tube results – SG#1 at 2700psig....159
Figure 8-12: Slim tube results – SG#1 at 2500psig....160
Figure 8-13: MMP plot for SG#1 161
Figure 8-14: MMP – Temperature relation of laboratory measured MMP data. ..164
Figure 8-15: MMP – Temperature relation of Oil A and CO_2. 165
Figure 8-16: MMP – Temperature relation of Oil A and SG#1. 166
Figure 8-17: MMP – Temperature relation of Oil A and SG#2. 167

Figure 8-18: RBA generated data 170
Figure 9-1: Flow diagram for procedure used in developing GA based MMP correlation. 176
Figure 9-2: Experimental data illustrating segregation in the data due to the oil composition. 179
Figure 9-3: Comparison of developed correlations.....182
Figure 9-4: Comparison of correlations from literature to developed correlations from this work.....183

LIST OF TABLES

Table 2-1: Screening criteria for application of CO_2 miscible flood.....20
Table 2-2: Target characteristics for immiscible carbon dioxide flood. 22
Table 2-3: Values for modification factor for component i (MF_i) 37
Table 3-1: Summary of samples taken for project.....50
Table 5-1: Oil A - Compositional Analysis of Recombined Reservoir Fluid 95
Table 5-2: Results from Constant Mass Study on Oil A at 279°F.....97
Table 5-3: Results from Constant Volume Depletion study on Oil A at 279°F.....100
Table 5-4: Oil A depletion formation volume factor and solution gas-oil ratio data corrected with flash liberation data from separator test.....100
Table 5-5: Oil A – data for produced gas streams during CVD test.....101
Table 5-6: Oil A – Composition of produced gas phase during CVD.....104
Table 5-7: Oil A – Composition of remaining liquid phase during CVD 105
Table 5-8: Results from Separator Tests on Oil A.....106
Table 5-9: Solubility-Swelling Test Results for Oil A with CO_2 108
Table 5-10: Solubility-Swelling Test Results for Oil A with SG#1.....109
Table 5-11: Solubility-Swelling Test – Change in saturation pressure and swelling factor with addition of injection gas 110
Table 5-12: Flash Calculation by EOS at 2500psia and 279°F: 112
Table 5-13: Viscosity Study of Oil A with added CO_2 and SG#1.....114
Table 6-1: Summary of basic core data 121
Table 6-2: Core Flood results.....123
Table 7-1: Simulation models to determine the effect of injection gas composition 127
Table 7-2: Gas compositions – CO_2, Ray Gas, SG#1 and SG#2.....128
Table 7-3: Gas compositions – Gas#1 to Gas#4.....128
Table 7-4: Gas compositions – Sam Gas, Bob Gas, Tim Gas and Ben Gas 129
Table 7-5: Experimental Core Flood Data.....132
Table 7-6: Simulated Flood Data.....133
Table 8-1: Compositions of oils used in miscibility studies.....150
Table 8-2: Gas compositions: CO_2, Field B gas, SG#1 and SG#2.....151
Table 8-3: Gas compositions – Gas#1 to Gas#4.....151

Table 8-4: Slim tube results – CO_2 at 3000psig 152
Table 8-5: Slim tube results – CO_2 at 2850psig 153
Table 8-6: Slim tube results – CO_2 at 2700psig 154
Table 8-7: Slim tube results – CO_2 at 2550psig 155
Table 8-8: Oil recovery at 1.2PV of CO_2 injected at injection pressure of test.....156
Table 8-9: Slim tube results – SG#1 at 3200psig 157
Table 8-10: Slim tube results – SG#1 at 3000psig 158
Table 8-11: Slim tube results – SG#1 at 2700psig 159
Table 8-12: Slim tube results – SG#1 at 2500psig 160
Table 8-13: Oil recovery at 1.2PV of SG#1 injected at injection pressure of test 161
Table 8-14: Laboratory measured MMP (psia) data by Slim Tube (ST) and RBA for CO_2, SG#1 and SG#2 164
Table 8-15: Correlated and measured results for MMP (psia) of Oil A with CO_2. 165
Table 8-16: Correlated and measured results for MMP (psia) of Oil A with SG#1. 166
Table 8-17: Correlated and measured results for MMP (psia) of Oil A with SG#2. 167
Table 8-18: Measured RBA MMPs for Gas#1 – Gas#4. 169
Table 9-1: Testing of correlated data 178
Table 9-2: Measured and Correlated MMP values.....185
Table 9-3: Comparison of developed correlations to correlations from literature 184

NOMENCLATURE

Nomenclature and units used throughout this thesis are as follows:

ENGLISH

Symbol	Description	Unit
A	Cross sectional area of core plug	cm^2
BHP	Bottom hole pressure	psi
B_g	Gas formation volume factor	rcf/scf
B_o	Oil formation volume factor	rb/stb
B_{od}	Depletion oil formation volume factor	rb/stb
B_{odb}	Depletion oil formation volume factor at bubble point pressure	rb/stb
B_{of}	Flash oil formation volume factor	rb/stb
B_{ofb}	Flash oil formation volume factor at bubble point pressure	rb/stb
B_{oi}	Initial oil formation volume factor	rb/stb
B_t	Total formation volume factor	rb/stb
B_{td}	Depletion total formation volume factor	rb/stb
C_1	Constant for oil viscosity	
C_2	Constant for oil viscosity	
C_g	Constant for GA fitness factor determination	
c_o	Oil compressibility	psi^{-1}
D	Plug diameter	cm
E	Gas expansion factor	scf/rcf
E_A	Areal sweep efficiency	
E_D	Displacement efficiency	
E_M	Mobilization efficiency	
E_R	Overall recovery efficiency	
E_V	Vertical sweep efficiency	
F_R	Mole fraction of intermediates	
$Fit(i)$	Average fitness of chromosome i	
GHV	Gross heating value	BTU/ft^3
GHV_i	Gross heating value for component i	BTU/ft^3
I	Oil characterization index	
k	Permeability	mD
L	Core plug length	cm
$Liq\%$	Liquid Percent	
m	Mass	
M	Mole fraction	mol%
M_i	Mole fraction of component i	mol%
M_{C1}	Mole fraction of methane and nitrogen in the reservoir fluid	mol%

M_{nC5}	The mole fraction nC_5 in the injection gas stream	mol%
M_{C5+}	Mole fraction of C_5+ in the oil	mol%
MW	Molecular weight	g.mol
MW_i	Molecular weight of component i	g.mol
MW_{inj}	Molecular weight of injection gas	g.mol
MW_{air}	Mole weight of air	g.mol
MW_{C5+}	Molecular weight of C_5+ of the reservoir fluid	g.mol
MW_{C7+}	Molecular weight of C_7+ component in stock tank oil	g.mol
MF_i	Modification Factor of component i	
MMP	Minimum miscibility Pressure	psia
MMP_{base}	MMP for base injection gas (no nC_5), psia	psia
MMP_{cal}	Calculated MMP	psia
MMP_{exp}	Experimental MMP	psia
$MMP_{GA\text{-}nC5.enriched}$	GA-based MMP for nC_5 enriched gas, psia	psia
$MMP_{LRM1\text{-}nC5\ enriched}$	The MMP for the nC_5 enriched gas correlated with LRM1	psia
$MMP_{LRM2\text{-}nC5\ enriched}$	The MMP for the nC_5 enriched gas correlated with LRM1	psia
$MMP_{impure(MPa)}$	Impure CO_2 MMP	MPa
$MMP_{pure(MPa)}$	Pure CO_2 MMP	MPa
n	Number of moles	
NHV	Net heating value	BTU/ft^3
NHV_i	Net heating value of component i	BTU/ft^3
P	Pressure	psia
P_c	Critical pressure	psia
$P_{C,CO2}$	Critical Pressure of CO_2	psia
$P_{C,inj}$	Critical pressure of injection gas	psia
P_{cw}	Weight fraction based critical pressure	psia
$P_{cw\text{-}base}$	Weight averaged pseudo-critical pressure of the base gas (no nC_5)	psia
$P_{cw\text{-}nC5}$	Weight averaged pseudo-critical pressure of the injected nC_5 enriched gas	psia
P_{pc}	psuedo-critical pressure	psia
P_{pr}	psuedo-reduced pressure	
P_R	Reservoir pressure	psi
P_{sat}	Saturation pressure	psia
$PFit(i,j)$	Fitness function of GA correlation for data number j of chromosome i	
pen	Penalty function, used for GA fitness factor determination	
q	flow rate	cc/sec
r	radius	ft, in
r_e	effective reservoir radius	ft

r_w	well bore radius	ft
R_s	Solution GOR	scf/stb
R_{sd}	Depletion solution GOR	scf/stb
R_{sdb}	Depletion solution GOR at bubble point	scf/stb
R_{sfb}	Flash solution GOR at bubble point	scf/stb
$\overline{S_o}$	Average oil saturation in swept zone	
S_{oi}	Initial oil saturation	
S_{orp}	Ultimate residual oil saturation	
T	Temperature	
T_c	Critical temperature	
$T_{c,inj}$	Critical temperature of injection gas	K
T_{ci}	Critical temperature of the gas component i, °F.	°F
T_{Ci}	Critical temperature of component i	K
T_{CM}	Critical temperature of the mix	K
T_{cm}	Pseudo-critical temperature of the mixture	°F
T_{cw}	Weight fraction based critical temperature	°F
$T_{cw\text{-}base}$	Weight averaged pseudo-critical temperature of the base gas (no nC_5)	°F
$T_{cw\text{-}nC5}$	weight average pseudo-critical of the injected nC_5 enriched gas	°F
T_{pc}	psuedo-critical temperature	
T_{pr}	psuedo-reduced temperature	
T_{res}	Reservoir temperature	°F
T_{RES}	Reservoir temperature	K
TE_o	Oil thermal expansion	$°F^{-1}$
t_{roll}	Roll time	sec
V	Volume	cc
V_B	Bulk volume	cc
V_P	Pore volume	cc
V_g	Gas volume	cf
$V_{g,res}$	Gas volume at reservoir conditions	rcf
$V_{g,surf}$	Gas volume at surface conditions	scf
$V_{g,cell}$	Gas cell volume	cc
V_o	Oil volume	bbl
$V_{o,res}$	Oil volume at reservoir conditions	rbbl
$V_{o,surf}$	Oil volume at surface conditions	stb
$V_{o,cell}$	Oil cell volume	cc
$V_{t,res}$	Total volume at reservoir conditions	rbbl
$V_{t,surf}$	Total volume at surface conditions	stb
V_{pump}	Pump volume	cc
$V_{pump,sat}$	Pump volume at saturation pressure	cc

V_{rel}	Relative total volume, swollen volume or swelling factor	
V_{sat}	Volume at the saturation pressure	cc
$V_{sat(new)}$	New saturation volume	cc
$V_{sat(orig.)}$	Original saturation volume	cc
Vol/Int	The ratio of volatile components (methane and nitrogen) to intermediate components (ethane to butane)	
W_{dry}	Dry weight of core plug	gm
w_i	Weight fraction of component i	wt%
W_{sat}	Saturated weight of core plug	gm
Y	The Y-function	
y_2	Mole fraction of non-CO_2 component in injection gas	
y_i	Mole fraction of component i	
Z	Compressibility factor (Z)	
Z_{sc}	Compressibility factor (Z) at standard conditions	

GREEK

Symbol	**Description**	**Unit**
α	Slope of the relationship between $MMP_{nC5\ enriched}$ / MMP_{base} vs $M_{C5+,oil}$ / MW_{C5+}	
α_{inj}	Johnson and Pollin (1981) Injection gas constant	psia/K
β_{GA}	GA multiplication factor	
β	Intercept of the relationship between $MMP_{nC5\ enriched}$ / MMP_{base} vs $M_{C5+,oil}$ / MW_{C5+}	
Δ	Difference	
ϕ_e	Effective porosity	
γ_G	Gas Gravity	
λ_{GA}	GA multiplication factor	
μ	Viscosity	cP
μ_g	Gas viscosity	cP
μ_o	Oil viscosity	cP
μ_w	Water viscosity	cP
ρ_{oil}	Oil density	gm/cc, lb/ft^3
ρ_r	reduced density	
ρ_{water}	Density of water	gm/cc, lb/ft^3
ρ_{steel}	Density of steel	gm/cc, lb/ft^3
ρ_{steel}	Density of steel	gm/cc, lb/ft^3

ACRONYMS

Acronym	**Description**
CCE	Constant Composition Expansion
CGR	Condensate Gas Ration
CME	Constant Mass Expansion
CMS	Constant Mass Study
CVD	Constant Volume Depletion
EOR	Enhanced Oil Recovery
FID	Flame Ionisation Detector
FVF	Formation Volume Factor
GC	Gas Chromatograph
GOR	Gas Oil Ratio
MMP	Minimum Miscibility Pressure
PV	Pore Volume
PVT	Pressure, Volume, Temperature
RBA	Rising Bubble Apparatus
SARA	Saturates, Aromatics, Resins, Asphaltenes
TCD	Thermal Conductivity Detector
WFT	Wireline Formation Tester

1 INTRODUCTION

Throughout the world's oil reservoirs, approximately one third of reserves initially in place are recovered by primary recovery methods. Several Enhanced Oil Recovery (EOR) techniques exist to increase the recovery of oil from reservoirs including thermal and chemical techniques, air, nitrogen, hydrocarbon gas and carbon dioxide injection. The applicability of each EOR method is dependant on the reservoir pressure and temperature, reservoir fluid and rock properties, as well as the availability of material to be injected.

The Cooper Basin is Australia's largest onshore oil and gas development. It has been supplying gas to Adelaide since 1969 and to Sydney since 1976. The region's oil reservoirs are typically very tight resulting in low oil recoveries. Water flooding is not an option due to the low permeabilities. However, miscible gas flooding for EOR could be an option.

This Ph.D. research project targets Cooper Basin oil reservoirs of very low permeability (approximately 1mD) where injectivities required for water flooding are not achievable. However, the use of injection gases such as CO_2 would not have injectivity problems. CO_2 is abundant in the region and available for EOR use. CO_2 was compared to other CO_2-rich injection gases with a hydrocarbon content including pentane plus components. While the effect of components up to butane has been investigated in the past, the effect of n-pentane has on impure CO_2 gas streams has not.

One particular field of the Cooper Basin was investigated in detail (Field A). However, since similar reservoir and fluid characteristics of Field A are common to the region it is expected that the data measured and developed has applications to many other oil reservoirs of the region (Pecanek and Paton, 1984, Pitt, 1986, Schulz-Rojahn and Phillips, 1989).

Furthermore, the information could be used to evaluate other oil reservoirs around the world where field characteristics coincide, such as the Jay/LEC fields in Florida and Alabama where published data from these fields was used for comparison and knowledge basis for this study (Christian *et al.,* 1981).

The aim of this Ph.D. project is to determine the applicability of CO_2 as an injection gas for Enhanced Oil Recovery (EOR) in the Cooper Basin oil reservoirs and to compare CO_2 with other possible CO_2-rich injection gases.

This research fills gaps in knowledge of CO_2 compatibility with the reservoir fluids from the targeted oil-bearing formations in the Cooper Basin.

The Cooper Basin stretches over the northeast corner of South Australia and southwest corner of Queensland in the centre of Australia as can be seen in **Figure 1-1**.

NOTE:
This figure is included on page 2 of the print copy of the thesis held in the University of Adelaide Library.

Figure 1-1: Location of the Cooper Basin and overlying basins (Neubauer, 2003).

Figure 1-2 is a map showing the location of the key area of study relative to nearby processing plant and a potential source gas field.

Figure 1-2: Map of Cooper Basin (modified from Bon and Sarma, 2004)

The oils and gases of the Cooper Basin region have high CO_2 which could be made available for an EOR project. This study looks at how applicable CO_2 is as an injection gas in the Cooper Basin in terms of the interaction between CO_2 and Field A reservoir fluid, and compares pure CO_2 to other CO_2-rich injection gases.

1.1 Regional Geology

The Cooper Basin is located in central Australia straddling the north-east corner of the South Australian border with south-western Queensland.

The Cooper Basin contains Permo-Triassic sediments deposited in glacial, fluvial and lacustrine environments (Kapel, 1966). Two major northeast-southwest

trending ridges (the Gidgealpa-Merrimelia-Innamincka and Murturee-Nappacoongee) separate three synclinal features, the Patchawarra, Nappamerri and Tenaperra Troughs (Rezae and Lemon, 1996). This is shown in **Figure 1-3**.

Oil and gas fields are found along the southern flank of the Patchawarra Trough with the majority of oil contained in the Tirrawarra Sandstone at depths of approximately 8850ft to 9850 ft (Neubauer, 2003).

NOTE:
This figure is included on page 4 of the print copy of the thesis held in the University of Adelaide Library.

Figure 1-3: Location and structure of the southern Cooper Basin (modified from Rezaee and Lemon, 1996).

Figure 1-4 shows the age and lithology of the Cooper Basin formations and underlying and overlying basins. The largest oil finds of the region are typically found in the Lower Permian Patchawarra and Tirrawarra sands.

Figure 1-4: Lithology and age of Cooper Basin formations and surrounding basins (Neubauer, 2003)

1.2 Data

Two field trips were made to the Cooper Basin, the first to acquire Field A reservoir fluid separator samples, and the second to collect wellhead gas samples from Field B. Two other reservoir fluid mixes were created (Oil B and Oil C) to provide additional data with a range of oils. In total 7 gases were used in the miscibility study. All gases used were synthetic mixes with the exception of SG#1 which was a mixture of pure CO_2 and Field B gas.

The data developed in the laboratory based component of the project is as follows:

- Fluid properties measured for reservoir fluid from Field A (Oil A).
- Compositional work was performed on all the fluids (both oils and gases).
- 8 successful Slim Tube tests were run.
- A reservoir condition core flood test using Field A core and reservoir fluid.
- Porosity and permeability measurements of Field A core.
- 45 Minimum Miscibility Pressure (MMP) measurements using the Rising Bubble Apparatus (RBA).

Further to this the compositions of four additional gases and reservoir properties used in simulation of the core flood was provided by Santos Limited. The majority of laboratory work was performed at the facilities of Petrolab Australia Pty. Ltd.

1.3 Project Aim

Aim: To determine the applicability of CO_2 as an injection gas for EOR in the Cooper Basin oil reservoirs and to compare CO_2 to other injection gas options for the region.

In order to accomplish the project aim, the following objectives were met:

A. Determination of reservoir fluid properties to aid evaluation of a possible CO_2 flood in an oil field in the Cooper Basin, Field A.
B. Compositional simulation of a core flood experiment to compare resulting production profiles using different production regimes and injection gases.

C. To investigate the effect of C_5+ and nC_5 on miscibility for CO_2-rich gases and development of a correlation to predict the effect on MMP due to nC_5 in CO_2-rich injection gas stream.

These objectives were achieved through the following agenda:

- To experimentally determine the PVT properties of Oil A.
- To experimentally determine the MMP and incremental recovery of oil due to a pure CO_2 and a CO_2-rich gas flood.
- To conduct a CO_2-rich synthetic gas reservoir condition core flood using a Field A rock-fluid system.
- To determine the sensitivity of the oil recovery to input parameters through simulation of the core flood.
- Through laboratory analysis, to investigate the effect of C_5+ components and nC_5.
- To develop a correlation for estimating the effect of nC_5 on MMP.

The motivation behind the above mentioned objectives are described with more detail in the following sections.

1.4 Motivation (A): Why should we investigate the potential for a CO_2 flood at Field A or other fields in the Cooper Basin?

Field A oil field is a very tight reservoir (permeability of 0.1 to 1mD) located in the Cooper Basin, South Australia. Due to the tight nature of the reservoir, water flooding injectivity pressures required would be unpractical, however as gases such as carbon dioxide have much smaller viscosities than that of water the viability of flooding the reservoir with a gas is much more viable. Additionally, several gas sources are viable from nearby locations that vary in CO_2 and hydrocarbon content.

The average porosity throughout the oil-bearing formations of Field A is low at approximately 7 to 10%. The initial reservoir pressure was approximately 4,200psig. The northeast part of the reservoir is still above the initial bubble point pressure at around 3150psig. The southwest pools have been depleted from

approximately 2,700 to 2,800psig. The oil is volatile (51°API) with a low viscosity (0.14 cP) at reservoir conditions. The reservoir temperatures are in the range of 250-300°F. Although there is indication of some aquifer support, not much data is available to analyse its impact.

To date the recovery has been only 3 to 4% of the 50 million barrels of original oil in place. It is envisaged that a suitable EOR scheme may help improve oil recovery. Simulation studies indicate the recovery at abandonment has been predicted at some 5 to 10%. It is estimated that the recovery could be increased to as much as 20 to 30% with gas flooding. In view of its low permeability and porosity, the application of water-based EOR processes faces severe injectivity problems. This brings appeal to more mobile injection fluids, such as hydrocarbon and CO_2 gases.

Within the Cooper Basin, oil is typically found in two formations, the Patchawarra Formation and the Tirrawarra Formation. Strong similarities are found in the oils found in the Tirrawarra and Patchawarra Formations within different fields of the Cooper Basin. For this reason it is believed that this data will be of use for other oil reservoirs of the region.

In order to determine the fluid properties of Field A an extensive laboratory study was performed to evaluate the possibility of a CO_2 flood at Field A. The laboratory work performed as part of this project includes:

- A full PVT study on reservoir fluid from Field A. This includes:
  - Compositional Analyses
  - Pressure-volume relations through a Constant Mass Study (CMS)
  - A Constant Volume Depletion Study (CVD)
  - A study of the viscosity-pressure relationship of Field A and the effect of pure CO_2 and SG#1 on the viscosity-pressure relationship of Field A.
- Solubility-swelling study with reservoir fluid from Field A and two injection gases, pure CO_2 and SG#1.

- A series of Slim Tube tests were run using Oil A with both pure CO_2 and SG#1 at reservoir temperature and a variety of injection pressures, with the aim of measuring the MMP of Oil A and the injection gases.
- Porosity and permeability was measured on Field A core plugs.
- A reservoir condition core flood with Field A core, Field A reservoir fluid and SG #1 at 3,000 psig.

An important part of ensuring the quality of the analysis was collection of representative reservoir fluid samples.

As part of this project, two trips were made to the Cooper Basin to collect Field A oil samples during a well test and Field B gas from the wellhead. Chapter 3 is dedicated to reservoir fluid sampling as it made up a fundamentally important part of the project.

Chapters 4 and 5 focus on the reservoir fluid analysis and Chapter 6 presents the results of the core experiments.

1.5 Motivation (B): How does pure CO_2 compare to other proposed injection gases?

Using CMG's compositional modelling software GEM, a reservoir condition core flood was simulated to create a base model. Once a satisfactory match was attained with the experimental data, the base model was modified to investigate how other proposed injection gases performed.

The injection gases investigated are as follows:

- Pure CO_2 and pure methane.
- The synthetic gases SG#1 and SG#2 made up from Field B gas (Ray Gas) and pure CO_2.
- Ray Gas, Sam Gas, Bob Gas, Ben Gas and Tim Gas: other readily available gases from the region which contain varying amounts of hydrocarbon and CO_2. All but Sam Gas contain over 20 mol% CO_2. The names of these gases have been modified to conserve confidentiality.

- Gas #1, Gas #2, Gas #3 and Gas #4: CO_2-rich gases with varying amounts of nC_5. The work done here overlaps with the motives of (C): Investigation of nC_5 on CO_2-rich injection gases.

Chapter 7 presents the results from the simulation studies performed.

1.6 Motivation (C): The effect of C_5+ and nC_5 on CO_2-Oil miscibility

During the early laboratory analyses, results suggested that having a pentanes plus fraction present in the injection gas stream could have a large effect on reducing the MMP to well below the predicted MMP values from existing correlations. This came from the lower than expected MMP result of the synthetic gas mixture SG#1 with Oil A. To further investigate the effect of C_5+ components a second synthetic gas mix was created from SG#1 adding C_5+ components in the same ratio as present in SG#1 to make SG#2 (Bon *et al.,* 2005). In order to further investigate this effect, yet simplify the investigation, the effect of nC_5 on a CO_2-rich injection gas investigated. For the investigation, a base synthetic gas blend was made from CO_2 and methane. To this 1 mol%, 3 mol% and 5 mol% nC_5 was added and the MMP was determined. By these means the effect of nC_5 on CO_2-rich MMP was determined.

To extend the applicability of the data, two synthetic oils were created (Oil B and Oil C). These were selected to broaden the range of the data and the oils were largely made up from reservoir fluid from other oil producing regions of Australia.

The MMP was measured by RBA using the four gases and the three oils at three temperatures (60, 80 and 100°C) to create a database of values large enough to find any trends.

A strong trend was found for the reduction in MMP with addition of nC_5. Based on this data correlations were developed using linear regression and Genetic Algorithm (GA) (Bon *et al.,* 2006, Emera, 2006).

Using the same core flood simulation model, production profiles were created for each of the enriched gas streams and compared. Furthermore, a brief economic

evaluation was performed by calculating the dollars revenue from oil recovery minus the cost of the injection gas by putting dollar figures on the components with a market value.

In order to achieve the above mentioned investigation the following work was performed:

- RBA measured MMP values compared to Slim Tube measured MMP values
- The measurement of MMP by RBA for three oils at three temperatures using four injection gases to develop a database of RBA measured MMP values with which to study the effect of nC_5 on a CO_2-rich gas stream
- Development of correlations to model the effect of nC_5 on a CO_2-rich gas stream

The results of the miscibility studies performed are presented in Chapter 8 and the development of correlations for the effect of nC_5 on CO_2-rich injection gases is presented in Chapter 9.

1.7 Summarised Conclusions from this Work

- A miscible CO_2 flood is achievable in Field A. This is likely to be the case in other Cooper Basin oil reservoirs.
- Miscibility for Field A reservoir fluid with CO_2 is achieved at approximately 2800psia at 279°F.
- Of the other possible injection gases SG#1, Tim Gas, Ray Gas, and Ben Gas also produce oil recoveries that are within 10% of that of pure CO_2. It is worth further investigating these gases for full economic benefit including pipelines, compression, gas processing and all other costs involved.
- Of the other possible injection gases methane, Sam gas and Bob gas give oil recoveries that are more than 10% less than that of pure CO_2. It is unlikely these gases will be viable injection gas options.
- A strong trend was found for the reduction in MMP with addition of nC_5 to a CO_2-rich injection gas. A correlation to match this trend was developed with an error of 3.2%.

- Another correlation for the reduction in MMP with addition of nC_5 to a CO_2-rich injection gas using the same dataset was developed with an added oil characterisation factor which further improved the error to 1.6%.
- The addition of nC_5 to the injection gas is not an economically viable option.

2 LITERATURE REVIEW

2.1 Introduction

This chapter gives a summary of the review of literature that formed a basis of information for this thesis and review of previously performed research in the area. The generalized gaps in knowledge aimed to be filled by this thesis are:

- Is CO_2 flooding a viable option at Field A?
- What other injection gases would make good options for a flood at Field A?
- What effect on MMP does retaining trace quantities of nC_5 or other heavy components have?
- What current research has already been performed on correlating the effect of impurities on CO_2 MMP and how can this information be used to help design other correlations for other impurities?

In order to answer these questions and create a basis of information the literature review looks at the following:

- General overview of EOR
- How CO_2 flooding can improve the recovery of oil
- Phase behaviour concepts behind oil-CO_2 interaction
- The role asphaltenes play in CO_2 flooding

2.2 Enhanced Oil Recovery

The injection of gas, chemicals or some form of thermal energy to stimulate a reservoirs production is generally termed Enhanced Oil Recovery.

The recovery of oil from a reservoir is generally divided into three forms; Primary, Secondary and Tertiary recovery, termed as such due to commonly being used in that chronological order. Primary recovery refers to the recovery of oil from the reservoirs own energy sources, such as depletion drive, rock and liquid expansion drive, aquifer drive, gas cap drive and gravity drainage. Secondary recovery is generally interpreted as some way to improve the recovery of oil through energies not from the reservoir. This often comes by way of pressure maintenance through injection of water or gas. Since water injection is so commonly used at this stage

the term secondary recovery has become nearly synonymous with water flooding. Tertiary recovery would then come after secondary recovery to further improve the recovery of oil and usually is used to describe processes such as polymer flooding, miscible gas flooding or thermal injection.

Although tertiary recovery is often considered as the tertiary phase in the production of a reservoir in chronological order (after primary and secondary recovery techniques) it is not always so since these techniques can be implement after primary production or even as the only recovery method. For this reason the term EOR has become more accepted within petroleum engineering literature.

2.2.1 Types of EOR Techniques

EOR techniques can be categorised as; polymer flooding, chemical injection, miscible injection, thermal injection or other techniques (such as microbial) (Klins, 1984, Green and Willhite, 1998).

Polymer Flooding is used when mobility control is required to prevent viscous fingering by thickening water with polymers or reducing gas mobility with foams. As such it improves the vertical and areal sweep efficiency.

Chemical Injection is the injection of chemicals such as alkali agents or surfactants are used to improve interfacial tension and phase behaviour and therefore reduce the displacement efficiency.

Thermal Injection is the injection of steam or hot water to decrease the viscosity of the reservoir fluid and as such is used in heavy oil fields. In some cases oxygen is injected in order to cause in-situ combustion with the reservoir fluid to create the thermal energy.

Miscible Flooding is the injection of a solvent that is miscible with the reservoir fluid in order to reduce residual oil saturations. This includes injection of hydrocarbon gases, CO_2 and LPG.

2.3 Recovery Efficiency and the Factors that Affect It

The efficiency of the recovery of oil from a reservoir is affected by a variety of parameters. In order to define the recovery efficiency it can be expressed simplistically as the following:

Eq. 2-1

$$E_R = E_A.E_V.E_D.E_M$$

Where:

E_R = overall recovery efficiency,

E_A = areal sweep efficiency,

E_V = vertical sweep efficiency,

E_D = displacement efficiency,

E_M = mobilization efficiency.

Several of these factors are a function of injected pore volumes of injection fluid and therefore pore volume of fluid injected would need to be maintained consistent need to be calculated at the same point of the flood.

2.3.1 Areal Sweep Efficiency

The areal sweep efficiency is defined as the fraction of the reservoir area invaded by the injection fluid. It can be affected by positioning of wells, fluid mobilities, and areal heterogeneity. It is a function of pore volumes of fluid injected. If viscous fingering occurs it would decrease the areal sweep efficiency. Polymer flooding can often be used to stabilise an injection front to improve areal sweep efficiency.

2.3.2 Vertical Sweep Efficiency

The vertical sweep efficiency is defined as the vertical section of the reservoir contacted by the injection fluid. It is primarily a function of vertical heterogeneity and gravity segregation. A high permeability streak or fracture within the reservoir will decrease the vertical sweep efficiency as injected fluid will flow through these.

2.3.3 Displacement Efficiency

The displacement efficiency is the fraction of movable oil that has been displaced in the swept zone. It can be expressed as:

Eq. 2-2

$$E_D = \frac{S_{oi} - \overline{S_o}}{S_{oi} - S_{orp}}$$

Where:

S_{oi} = initial oil saturation

$\overline{S_o}$ = average oil saturation in swept zone

S_{orp} = ultimate residual oil saturation

The displacement efficiency is affected by relative permeabilities and fluid viscosities.

2.3.4 Mobilization Efficiency

The mobilization efficiency is defined as the fraction of initial oil in place recovered by the recovery process. It can be seen as the ultimate recovery of the recovery process and can be expressed as:

Eq. 2-3

$$E_M = \frac{S_{oi}/B_{oi} - S_{orp}/B_{of}}{S_{oi}/B_{oi}}$$

Where:

B_{oi} = initial oil formation volume factor

B_{of} = final oil formation volume factor

The mobilization efficiency is affected by the ratio of capillary to viscous forces and phase behaviour of fluids. A miscible flood can improve the mobilization efficiency by decreasing the residual oil saturation.

2.4 Carbon Dioxide Flooding

The critical pressure and temperature of carbon dioxide is 73.0atm and 31.0°C respectively (1073psia and 87.8°F) (Chang, 1994). At pressures and temperatures above these carbon dioxide is supercritical. CO_2 can either displace oil by miscible or immiscible displacement.

Figure 2-1 shows the suitability of different gas injection processes as a function of the reservoir fluids reduced properties.

NOTE:
This figure is included on page 17 of the print copy of the thesis held in the University of Adelaide Library.

Figure 2-1: Suitability of CO_2 processes. CO_2 could possibly replace expensive and "greener" C_2-C_3 gases in many reservoirs, if available (Novosad, 1996).

The following topics go further into CO_2 flooding detailing how and why it can be used to enhance the recovery of oil.

2.4.1 Carbon Dioxide Miscible Flooding

First it is important to define miscibility and particularly to differentiate it from solubility, two terms which are often misused as if synonymous.

Definition:

"Solubility is defined as the ability of a limited amount of one substance to mix with another substance to form a single, homogeneous phase. Miscibility is defined as the ability of two or more substances to form a single homogeneous phase when mixed in all proportions" (Holm, 1986).

Carbon dioxide miscible flooding improves oil recovery by (Yellig and Metcalfe, 1980):

- Gas drive
- Swelling of the oil (therefore increasing the reservoir pressure)
- Decreasing the viscosity of the oil

Further to the above benefits of miscible CO_2 flooding, when a reservoir fluid and CO_2 are miscible there is no interfacial tension and thus capillary forces are eliminated. This has the implication of reducing the oil saturation below the residual oil saturation that would otherwise be achieved, thus yielding more recoverable oil.

Miscibility between fluids can be either first contact miscible or multi-contact miscible (also known as dynamic miscibility). If carbon dioxide is first contact miscible with a reservoir fluid then it will mix in all proportions as soon as the two fluids are contact one another, no matter what amounts of each component is used for the mixture (Stalkup, 1984).

2.4.2 The Vaporising and Condensing Drive Mechanisms

Multi-contact miscibility can be achieved through two techniques; the vaporising-gas drive and condensing gas-drive (Holm, 1986, Bradley, 1987).

In the vaporising-gas drive, a lean gas is injected. The leading edge of the injection gas will first vaporise the lighter components present in the reservoir fluid, such as, methane through to hexane. Then this mixture will progressively mix with heavier components until the leading edge of the injection gas is enriched enough such that it is miscible with the virgin reservoir fluid (Holm, 1986).

In a condensing-gas drive, an enriched gas with C_2+ components is injected and the heavier components are given up into the oil. When the oil becomes sufficiently enriched with these light hydrocarbon components it becomes miscible with the injection gas (Holm, 1986). In the condensing gas drive miscibility is achieved at the trailing edge. The enriched reservoir fluid becomes miscible with fresh injection gas.

Figure 2-2 (shown below) is a pseudo-ternary diagram for a hypothetical hydrocarbon system. Ternary diagrams can be quite useful to visualise the composition of a system or several systems on the same diagram for three component mixes, however, when more components exists they can be grouped into pseudo-components such as volatile, intermediate and heavy components. After drawing the ternary diagram for a reservoir fluid at known conditions of pressure and temperature, the two-phase envelope is drawn and the reservoir fluid composition can be placed accordingly. Remember, this two-phase envelope is the compositional conditions at the particular pressure and temperature at which the diagram is drawn at in which two-phases will exist.

Tie lines can then be drawn in by drawing the tangent to the critical point on the two-phase envelope (the critical tie line) and the tangent to the two-phase envelope that goes through the reservoir fluid composition (RF). This creates three zones. Based on these zones we can define the following:

- RF is first contact miscible with fluids whose composition fall in Zone 1,
- RF is multi-contact miscible with fluids whose composition fall in Zone 2 and
- RF is immiscible with fluids whose compositions fall in Zone 3.

The diagram can then be re-drawn at conditions of pressure and temperature for comparison at changes in conditions.

Looking at the multi-contact scenario, the ternary diagram enables us to envisage the CO_2-oil interaction in order to generate miscibility. A solvent in Zone 2 (for example "Z_2") would be multi-contact miscible with RF as the line drawn between RF and the solvent travels through the two-phase region (Alston *et al.,* 1985). This means that the solvent vaporises the lighter components of RF to make an

enriched solvent mixture with concentration at point "a_1". The solvent mixture at "a_1" then mixes with heavier components in the reservoir fluid to create a fluid which condenses with composition at "a_2". These process repeats until it reaches equilibrium at some point, shown in **Figure 2-2** as "A".

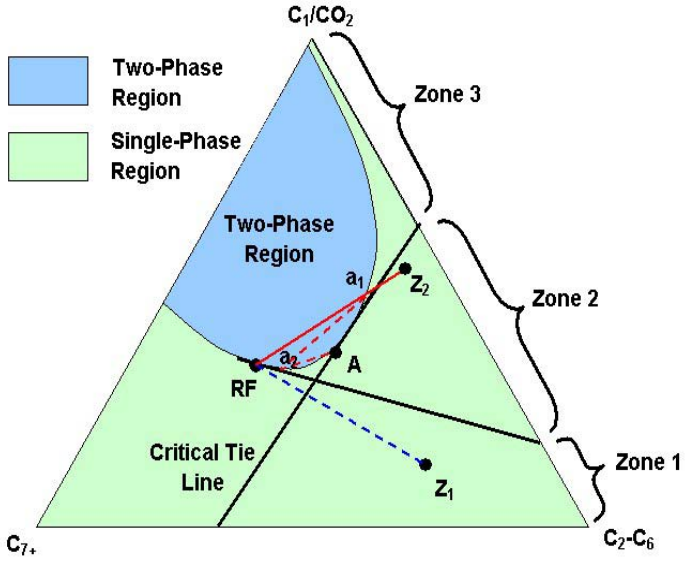

Figure 2-2: Pseudo-ternary diagram for a hypothetical hydrocarbon system diagram showing ranges of miscibility with a solvent.

Table 2-1 below, reproduced from Gozalpour *et al.,* 2005, lists depth versus oil gravity for screening whether a CO_2 flood would be a viable option in the reservoir.

Table 2-1: Screening criteria for application of CO_2 miscible flood (Gozalpour *et al.,* 2005).

Reservoir Parameter	Carcoana (1982)	Taber and Martin (1983)	Klins (1984)	Taber *et al.,* (1997)
Depth (m)	< 3000	> 700	< 914	i) > 1219; ii) > 1006 iii) > 853; iv) > 762
Temperature (°C)	< 90°C			
Pressure (MPa)	> 83		> 103	
Permeability (mD)	> 1			
Oil Gravity (°API)	> 40	> 26	> 30	i) 22-27; ii) 28-31.9 iii) 32-39; iv) > 40
Viscosity (cP)	< 2	< 15	< 12	< 10
Fraction of Oil Remaining	> 0.30	> 0.30	> 0.25	> 0.20

2.4.3 Carbon Dioxide Immiscible Flooding

Carbon dioxide can also be used to flood the reservoir immiscibly (Brush *et al.,* 2000, Dyer and Farouq Ali, 1989, Holm and Josendal, 1974). One such example is the immiscible flood at Bati Raman oilfield in Turkey (Spivak *et al.,* 1989, Sahin *et al.,* 2008). For an immiscible CO_2 flood the reservoir pressure is below the MMP and the flood operates similarly to a water flood.

Even for CO_2 floods with injection pressures just above the MMP, drawdown resulting from flow may drop the pressure below the MMP and it is possible to have both miscible and immiscible flooding within the same reservoir (Elsharkawy *et al.,* 1992).

In immiscible flooding, there exists an interface between the two fluids and thus, there also exists a capillary pressure caused by the interfacial tensions. The benefit of the flood is due to reservoir pressure maintenance and by displacing the fluid. Since the two fluids are immiscible, higher residual oil saturations can be expected than with a miscible flood (Dake, 1978).

Dyer and Farouq Ali (1989) concluded that immiscible flooding is not a substitute for miscible carbon dioxide flooding or thermal flooding but rather it should be used if the reservoir conditions are appropriate for it. Immiscible carbon dioxide flooding is mostly applicable for reservoirs with very heavy reservoir fluid (13-22°API) if the oil is very heavy then MMP will be too high for carbon dioxide miscibility with the oil at a reasonable pressure. Those reservoirs that are too deep or too thin for thermal flooding to be feasible are also potential candidates for carbon dioxide immiscible flooding. **Table 2-2**, reproduced from Dyer and Farouq Ali, 1989, shows the target characteristics for an immiscible flood. Reservoirs with these properties are regarded as potential candidates for immiscible flooding.

Table 2-2: Target characteristics for immiscible carbon dioxide flood.
(Dyer and Farouq Ali, 1989)

NOTE:
This table is included on page 22 of the print copy of the thesis held in the University of Adelaide Library.

2.4.4 Ways to Utilize CO_2 in EOR Process

CO_2 is rarely first-contact miscible with oil. It is usually multi-contact miscible, a process whereby the CO_2 first contacts the reservoir fluid and dissolves light components in the reservoir fluid. This fluid becomes a new mix and forms an interface between the CO_2 and the reservoir fluid, being miscible with both.

CO_2 floods rarely use pure CO_2 and will often contain varying amounts of impurities such as methane or other hydrocarbon components, H_2S, SO_2 or N_2. In some cases these impurities are retained or added to improve the miscibility of the CO_2 with the oil and in other cases it is more expensive to remove the impurity than to retain it.

When flooding with CO_2, it is often injected in alternating slug modes. Where CO_2 is very expensive, the utilization is reduced by injecting first a pre-determined slug of CO_2 followed by a cheaper chase gas such as N_2 or air. Thus, CO_2 is driven by a much larger volume of cheaper gas.

In many cases, water is used as the chase fluid. This process is called the Water-Alternating-Gas (WAG) or more appropriately, Water-Alternating-CO_2 ($WACO_2$) for a CO_2 flood. The primary role of these additional fluids is to control the mobility of CO_2 and/or to take advantage of gravity segregation. Some CO_2 floods are also carried out in combination with solvents such as natural gas liquids (NGL), H_2S or SO_2 to help reduce the MMP and maintain the miscibility throughout the reservoir.

2.5 CO_2-Oil Interaction

As previously mentioned, the critical pressure and temperature of carbon dioxide is 1073 psia and 87.8°F respectively (Chang, 1994). Since CO_2 floods will often be at pressures *and* temperatures above this it is important to keep in mind that at these conditions CO_2 is supercritical. Supercritical fluid is neither vapour nor liquid and tends to have properties somewhere in between those of either phase. Supercritical CO_2 has a low viscosity but high density.

Carbon dioxide mixes in oil mainly as a result of three mass transfer mechanisms; solubility, diffusion and dispersion (Dyer and Farouq Ali, 1989). Of these three mass transfer mechanisms, solubility accounts for the greater part of the mixing. Solubility is affected greatly by pressure and to a lesser degree by temperature and composition. Carbon dioxide is more soluble in hydrocarbons as a gas than it is when in the liquid phase. Carbon dioxide solubility decreases with increasing concentrations of nitrogen and methane and also decreases as the bubble point of the oil increases. Carbon dioxide is more soluble in oil than it is in water.

In water the carbon dioxide solubility is dependant on the salinity, pressure and temperature of the water, with solubility decreasing with increasing salinity (Dyer and Farouq Ali, 1989).

Carbon dioxide also mixes with oil through diffusion. Diffusion helps the carbon dioxide mix in particular with heavier oils, reducing the density and viscosity of the fluid (Donaldson *et al.,* 1985).

Due to the velocity of flow, additional mixing can occur as a result of dispersive forces of attraction that occur within molecules of high polarity such as hydrocarbons. However, the mixing as a result of dispersion is far less than that due to solubility or diffusion (Dyer and Farouq Ali, 1989).

2.5.1 CO_2 Solubility in Oil and the Swelling Factor

Consider the oil phase in a separator at an elevated pressure. It will contain gas dissolved in solution. When this liquid is flashed to the stock tank, the gas will come out of solution and, although the liquid decompresses (resulting in an

increase in volume), the volume of oil will shrink as a result of gas molecules coming out of solution. The ratio of the final volume (depressurised) to the initial volume (with gas in solution) gives the shrinkage of the oil.

Swelling is the reverse of the processes occurring for shrinkage to take place. When CO_2 mixes with a reservoir fluid and dissolves to form a single-phase, the new mix will have a larger volume than before and as such the volume has swollen. Quantifying the amount of swelling is important as this will contribute to the energy available to produce the reservoir fluid and the change in volumes within the reservoir. For this reason, it is common to undertake laboratory solubility-swelling tests as part of an analyses program for evaluation of a gas flood and compatibility of the gas and reservoir fluid.

With solubility-swelling data the volume changes within the reservoir due to a gas injection project will be known.

2.6 Corrosive/Scaling Effects of CO_2

The water holding capacity of CO_2 under given conditions of pressure and temperature to design cost-effective facilities are determined by the corrosive and scaling effects of CO_2. CO_2 dissolves in water forming carbonic acid (H_2CO3). This can react with the tubing and surface facilities corroding them. It can also dissolve carbonates and deposit them elsewhere within the reservoir. It is to be noted that liquid water is much more corrosive than water vapour.

2.7 Minimum Miscibility Pressure

Definition:

The Minimum Miscibility Pressure (MMP) is the lowest pressure at which multi-contact miscibility can be achieved.

Miscibility can be thought of as mixing of two fluids dynamically, whereas solubility is the mixing of two fluids statically. MMP is a function of a variety of parameters, the CO_2 flood may either be miscible or immiscible with the reservoir fluid. The main factors affecting miscibility are the reservoir fluid composition, injection gas

composition and reservoir temperature. These factors and how they affect miscibility are discussed in the following section.

2.7.1 Parameters that Impact MMP

Below the MMP the recovery of oil increases rapidly with an increase in injection pressure. Injection of CO_2 at higher pressures will result in a greater oil recovery, however, above the MMP the recovery increase is much smaller. The relationship of oil recovery to injection pressure is more or less linear on either side of the MMP and therefore the MMP can be defined as the break-over point on the plot of oil recovery to injection pressure.

However, the cost of injection increases at higher pressures due to the cost of compressing the CO_2. Because of this, knowing the MMP is very important in order to maximise profits from an injection project.

Yellig and Metcalfe (1980) studied the effects of temperature and composition on the CO_2 MMP. The MMP was determined experimentally by the Slim Tube method. This paper came to the conclusion that the Slim Tube method is a useful and reproducible technique for determining the CO_2 MMP for a reservoir oil. It also stated that, for the oils considered, the reservoir fluid composition had little or no effect on the MMP and temperature affected the CO_2 MMP linearly at approximately 15 psi/°F.

Alston *et al.,* (1985) concluded that the primary factors affecting the CO_2 MMP are the temperature and the pentanes plus composition of the reservoir fluid.

Most correlations used to determine the MMP agree with Alston *et al.,* (1985), in that the main parameters affecting the MMP are as follows (Holm and Josendal (1974), Sebastian *et al.,* (1985), Glasø (1985), Emera and Sarma (2005)):

- Composition of the reservoir fluid (often incorporated through the molecular weight of C_5+),
- Composition of the injection gas (often incorporated through the critical temperature of the gas), and
- Reservoir temperature.

Reservoir fluid composition

CO_2 is more miscible with the intermediate components in reservoir fluid than it is with the heavy or the light components. Thus the heavier the reservoir fluid the less miscible it is. Also the richer it is in methane the less miscible. However, CO_2 can achieve miscibility with heavy components in the reservoir fluid through multiple contact miscibility. Therefore, MMP is lower for oils with a larger the intermediate fraction. MMP is higher for oils with a larger fraction of heavy components.

Injection Gas Composition

Methane and nitrogen is less miscible with reservoir fluids than CO_2 is. They are commonly the impure components found in injection gas. Thus, having more of these substances in the injection gas will increase the MMP.

Reservoir Temperature

CO_2 MMP increases with increasing temperature (Holm and Josendal, 1978, Yellig and Metcalfe, 1980, Mungan, 1981). Therefore deeper, hotter reservoirs have higher MMP values.

2.8 Methods to Determine the MMP

The following methods exist for determination of MMP:

- Measurement by Slim Tube (considered the industry standard)
- Measurement by Rising Bubble Apparatus
- Calculation using an appropriate empirical correlation
- Calculation using equation of state software

The following sections go into these methods with more detail.

2.8.1 The Slim Tube Test

The Slim Tube Test involves saturating the Slim Tube with reservoir fluid and then flooding the reservoir fluid with the solvent. The incremental oil produced through the flooding of the reservoir fluid with the solvent is measured. The test takes place at reservoir temperature and a user defined pressure and is repeated for

multiple pressures. The Slim Tube test is considered the industry standard for MMP measurements.

The justification of having a longer Slim Tube is to minimize the effects of the transition zone of the injected fluid in the reservoir fluid. And by having a thinner Slim Tube viscous fingering can be avoided. With respect to the packing of the column there are differences in opinions within literature, some say it makes little difference while others claim that the difference in dispersion levels from differently packed column affects the oil recovery. The porosity tends to have little effect; generally a column of 30% or greater porosity is used.

It is best to keep the pressure differential of the Slim Tube test low (with a high permeability column) because in doing so the pressure at which the MMP is measured remains consistent.

The Slim Tube test can be used to determine incremental recoveries. However, the core flood incremental recoveries are more accurate as they are more representative of the true reservoir conditions and in modelling the fluid flow. Also, as no water is present in the Slim Tube, the residual oil saturation determined excludes the relative permeability relationships between oil and water, and connate water saturation is not measured at all. However, as this project will also incorporate a core flood, the Slim Tube will be used solely for the determination of MMP and to verify trends in results experienced in the core flood.

Generally the MMP is considered to be the break-over point on the graphing of oil recovery after 1.2 pore volumes (PV) of injected fluid versus injection pressure, created from at least several Slim Tube tests. The points must be taken from tests with the same reservoir fluid, injection gas, test temperature and using the same experimental set-up with injection pressure being the only variable.

In the absence of multiple test results (usually due to time and budget constraints) other criteria are commonly taken to define multi-contact miscibility or immiscibility, such as the oil recovery being over 90% at 1.2 PV of fluid injected (Williams *et al.,* 1980). Furthermore, sometimes the recovery at 1.0 PV of fluid injected is used or a

cut-off gas-oil ratio (GOR) in heavier oils where breakthrough may occur well before 1.0 PV of fluid injected (Danesh, 1998).

2.8.2 The Rising Bubble Apparatus Method for Determination of MMP

Another way in which the MMP can be measured is by using the RBA (Christiansen *et al.,* 1987). Elsharkawy *et al.,* 1992, compared the two methods. This was based on analysis that was performed on twelve different systems. From their study they concluded that the MMP measurements by the RBA were in good agreement with the point in the Slim Tube test at which the oil recovery improved less than 1% per 100 psi incremental pressure. The RBA is considerably faster in determining the MMP, taking only 1-2 hours while the Slim Tube test can take as long as a week to complete.

Asphaltene precipitation has minimal effect on the RBA. If asphaltenes precipitate the rising bubble should still be clearly visible, thus not affecting the test. If asphaltenes precipitate inside a Slim Tube the permeability of the column is altered and the column may not be completely repairable.

For both RBA and Slim Tube, the measurement of MMP is only of any practical value at pressures above the bubble-point pressure of the reservoir fluid as below the bubble-point pressure the composition will vary.

Although the RBA is commonly believed to be only appropriate for measuring the MMP when miscibility develops by vaporising drive mechanism, it can also be used to measure MMP when miscibility develops by condensing drive mechanism as described in the discussion between Poettmann *et al.* (1992) and Sibbald *et al.* (1992).

2.9 Correlations for Determining the MMP

2.9.1 Cronquist (1978)

In 1978 Cronquist proposed the following CO_2 MMP correlation:

Eq. 2-4

$$MMP = 15.988 * T_{res}^{(0.744206 + 0.0011038 * MW_{C_5^+} + 0.0015279 * M_{C_1})}$$

Where:

MMP = Minimum Miscibility Pressure

T_{res} = Reservoir temperature, °F

MW_{C_5+} = Molecular Weight of the pentanes plus fraction of the reservoir fluid

M_{C_1} = Mole fraction of methane and nitrogen in the reservoir fluid

The reservoir fluid was characterised using the molecular weight of the C_5+ fraction and the mole percent of nitrogen and methane in the reservoir fluid. The Correlation was based on 58 experimental MMP measurements from a number of sources using oils ranging from 23.7 to 44 °API and reservoir temperatures from 77 to 248 °F. The MMP values ranged from 1,076 to 5,000 psi. Average error between predicted and experimental values was 310 psi and the maximum error was 1,700 psi. One likely major factor adding to the error was that the MMP values came from different sources with different criteria for defining MMP (Stalkup, 1984).

2.9.2 Holm and Josendal (1978) and Mungan (1981)

In 1978 Holm and Josendal presented a graphical correlation for MMP as a function of temperature and mole weight of C_5+ of the reservoir fluid. In 1981, Mungan presented further data for heavier oils in the same format. **Figure 2-3** shown below shows both these graphical correlations.

NOTE:
This figure is included on page 30 of the print copy of the thesis held in the University of Adelaide Library.

Figure 2-3: MMP as a function of reservoir temperature and mole weight of the C_5+ component in the reservoir fluid (Mungan, 1981).

2.9.3 Yellig and Metcalfe (1980)

Yellig and Metcalfe in 1980 proposed a pure CO_2 MMP correlation based on the reservoir temperature. They also stated that if the calculated MMP is less than the bubble point pressure of the reservoir fluid that the bubble point pressure should be taken as the MMP. The correlation is expressed as:

Eq. 2-5

$$MMP = 1833.7217 + 2.2518055 \times T_{res} + 0.01800674 \times T_{res}^2 - 103949.93/T_{res}$$

Yellig and Metcalfe (1980) believed that the oil composition and quantity should have an effect on the CO_2 MMP and as such, in order to model this effect, they created their four oils by varying the quantities of three lumped fractions; the light fraction (C_1, N_2 and CO_2), the intermediate fraction (C_2-C_6) and the heavy fraction (C_7+). Only one of the oil mixtures had a variation in C_2-C_6 molar ratios. All other lumped fractions had consistent properties. They were surprised to find that the oil composition had little or no effect at lower temperatures and only a small effect at higher temperatures.

As such they concluded that, for the oils used in their study; (a) temperature increases CO_2 MMP by approximately 15 psi/°F over the range of 95-192°F (b) there is no effect due to oil composition and (c) there is only a minor effect of oil composition on CO_2 MMP at temperatures where vaporization mechanism is predominant.

The conclusion that oil composition has little effect on CO_2 MMP has since been proven wrong. In defence of the authors, at the time of the study very little literature data was available and they went through the laborious task of creating their own MMP data bank with Slim Tube tests. More data was required and the lack of great variation in the four oils used in their study was likely to be the reason that little variation was seen in resultant MMP measurements due to changes in oil composition.

2.9.4 Johnson and Pollin (1981)

Johnson and Pollin (1981) developed a CO_2 MMP correlation for the temperature range of 300K to 410K, which tolerated up to 20 mol% methane and nitrogen impurities. The correlation is shown below:

Eq. 2-6

$$MMP - P_{C,inj} = \alpha_{inj}(T_{RES} - T_{C,inj}) + I(0.285 * MW - MW_{inj})^2$$

Where:

$P_{C,inj}$ = Critical pressure of injection gas (psia)

T_{RES} = Reservoir temperature (K)

$T_{c,inj}$ = Critical temperature of injection gas (K)

MW = Molecular weight of reservoir fluid

MW_{inj} = Molecular weight of injection gas

I = oil characterization index

α_{inj} = 18.9psia/K for pure CO_2

The oil characterization index is a function of molecular weight and API gravity and is expressed by the following equation:

Eq. 2-7

$$I = C_{11} + C_{21}MW + C_{31}MW^2 + C_{41}MW^3 + (C_{12} + C_{22}MW)\rho + C_{13}\rho^2$$

Where:

C_{11} = -11.73

C_{12} = 0.1362

C_{13} = -7.222 x 10^{-5}

C_{21} = 6.313 x 10^{-2}

C_{22} = 1.138 x 10^{-5}

C_{31} = -1.954 x 10^{-4}

C_{41} = 2.502 x 10^{-7}

For gas mixtures of CO_2 with N_2, the injection as constant (α_{inj}) becomes:

Eq. 2-8

$$\alpha_{inj} = 10.5 \times (1.8 + \frac{10^3 y_2}{T_{RES} - T_{C,inj}})$$

For gas mixtures of CO_2 with CH_4, the injection as constant (α_{inj}) becomes:

Eq. 2-9

$$\alpha_{inj} = 10.5 \times (1.8 + \frac{10^2 y_2}{T_{RES} - T_{C,inj}})$$

Where:

y_2 = mole fraction of non-CO_2 component in injection gas

As oppose to most other MMP correlations, this correlation is sensitive to changes in reservoir composition through the molecular weight and the API gravity of the entire reservoir fluid. Most other MMP correlations split the reservoir fluid into the light, intermediate and heavy components. They have also concentrated heavily on parameters influenced by a change in injection gas composition ($P_{C,inj}$, $T_{C,inj}$, M_{inj} and y_2) while other correlations have only used one or two of these parameters to model changes in injection gas composition.

2.9.5 Sebastian, Wenger and Renner (1985)

Sebastian *et al.* (1985) derived a correlation to predict MMP for impure gas streams. It used the pure MMP and pseudo-critical temperature of the injection gas as input parameters. However, this correlation does not actually calculate an MMP itself, rather it uses the MMP calculated from another correlation or measured in a laboratory and then uses that value to calculate the MMP for the same reservoir fluid with an impure CO_2 injection gas. The correlation is shown below:

Eq. 2-10

$$MMP_{impure}/MMP = 1.0 - 2.13\times10^{-2}(T_{CM} - 304.2) + 2.51\times10^{-4}(T_{CM} - 304.2)^2 - 2.35\times10^{-7}(T_{CM} - 304.2)^3$$

$$T_{CM} = \sum_{i=1}^{N} y_i \times T_{Ci}$$

Where:

MMP_{impure} = Impure CO_2 MMP (psia)

MMP = Pure CO_2 MMP (psia)

T_{CM} = critical temperature of the mix (K)

T_{Ci} = critical temperature of component i (K)

y_i = Mole fraction of component i

2.9.6 Alston, Kokolis and James (1985)

Alston *et al.,* 1985, looked at correlations for CO_2 MMP for pure and impure CO_2 streams. Their correlation added corrections to previously derived correlations. The final mathematical equation representing MMP for an impure CO_2 stream is as shown below:

Eq. 2-11

$$MMP = 8.78 * 10^{-4} * T^{1.06} * MW_{C_5+}^{1.78} * \left(Vol/Int\right)^{0.136} * \left(87.8/T_{cm}\right)^{(169.89/T_{cm})}$$

$$T_{cm} = \sum_{i=1}^{n} w_i T_{ci}$$

Where:

Vol/Int = the ratio of volatile components (methane and nitrogen) to intermediate components (ethane to butane)

MW_{C_5+} = Molecular Weight of C_5+ of the reservoir fluid

T_{cm} = the pseudo-critical temperature of the mixture (°F)

w_i = weight fraction of component i

T_{ci} = critical temperature of component i (°F) (T_c = 87.8°F for CO_2)

2.9.7 Glasø (1985)

Glasø in 1985 modelled CO_2 MMP by the following equation:

Eq. 2-12

$$MMP = 810.0 - 3.404 \times MW_{C_7+} + (1.700 \times 10^{-9} \times MW_{C_7+}^{3.730} \times e^{786.8 * MW_{C_7+}^{-1.058}}) \times T_{res}$$

Where:

MW_{C_7+} = Molecular weight of C_7+ component in stock tank oil

When the mole fraction of intermediates (F_R) <18%, the correlation is:

Eq. 2-13

$$MMP = 2947.9 - 3.404 \times MW_{C_7+} + (1.7 \times 10^{-9} \times MW_{C_7+}^{3.73} \times e^{786.8 \times MW_{C_7+}^{-1.058}}) \times T_{res} - 121.2 \times F_R$$

In his paper, Glasø plots MMP derived from experimental work against the MMP calculated from his correlation. It can be seen that at lower pressures, the correlation predicts slightly high while at higher pressures the accuracy decreases and the correlation predicts lower than experimental MMP data. Glasø's correlation predicts that a larger fraction of volatile components in the reservoir fluid results in a lower MMP.

2.9.8 Yuan, Johns and Egwuenu (2005)

Yuan *et al.,* (2005) developed pure and impure CO_2 MMP correlations.

For their pure CO_2 MMP correlation, Yuan *et al.* used 70 MMP measurements and fitted a quadratic equation to the data. The input data had reservoir temperatures in the range of 120°F to 300°F. The correlation used three input parameters; the reservoir temperature, the C_2-C_6 mole fraction in the oil and the molecular weight of the C_7+ fraction. The correlation gave an absolute average error of 6.6% and is expressed as follows:

Eq. 2-14

$$MMP = a_1 + a_2 MW_{C_{7+}} + a_3 P_{C_{2-6}} + \left(a_4 + a_5 MW_{C_{7+}} + a_6 \frac{P_{C_{2-6}}}{MW_{C_{7+}}} \right) T_{res}$$
$$+ \left(a_7 + a_8 MW_{C_{7+}} + a_9 MW_{C_{7+}}{}^2 + a_{10} P_{C_{2-6}} \right) T_{res}{}^2$$

Where:

a_1 = -1.4634 x 10^3

a_2 = 6.612

a_3 = -44.979

a_4 = 2.139

a_5 = 0.11667

a_6 = 8.1661 x 10^3

a_7 = -0.12258

a_8 = 1.2883 x 10^{-3}

a_9 = -4.0152 x 10^{-6}

a_{10} = -9.2577 x 10^{-4}

The impure CO_2 MMP correlation developed in this work was designed to tolerate methane impurities only. The reservoir temperatures of the input data used varied from 110°F to 300°F. The correlation is as follows:

Eq. 2-15

$$\frac{MMP_{impure}}{MMP_{pure}} = 1 + m\left(P_{CO_2} - 100\right)$$

Eq. 2-16

$$m = a_1 + a_2 MW_{C_7+} + a_3 P_{C_{2-6}} + \left(a_4 + a_5 MW_{C_7+} + a_6 \frac{P_{C_{2-6}}}{MW_{C_7+}}\right) T_{res}$$

$$+ \left(a_7 + a_8 MW_{C_7+} + a_9 MW_{C_7+}{}^2 + a_{10} P_{C_{2-6}}\right) T_{res}{}^2$$

Where:

a_1 = -6.599 x 10^{-2}

a_2 = -1.5246 x 10^{-4}

a_3 = 1.3807 x 10^{-3}

a_4 = 6.2384 x 10^{-4}

a_5 = -6.7725 x 10^{-7}

a_6 = -2.7344 x 10^{-2}

a_7 = -2.6953 x 10^{-6}

a_8 = 1.7279 x 10^{-8}

a_9 = -3.1436 x 10^{-11}

a_{10} = -1.9566 x 10^{-8}

2.9.9 Emera and Sarma (2005)

Emera and Sarma in 2005 presented a pure CO_2 MMP correlation. These correlations were developed using the Genetic Algorithm (GA). For oil with bubble point pressure less than 0.345 MPa:

Eq. 2-17

$$MMP_{pure(MPa)} = 7.43497 \times 10^{-5} \times \left(T_{res}\right)^{1.1669} \times MW_{C_5+}{}^{1.201} \times \left(\frac{Vol}{Int}\right)^{0.109}$$

Where:

$MMP_{pure(MPa)}$ = MMP of pure CO_2, (MPa)

For impure gas streams, Emera and Sarma (2005) presented the following correlation:

Eq. 2-18

$$\frac{MMP_{impure(MPa)}}{MMP_{pure(MPa)}} = \frac{P_{C,CO_2}}{P_{CW}}\left[6.606 - 29.69\times\left(\frac{T_{CW}}{T_{C,CO_2}}\right) + 109.5\times\left(\frac{T_{CW}}{T_{C,CO_2}}\right)^2 - 213.363\times\left(\frac{T_{CW}}{T_{C,CO_2}}\right)^3 + 208.366\times\left(\frac{T_{CW}}{T_{C,CO_2}}\right)^4 - 98.46\times\left(\frac{T_{CW}}{T_{C,CO_2}}\right)^5 + 18.009\times\left(\frac{T_{CW}}{T_{C,CO_2}}\right)^6\right]$$

Where:

$MMP_{impure,MPa}$ = MMP of impure CO_2, (MPa)

$P_{C,CO2}$ = Critical pressure of CO_2, (MPa)

$P_{cw} = \sum_{i=1}^{n} w_i P_{Ci}$, (MPa)

$T_{cw} = \sum_{i=1}^{n} MF_i w_i T_{ci}$, (°F)

$T_{C,CO2}$ = Critical temperature of CO_2, (°F)

MF_i = Modification Factor of component i

Values of MF_i were as shown in **Table 2-3**.

Table 2-3: Values for modification factor for component i (MF_i)

Component	MF_i
SO_2	0.3
H_2S	0.59
CO_2	1.0
C_2	1.1
C_1	1.6
N_2	1.9
All other components	1.0

2.9.10 Summary of Selected Correlations from Literature

Summarising the selected correlations from literature that have been looked at, the key parameters that need to be accounted for when modelling CO_2 MMP are:

- The reservoir temperature (or temperature at which the MMP is desired)
- The reservoir fluid composition
- The injection gas composition

One key observation made though is that while most use the molecular weight of the plus fraction in the liquid to characterise the reservoir fluid (commonly the C_5+ or C_7+ where stock tank liquid data will give reliably consistent data), not all quantify this fraction. This can have the effect of erroneous calculations for fluids rich in intermediate components C_2-C_6 that will have lower MMP values than oils with a smaller amount of intermediates but the same molecular weight of C_7+. The correlations that account for the quantity of either heavy or intermediate fraction tend to have better accuracies (in accounting for one it indirectly accounts for the other). Therefore, ideally a correlation should ensure it characterises all components in the oil to improve accuracy. In the past calculations would become too complex with sophisticated correlations and therefore characterising the oil with a stock tank oil property like molecular weight or density which worked quite well and was very simple to measure and use. These days computational power available makes using sophisticated correlations very simple and there is no reason to not use more input parameters in order to improve error, be it only slightly.

One major drawback is that the best way to create a new correlation today is to use as many measurements as possible, therefore you are constrained to the input literature has published and how the literature characterised its oil.

For pure CO_2, the injection gas composition is not an issue as only input data for pure CO_2 is used. Therefore, injection gas composition is an issue only for impure gas mixes because these correlations usually try to cater for more than one impurity to broaden the applicability of the correlation. The composition of the gas mix tends to be well correlated using the pseudo-critical properties (pressure and temperature) of the gas mix as this takes into account the mole percent of all

components in the gas. Some correlations have found that using the weight percent rather than mole percent yields better results and then have further improved accuracy by adding multiplying factors depending on which “impure” component is in the mix (Emera and Sarma, 2005).

Characterizing the oil fraction presents the best opportunity for improvement in the CO_2 MMP correlations. Molecular weight *and* mole percent of a lumped component should be used and all the components should be taken into account (heavy, intermediate *and* light components).

The problem that presents with this is that the most accurate correlations use as many data points as possible. Emera and Sarma (2005) and Yuan *et al.,* (2005) present excellent summaries of previously published data. The previously published data is usually summarised and often only the input data used for a particular correlation is given. Complete compositions of the reservoir fluids need to be pieced back together and are not always given. Often, methane, nitrogen and CO_2 fractions in the oil are not given. Sometimes the molecular weight of the C_5+ fraction is used and sometimes the molecular weight of the C_7+ fraction is used. Therefore, in designing a new correlation, the best option is to use as much data as is available in literature but you are constrained by what is available. The other option is to create new data and measure all the data that would best suit the correlation, however, time constraints will tend to limit the amount of data that can be measured and therefore the accuracy.

Also, it is important to always check the ranges of the correlation prior to use as there may be a good reason for it not being recommended outside of the given ranges. For example, some correlations for impure CO_2 are specific for certain impurities and while the correlation may take into account the non-CO_2 component, this may only be valid for a particular impurity.

Looking at **Figure 2-3** shown earlier in this chapter, it can be seen that temperature tends away from linearity at higher temperatures, and this varies with fluid composition. Therefore, usage of correlations outside of the recommended

ranges for temperatures or reservoir fluid types is likely to produce an error of some sort.

2.9.11 Effects of Impurities on CO_2 MMP

A brief description of the main impurities that can be in a CO_2 injection stream follows:

Methane (CH_4): This is a very common impurity that may be founding a CO_2 injection gas stream as it is of low cost and the most common component in hydrocarbon systems. However, it will increase the MMP and therefore lower oil recoveries can be expected from a methane-rich injection gas. (Emera and Sarma, 2005, Yuan *et al.,* 2005, Alston *et al.,* 1985, Yellig and Metcalfe, 1980).

Nitrogen (N_2): Also a common impurity that may be found in a CO_2 injection gas stream or often makes up a large portion of a flue gas injection. It is an interesting component and one that could do with further research. Research to date has shown that N_2 MMP increases and decreases depending on reservoir fluid composition and temperature range. Normally you would expect N_2 to increase the MMP and this is what most correlations predict (Emera and Sarma, 2005, Alston *et al.,* 1985, Johnson and Pollin, 1981). However, for volatile oils at high temperatures N_2 MMP will decrease with increases in temperatures (Firoozabadi and Aziz, 1986, Christiansen, 1981). This is dependant on reservoir fluid composition but can be seen at normal reservoir temperatures (100°F to 300°F) with lighter oils being more likely to observe improved MMP measurements with increased temperature (Sebastian and Lawrence, 1992).

Ethane (C_2H_6): Has similar thermodynamic properties to CO_2 and tends to have little effect on the CO_2 MMP (Emera and Sarma, 2005).

Propane (C_3H_8) and Butane (C_4H_{10}): Mixes better with reservoir fluids than CO_2 and therefore has the effect of lowering the MMP.

Pentane (C_5H_{12}): Mixes better with reservoir fluids than CO_2 and therefore has the effect of lowering the MMP. The effect of pentane on CO_2 MMP has previously not been analysed to great depth and is one of the key investigations of this thesis.

Hydrogen Sulphide (H_2S): Has similar thermodynamic properties to CO_2 and tends to have little effect on the CO_2 MMP (Emera and Sarma, 2005).

Hydrocarbon Gas Mixtures: Often hydrocarbon gas mixtures are used. The mixtures usually contain high methane contents and may or may not contain high volumes of CO_2, H_2S or other non-hydrocarbon components (but remain largely hydrocarbon gas mixtures). The thermodynamic properties and phase behaviour of the mix dictate the MMP of the gas with the reservoir fluid. These mixtures usually will achieve MMP through vaporising-condensing processes whereby not only are light components from the reservoir fluid vaporised into the injection gas to for a bank but also heavier components in the gas stream are condensed into the reservoir fluid.

Pentane plus fraction (C_5+): Part of the investigations performed in this thesis also looked at the effect of C_5+ components on CO_2 MMP. Generally speaking all hydrocarbon components propane and heavier that are at equilibrium in a vapour phase will have the effect of reducing the CO_2 MMP (Bon and Sarma, 2005).

2.10 Asphaltenes – Their Role in CO_2 Flooding

As per standard test method IP-143, asphaltenes are defined as the wax free fraction in a crude oil soluble in toluene but insoluble in n-heptane.

The role of asphaltene precipitation is very relevant to CO_2 flooding as light paraffins and gases, including carbon dioxide, destabilize asphaltenes that exist in solution, and cause them to precipitate (Danesh *et al.,* 1988). Once precipitated, they can clog the reservoir pores, altering permeability, and clogging tubing, separators, pipelines and other production facilities. **Figure 2-4**, shows the places where asphaltenes can precipitate. Generally speaking, the further upstream asphaltene precipitates, the bigger the problem. The asphaltene particles have been found to affect the reservoir in a similar manner to fines migration.

NOTE:
This figure is included on page 42 of the print copy of the thesis held in the University of Adelaide Library.

Figure 2-4: Asphaltene precipitation and potential locations of clogging (Jamaluddin *et al.,* 2001)

Asphaltene precipitation is a subject that is not yet fully understood. The structure of asphaltenes can vary and different asphaltenes tend to have different properties. This is noticed in several aspects such as the stability in solution, reversibility of precipitation, the onset of asphaltenes, melting point and other such characteristics.

Asphaltenes are a black friable material. When heated they often swell and decompose leaving a carbonaceous material and volatile products. Analysis indicates that they contain a dense polynuclear aromatic nucleus with alkyl and alicyclic chains and scattered presence of heteroatoms such as nitrogen, sulphur and oxygen. The number of nuclei can range from six to more than twenty, however no conclusion has been met as to the structure of an asphaltene.

For paraffinic solvents of carbon chain larger than n-heptane, asphaltene precipitation remains relatively constant. For paraffins of less carbon content than n-heptane, asphaltene precipitation increases greatly with smaller carbon chained

paraffin. This is illustrated in **Figure 2-5** which shows what a typical plot of carbon number of n-paraffin solvent versus percent by weight of asphaltenes precipitated.

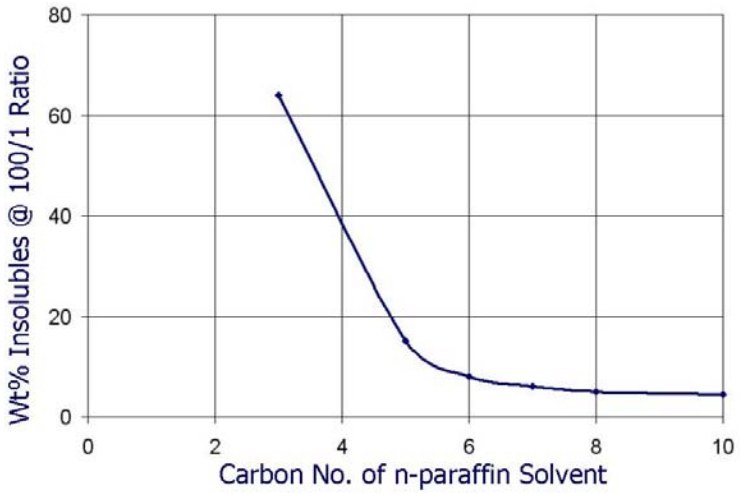

Figure 2-5: Example of effect of n-paraffin solvent carbon number on insolubles.

The Institute of Petroleum (IP) test number 143 is the standard method for measuring asphaltene content of dead crude. IP 143 essentially requires dissolving the crude in the solvent (either n-pentane or n-heptane) and filtering the solids (asphaltenes) that have precipitated due to the addition of solvent.

One important fact that has been noticed is that the fraction of asphaltene precipitated and fraction of asphaltene initially in the crude have no correlation. This is clearly evident when looking at industry experience. The crude from the Boscan field in eastern Venezuela has an asphaltene content by weight of 17%, yet suffers no problems in production. On the other hand, the Hassi Messaud field in Algeria has a 0.062% asphaltene content and has suffered large problems due to asphaltene precipitation (de Boer *et al*, 1995). This is due to the other properties of the oils, mainly composition. The Boscan crude is much heavier crude than the Hassi Messaud oil with API gravities of 10.2 and 45.0 respectively.

2.10.1 The Role of Resins on Asphaltene Precipitation

The polarity of the SARA fractions goes in the following order:

Saturates → Aromatics → Resins → Asphaltenes

There is still a great amount of uncertainty within the science of asphaltenes. It has, however, been generally accepted that under initial reservoir conditions the asphaltenes are in solution. Two main schools of thought have spawned from this; the first believing that asphaltene precipitation is a thermodynamic phenomenon that occurs due to change in reservoir PVT conditions and oil composition and that such a process should therefore be thermodynamically reversible. The other belief is that asphaltenes are solids suspended colloidally in the crude oil and remain suspended due to resin molecules, and that this process is irreversible.

The colloidal model believes that, due to the higher polarity of resin molecules, the resin molecules are attracted to the asphaltene micelles and keep them suspended in solution. Therefore, a higher resin to asphaltene ratio is desirable (**Figure 2-6**).

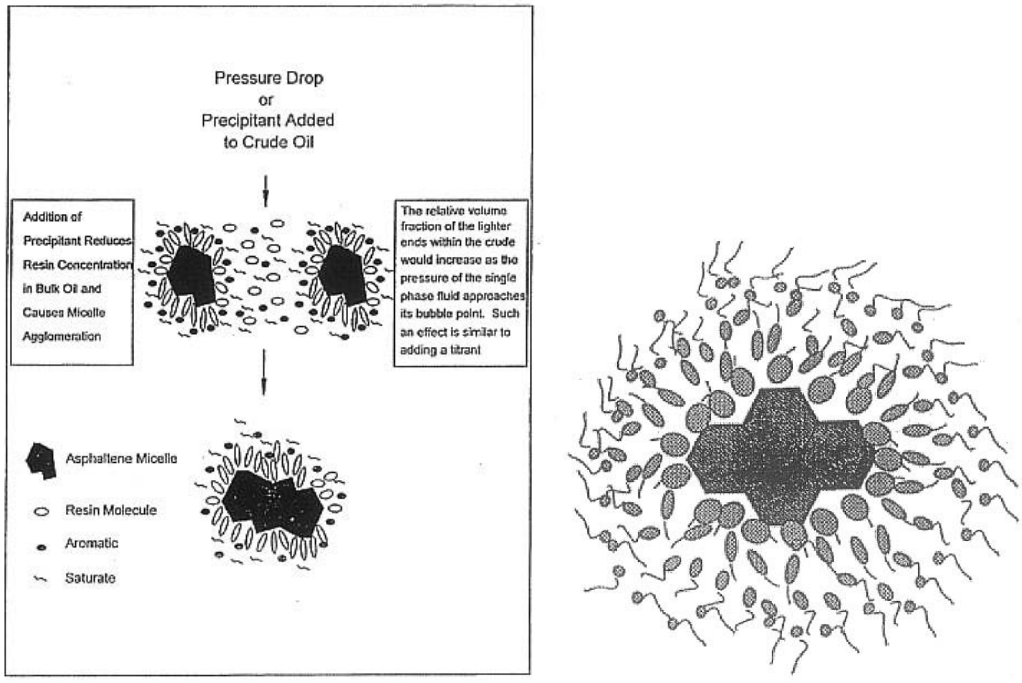

Figure 2-6 (left): Illustrating asphaltene micelle agglomeration due to reduction in resin concentration (Hammami *et al.,* 1998), and (right): Asphaltene micelle suspended by resin molecules (Hammami *et al.,* 1998).

For pressures below the bubble point of an oil, asphaltene solubility increases rapidly with a decrease in pressure. This is due to the light components of the oil being released from solution, changing the fluid composition and thus, making the

asphaltenes more soluble in the remaining liquid. At pressures above the bubble point, the asphaltene solubility increases with an increase in pressure. This is illustrated by **Figure 2-7**, shown below (de Boer *et al*, 1995). This indicates a minimum in asphaltene solubility at the bubble point.

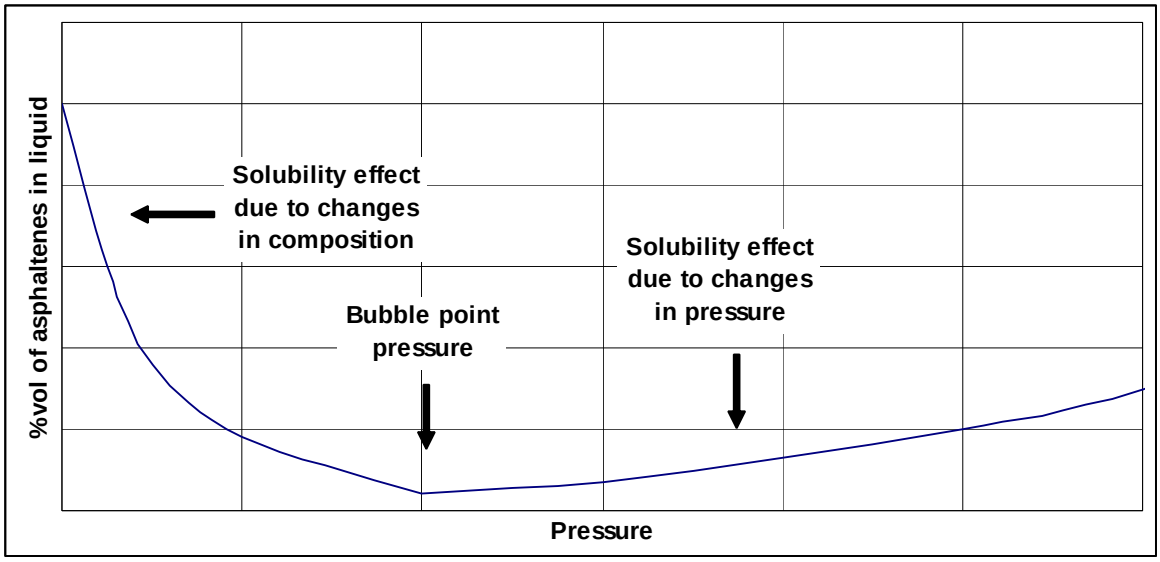

Figure 2-7: Asphaltene percent by volume in solution versus pressure.

2.10.2 Screening Criteria

De Boer *et al.,* 1995 presented the following screening criteria (**Figure 2-8**). This criteria puts together two of the concepts mentioned above and shown in **Figure 2-5** and **Figure 2-7** in that:

- Asphaltene stability is directly related to the density of the crude. Asphaltenes are more stable in high density crudes (low API gravities).
- Asphaltene stability is directly related to the difference between initial reservoir pressure and saturation pressure (the degree of undersaturation). If the difference is large, there is more likelihood that asphaltenes will be destabilized by the change in pressure prior to reaching saturation pressure. If the crude is already saturated, solubility should only increase.

Field data has been superimposed on the chart to illustrate its validity. H.M. represents the conditions of the Hassi Messaud field in Algeria and BO represents the conditions of the Boscan field in Venezuela.

NOTE:
This figure is included on page 46 of the print copy of the thesis held in the University of Adelaide Library.

Figure 2-8: de Boer plot for screening reservoirs with possible asphaltene precipitation problems (de Boer *et al.*,1995).

Using results from SARA analyses, Stankiewicz *et al.,* in 2002 plotted the Saturate/Aromatic fraction of different crudes against the Asphaltene/Resin fraction and made not of the asphaltene stability of the crude. The result was the diagram shown below (**Figure 2-9**). From this it can be concluded that asphaltenes are most stable in oils with a high resin to asphaltene ratio and high aromatics to saturates ratio.

Figure 2-9: SARA stability screening (Stankiewicz, *et al.,* 2002)

2.10.3 Asphaltene Deposition Envelope (ADE)

The knowledge of pressure and temperature effects as well as compositional changes on asphaltene deposition allows us to develop an asphaltene deposition envelope (ADE) for a crude oil. An example of an ADE super imposed on a phase diagram is shown below in **Figure 2-10**.

Figure 2-10: Asphaltene depositional envelope (ADE), superimposed upon a reservoir fluid phase envelope (Jamaluddin *et al.,* 2001).

Another problem induced by asphaltene precipitation is that the asphaltene particles are highly polar and when they precipitate they adhere to the rock particles. This has the effect of changing water wet reservoirs to intermediate wettability or even oil wet reservoirs (Amroun and Tiab, 2001, Danesh *et al*, 1988, Wolcott *et al*, 1989). In doing so, it alters the relative permeability curve.

2.10.4 Reversibility of Asphaltene Precipitation

Hammami *et al.* (2000) plotted pressure against the absorbed laser power. By these means they could detect the onset of asphaltene precipitation. They plotted the depressurisation and repressurisation of the system with noticeable hysteresis between the two events. However, what the study showed was that even though the reservoir fluid could cause severe asphaltene precipitation problems, in this particular case the precipitation could be reversed by a significant degree by altering the operating conditions.

Hirschberg *et al.,* (1984), made the assumptions that asphaltene precipitation is reversible. They did this because, for their thermodynamic relationships to hold true the process must be reversible. They stated that the theory of the irreversibility of asphaltenes is mainly based on titration experiments. In these

experiments the asphaltenes are redissolved in a solvent after already being precipitated by some precipitant. This seems possible only up to a limited amount of precipitant. They also stated that this is not evidence of irreversibility because the addition of solvent is not the reverse of adding precipitant. The re-dissolution of asphaltenes could take much more equilibrium time to complete.

3 RESERVOIR FLUID SAMPLING

Fluid samples were an essential part of this project, without which the analysis could not have been performed. Two field trips to the Cooper Basin were necessary to obtain samples for the project work at two different reservoirs. As part of the project work literature on sampling and different sampling techniques was reviewed extensively (Bon *et al.,* 2007). It cannot be stressed enough the importance of sampling in producing top quality fluid analysis data. It was therefore considered significant to dedicate a chapter to fluid sampling as it was an important part of the project.

3.1 Summary of Samples Taken for This Project

Separator oil and gas were taken at Field A during a well test. Prior to sampling it was estimated that a large 2 litre reservoir fluid mix would be required to perform all the proposed analyses. Large volumes were sampled to ensure enough sample was available to make two 2 litre mixes at reservoir conditions. Separator gas samples were taken into pre-evacuated 20L cylinders and separator oil samples were taken by brine displacement. Gas from Field B was taken at the wellhead. These were sampled directly into pre-evacuated cylinders. A summary of the fluid samples taken for this project shown in **Table 3-1**.

Table 3-1: Summary of samples taken for project

Field	Number of Samples	Sample Type	Sample Volume
Field A	8	Separator Gas	20L
Field A	2	Separator Oil	10L
Field A	2	Separator Gas	500cc
Field A	2	Separator Oil	500cc
Field B	4	Wellhead Gas	20L

Upon arrival to the laboratory, the Field A samples were quality checked and had compositional analyses performed. Once a suitable GOR was decided upon the separator gas and separator oil samples were recombined.

3.2 Review of Literature on Sampling and Different Sampling Techniques

Pressure/volume/temperature (PVT) fluid properties are an integral part of determining the ultimate oil recovery and characterization of a reservoir, and are a vital tool in our attempts to enhance the reservoir's productive capability. However, as the experimental procedures to obtain these are time consuming and expensive, they are often based on analyses of a few reservoir-fluid samples, which are then applied to the entire reservoir. Therefore, it is of utmost importance to ensure that representative samples are taken, as they are fundamental to the reliability and accuracy of a study.

Critical to the successful sampling of a reservoir fluid is the correct employment of sampling procedures and well conditioning prior to and during sampling. There are two general methods of sampling; surface and subsurface sampling. However, within these there exist different methods that can be more applicable to a particular type of reservoir fluid than to another. Further to this, well conditioning can differ depending on the type of reservoir fluid. Sampling methods including single-phase sampling and iso-kinetic sampling, which have been used increasingly in the last decade, will be discussed with some detail as will preserving the representativeness of other components in the sample including asphaltenes, mercury and sulphur compounds.

Reservoir fluid samples are obtained for a number of reasons including:

- PVT analysis for subsequent engineering calculations.
- Determination of the components that exist in a particular reservoir to have an understanding of the economic value of the fluid.
- To obtain knowledge of the content of certain components that exist in the reservoir fluid for further planning and future drilling programs, such as the content of sulphur compounds and carbon dioxide and the corrosiveness of the fluid. This will impact the material used for casing, tubing and surface equipment that may be necessary.
- To obtain knowledge of the fluids ability to flow through production tubing, pipelines etc. and possible problems that may arise because of viscosity changes due to precipitation of solids such as wax and/or of asphaltene.

- To determine the contaminating components that affect plant design such as the mercury content, sulphur components and radioactive components.
- The sample can provide more about the reservoir. For example, if a gas sample is obtained and it is then determined that the dew point pressure of the sample is equal to the reservoir pressure then this is indicative that it is likely there is an oil leg deeper within the reservoir.

Mostly the samples are required to obtain a better knowledge of a combination of these effects; however, it must be kept in mind that often the sample is not required to solve *all* of these issues.

The properties of fluid samples from oil and gas reservoirs, at original conditions and as found at different stages during production, have been of great interest for as long as the oil industry has had reservoir engineers. The quality of these samples is of utmost importance to make the right reservoir management decisions and the constantly improving compositional data is helping the downstream industry with planning facilities. Further improvement of more detailed fluid properties is being expected and the fact that many of the specialists in this field are being renamed flow assurance experts highlights the downstream's need for good quality compositional, fluid property and phase behaviour data.

Bottom-hole sampling goes back more than 60 years (Reudelhuber, 1957, Fevang and Whitson, 1994) when most operating oil companies had their own design of bottom-hole samplers. These were either flow through samplers, purging fluid constantly, or previously evacuated chambers that when activated by clocks or other mechanical devices trapped downhole fluid samples.

There was greater consensus in surface sampling and most everyone agreed on the way to sample from separators and in some cases from the wellhead. From very early on the engineers were aware of occasional carry over of entrained liquid droplets in the gas phase and early attempts of iso-kinetic sampling were initially superseded by improving the separation properties of the separators, increasing their size and/or lowering the flow rates to allow more time for equilibrium (Fevang and Whitson, 1994).

The biggest challenge lies in improving the quality of the ever more popular open-hole wireline samples taken with wireline formation testers (WFT). WFT were first introduced to the industry in 1955 (Ayan *et al.,* 1996). The main purpose of the tool was to measure a formation pressure point and collect a fluid sample. It wasn't until the mid-seventies that much advance was made on the tools technology. The samples taken with these tools were completely discredited by the fluid experts until the early nineties when tool technology improved greatly addressing issues particularly relating to fluid typing and sampling. As a result these samplers are of irreplaceable importance today.

All these issues have been addressed again since then, and changes and improvements are being made wherever possible and will continue to be ongoing. Representative samples taken with typical single-phase bottomhole samplers are often taken for reservoir-fluid composition, PVT analysis, and, depending on the reservoir, asphaltene studies. However, these tools are often not suitable for measuring the content of sulphur or mercury compounds. A good knowledge of the wax content and problems that may arise due to wax can be obtained from studies performed on stock tank oil. Sulphur compounds and mercury are mostly present in the gas stream, so analysis can be performed on separator or wellhead gas streams. While ideally all the parameters could be obtained from the same sample, in practice, different samples can suit different needs. First and foremost, the need for the sample should be established so the correct samples can be taken. This can avoid extra costs of sampling for parameters that will not be measured, or the cost of having to go back and sample again. But key to a successful sampling program is to first answer the question: "*What are you sampling for?*".

This chapter aims at discussing different sampling methods and what they are most suited for. The focus is on obtaining representative samples of live reservoir fluid for the aim of characterizing the reservoir production, however also touches on some of the downstream issues.

3.3 Understanding our Reservoir Processes

Immediately after a well is drilled, the well will first go online with a cleanup-flow period of reasonably hard flow to push drilling fluids out of the near-wellbore region and the wellbore (Reudelhuber, 1957; McCain and Alexander, 1992; El-Banbi and McCain, 2001; Cobenas and Crotti, 1999; Strong *et al.,* 1993; Towler, 1989). Depending on how undersaturated the reservoir fluid is (sometimes not at all), the pressure drop induced to create the flow may result in a drawdown of pressure below the saturation pressure. This causes either dissolved gas (for oil wells) or dissolved condensate (for gas wells) to come out of solution. The subsequent effects are discussed further for each reservoir type.

3.3.1 Undersaturated Oil Reservoirs

In principle, sampling undersaturated oil reservoirs should be the simplest. Ideally, if the reservoir is greatly undersaturated, the drawdown because of flowing the well never pulls the flowing bottomhole pressure below the saturation pressure, and thus the wellbore will have virgin reservoir fluid flowing through it.

If because of cleanup flow or any other reason the reservoir is drawn down below the bubblepoint pressure, then the two-phase fluid needs to be driven out with virgin reservoir fluid. This can be done by flowing at a lower rate, hence minimizing the drawdown so flowing bottomhole pressure is still above the saturation pressure. Initially, because of capillary pressure effects, released solution gas will remain immobile in the pore spaces until a critical gas saturation is achieved, and after that an excess of gas may flow.

At the surface, monitoring the GOR can indicate when the sampling operation should start. Initially, the GOR will be too low. A rate should be sought such that a stable GOR is attained after prolonged flow.

For bottomhole samples, the fluid entering the wellbore needs to be single phase. If considerable water is flowing together with the oil, the flow may not be great enough to push the water from the wellbore. To avoid sampling water, a static gradient should be run before sampling.

For surface samples, so long as the fluid (assuming two-phase flow of gas and liquid flowing into and up the wellbore) is in the same ratio as the original reservoir fluid, the separator samples will be good.

3.3.2 Saturated Oil Reservoirs

Sampling saturated reservoirs is not simple because flowing the reservoir results in a drawdown, which will pull the flowing bottomhole pressure below the bubblepoint pressure (Reudelhuber, 1957; Strong *et al.,* 1993; Towler, 1989; Dake, 1994). Therefore any flow will result in the release of solution gas from the reservoir fluid. Because of this, separator samples should be taken. Bottomhole samples are not recommended, as they may collect a disproportionate amount of liquid or gas (Towler, 1989).

Shutting in the reservoir to build up pressure again will redissolve gas into the oil (Towler, 1989). Obtaining a stable GOR is more difficult for saturated oil reservoirs. However, by flowing at a lower rate, a stabilized flow can eventually be reached and a constant GOR can be observed. The fluid (although flowing in two-phases) carries the liquid and the gas at the same GOR as in the virgin reservoir fluid.

If the only option is bottomhole sampling, the sample should be taken at a trickle flow so that the drawdown is as small as possible, therefore minimizing disturbance to the solution gas in the pores and maximizing solution gas dissolved within the liquid. If a gas cap exists, the pressure at the gas/oil contact (GOC) should be used as the saturation pressure for the reservoir fluid.

3.3.3 Gas-Condensate Reservoirs

Similarly to an undersaturated oil reservoir, if a gas/condensate reservoir is undersaturated, provided the well is not drawn down below the dewpoint pressure, condensate will stay in solution.

If the reservoir fluid is saturated or reservoir pressure is near the dewpoint pressure, a flow period resulting in a drawdown will inevitably result in condensate coming out of the solution. Similar to the gas in saturated oil, the condensate that

initially comes out of solution will fill pore space until a critical saturation is reached. This fluid needs to be flushed out with virgin reservoir fluid. After this, condensate will flow with the gas through the wellbore. For surface sampling, another problem arises: The flow rate must be large enough to carry the condensate to the surface, but if the flow is too high, stable flow will not be achieved, and perhaps there will even be poor separation at the separator because the fluid has little time to reach equilibrium.

The condensate dropout in the near-wellbore region can also reduce permeability as condensate drops out and fills pore spaces. This can sometimes severely affect the flow and can be a big issue particularly in low-permeability reservoirs.

Reducing the flow rate results in an increase in the flowing bottomhole pressure and the pressure in the drainage radius. This causes some of the condensate in the pore spaces to revaporise, decreasing the GOR below that of the virgin reservoir fluid. After a rate reduction, one must wait a period of days or even months for low-permeability reservoirs before sampling (McCain and Alexander 1992).

3.4 Well Conditioning

PVT samples need to represent the fluid to be produced from the reservoir. The sooner the well is sampled after drilling, the greater the chances of representative sampling, because it is more likely that pressure drops that can create two phases in the reservoir have not occurred (Dake, 1994, Amyx *et al.,* 1960). If the reservoir fluid in the near-wellbore region has been drawn into two phases, well conditioning is applied to correct this effect and bring single-phase fluid back into the wellbore and its vicinity.

Because WFT are generally run immediately after drilling when no flow or drawdown has yet occurred, usually no rigorous conditioning is necessary besides eliminating as much drilling fluid as possible. This is especially important when oil-based mud (OBM) has been used during drilling. The drilling fluid is removed with a pump-out option of the WFT (Michaels *et al.,* 1995), where the reservoir fluid is passed over a variety of sensors and then into the annulus until indications of

maximum purity are obtained. After this, the flow of fluid is directed to the sample chamber.

Exposing the reservoir fluid to lower-than-original reservoir pressures can cause the fluid to go into two or three phases, depending on its saturation pressure and phase behaviour.

The pressure will have to be increased to above the saturation pressure with a stepwise approach of brief flowing periods and shut-in periods with successively lower rates to return the fluid flowing through the well back to its original state. This is continued until the lowest rate at which there exists a stable GOR is established. When this happens, it implies that single-phase fluid is flowing into the wellbore. This is generally followed by a longer shut-in period in order to build up the bottomhole pressure at the wellbore. This stable GOR can be confirmed by trial-and-error bottomhole sampling, which is expensive; can be assumed because of stable wellhead pressure after several reduced-rate flow periods; or, preferably, can be determined by measuring the GOR while producing through a test separator. In the last case, separator samples should always be taken also, to confirm the quality of the bottomhole samples and to provide backup samples in the case of near-saturated pressures that cannot be reconditioned easily.

If taking surface samples, the criterion of having single-phase representative reservoir fluid in the shut-in wellbore is superseded by the influx of two-phase fluid, where the gas and oil flow at the GOR of the virgin reservoir fluid.

For gas/condensate reservoirs, surface sampling through a stable separator is recommended. The well is usually produced at successively higher rates (McCain and Alexander, 1992). Retrograde liquid dropout will occur once the reservoir is drawn down into two phases. This liquid will accumulate in the near-wellbore region; but eventually, with continued flow of fluid through those pore spaces, this same fluid will be mobilized, and its production will result in a constant Condensate-Gas Ratio (CGR). The best samples will be taken at the lowest rate that produces a stable CGR, but it is recommended to take duplicate sets at other rates as well.

The conditioning principle extends into conditioning or cleaning/purging of the wellbore, separators, sampling lines, equipment, and cylinders of all foreign material.

3.5 Reservoir Fluid Sampling Methods

Reservoir fluid sampling techniques can be generalized into two groups sub-surface and surface.

The following flow chart (**Figure 3-1**) splits up sampling methods based on saturation of the fluid.

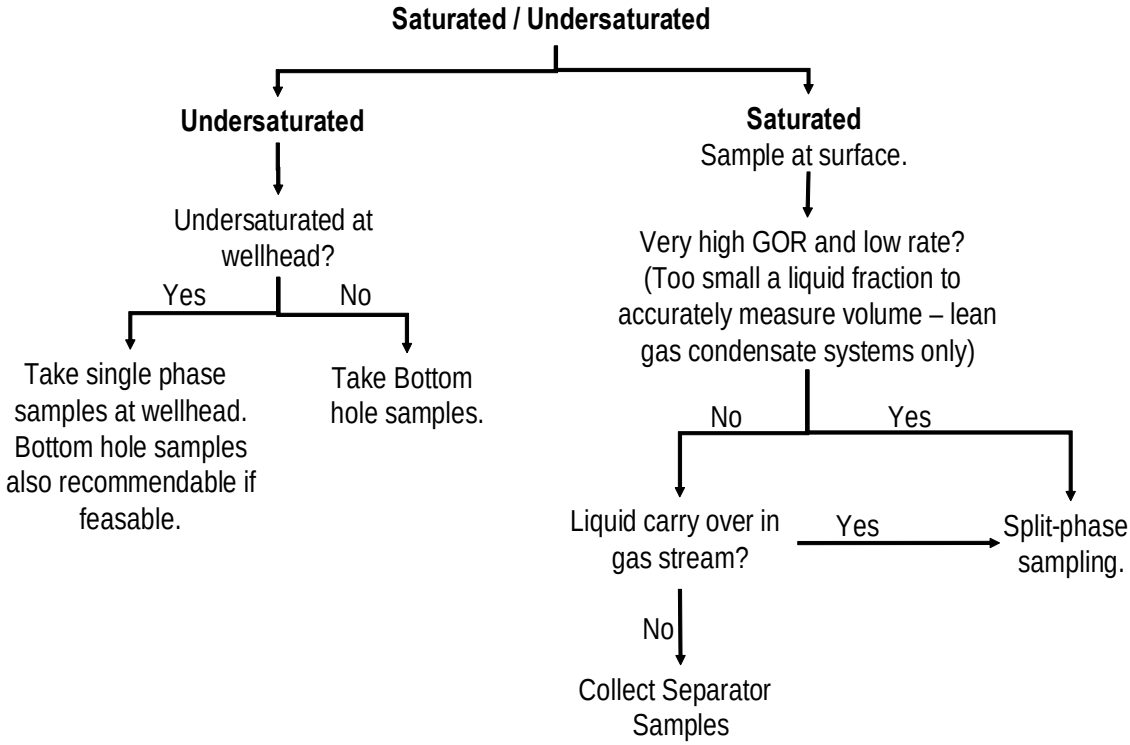

Figure 3-1: Flow chart of sampling process based on fluid saturation.

3.5.1 Surface Sampling Techniques

1. Separator samples, from test or production separators. Often recommended for gas-condensates, saturated black oils and volatile oils. The equilibrium separator liquid and gas are recombined in their produced ratio to obtain representative reservoir-fluid samples.
2. Wellhead samples, for undersaturated fluids still in single phase at well head conditions.

3. Split-phase sampling or iso-kinetic sampling – scaled down reconditioned homogeneous two phase flow through a mini-separator. Split-phase sampling is performed either on wellhead gas or the produced gas stream from a separator (see **Figure 3-2**).
4. From pipelines or plant flow lines.

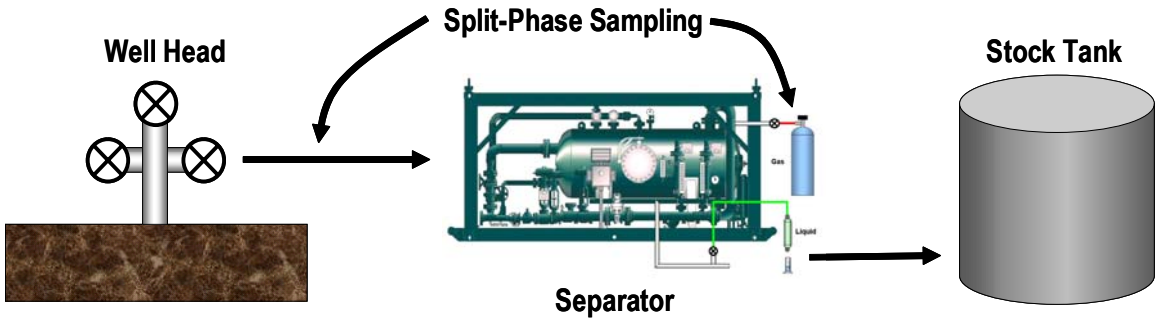

Figure 3-2: Surface sampling methods

Whichever way we choose to take reservoir fluid samples, it is essential to ensure that the actual fluid obtained is as close as possible to the virgin fluid discovered in the reservoir to ensure it is as representative as possible. To do that, all wells usually have to be conditioned to bring such fluid into the well bore or separator. Since this process is more complicated than it sounds it is recommended to take samples in more than one way, to therefore obtain differently conditioned fluids from the same reservoir to better define its properties.

The advantage of awareness of all new developments, should also allow us to evaluate simpler situations with simpler sampling solutions while at the same time provide solutions for more complex problems when required.

Separator Sampling

A recommended guideline to good separator sampling is to flow the well through the separator at a stable pressure, temperature, and GOR for two to three separator volumes to ensure that the fluid that collected in the separator at any other points in the equilibrium state is flushed out. At any pressure and temperature (within the two-phase conditions), the gas and liquid coexist in equilibrium. The individual components of the reservoir fluid coexist, to some degree, in both phases. The ratio of the fraction of a component in the gas phase

to its fraction in the liquid phase is termed the K-value. If either pressure or temperature is changed drastically, the K-value will change, and hence some of the component that exists in the gas phase may condense, or conversely, some of the component that exists in the liquid phase may vaporize. When the samples are taken, the pressure and temperature of the separator are recorded along with—as accurately as possible—the gas- and liquid-flow rates. Furthermore, the GOR should be based on oil-flow rate at separator conditions, and the correction factors used should be noted (Williams, 1994). No matter how good the sampling and well conditioning are, if the rates measured and subsequent GOR are incorrect, the recombined sample will be unrepresentative.

Separator samples can be taken by the following methods.
For gases:

- Sampled directly into an evacuated cylinder (preferred method)
- If evacuated cylinders are not available, the air in the cylinder can be removed by dilution. Filling the bottle and emptying prior to sampling.

For liquids:

- Brine displacement (preferred method). Cylinder is first filled with brine. The brine is then displaced with separator liquid ensuring fluid remains at separator pressure throughout the sampling.
- Evacuated cylinder. The fluid is sampled directly into an evacuated cylinder as for a gas sample. Although the sample will separate into two phases within the cylinder, since the fluid is single phase up to cylinder valve the sample will be representative. However, if the sample is taken too quickly it will separate into two phases in the flow lines prior to entering the cylinder and a poor sample will be taken. For this reason brine displacement is preferred.
- Separator-gas displacement. Sample cylinder is first filled with separator gas, this is then displaced as the fluid enters the bottle (from the bottom)

Wellhead Sampling

Sampling at the wellhead is only done if it is known that the wellhead pressure and temperature is above the reservoir fluids saturation pressure. Dry gases can be

sampled at the wellhead as well as some lean gases and low GOR oils. However if the sample is flowing in two-phases at the wellhead then an unrepresentative sample will be taken as the two individual phases will not flow into the cylinder in the same ratio as they exist in the reservoir.

Split-Phase Sampling

Iso-kinetic or split-phase sampling can be used to sample wellhead gas streams (particularly rich gases), two-phase well-head fluid or to measure the volume of entrained liquid in a gas stream, such as at the gas outlet of a separator (Williams, 1994, Dybdahl, 2006, Amyx *et al.,* 1960, Riley *et al.,* 1979). Once a stable GOR is established, the two-phase fluid mixed using a mixing head. The mixing head is designed to homogeneously spread the liquid droplets carried through with the vapour. A probe then collects the gas and liquid sample at the corresponding GOR. An online laboratory ensures that GOR is stable prior to sampling and a mini-separator separates the fluid into the correct ratio.

Split-phase sampling is applicable particularly for gas-condensate reservoirs that produce at low rates with low CGR. It is also applicable for separator gas streams with a large volume of entrained liquid to correct the CGR and improve the separator test data; in this case it is not replacing the separator test but improving the data. However, this method of sampling is not always economic and also not always better than simultaneously obtained separator samples.

Split-phase sampling technology is over 60 years old (Fevang, 1994), however in recent years has been used increasingly. The technology has improved, particularly in the measurement of GOR as it is distributed through the cross section of the pipe (not actually homogenous). Previously it was assumed that the mixing head perfectly distributed the liquid droplets across the pipe cross section. This assumption was found to be not exactly correct, so to improve the GOR measurement and minimize the error due to this effect, the probe now samples at three different points across the pipe and averages the result (Dybdahl, 2006).

A simple alternative to needing to measure the volume of liquid carry over is to flow at a lower rate, if possible, so that the fluid has more time to reach equilibrium in the separator (Fevang, 1994).

Another simple alternative is to take the separator gas samples as normally done. These, will bring the entrained liquid along with them. Once in the lab, the gas samples are returned to separator conditions by heating to separator temperature. The cylinder is placed vertically upside down allowing the entrained liquid to dropout and flow to the bottom of the cylinder. This liquid can then be removed, analysed and the volume measured and then both mathematically and physically added to the total well stream composition.

3.5.2 Sub-surface Sampling Techniques

1. Slickline run tools usually in cased holes using conventional flow through or pistonned samplers. This method is recommended for normal undersaturated oil reservoirs and undersaturated gas reservoirs where there is difficulty in obtaining a good quality surface sample.
2. Single-phase samplers: tools with pressure compensation for sampling and maintaining the fluid single phase. This is recommended for undersaturated oil and gas reservoir fluids with possible solids (wax / asphaltenes) precipitation problems.
3. Exothermic samplers: These samplers not only keep the sample pressure compensated but also temperature compensated to further reduce any chance of solids precipitation prior to sample transfer and analysis.
4. Wireline Formation Testers run with electrical line, tied into the logging string, usually taken in open holes prior to casing being set. There are a range of proprietary samplers with only subtle differences in tools from different companies. These types of tools are referred to as Wireline Formation Testers (WFT).
5. Pressure compensated WFT for single-phase sampling open hole.
6. Samples taken during open-hole drill stem testing (DST).
7. Samplers taken with a sub carried in the drillstring accommodating the samplers described in the above described points 1, 2 and 3.

3.5.3 Sampling Heavy Oils

Difficulties arise when sampling heavy oils because of the high viscosity of the fluid. For bottomhole sampling, generally speaking, samples are best taken with a WFT (Achourov *et al.,* 2006; Nagarajan *et al.,* 2006; Morton *et al.,* 2005). Having said that, successful samples have been taken with DST-type bottomhole samplers, but these are applicable only if the reservoir is undersaturated. If the reservoir is saturated, the WFT are recommended. The key issues with bottomhole sampling of heavy oils are as follows (Achourov *et al.,* 2006; Nagarajan *et al.,* 2006; Morton *et al.,* 2005).

- ***Pressure Drawdown***. The pressure drawdown should be minimized so that the fluid remains single phase, sand production is controlled, and foaming can be minimized. The drawback is that a low drawdown may not mobilize the high-viscosity fluid.
- ***Mud Contamination***. The mud filtrate in the near-wellbore region needs to be cleaned up with the pump-out option of the WFT. However, with an extended period of pumping, the risk of the pump getting stuck is increased. With OBM, contamination poses a particular issue because excessive miscible contamination will result in unrepresentative samples.
- ***Dual Packer***. The conventional small probe and rubber packer are not applicable for heavy oils. It is recommended that a dual-packer module be used to hydraulically isolate the formation. With the dual-packer module, the flow area is increased, lowering the drawdown. The risks are in a poor-packer seal or leak, if seating and/or inflation fail.

Surface sampling may also be an option with heavy-oil reservoirs. An easy way of acceptable accuracy is to recombine crude from the wellhead and gas from the annulus or the wellhead, provided an accurate GOR can be attained. Extrapolating into a PVT study on a recombined reservoir fluid with a GOR that is too high is acceptable if the real GOR is known only after the study is performed. Separator tests are usually performed on fluid with added diluents to decrease the viscosity and, provided good volumetrics are kept track of, an accurate GOR can be back-calculated for the wellhead samples. In important cases, it might be necessary to convince the operator to cut the diluents for as short a time as possible to obtain good-quality separator samples of uncontaminated composition. GOR

measurements might be weak because most of the solution gas will stay in the separator liquid and will not be measured with the liberated separator gas.

3.6 Other Components of Interest

3.6.1 Asphaltenes

If sampling a reservoir and the engineer is very confident that asphaltenes will not be a problem and no study is intended to be done for solids, then single phase or exothermic sampling tools are surplus.

However, in fields where asphaltene problems may arise and the samples are intended for asphaltene analysis, the samples should be taken single-phase so to preserve the asphaltenes in solution for subsequent analysis. Although the sampling and analysis of asphaltenes are costly, a prior knowledge of the problems the field may have can be of great economic benefit in the long run. However, if analysis has already been done and/or no asphaltene analysis is intended for the samples, single-phase sampling may not be required.

Asphaltene problems should also be kept in mind in particularly if gas injection at some stage in the reservoirs life is intended. It may be too late to take representative samples later.

Analysis for asphaltenes performed on live single-phase fluid is performed in laboratories with specialized equipment. However, some analysis can be performed onsite, if required, on stock tank fluids on site such as weight percent of asphaltenes in stock tank oil by n-heptane precipitation or SARA analysis.

The reversibility of asphaltene precipitation is questionable. For this reason single-phase and exothermic samplers were designed, so that the sample does not cross the OAP prior to analysis.

3.6.2 Wax

Wax can be treated and controlled by maintaining high temperature and pressure. If any indication of wax issues are encountered during WFT sampling the transfer of samples to cylinders for further analysis becomes more difficult. The solidified

wax is a third phase and needs to be re-dissolved into the fluid prior to transferring the sample into sample cylinders. This is performed with a prolonged period of heating at reservoir temperature and stirring (even as long as 12 hours for severe cases). If a mixing mechanism exists in the sample chamber, this time can be shortened otherwise stirring has to be done by gravity, lifting one end of the chamber for a half hour, and then the other end. Patience is required.

3.6.3 Sulphur Compounds

Sampling for analysis of the sulphur content present in the reservoir fluid is not easy and still developing. The key issue is that sulphur compounds such as H_2S, mercaptans (RSH) and carbonyl sulphide (COS) are adsorbed by the walls of cylinders or sample chambers, particularly those made of stainless-steel (Elshahawi and Hashem, 2005). Alternate materials are recommended to preserve the content of the sulphur compounds, this is particularly important if analysis is to be done in a laboratory as the time required for the sample to reach the laboratory (be it only a week) is enough for the analysis to measure greatly reduced H_2S contents.

This problem is, for now, best solved using current technology in metallurgy by using cylinders made from other materials and metal alloys. In addition to this, coatings have been made to reduce the reaction of conventional stainless-steel cylinders with H_2S. These coatings tend to be either polytetrafluoroethylene (PTFE)-based or the latest generation of cylinders, which are silicon-based (Elshahawi and Hashem, 2005, Dybdahl, 2006).

When taking WFT samples, adsorption often occurs in the flow lines into the sample chambers and, most of all at the pumping unit.

The error margin due to adsorbed sulphur is less if there is higher sulphur content in the sample. This is because, even though a larger volume is adsorbed, it is a smaller fraction.

Some analysis can also be performed on-site. Again, an issue still remains as to whether the sulphur compounds are adhering to the walls of the tubing, casing and

surface equipment prior to being sampled for analysis. Typical analysis for sulphur compounds are as follows (Elshahawi and Hashem, 2005):

- Potentiometric titration
- Iodometric titration (highly accurate but time consuming)
- Tutwiler method (higher concentrations)
- Gas Chromatography
- Gas detection tubes

Further to this, downhole sensors now exist to at least give an indication of whether surface measured sulphur compound concentrations are wrong or approximate. The future of measurement of concentrations of sulphur compounds is likely to be in improvement of this technology.

3.6.4 Mercury Content

The mercury content in the well-stream is also important to measure to determine whether extra requirements are necessary in the refining process. Mercury can cause metallic parts to fail by amalgamating and changing the mechanical properties of the metal, particularly aluminium or copper.

Similarly to sulphur compounds, the measurable mercury content decreases with time because it is adsorbed onto the walls of stainless-steel cylinders and sample chambers. On-site analysis can be performed on the separator gas stream. In general, the mercury compounds that may naturally occur in a reservoir fluid are elemental mercury (Hg^0) in hydrocarbon-gas streams and both elemental mercury and organic mercury [$Hg(C_xH_y)_2$] in hydrocarbon-liquid streams (Wilhelm and McArthur, 1995).

The mercury compounds are removed by passing the gas through a permanganate solution. The solution is analysed in a lab by atomic absorption spectroscopy (AAS). This can also be performed on stock tank liquid/condensates. The samples should be kept in glass vials with minimal head space for transportation to the lab.

The mercury content in gas can also be measured using a gold-film mercury-vapour analyser (Bingham, 1990). These mercury detectors have a small built-in pump that takes in a volume of gas through the sample probe, which consists of a film of gold onto which the mercury adsorbs. The mercury detectors operate at atmospheric pressure. One method of using these machines is to pass the gas through a plastic bottle with an outlet to maintain pressure at atmospheric pressure and another outlet for the gas that is to be passed through the machine.

3.6.5 Oil Based Mud

For WFT sampling, the use of Oil Based Mud's (OBM) can contaminate samples. If this is the case for oil wells, depending on the severity of the contamination, the composition can be back calculated if the OBM composition is known. This is done by determining the composition of the contaminated oil sample, then a sample with a known added volume of OBM, and the full OBM composition. Based on this the OBM components can be mathematically removed from the contaminated oil composition (Dybdahl, 2006).

With gas-condensates a much smaller contamination will have more sever effects. Not only in terms of the composition but measured dew points can be far too high. However, the same principle as for oils can be applied to gases.

3.7 Chapter Summary

- Sample as early as possible in the life of the reservoir. Generally speaking, the earlier you sample the higher the likelihood of obtaining representative samples.
- Well conditioning is of utmost importance. Ensure the well is conditioned as best possible prior to sampling. The preparation of a good conditioning program will improve sample quality.
- Keep your WFT samples under pressure and transfer them into a cylinder. It is common for these samples to be released to stock tank conditions and only some basic analyses performed. However, advanced technology in this area has greatly improved the quality of these samples which should be considered representative until proven not so, rather than the opposite. The chance to collect bottom hole or separator samples later may not come.

However, bear in mind that WFT samples still require a drawdown and suffer problems from drilling fluid issues and may not be representative. But don't dump them until some analysis has been done.

- When in doubt take both surface and bottom-hole samples.
- If no asphaltene or solids present you may be able to use a cheaper alternative to single-phase sampling
- If asphaltenes may be a problem, take single phase samples.
- More research needs to be done on temperature dependence of asphaltenes and this be translated into better design of exothermic samplers. Since single-phase sampling has advanced, comparative studies should be performed on conventional samples versus single-phase samples for different reservoir and asphaltene types.
- For difficult situations, a good hindsight quality check is to compare the laboratory or on-site live reservoir fluid density with the one calculated from the pressure gradients during well logging. The new developments in the field are excellent advances and should be used to improve sampling. However, the problem should not be over complicated and complex solutions should be used only when necessary.

4 METHODOLOGY AND PROCEDURES OF RESERVOIR FLUID ANALYSES PERFORMED

A brief description of the laboratory tests performed in analysing Field A reservoir fluid follows. In many of the tests (those with live reservoir fluid), the key reservoir conditions of temperature and pressure were adhered to. The analyses performed were classified into the following categories:

- Determination of Asphaltene Content
- Quality Checks and Compositional Analyses
- PVT Analysis
    - Pressure-Volume relations through Constant Mass Study (CMS)
    - Constant Volume Depletion Study (CVD)
    - Viscosity-Pressure relations
    - Separator Test
    - Solubility Swelling

4.1 Determination of Asphaltene Content

One of the first things that should be considered when evaluating a CO_2 flood is the possibility of asphaltene precipitation. The injection of CO_2 can destabilize asphaltenes and cause them to come out of solution. If this happens it can cause serious problems with costly repercussions. Asphaltenes can clog production pipe lines, the tubing string, or in worse case scenarios, it can clog the pores of the reservoir near the well bore creating a high skin factor. As a result, we decided to do some asphaltene analysis on Oil A in order to get a better idea of whether asphaltenes may be a problem or not. The asphaltene content of Oil A was measured by asphaltene precipitation with n-heptane and SARA analysis. Further to this, during Slim Tube and core flood tests performed with live reservoir fluid at reservoir conditions, the pressure differential over the packed medium was measured – a sudden increase in pressure differential would be due to a flow restriction of some type, possibly asphaltene precipitation.

4.1.1 IP 143 - Asphaltene Precipitation with n-heptane

Asphaltene precipitation with n-heptane otherwise known as IP 143 (also known as ASTM D2007-80) is performed at atmospheric conditions to measure the percentage by weight of asphaltenes in a crude oil sample. It follows the definition of asphaltenes as the insoluble fraction in n-heptane.

1. Mix the reservoir oil and solvent and agitate for 1 hour. The mixture should be no less than 10mL per 1 gram of oil.
2. Filter the mixture through a pre-weighed 0.45μm filter. If remnants from the previous step still remain, rinse the container with solvent and pass through the filter.
3. Oven dry the filter with solids at a temperature below 200°F and then weigh the filter paper.
4. Re-dissolve solids from the filter in toluene, and filter again through a new 0.45μm filter.
5. Again, oven dry the filter with solids at a temperature below 200°F and then weigh the filter paper.

If nC_5 is used, step 3 gives the nC_7 insoluble. Steps 3-5 give the nC_5 asphaltenes and inorganics, carbenes and carboids.

4.1.2 SARA Analysis Method

The SARA (Saturates, Aromatics, Resins, Asphaltenes) analysis test is carried out to determine the content (percentage by weight) of saturates, aromatics, resins and asphaltenes in the oil sample. Results of the analysis in terms of saturate to aromatic and asphaltene to resin ratios could act as an indicator of the asphaltene problem. The former measures the solvency of asphaltenes while the latter is an indication of its colloidal state in the oil. Higher content of aromatics strengthens the asphaltene solvency (i.e., it becomes more stable in the reservoir oil). Resins stabilize asphaltene in oil and hence, a low asphaltene-to-resin ratio ensures a better colloidal stabilization. Between the two, the asphaltene to resin ratio has a greater impact on the stability.

The analysis is carried out in atmospheric conditions using the following ASTM D 2007-86 procedures:

- The volatile material is removed by distilling the dead oil.
- The asphaltene is first precipitated by adding n-heptane to the residue.
- The sample is then filtered and asphaltene is removed and weighed.
- The filtrate (maltenes) that contains saturates, aromatic compounds and resins that are separated through open column liquid chromatography using n-pentane as the carrier fluid.
- Two columns are used, the first with attapulgus clay and the second containing silica gel.
- The aromatics are adsorbed by the silica gel, resins are adsorbed by the attapulgus clay and saturates pass through both columns with the n-pentane.
- Aromatics are then removed from the silica gel using toluene. Resins are removed from the attapulgus clay with a toluene/acetone (50/50) mix.
- Solvents are then removed by evaporation

4.2 Quality Checks and Compositional Analyses

Quality checks are performed on all samples prior to analysis to ensure that representative samples have been taken. Once this is done, the composition of the samples is determined. The methods used to perform these are described below.

4.2.1 Quality Checks of Separator Liquids by measurement of Saturation Pressure

Once the separator liquid samples are returned to the laboratory, their quality is checked by measurement of the sample's saturation pressure. This is done through the injection of known volumes of mercury into the sample cylinder (thus compressing the sample) and recording the pressure at each volume increment. When the sample is in two phases the gas compressibility cushions the decrease in volume of the sample and the pressure increment will be small. Once the sample is in single phase the compressibility of the fluid is much smaller and the pressure increases far more with a decrease in sample volume. Thus, by plotting the volume of mercury injected against the pressure, the bubble point pressure of

the separator liquid sample can be determined. This can be seen in **Figure 4-1** shown below.

If done at the separator temperature, the bubble point pressure should be very close to the separator pressure at the time of sampling and the duplicate samples should have similar bubble point pressure to one another. If this is the case then the samples can be confidently assumed to be representative.

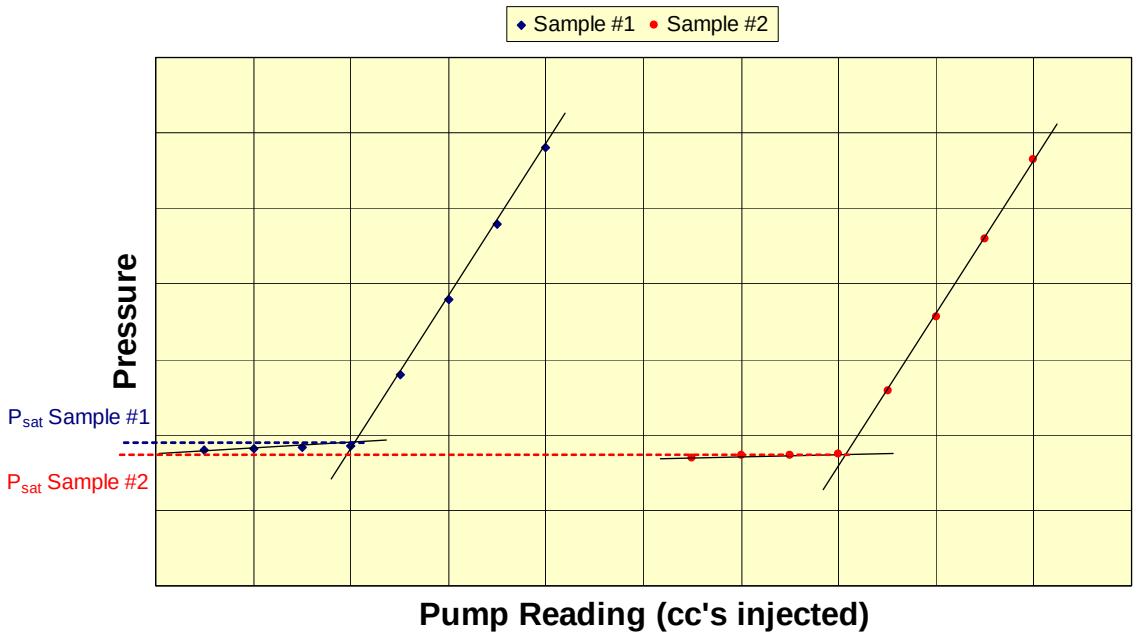

Figure 4-1: Determination of bubble point pressure from pressure – volume relationship.

4.2.2 Compositional Analysis of Separator Gas

The composition of the separator gas is measured by passing the gas through a gas chromatograph (GC). Two different columns and detectors are used in order to do this. The Thermal Conductivity Detector (TCD) is used to determine the mole percent of the lighter components - methane through to n-butane, and the carbon dioxide and nitrogen. A Flame Ionization Detector (FID) is used to determine the mole percent of n-butane through to dodecanes (carbon dioxide and nitrogen are not sensed by the FID, hence the need for two detectors). N-butane is overlapped in order to synchronize the detector readings of the two detectors. The resultants are the chromatograms shown in **Figure 4-2** and **Figure 4-3**. The peak areas are calculated through integration of the chromatogram and the weight percent can

then be calculated as the fraction of a components area over the total area. The mole percent can then be calculated from this using the individual molecular weight of each substance.

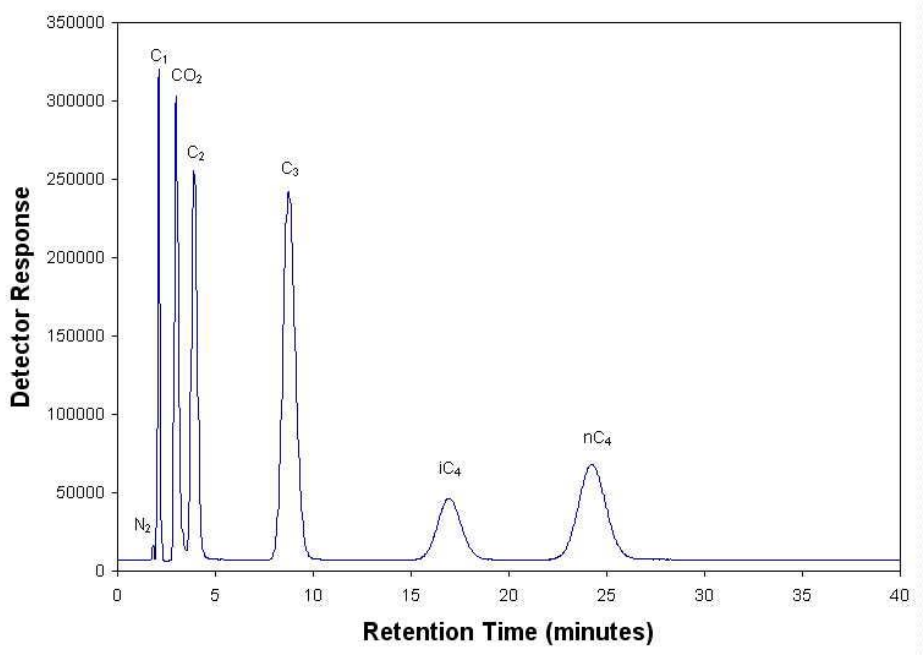

Figure 4-2: Typical TCD chromatogram of gas sample

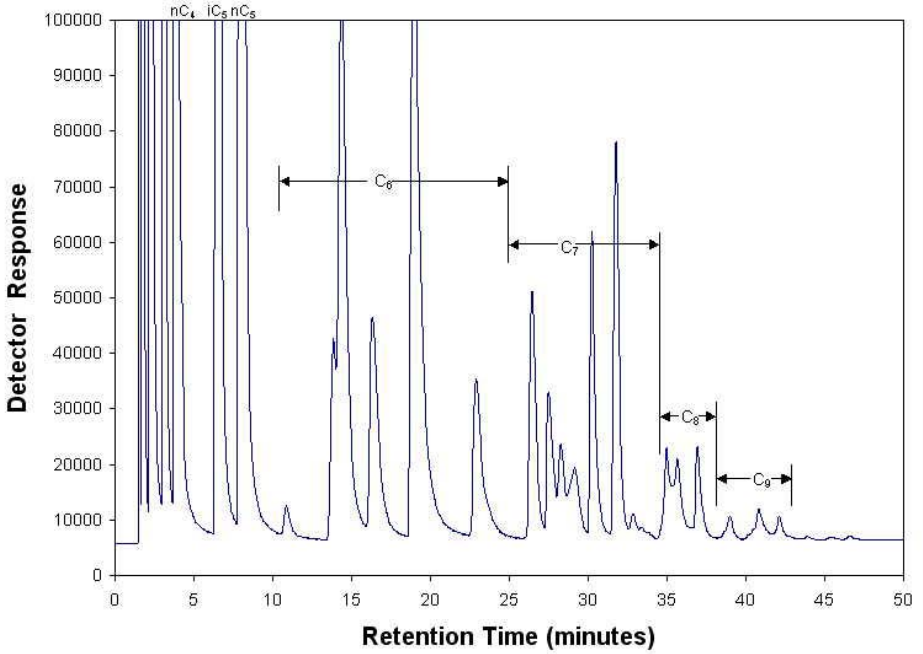

Figure 4-3: Typical FID chromatogram of gas sample.

Gas Sheet Calculations

In order to calculate the gas composition and factors based upon this the following is performed:

- The GC detector delivers an output.
- The peak from the chromatogram is integrated for each component giving a peak area
- The sum of the areas for all the peaks give the total area.
- From calibration runs, the area is corrected. The GC is calibrated monthly and using a standardized gas which has a known composition. Based on this the calibration factors are developed and updated monthly.
- The fraction of the peak area over the total area gives a weight percent.
- The wt% is converted to mol% using the molecular weight through the following equation:

Eq. 4-1

$$M = wt\% / MW$$

- This fraction is then renormalized and reported as a mol %.

Further to this the properties of the gas stream that follow are also reported. With each property the equation used to determine that property is shown.

Gas Stream Molecular Weight (MW):

Eq. 4-2

$$MW = \sum_{i}^{1-12+} MW_i \times M_i$$

Eq. 4-3

$$MW_{C6+} = \frac{\sum_{i}^{6-12+} MW_i \times M_i}{\sum_{i}^{6-12+} M_i}$$

For MW_{C7+}, MW_{C10+}, MW_{C11+} and MW_{C12+}, as for MW_{C6+}, replacing i = 6…12+ with i = 7…12+, i = 10…12+, i = 11…12+ and i = 12+ respectively.

Gas Gravity (γ_G):

Eq. 4-4

$$\gamma_G = \frac{MW}{MW_{air}} * Z_{SC} \quad ; MW_{air} = 28.9644\ g.mol$$

Pseudo-Critical Pressure and Temperature (P_{pc}, T_{pc}):

Eq. 4-5

$$P_{pc} = \sum_{i}^{1-12+} M_i * P_{ci}$$

Eq. 4-6

$$T_{pc} = \sum_{i}^{1-12+} M_i * T_{ci}$$

Pseudo-Reduced Pressure and Temperature (P_{pr}, T_{pr}):

Eq. 4-7

$$P_{pr} = P \big/ P_{pc}$$

Eq. 4-8

$$T_{pr} = T \big/ T_{pc}$$

Gross Heating Value (GHV):

Eq. 4-9

$$GHV = \frac{\sum_{i}^{1-12+} M_i \times GHV_i}{Z_{SC}}$$

Nett Heating Value (NHV):

Eq. 4-10

$$NHV = \frac{\sum_{i}^{1-12+} mol\%_i \times NHV_i}{Z_{SC}}$$

Wobbe Index:

Eq. 4-11

$$Wobbe\ Index = GHV \Big/ \sqrt{\gamma_G}$$

Compressibility Factor at Pressure and Temperature (Z):

For calculation of the compressibility factor at a nominated pressure and temperature the Dranchuk and Abou Kassem (1975) correlation was used. This correlation is based on the graphical correlation by Standing and Katz (1942).

Eq. 4-12

$$Z = \left[A_1 + \frac{A_2}{T_{pr}} + \frac{A_3}{T_{pr}^3} + \frac{A_4}{T_{pr}^4} + \frac{A_5}{T_{pr}^5} \right] \rho_r + \left[A_6 + \frac{A_7}{T_{pr}} + \frac{A_8}{T_{pr}^2} \right] \rho_r^2 - A_9 \left[\frac{A_7}{T_{pr}} + \frac{A_8}{T_{pr}^2} \right] \rho_r^5$$

$$+ A_{10}(1 + A_{11}\rho_r^2) \frac{\rho_r^2}{T_{pr}^3} \times EXP\left[-A_{11}\rho_r^2 \right] + 1$$

Where:

Eq. 4-13

$$\rho_r = \frac{0.27 P_{pr}}{Z T_{pr}}$$

The correlation was developed using non-linear regression to fit 1500 data points to the graphical correlation, producing 11 coefficients as shown below:

A1 = 0.3265

A2 = -1.0700

A3 = -0.5339

A4 = 0.01569

A5 = -0.05165

A6 = 0.5475

A7 = -0.7361

A8 = 0.1844

A9 = 0.1056

A10 = 0.6134

A11 = 0.721

Furthermore, you may notice that ρ_r, used in the calculation requires Z to calculate, hence it is an iterative process. An initial value of Z = 1 can be used to begin, after calculation of Z, insert this value into the calculation of ρ_r and begin again.

4.2.3 Compositional Analysis of Separator Liquid by Flash Separation to Stock Tank conditions

Determining the composition of a separator liquid requires flashing the liquid and gas to stock tank conditions. The volumes of the two phases are measured accurately so that they can be mathematically recombined to give the composition of the liquid at pressure. The gas that comes out of solution is passed through a gas chromatograph and the liquid is injected into a capillary column and passed through a FID. From the chromatograms the mole percent of the components is determined. **Figure 4-4**, shown below, is an example liquid chromatogram.

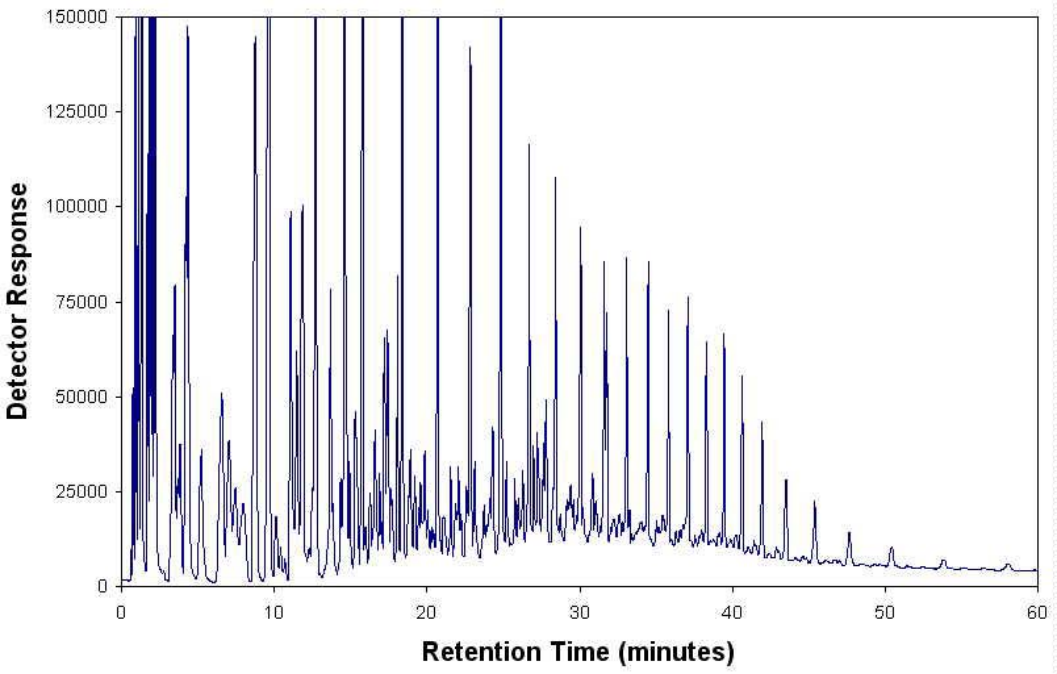

Figure 4-4: Typical FID liquid chromatogram

Fingerprint Calculations

In order to calculate the liquid composition and factors based upon this, similarly to the gas composition calculations, the following is performed:

- The GC detector delivers an output.

- The peak from the chromatogram is integrated for each component giving a peak area
- The sum of the areas for all the peaks give the total area.
- From calibration runs, the area is corrected. The GC is calibrated monthly and using a standardized gas which has a known composition. Based on this the calibration factors are developed and updated monthly.
- The fraction of the peak area over the total area gives a weight percent.
- The wt% is converted to mol% using Eq. 4-1.
- This fraction is then renormalized and reported as a mol %.

Further to this we report the molecular weight and density of the stock tank liquid, calculated by the following method:

Molecular Weight (MW):

Molecular Weight for the sample or a lumped fraction can be calculated using Eq. 4-2 and Eq. 4-3 respectively.

Density at 60°F ($\rho_{60°F}$):

Eq. 4-14

$$\rho_{60°F} = \frac{\sum_{i}^{1-34+} w_i}{\sum_{i}^{1-34+} V_i}$$

4.3 PVT Analysis

The following PVT tests, described in the following section, were performed to determine the following relevant fluid parameters:

- Formation Volume Factors (B_o and B_g)
- Gas Oil Ratio (GOR)
- Saturation pressure (P_{sat})
- Oil and Gas Viscosity (μ) at High Pressure
- Oil and Gas Density (ρ) at High Pressure

- Oil compressibility, Oil thermal Expansion, Y-function, Relative volume, Saturation Pressure,

The experiments performed include:

- Constant Mass Study
- Constant Volume Depletion
- Solubility and Swelling of CO_2 in Oil
- Separator Test
- High Pressure Viscosity of Oil

4.3.1 Constant Mass Study

The CMS is a test performed with a known quantity of representative reservoir fluid sample, which remains constant throughout the test. It is also known as a Constant Composition Expansion test (CCE) or a Constant Mass Expansion test (CME). The CMS is a flash liberation process, since the sample composition remains constant and as gas is liberated from solution, it remains in contact with the liquid and equilibrium is attained with all components still present.

From the CMS the following can be determined:

- Reservoir temperature saturation pressure
- Ambient temperature saturation pressure
- Relative Volume – Pressure relationship
- Compressibility
- Y-function
- Thermal Expansion

A fixed volume of reservoir fluid is charged into a high pressure PVT cell well above the saturation pressure of the fluid. The cell volume is increased in small increments, with the pressure being recorded after each volume increment and after it reaches equilibrium. When the cell reaches the samples bubble point, the first bubble of gas evolves. The compressibility of the two phases now present in the cell drastically increases due to the gas compressibility being much larger than that of a liquid. This can be seen when the cell pressure is plotted against the

sample volume and is illustrated in **Figure 4-5**. The test can be described step by step as follows (Ahmed, 1989):

- The cell starts at a pressure well above the bubble point pressure as in the cell diagram on the far left of **Figure 4-5**.
- The pump is backed off to increase the cell volume and the new cell pressure is recorded. In the second diagram from the left in **Figure 4-5**, the bubble point (P_b) is reached and the first bubble of gas is formed. Looking at the pressure - volume (P-V) plot under each cell, the single-phase part of the curve is quite linear.
- In the cell diagram third from the left, the cell volume is further increased, such that the cell pressure is now P_3, which is less that the bubble point pressure. More gas has come out of solution, as a result the sample compressibility changes drastically. This is illustrated in the P-V plot by the deviation from linearity.
- The cell volume is further expanded and the pressure continues to decrease, however it decreases less with a step increase in sample volume.

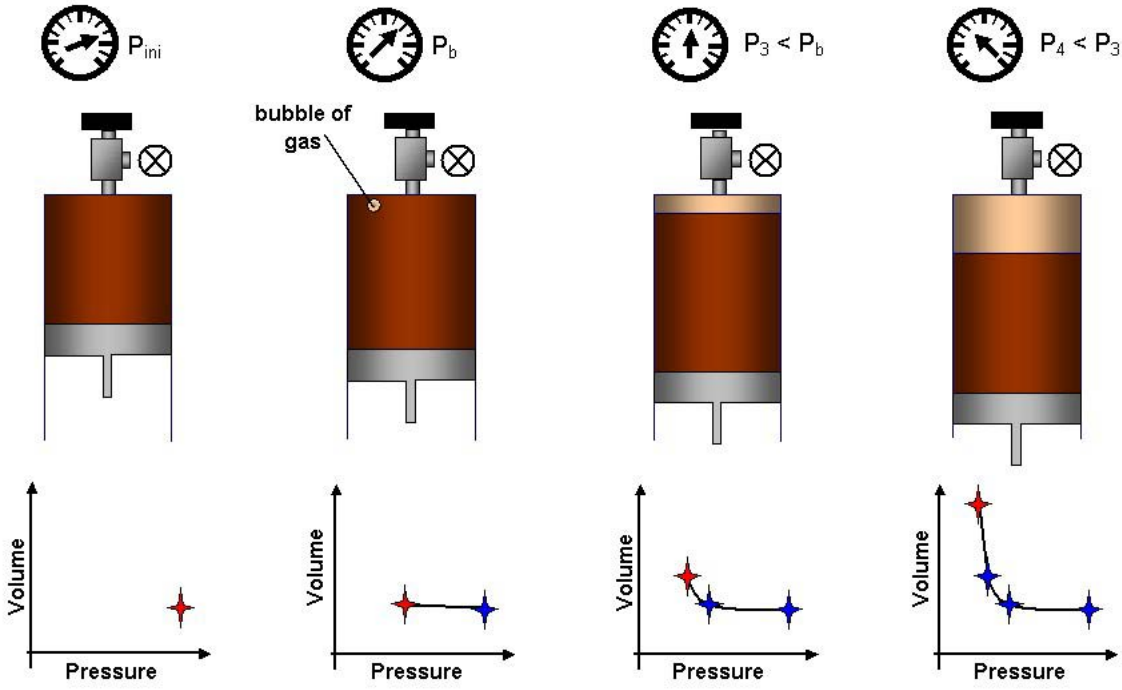

Figure 4-5: Schematic representation of the CMS experiment and relative volume plot

In reality, many more measurements would be made throughout the test. The volume is expressed as a fraction of the volume at the saturation pressure (relative volume). **Figure 4-6** shows an example P-V plot with real data. It is to be noted that there is a concentration of measurements around the saturation pressure as this is the most important measurement of the test and accuracy is improved with more measurements.

Reporting CMS Data

Relative Volume

The relative volume is determined from the ratio of the pump volume at a pressure over the pump volume at saturation pressure (Standing, 1977).

Eq. 4-15

$$V_{rel} = \frac{V_{pump}}{V_{pump,sat}}$$

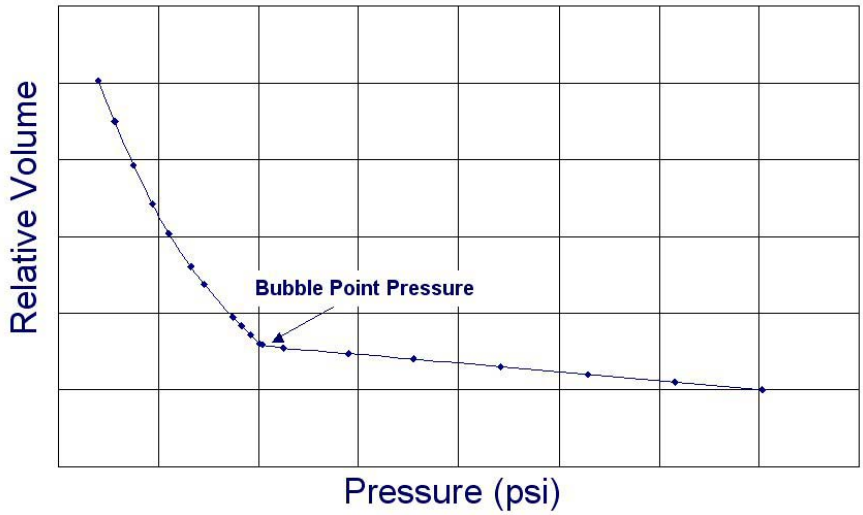

Figure 4-6: Pressure – relative volume relationship from constant mass study

Oil Compressibility

From the same measured data the isothermal oil compressibility can also be determined from the following equation (Standing, 1977):

Eq. 4-16

$$c_o = -\frac{1}{V_o} * \left(\frac{dV_o}{dP} \right)$$

Where:

c_o = oil compressibility (psi^{-1})

V_o = volume of the oil at pressure (cc)

P = experimental pressure (psi)

Oil Thermal Expansion

The thermal expansion of the oil above the bubble point pressure is determined by running the test at ambient temperature as well as reservoir temperature. The thermal expansion can then be calculated by dividing the relative volumes at each pressure (Standing, 1977).

Eq. 4-17

$$TE_o = -\frac{1}{V_o}\left(\frac{\partial V_o}{\partial T}\right)_P$$

Where:

TE_o = oil thermal expansion

T = experimental temperature

Y-function

After the saturation pressure is reached, the Y-function can be determined. The Y-function can be described as a relationship to smooth the pressure-volume data at pressures below the saturation pressure. It is determined by the following equation (Standing, 1977):

Eq. 4-18

$$Y = \left(\frac{P_{sat} - P}{P}\right) \Big/ \left(\frac{V}{V_{sat}} - 1\right)$$

Where: Y = the Y-function (an empirical value)

P = pressure at any point in the experiment

V = two-phase volume at pressure

V_{sat} = volume at the saturation pressure

P_{sat} = saturation pressure

4.3.2 Constant Volume Depletion on Volatile Oil Systems

The CVD test is performed to determine the following PVT parameters as a function of pressure at reservoir temperature:

- Oil, Gas and Total Formation Volume Factors
- Gas Expansion Factor
- Solution Gas Oil Ratio
- Compressibility or Z-factor
- Gas Gravity and Viscosity
- Oil Density
- Compositional analysis of liberated gas and residual oil
- Liquid Volume Percent

The CVD test is designed for gas condensate or volatile oil reservoir fluid systems. An alternate test, good enough for low shrinkage black oils, is the Differential Vaporization (DV) test. The CVD is a more difficult and time consuming test and therefore is generally only performed for volatile oils and gas condensate systems. For volatile oils that are rich in intermediates, the DV gives high values for both oil formation volume factor (FVF) and GOR (Jacoby *et al.,* 1957). The difference between the CVD and DV is that in the DV test, the entire gas cap is pushed out of the cell at each stage. Therefore, the volume of sample remaining in the cell decreases after each step (Ahmed, 1989). This is an allowable simplification for black oil reservoirs producing relatively lean solution gas but does not account for liquids produced from rich gases present in gas condensates and volatile oils.
The test is shown in **Figure 5-7** and the method is summarized below.

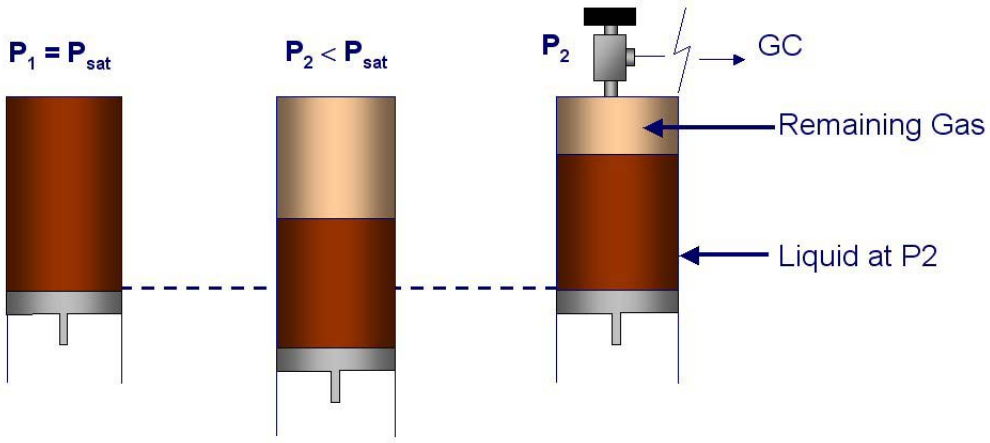

Figure 4-7: The CVD experiment

A measured volume of representative reservoir fluid, with a known overall composition (c_i) is charged into a windowed PVT cell at the saturation pressure, (P_{sat}). The cell is always maintained at the reservoir temperature throughout the entire test. The initial volume (V_i) of saturated reservoir fluid is recorded as the reference volume for the test.

The pressure is drawn down to some pressure below the saturation pressure. This causes the gas to come out of solution. The top valve of the cell is then opened (in a controlled manner) and the released gas is pushed out until the sample is back at the initial volume. The atmospheric volume and composition of the gas released is measured. The remaining liquid volume is determined by measuring the liquid level (between the piston and the gas-oil level) visually through the window in the cell.

After this, the pressure is dropped again to another pressure by withdrawing the piston and the process is repeated. This is repeated several more times until measurements have been made at eight different pressure steps. At the last step (the abandonment pressure) the volume and composition of the remaining fluid is determined by flashing it to stock tank conditions.

Thus, differentially from the liquid volume measurements at each pressure step the volume of gas remaining in the cell is known. Since the volume of gas liberated is also known, solution GOR and oil FVF can be determined at each pressure.

Also, from the measured change in cell volume during the removal of excess gas, which is also measured at stock tank conditions, the gas compressibility, formation volume and expansion factors can also be determined.

Since the composition of gas removed at each pressure step is determined and the composition of the initial sample is known, from a material balance calculation, the calculated composition of the remaining fluid can be compared with the actual flashed off abandonment fluid and the quality of the experiment checked.

Generation of Results for CVD

During the CVD test the pressures, volumes and temperatures are all physically measured. From these measurements, the PVT parameters can be derived. The PVT parameters are all essentially dimensionless factors to enable the data to be translated from cell volumes (in the order of 100cc) to reservoir volumes (in the order of millions or even billions of barrels). Although correlations exist for all the PVT paraemeters derived from the CVD, from the measurements of P, V and T during the CVD experiment the CVD provides *measured* values, of key importance in tuning fluid models and subsequent fluid-flow simulations. While good correlations exist for PVT parameters such as the Z-factor and saturation pressure, laboratory measured data still and will always yield the most accurate data to use for subsequent engineering calculations. This is due to the simple fact that the correlations are based upon laboratory attained data. This difference is particularly apparent for data such as that of Oil A, which is high in CO_2.

The following data is reported from the results of the CVD:

- The properties of the produced gas stream, as a function of pressure: Gas compositions, Cumulative Produced Gas, Gas FVF (B_G), Z-Factor (Z), expansion factor (E), gas gravity (γ_G) and gas viscosity (μ_G)
- The properties of the oil / reservoir fluid remaining in the cell as a function of pressure: liquid compositions, depletion solution GOR (R_{sd}), depletion oil FVF (B_{od}), depletion total FVF (B_{td}), Liq%, Oil Density (ρ_o)

- Depletion liberation data (from CVD) corrected with flash liberation data (from separator test): GOR Corrected (R_s), Corrected Oil FVF (B_o), Corrected Total FVF (B_t)

For example, if the bubble point pressure is 2350psig, and the first CVD pressure step is to 2200psig, the pump needs to be backed a certain volume in order to attain an equilibrium fluid at 2200psig, say some 5cc. Once equilibrium is reached the valve is cracked open and 5cc of gas at 2200psig and 279°F is pushed out to standard conditions. At standard conditions the volume of the gas is likely to be several litres. Therefore, in this example, the volume of the gas at reservoir conditions of 2200psig and 279°F is 5cc. The volume of the same gas at surface conditions (0psig, 60°F) is several litres. The gas FVF can be calculated using:

Eq. 4-19

$$B_g = \frac{V_{g,surf}}{V_{g,res}}$$

Z-Factor (Z):

Rearranging the equation of state, we can write the equation as:

Eq. 4-20

$$Z = \frac{PV}{nRT}$$

All the data on the right had side of the equation is measured, therefore Z can be easily attained. The Z-factor is measured at each step by measuring the displaced gas volume at pressure and temperature and then at stock tank conditions.

Expansion Factor (E):

The gas expansion factor is, by definition, the gas FVF, i.e.:

Eq. 4-21

$$E = \frac{1}{B_g}$$

Gas gravity (γ_G):

Gas gravity can be calculated using Eq. 4-4.

Gas viscosity (μ_G):

Gas viscosity can be measured by passing the gas through a capillary at a set flow rate and measuring the pressure difference over the capillary. Using this information and Poiseuille's law we can obtain the gas viscosity:

Eq. 4-22

$$\mu_g = \frac{3.14 * r^4 * (\Delta P)}{8 * Q * L}$$

Where:

μ_g = Viscosity

r = Radius of Capillary

ΔP = Differential Pressure over the Capillary

L = Length of Capillary

Q = Flow rate through Capillary

Liquid compositions:

The composition of the fluid remaining at abandonment is measured by flashing it to stock tank conditions.

Depletion solution GOR (R_{sd}):

The cathetometer readings provide the volume of the liquid and gas in the cell. From these readings we, pump readings and readings of produced gas volumes can get the formation volume factors.

Eq. 4-23

$$R_{sd} = \frac{V_{g,surf}}{V_{o,surf}}$$

Depletion oil FVF (B_{od}):

Eq. 4-24

$$B_{od} = \frac{V_{o,surf}}{V_{o,res}}$$

Depletion total FVF (B_{td}):

Eq. 4-25

$$B_{td} = \frac{V_{t,surf}}{V_{t,res}}$$

Liquid percent (Liq%):

Eq. 4-26

$$Liq\% = \frac{V_{g,cell}}{V_{o,cell}} \times 100$$

Oil Density (ρ_o):

Eq. 4-27

$$\rho_o = \frac{m_{o,cell}}{V_{o,cell}}$$

Solution GOR Corrected (R_s):

Eq. 4-28

$$R_s = R_{sfb} - \left(R_{sdb} - R_{sd}\right) \times \left(B_{ofb} \middle/ B_{odb} \right)$$

Corrected Oil FVF (B_o):

Eq. 4-29

$$B_o = B_{od} \times \left(B_{ofb} \middle/ B_{odb} \right)$$

Corrected Total FVF (B_t):

Eq. 4-30

$$B_t = B_{td} \times \left(B_{ofb} \middle/ B_{odb} \right)$$

4.3.3 Separator Test on Physically Recombined Separator Samples

In the separator test, a PVT cell is maintained at separator temperature and pressure and the reservoir fluid is allowed to separate at those conditions. This is done by supplying a back pressure with compressed air. In doing this, the air supplies a compressible cushion and thus the pressure does not change throughout the test once the conditions are established. The cell is well insulated to maintain the separator temperature steady. The solution gas at separator conditions is pushed out and the volume and composition of the gas is measured.

The remaining separator liquid is flashed out of the cell to stock tank conditions and the gas and oil volumes and the composition are measured.

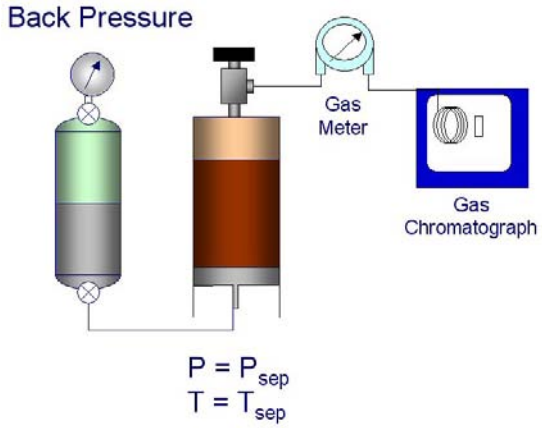

Figure 4-8: Separator test schematic.

4.3.4 High Pressure (Rolling Ball) Viscosity on Physically Recombined Separator Samples

The high pressure viscosity is evaluated using a Rolling Ball Viscometer. The viscometer maintains the fluid at reservoir temperature and high pressure and comprises of a cylinder with an inner diameter known to high accuracy, and a steel ball with a diameter also known to high accuracy. The time taken for the ball to move from the top of the viscometer to the bottom is measured. When the ball reaches the bottom it stops the clock by completing a circuit with a probe located at the bottom of the viscometer. The viscosity is the then measured by the following equation:

Eq. 4-31

$$\mu_o = \left[\left(\rho_{steel} - \rho_{oil} \right) * t_{roll} - C_1 \right] * C_2$$

Where:

μ_o = Viscosity of oil

ρ_{steel} = Steel density

ρ_{oil} = Oil density

t_{roll} = Roll time

C_1 = The intercept of the plot of the equation displayed as μ versus $\Delta\rho.T_{roll}$. This is predetermined from calibration tests.

C_2 = The inverse of the gradient of the of the plot of the equation displayed as μ versus $\Delta\rho.T_{roll}$. This is predetermined from calibration tests with a fluid of known viscosity

The test is run at several pressures above and below the bubble point to obtain a curve of viscosity versus pressure. The sample is charged into the cell at a pressure well above the bubble point and the time for the ball to roll through the reservoir fluid is taken until several repeated values are obtained. The pressure in the cell is then dropped by releasing some fluid and the again the time for the ball to roll through the reservoir fluid is taken.

The resultant is the plot shown below (**Figure 4-9**). What is observed is that the viscosity decreases with decreasing pressure until the saturation pressure due to the decompression of the reservoir fluid. When below the bubble point pressure, the gas comes out of solution leaving a heavier reservoir fluid and the viscosity increases again. Due to the constantly changing composition of the fluid the relationship below the bubble point is not linear.

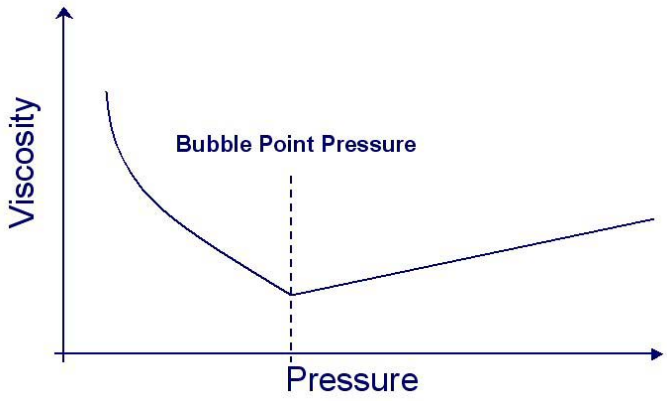

Figure 4-9: Viscosity of a crude oil at elevated pressures.

4.3.5 Solubility and Swelling Tests

Solubility – Swelling tests should be conducted when considering an injection project, be it, gas injection into an oil reservoir or dry gas cycling into a gas condensate system. The test is intended to measure the degree to which the injection gas will dissolve in the reservoir fluid and the pressure at which a single phase exists. From the experiment the following data can be obtained (Ahmed, 1989):

- The relationship of saturation pressure and volume of gas injected
- The volume of the new saturated mixture. This is compared to the volume of the original saturated reservoir fluid.

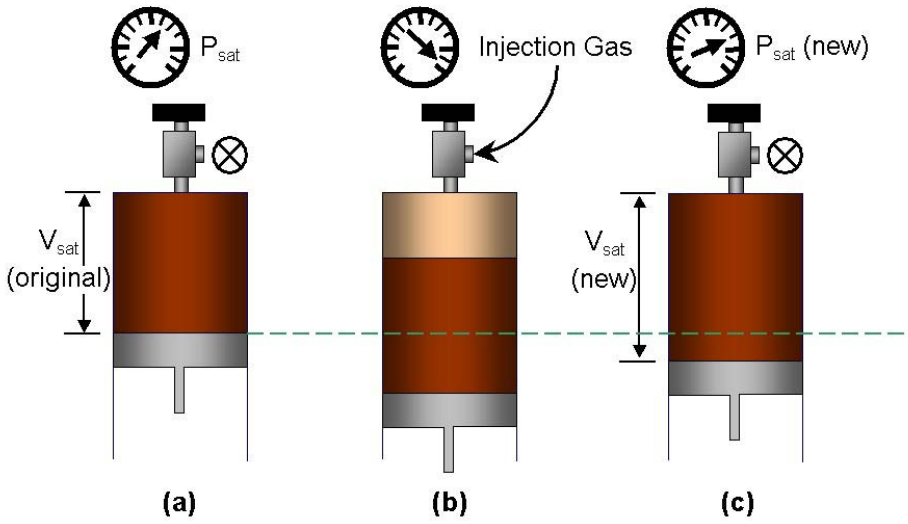

Figure 4-10: Schematic representation of the solubility-swelling test

When CO_2 dissolves in oil it has the effect of swelling the oil. The amount of swelling experienced by a crude oil and the increase in the saturation pressure as a result of CO_2 injection can be determined by the solubility-swelling test. The test is performed as follows (**Figure 4-10**):

- A high pressure PVT cell is charged with a pre-determined volume of single-phase reservoir fluid at reservoir temperature.
- To this a known volume of injection gas is charged to the cell, maintaining the same cell temperature conditions.
- The contents of the cell are pressurized and mixed to establish equilibrium and the increase in saturation volume as a result of the injection gas is measured.
- This is repeated for increasing volumes of injection gas up to approximately 80mol% injection gas (can also be reported as a gas-oil ratio).

The swelling factor is determined as the ratio of the oil volumes at new saturation pressure to the original saturation pressure.

Eq. 4-32

$$V_{rel} = \frac{V_{sat(new)}}{V_{sat(orig.)}}$$

Where:

V_{rel} = relative total volume, swollen volume or swelling factor

$V_{sat(orig.)}$ = original saturation volume

$V_{sat(new)}$ = new saturation volume

At each incremental addition of CO_2, a CMS is performed. From this the pressure-volume properties can be compared to that of the original reservoir fluid. Also, during the CMS the new saturation pressure is measured.

The pressure at which the two fluids dissolve to form one phase (the new saturation pressure) is the pressure at which the two fluids are considered soluble with one another. The new relative volume at this pressure compared to the relative volume at saturation of the pure reservoir fluid without the injection fluid gives the amount of swelling undergone.

5 DISCUSSION AND RESULTS OF RESERVOIR FLUID STUDIES

This chapter presents discussion of the results of the fluid analyses performed. The experimental methodology for the results discussed in this chapter was presented in the previous chapter (Chapter 4 - Methodology and Procedures of Reservoir Fluid Analyses Performed).

5.1 Asphaltene Precipitation Analysis

As it is well documented that adding injection gas can precipitate solids from the crude and damage the project (de Boer *et al.,* 1995, Stankiewicz *et al.,* 2002, Danesh *et al.,* 1988), SARA and Asphaltene content experiments were done on the recovered stock tank liquid.

The asphaltene content by means of n-heptane precipitation (IP 143) was 0.08 wt% a quantity confirmed in the SARA test which gave the Saturates, Aromatics, Resins and Asphaltenes fraction by weight respectively as 42.0%, 1.1%, 33.2% and 0.1%. The remaining 23.6% is loss and can be assumed to be made up mainly of saturates and aromatics as the boiling point of the solvents boiled off at the end of the test is very similar to that of the saturates pentane, hexane and heptane.

Even though small concentrations of asphaltenes as found in the Oil A, these concentrations could indeed cause severe production problems. However, the rather high amount of resins makes it very unlikely for those solids to precipitate. Furthermore, from production history to date no asphaltene problems have been detected. The asphaltene to resin ratio for Oil A is 0.003 placing it in the stable part of the Stankiewicz plot (Chapter 3: Literature Review, **Figure 2-9**, Stankiewicz *et al.,* 2002).

The recombined sample was also charged into a visual PVT cell. The precipitation of solids was checked visually in the cell. No visual evidence of solids was reported during the PVT analysis in the visual PVT cell. Further to this, during the

Slim Tube experiments no build up of solids was detected – this would be detected by the pressure differential over the Slim Tube.

5.2 Reservoir Fluid Analyses

5.2.1 Quality Checks and Compositional Analysis

Eight 20 litre primary separator gas samples were taken together with two 10 litre and two 500cc primary separator liquid samples from the subject well at Field A. It was found that the samples taken were representative and sample quality had been preserved during transportation. The compositional analysis reconfirmed this.

The Oil A recombined reservoir fluid composition and properties can be found on **Table 5-1**.

Table 5-1: Oil A - Compositional Analysis of Recombined Reservoir Fluid

Component		Stock Tank Liquid Mol %	Stock Tank Gas Mol %	Recombined Reservoir Fluid Mol %
Hydrogen Sulphide	H_2S	0.00	0.00	0.00
Carbon Dioxide	CO_2	0.34	23.78	15.57
Nitrogen	N_2	0.00	1.13	0.73
Methane	C_1	0.21	36.74	23.95
Ethane	C_2	0.44	13.17	8.71
Propane	C_3	1.49	12.47	8.63
Iso-Butane	iC_4	0.91	3.05	2.30
N-Butane	nC_4	2.23	5.20	4.16
Iso-Pentane	iC_5	1.58	1.40	1.46
N-Pentane	nC_5	2.04	1.41	1.63
Hexanes	C_6	8.96	0.87	3.70
Heptanes	C_7	20.66	0.47	7.54
Octanes	C_8	10.60	0.13	3.80
Nonanes	C_9	11.07	0.06	3.91
Decanes	C_{10}	8.07	0.03	2.84
Undecanes	C_{11}	5.09	0.02	1.79
Dodecanes Plus	$C_{12}+$	26.31	0.07	9.28
TOTAL		100.00	100.00	100.00
Ratios				
Molar Ratio	:	0.3501	0.6499	1
Mass Ratio	:	0.6794	0.3206	1
Liquid Ratio (bbl/bbl)	:	1 @ SC	--	2.0844 @ P and T*
Gas Liquid Ratio	:	1bbl @ SC	1410 scf	--
Stream Properties				
Molecular Weight	:	135.9	34.54	70.03
Density obs. (gm/cc)	:	0.7761 @ 60 °F	--	0.5495 @ P and T*
Gravity (AIR = 1.000)	:	50.7 °API @ 60 °F	1.202	125.8
GHV (BTU/scf)	:	--	1401	--
Hexanes Plus Properties				
Mol %	:	90.75	1.65	32.86
Molecular Weight	:	143.8	95.9	142.2
Density (gm/cc @ 60 °F)	:	0.7869	0.6836	0.7843
Gravity (°API @ 60 °F)	:	48.1	75.3	48.7
Heptanes Plus Properties				
Mol %	:	81.79	0.78	29.16
Molecular Weight	:	150.4	109.2	149.6
Density (gm/cc @ 60 °F)	:	0.7941	0.7007	0.7928
Gravity (°API @ 60 °F)	:	46.5	70.2	46.8
Decanes Plus Properties				
Mol %	:	39.46	0.12	13.91
Molecular Weight	:	198.7	157.2	198.3
Density (gm/cc @ 60 °F)	:	0.8286	0.7489	0.8281
Gravity (°API @ 60 °F)	:	39.1	57.3	39.2
Undecanes Plus Properties				
Mol %	:	31.40	0.09	11.07
Molecular Weight	:	215.3	164.9	214.9
Density (gm/cc @ 60 °F)	:	0.8373	0.7552	0.8369
Gravity (°API @ 60 °F)	:	37.3	55.7	37.4
Dodecanes Plus Properties				
Mol %	:	26.31	0.07	9.28
Molecular Weight	:	228.5	170	228.2
Density (gm/cc @ 60 °F)	:	0.8437	0.7592	0.8433
Gravity (°API @ 60 °F)	:	36.1	54.7	36.1

* (P)ressure : 2350 psig * (T)emperature : 279 °F

5.2.2 Constant Mass Study on Physically Recombined Separator Samples

The separator products were then physically recombined at a predicted GOR with an aim to have a saturation pressure close to the estimated reservoir pressure at the start of the potential gas injection project.

In a visual PVT cell the reservoir fluid was thermally expanded to the reservoir temperature of 279°F. During the constant mass study the physically recombined sample was found to have a bubble point of 2350psig. This can be seen from the relative volume versus pressure plot (**Figure 5-1**). When the fluid is in single phase, due to the relatively low compressibility of the liquid phase, the decrease in pressure with an increase in volume is not as large as when in two phases due to the gas that is present in the two phase fluid.

The Y-function, also shown in **Figure 5-1**, is a dimensionless function of pressure and temperature to describe the pressure volume relationship at pressures below the bubble point. It is a linear relationship and increases with pressure. As it approaches the bubble point it deviates from linearity.

The oil thermal expansion plot (**Figure 5-2**) shows the change in the relative volume per degree Fahrenheit, measured by repeating the pressure volume relationship at a different temperature. What can be seen is that at higher pressures, due to the reservoir fluid being more compressed, the change is not as large as at lower pressures. The plot extends only down to the bubble point pressure. At pressures below the bubble point pressure, the composition of the liquid changes with each decrease in pressure step and the thermal expansion cannot be compared to the single phase fluid at another temperature. At the bubble point pressure, the thermal expansion is just under $11 * 10^{-4}$ / °F and at the current reservoir pressure of 3150 psig it is just over $9 * 10^{-4}$ / °F.

Also on **Figure 5-2** is the compressibility plot. As for the oil thermal expansion this is measured only above the bubble point pressure for the single phase fluid. The compressibility plot shows how the oil relative volume changes with pressure. At lower pressures the volume is larger due to decompression and, conversely, at higher pressure the volume is lower. At the bubble point pressure, the oil

compressibility is approximately 47 * 10^{-6} / psi and at the current reservoir pressure of 3150psi it is approximately 34 * 10^{-6} / psi.

Table 5-2: Results from CMS on Oil A at 279°F

Pressure (psig)	**Relative Volume (V/V_{sat})** (1)	**Oil Compressibility ($x10^{-6}$)($psig^{-1}$)** (2)	**Y Function ($psig^{-1}$)** (3)	**Thermal Expansion ($x10^{-4}$)($°F^{-1}$)** (4)	**Oil Viscosity (Centipoise)** (5)
5000	0.9153	22.37		7.46	0.180
4500	0.9270	25.19		7.87	0.172
4000	0.9402	28.20		8.32	0.165
3500	0.9553	31.61		8.87	0.157
3000	0.9727	35.74		9.50	0.149
2800	0.9801	37.89		9.82	0.146
2500	0.9929	42.93		10.42	0.142
2350*	1.0000	47.21		10.80	0.139
2300	1.0172		1.264		0.142
2200	1.0481		1.417		0.147
2100	1.0804		1.480		0.153
2000	1.1176		1.488		0.158
1800	1.2115		1.445		0.169
1600	1.3348		1.400		0.180
1400	1.5019		1.352		0.192
1200	1.7338		1.306		0.205
1000	2.0723		1.259		0.218
800	2.5973		1.213		0.233
600	3.5014		1.166		0.254
500	4.2371		1.143		0.266
0					0.390

* Saturation Pressure

(1) Barrels at indicated pressure per barrel at saturation pressure
(2) Oil Compressibility = - (1 / V) * (dV / dP)
(3) Y Function = (P_{sat} – P) / (P) * (V / V_{sat} – 1)
(4) Thermal Expansion = - (1 / V) * (dV / dT)
(5) Oil Viscosity below Bubble Point from Depleted Oil

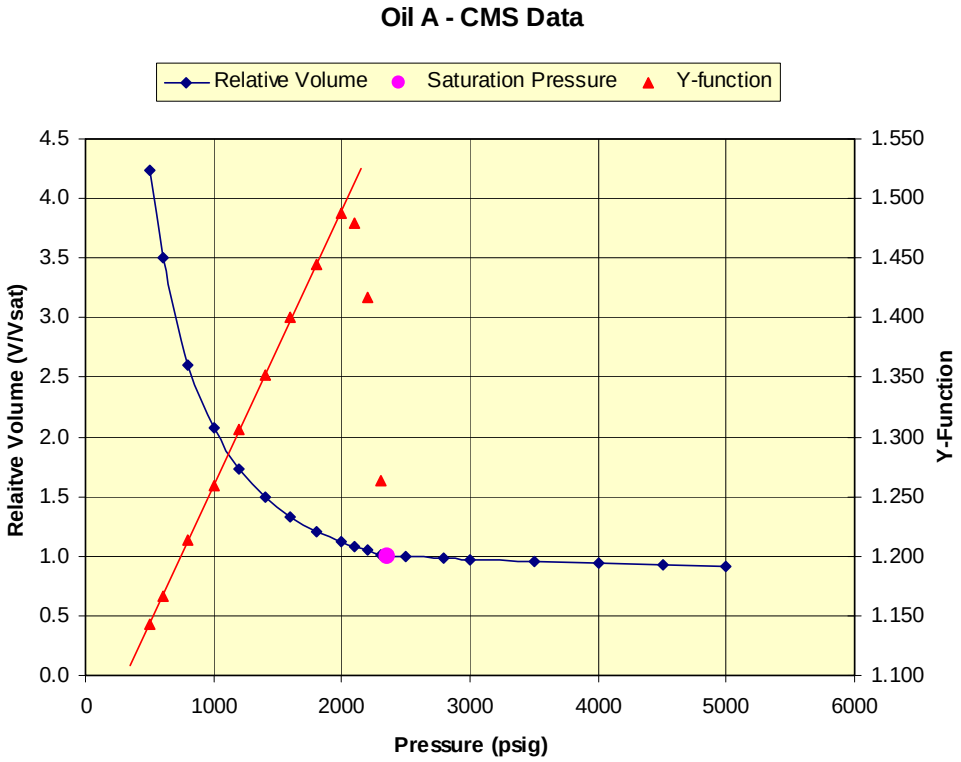

Figure 5-1: Oil A relative volume plot (P-V Relationship)

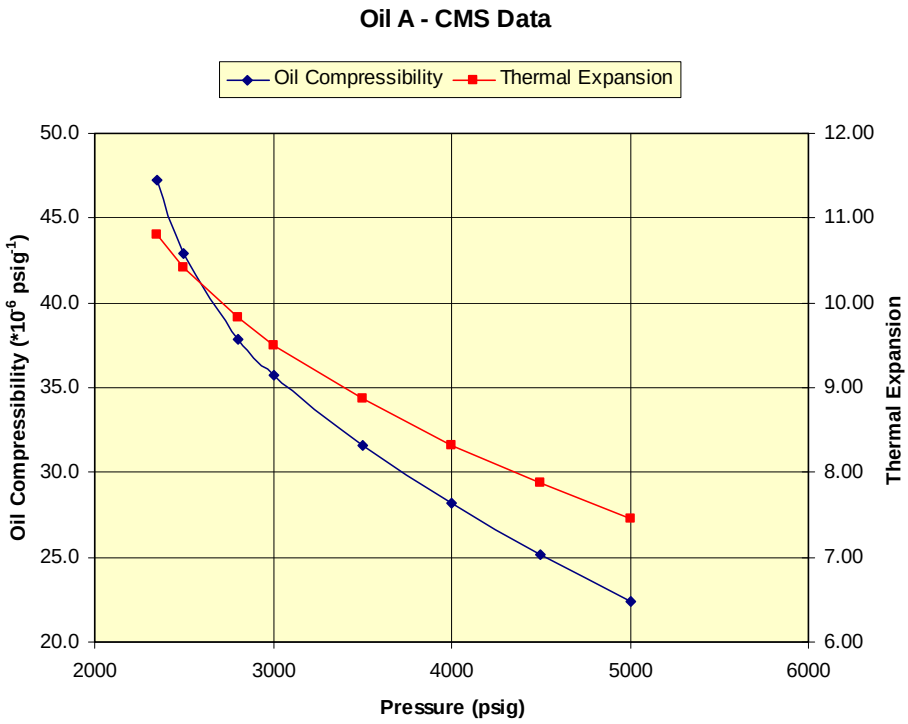

Figure 5-2: Oil A compressibility and thermal expansion

5.2.3 Constant Volume Depletion

Due to the volatile nature of Oil A, the reservoir fluid was depleted in the PVT cell by means of a CVD. At each depletion pressure, the amount and composition of the produced gas phase were determined and additional measurements of the liquid phase volumes enabled us to calculate their densities and compositions, solution gas oil ratios and their equilibrium (K-values). The good match between the two reported liquid compositions at the abandonment pressure of 300 psig, one physically measured and one calculated, indicate an accurate material balance.

From the constant volume depletion test and after correcting the depletion data with data from the separator test, an oil formation volume factor of 1.998 rb/stb; and a gas oil ratio of 1263 scf/stb was obtained when the reservoir fluid was taken from the saturation pressure to separator conditions.

Table 5-3 shows the oil results of the CVD volumetrics – hence the GOR, oil FVF, total FVF, liquid percent and oil density. **Table 5-4** shows the volumetrics results corrected with data from the separator test. The oil FVF and GOR are graphically shown in **Figure 5-3**. **Table 5-5** shows the properties of the produced gas, these are represented graphically in **Figure 5-4**, **Figure 5-5** and **Figure 5-6**. The properties of the produced gas stream at each step were developed based on compositional analysis, these are reported on **Table 5-6**. The composition of the liquid remaining in the cell at each pressure step was then calculated based on the volume and composition of produced gas and the volume of gas and liquid in the cell (**Table 5-7**).

Table 5-3: Results from CVD study on Oil A at 279°F

Pressure (psig)	Gas-Oil Ratio (SCF/Bbl) (1)	Oil Formation Volume Factor (Bo) (2)	Total Formation Volume Factor (Bt) (3)	Percent Liquid (%) (4)	Oil Density (gm/cc)	
4000	1444	2.0477	2.0477	100	0.5844	***
3500	1444	2.0806	2.0806	100	0.5752	***
3000	1444	2.1185	2.1185	100	0.5649	***
2800	1444	2.1346	2.1346	100	0.5606	***
2500	1444	2.1625	2.1625	100	0.5534	***
2350	1444	2.1779	2.1779	100	0.5495	
2200	1228	2.0056	2.2569	92.09	0.5674	
2000	1059	1.8854	2.393	86.57	0.581	
1750	884	1.7711	2.6506	81.32	0.5931	
1500	740	1.6742	3.0131	76.87	0.6049	
1250	608	1.577	3.5595	72.41	0.6192	
900	449	1.4565	4.8988	66.88	0.6394	
600	305	1.3629	7.491	62.58	0.6514	
300	147	1.2519	15.5427	57.48	0.6675	
0	0	1.1267		51.73	0.6955	

* Saturation Pressure
** Values above Saturation Pressure from Constant Mass Study

(1) Cubic feet of gas at 14.696 psia and 60 °F per barrel of residual oil at 60 °F
(2) Barrels of oil at indicated pressure and temperature per barrel of residual oil at 60 °F
(3) Barrels of oil plus liberated gas at indicated pressure and temperature per barrel of residual oil at 60 °F
(4) Percent liquid of total hydrocarbon in pore space

Table 5-4: Oil A depletion formation volume factor and solution gas-oil ratio data corrected with flash liberation data from separator test

1st STAGE SEPARATOR DATA : Pressure (psig) = 180 Temperature (°F) = 79
Bofb = 2.00 Rsfb (scf/STB) = 1263
DEPLETION DATA : Bodb = 2.18 Rsdb (scf/STB) = 1444

(2) Bo = Bod * (Bofb / Bodb)
(4) Bt = Btd * (Bofb / Bodb)
(6) Rs = Rsfb - (Rsdb -Rsd) * (Bofb / Bodb)

Pressure (psig)	(Bod) (1)	(Bo) (2)	(Btd) (3)	(Bt) (4)	(Rsd) (scf/STB) (5)	(Rs) (scf/STB) (6)
2800	2.1346	1.9583	2.1346	1.9583	1444	1263
2350*	2.1779	1.9980	2.1779	1.9980	1444	1263
2200	2.0056	1.9610	2.2569	2.2547	1228	1151
2000	1.8854	1.8836	2.393	2.3906	1059	996
1750	1.7711	1.7693	2.6506	2.6479	884	836
1500	1.6742	1.6726	3.0131	3.0101	740	703
1250	1.577	1.5754	3.5595	3.5559	608	582
900	1.4565	1.4551	4.8988	4.8939	449	436
600	1.3629	1.3616	7.491	7.4835	305	305
300	1.2519	1.2507	15.5427	15.5272	147	159
0	1.1267	1.1267			0	0

*Saturation Pressure

(1) Barrels of oil at indicated pressure and temperature per barrel of residual oil at 60 °F
(2) Barrels of oil at indicated pressure and temperature per barrel of stock tank oil at 60 °F
(3) Barrels of oil plus liberated gas at indicated pressure and temperature per barrel of residual oil at 60 °F
(4) Barrels of oil plus liberated gas at indicated pressure and temperature per barrel of stock tank oil at 60 °F
(5) Cubic feet of gas at 14.696 psia and 60 °F per barrel of residual oil at 60 °F
(6) Cubic feet of gas at 14.696 psia and 60 °F per barrel of stock tank oil at 60 °F

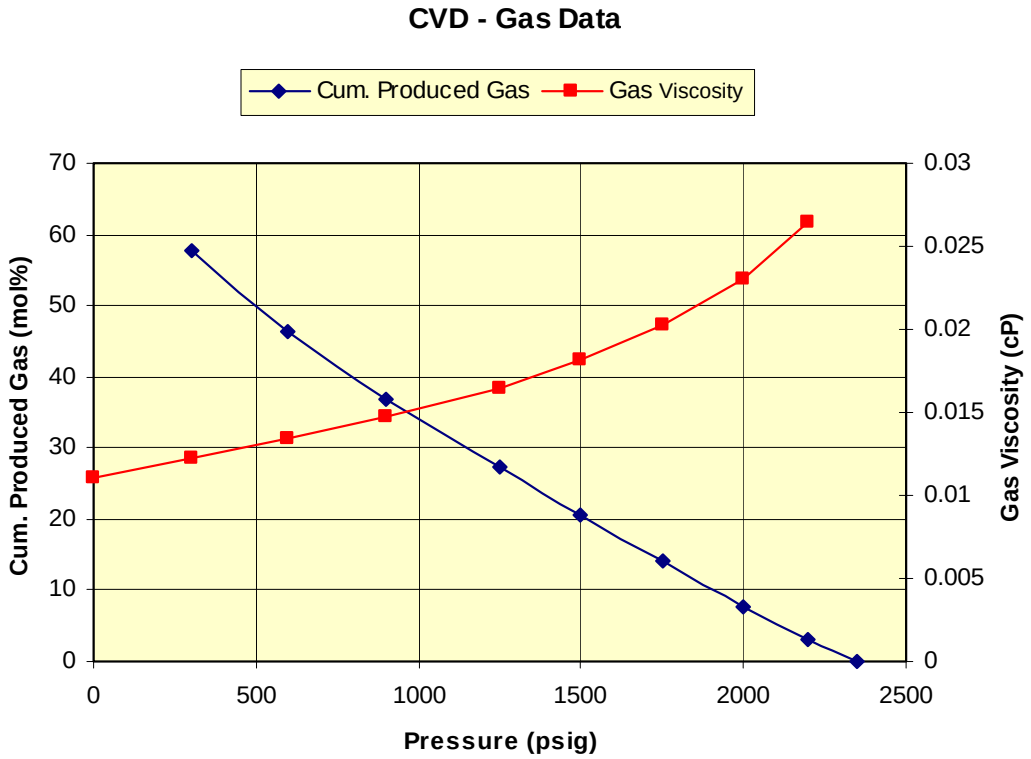

Figure 5-4: Oil A data for produced gas streams during CVD test

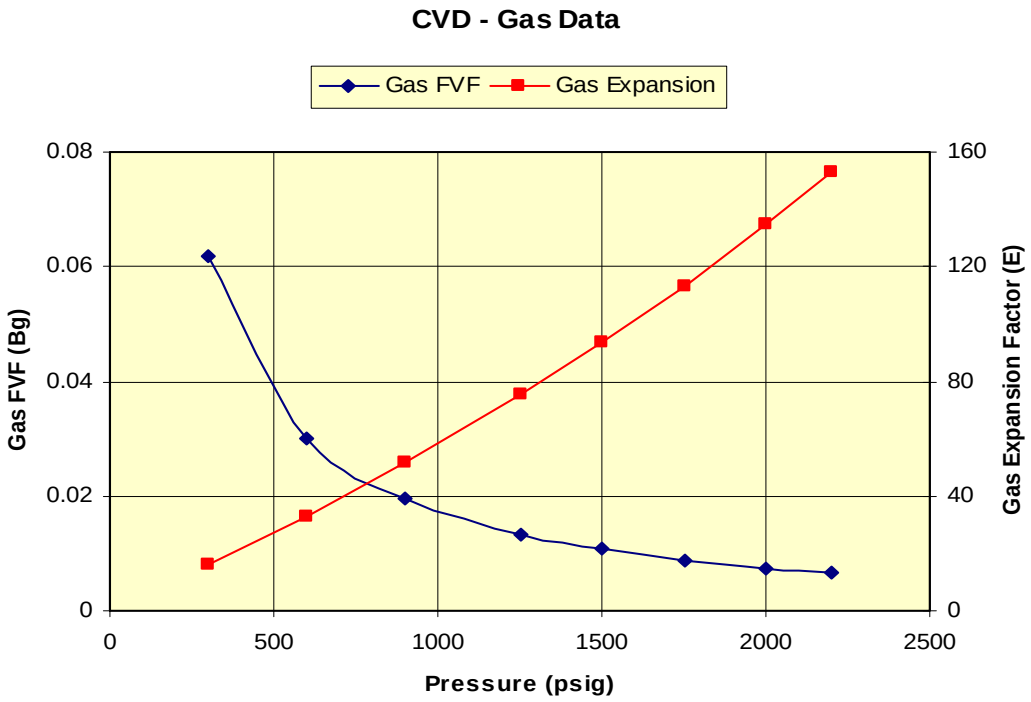

Figure 5-5: Oil A data for produced gas streams during CVD test

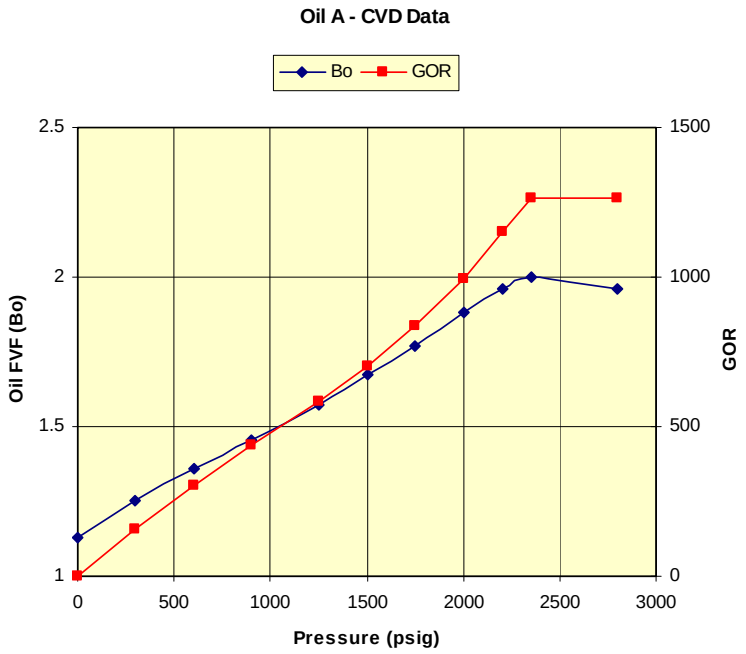

Figure 5-3: Oil A formation volume factor and solution GOR after correction with separator test data

Table 5-5: Oil A – data for produced gas streams during CVD test

CONSTANT VOLUME DEPLETION STUDY

@ 279 °F

Using Recombined Reservoir Fluid

Pressure (psig)	Cumulative Produced Gas Phase (1)	Gas Formation Volume Factor (Bg) (2)	Gas Expansion Factor (E) (3)	Deviation Factor (Z)	Gas Gravity (Air = 1.00)	Gas Viscosity (Centipoise) (4)
2350*	0					
2200	3.169	0.00653	153.24	0.692	1.253	0.0265
2000	7.633	0.0074	135.13	0.714	1.202	0.023
1750	14.068	0.00882	113.42	0.745	1.192	0.0202
1500	20.532	0.01067	93.73	0.774	1.193	0.0181
1250	27.194	0.01331	75.13	0.806	1.209	0.0165
900	36.92	0.01941	51.52	0.85	1.252	0.0147
600	46.441	0.03021	33.11	0.889	1.311	0.0134
300	57.573	0.06184	16.17	0.932	1.419	0.0122
0				1	1.573	0.0111

* Saturation Pressure

(1) Gas phase produced : Cumulative mol percent of initial fluid

(2) Cubic feet of gas at indicated pressure and temperature per cubic foot at 14.696 psia and 60 °F

(3) Cubic feet of gas at 14.696 psia and 60 °F per cubic foot at indicated pressure and temperature

(4) Calculated from correlation of Lee *et al.*, 1966

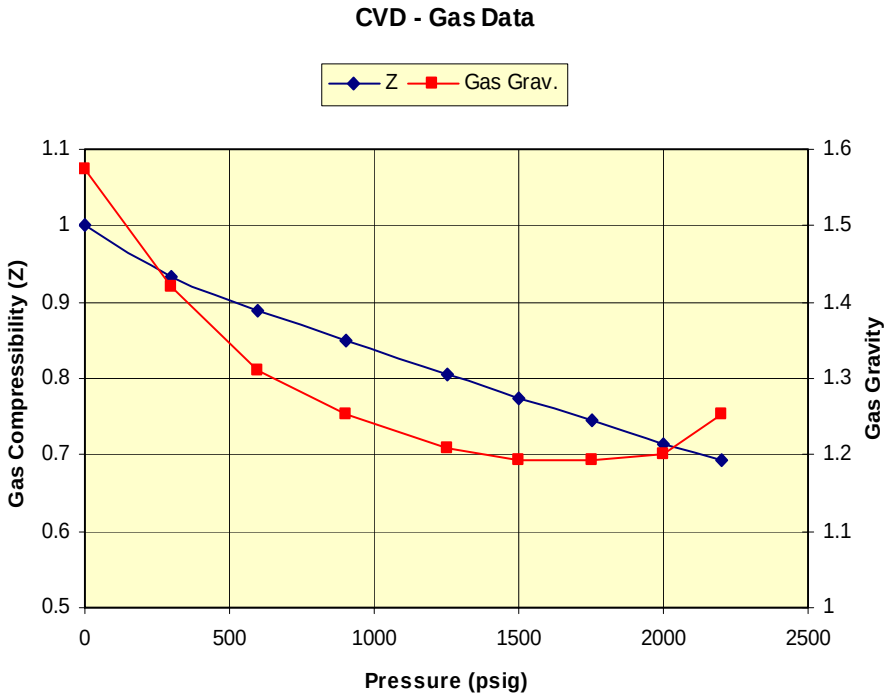

Figure 5-6 Oil A - data for produced gas streams during CVD test

Table 5-6: Oil A – Composition of produced gas phase during CVD

		*Well Stream	Produced Gas Streams							
		2350	2200	2000	1750	1500	1250	900	600	300
		Mol %	Mol %	Mol %	Mol %	Mol %	Mol %	Mol %	Mol %	Mol %
Hydrogen Sulphide	H_2S	0.00	0.00	0.00	0.00	0.00	0.00	0.00	0.00	0.00
Carbon Dioxide	CO_2	15.57	22.61	23.13	23.93	24.14	24.39	24.63	23.14	21.14
Nitrogen	N_2	0.73	1.95	1.82	1.74	1.51	1.31	1.10	0.90	0.60
Methane	C_1	23.95	44.00	44.70	43.70	43.07	41.57	38.13	34.98	29.42
Ethane	C_2	8.71	9.90	10.34	10.81	11.11	11.62	12.50	12.91	13.00
Propane	C_3	8.63	7.53	7.65	7.98	8.35	8.70	9.92	11.51	14.22
Iso-Butane	iC_4	2.30	1.72	1.73	1.77	1.81	1.92	2.20	2.70	3.47
N-Butane	nC_4	4.16	3.07	3.03	3.12	3.17	3.42	3.85	4.78	6.24
Iso-Pentane	iC_5	1.46	1.01	1.01	1.00	1.02	1.10	1.19	1.44	1.99
N-Pentane	nC_5	1.63	1.17	1.17	1.16	1.17	1.25	1.35	1.64	2.23
Hexanes	C_6	3.70	1.63	1.43	1.37	1.38	1.43	1.61	2.16	3.40
Heptanes	C_7	7.54	1.89	1.57	1.44	1.43	1.48	1.63	1.78	1.99
Octanes	C_8	3.80	1.45	0.85	0.71	0.70	0.71	0.75	0.83	0.95
Nonanes	C_9	3.91	0.81	0.63	0.54	0.51	0.52	0.55	0.61	0.68
Decanes	C_{10}	2.84	0.50	0.39	0.31	0.28	0.27	0.28	0.30	0.33
Undecanes	C_{11}	1.79	0.26	0.19	0.15	0.14	0.14	0.17	0.20	0.24
Dodecanes Plus	C_{12}+	9.28	0.50	0.36	0.27	0.21	0.17	0.14	0.12	0.10
Total		100.00	100.00	100.00	100.00	100.00	100.00	100.00	100.00	100.00
Stream Properties										
Molecular Weight		70.03	36.01	34.57	34.29	34.31	34.77	35.99	37.62	40.63
Gravity (AIR = 1.000)		2.443	1.253	1.202	1.192	1.193	1.209	1.252	1.311	1.419
Gross HV (BTU/SCF)		3515	1492	1404	1370	1370	1392	1456	1587	1810
Nett HV (BTU/SCF)		3251	1367	1285	1254	1254	1274	1334	1456	1663
Wobbe Index		2249	1333	1280	1255	1254	1266	1301	1386	1519
Critical Pressure (psia)		606.2	724.9	732.2	737.4	739	739.5	738.4	727.2	709.4
Critical Temperature (°R)		706.1	509.1	500.4	500.2	502	507.5	520.3	537.2	567.3
GPM Content										
Ethane Plus		26.505	10.367	9.71	9.633	9.763	10.18	11.214	12.775	15.364
Propane Plus		24.174	7.717	6.943	6.74	6.79	7.07	7.869	9.32	11.885
Butanes Plus		21.794	5.641	4.833	4.539	4.487	4.671	5.133	6.146	7.964
Pentanes Plus		19.728	4.109	3.311	2.974	2.894	2.963	3.198	3.753	4.859
Hexanes Plus Properties										
Mol %		32.86	7.04	5.42	4.79	4.65	4.72	5.13	6	7.69
Molecular Weight		142.2	110.7	108.7	106.3	104.5	103.2	102.2	100.7	98.5
Density (gm/cc @ 60 °F)		0.7843	0.748	0.7456	0.7426	0.7404	0.7387	0.7374	0.7354	0.7325
Gravity (°API @ 60 °F)		48.7	57.5	58.1	58.9	59.4	59.9	60.2	60.7	61.5
Heptanes Plus Properties										
Mol %		29.16	5.41	3.99	3.42	3.27	3.29	3.52	3.84	4.29
Molecular Weight		149.6	118.8	117.5	115.2	113.2	111.6	110.5	110.1	110
Density (gm/cc @ 60 °F)		0.7928	0.7575	0.7561	0.7534	0.751	0.7491	0.7478	0.7472	0.7471
Gravity (°API @ 60 °F)		46.8	55.1	55.5	56.1	56.7	57.2	57.5	57.7	57.7
Decanes Plus Properties										
Mol %		13.91	1.26	0.94	0.73	0.63	0.58	0.59	0.62	0.67
Molecular Weight		198.3	165.1	160.7	156.8	152.8	148.4	145.4	143.8	144.5
Density (gm/cc @ 60 °F)		0.8281	0.8036	0.7997	0.7963	0.7925	0.7884	0.7855	0.7839	0.7847
Gravity (°API @ 60 °F)		39.2	44.4	45.3	46	46.9	47.8	48.5	48.8	48.7
Undecanes Plus Properties										
Mol %		11.07	0.76	0.55	0.42	0.35	0.31	0.31	0.32	0.34
Molecular Weight		214.9	185.5	179.6	173.7	167.8	161	155.7	152.9	154.7
Density (gm/cc @ 60 °F)		0.8369	0.8206	0.8159	0.811	0.806	0.8	0.7953	0.7927	0.7944
Gravity (°API @ 60 °F)		37.4	40.8	41.8	42.8	43.9	45.2	46.3	46.8	46.5
Dodecanes Plus Properties										
Molecular Weight		228.2	205.5	196.8	188.5	181.6	172.5	166.3	162.7	173.3
Density (gm/cc @ 60 °F)		0.8433	0.8359	0.8294	0.823	0.8175	0.81	0.8047	0.8016	0.8107
Gravity (°API @ 60 °F)		36.1	37.6	38.9	40.3	41.4	43	44.2	44.9	42.9

* Original Reservoir Fluid

Table 5-7: Oil A – Composition of remaining liquid phase during CVD

		2200 Mol %	2000 Mol %	1750 Mol %	1500 Mol %	1250 Mol %	900 Mol %	600 Mol %	300 Mol %	300 Mol %
Hydrogen Sulphide	H_2S	0.00	0.00	0.00	0.00	0.00	0.00	0.00	0.00	0.00
Carbon Dioxide	CO_2	14.81	13.99	12.81	11.65	10.33	8.23	6.29	3.51	2.93
Nitrogen	N_2	0.60	0.49	0.37	0.30	0.23	0.15	0.08	0.02	0.03
Methane	C_1	21.79	19.60	17.12	14.64	12.24	9.23	6.01	2.04	2.22
Ethane	C_2	8.58	8.38	8.06	7.70	7.22	6.27	5.20	3.54	3.93
Propane	C_3	8.75	8.84	8.89	8.88	8.83	8.42	7.65	5.80	4.90
Iso-Butane	iC_4	2.36	2.42	2.49	2.55	2.59	2.59	2.47	2.13	2.68
N-Butane	nC_4	4.28	4.40	4.52	4.65	4.72	4.76	4.58	3.97	5.62
Iso-Pentane	iC_5	1.51	1.55	1.62	1.67	1.71	1.77	1.77	1.63	2.42
N-Pentane	nC_5	1.68	1.73	1.79	1.85	1.89	1.95	1.94	1.78	3.13
Hexanes	C_6	3.92	4.17	4.48	4.79	5.12	5.58	5.98	6.32	9.28
Heptanes Plus	C_7+	31.72	34.43	37.85	41.32	45.12	51.05	58.03	69.26	62.86
Total		100.00	100.00	100.00	100.00	100.00	100.00	100.00	100.00	100.00
Stream Properties										
Molecular Weight		74.0	77.7	82.5	87.3	92.4	100.3	109.3	123.3	115.8
Density @ P & T		0.575	0.582	0.59	0.596	0.602	0.608	0.615	0.626	0.61
Hexanes Plus Properties										
Mol %		35.64	38.60	42.33	46.11	50.24	56.63	64.01	75.58	72.14
Molecular Weight		143.6	143.9	144.4	144.8	145.2	145.8	146.6	147.9	141.4
Density (gm/cc @ 60 °F)		0.783	0.783	0.784	0.784	0.785	0.785	0.786	0.787	0.781
Gravity (°API @ 60 °F)		49.0	48.9	48.8	48.7	48.6	48.5	48.3	48.0	49.6
Heptanes Plus Properties										
Molecular Weight		150.9	151.2	151.5	151.8	152.1	152.6	153.1	153.7	149.9
Density (gm/cc @ 60 °F)		0.791	0.791	0.791	0.792	0.792	0.792	0.793	0.793	0.79
Gravity (°API @ 60 °F)		47.3	47.2	47.1	47.1	47	46.9	46.8	46.7	47.5

5.2.4 Separator Test

Three single stage separator tests were performed to determine the effects of separator pressure and temperature upon gas - oil ratio, stock tank oil gravity and formation volume factor. One test was performed at the separator conditions during sampling (245psig and 79°F) and the other two at the same temperature and pressures of 150psig and 50psig. It was found that field separator conditions can be slightly improved by dropping the separator pressure to around 160 psig as at these conditions the oil formation volume factor and GOR is at a minimum and the API gravity of the liquid is at a maximum, thus maximising the volume of liquid captured. This can be seen from **Figure 5-7** and **Table 5-8**.

Table 5-8: Results from Separator Tests on Oil A

Separator Pressure (psig)	Separator Temperature (°F)	Gas/Oil Ratio (1)	Density (@ 60 °F) °API	Density (@ 60 °F) (gm/cc)	Formation Volume Factor (2)	Shrinkage Factor (3)	Gas Gravity (Air = 1)
Test # 1							
245	79	963				0.819	1.014
	TO						
0	79	324	49.8	0.7796	2.014	0.99	1.582
	Total GOR	1287					
Test # 2							
150	79	1072				0.879	1.074
	TO						
0	79	195	49.9	0.7792	2.000	0.99	1.626
	Total GOR	1267					
Test # 3							
50	79	1238				0.945	1.123
	TO						
0	79	74	49.7	0.7801	2.035	0.99	1.591
	Total GOR	1312					
Test # 4							
0	79	1410	49.4	0.7814	2.084	0.99	1.202
	Total GOR	1410					

(1) Gas/Oil Ratio is reported as cubic feet of gas @ 14.696 psia and 60 °F per barrel of stock tank oil @ 60 °F
(2) Formation Volume Factor is reported as barrels of saturated oil @ 2350 psig and 279°F per barrel of stock tank oil @ 60 °F
(3) Shrinkage Factor is reported as barrels of stock tank oil at @ 60 °F per barrel of separator liquid at separator conditions

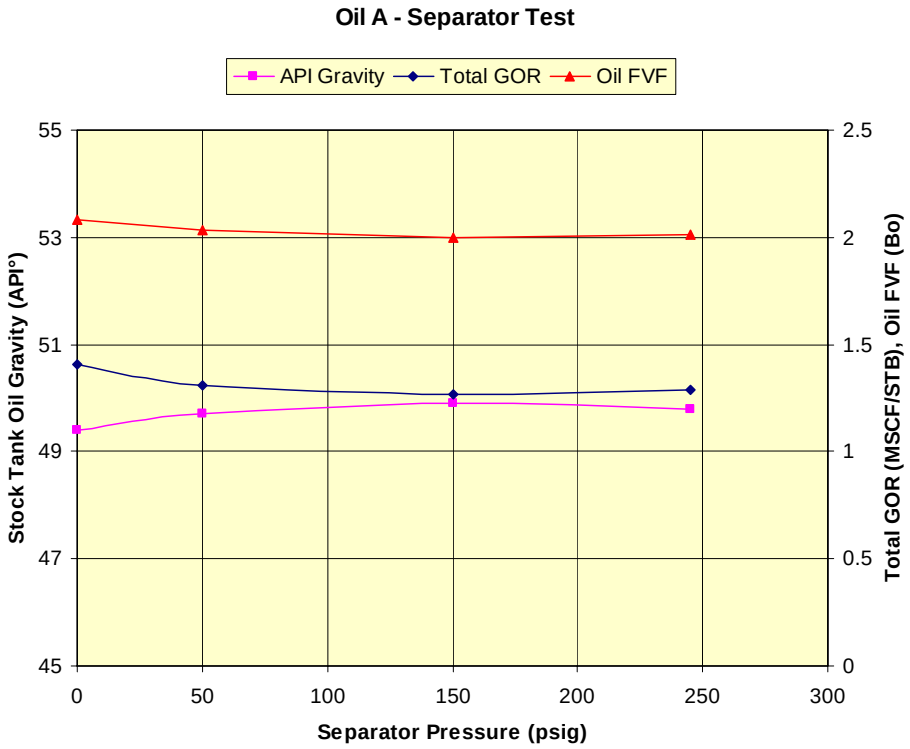

Figure 5-7: Oil A separator test data

5.2.5 Solubility Swelling Tests

Solubility-swelling tests were conducted on the reservoir fluid with CO_2 and SG#1. It was found that the addition of the injection gas caused the saturation pressure to increase and that SG#1 increased the saturation pressure more than the pure CO_2 did. This is likely to be due to the large presence of methane in the non-CO_2 components of SG#1. **Figures 5-8** and **5-9** and **Tables 5-10** and **5-11** show the relative volume data for CO_2 and SG#1 respectively.

By plotting the relative volume at saturation after addition of injection gas (or swelling factor) against the saturation pressure (or the pressure at which the injection gas is soluble) we obtain the plot shown in **Figure 5-9**, the data can be found on **Table 5-11**. From this we can see that at corresponding pressures, the pure CO_2 swells the oil more than the synthetic gas does. **Figure 5-10** shows the effect of addiction of gas on the saturation pressure of the mixture.

Table 5-9: Solubility-Swelling Test Results for Oil A with CO_2

100 mol% Oil A 0 mol% CO_2		80 mol% Oil A 20 mol% CO_2		60 mol% Oil A 40 mol% CO_2		40 mol% Oil A 60 mol% CO_2	
Pressure (psig)	Relative Volume	Pressure (psig)	Relative Volume	Pressure (psig)	Relative Volume	Pressure (psig)	Relative Volume
5000	0.91	5000	1.05	5000	1.25	5000	1.72
4000	0.93	4500	1.05	4500	1.28	4500	1.77
3500	0.95	4000	1.08	4000	1.32	4000	1.84
3000	0.97	3500	1.10	3500	1.36	3800	1.87
2500	0.99	3000	1.13	3200	1.40	3600	1.92
2350	1.00	2683	1.15	2955	1.42	3387	1.97

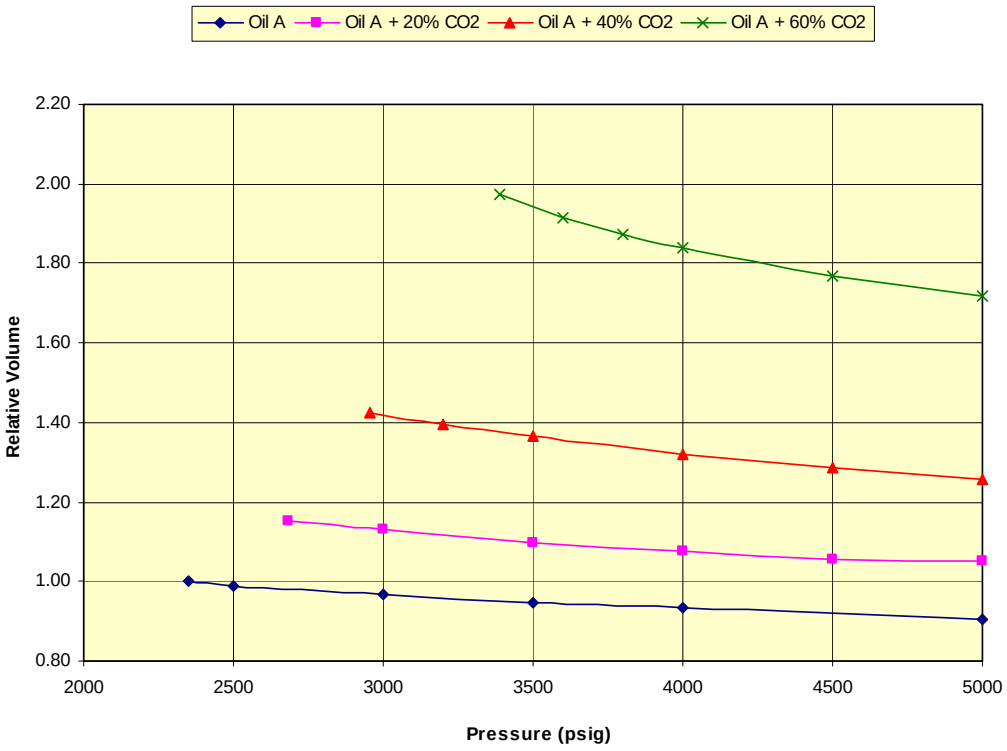

Figure 5-8: Solubility-Swelling Test for Oil A with CO_2 – Relative Volume increase with increase in gas

Table 5-10: Solubility-Swelling Test Results for Oil A with SG#1

100 mol% Oil A 0 mol% SG#1		80 mol% Oil A 20 mol% SG#1		60 mol% Oil A 40 mol% SG#1		40 mol% Oil A 60 mol% SG#1	
Pressure (psig)	Relative Volume	Pressure (psig)	Relative Volume	Pressure (psig)	Relative Volume	Pressure (psig)	Relative Volume
5000	0.90	5000	1.05	5000	1.31	5000	1.87
4500	0.91	4500	1.07	4500	1.34	4800	1.89
4000	0.92	4000	1.09	4000	1.38	4500	1.94
3500	0.94	3500	1.12	3500	1.44	4000	2.02
3000	0.96	3000	1.15	3300	1.46	3800	2.06
2350	1.00	2733	1.18	3090	1.50	3590	2.12

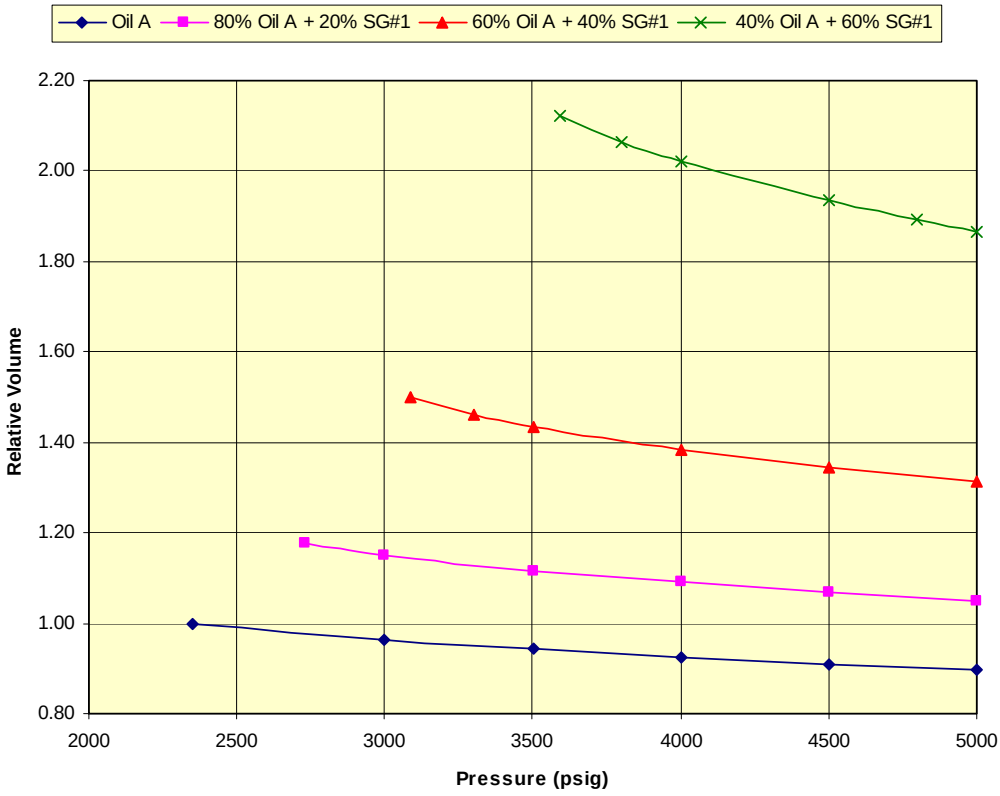

Figure 5-9: Solubility-Swelling Test for Oil A with SG#1 – Relative Volume increase with increase in gas

Table 5-11: Solubility-Swelling Test – Change in saturation pressure and swelling factor with addition of injection gas

Oil A and CO_2			Oil A and SG#1		
Injection Fluid (Mol %)	Saturation Pressure (psig)	Relative Volume	Injection Fluid (Mol %)	Saturation Pressure (psig)	Relative Volume
0	2350	1.00	0	2350	1.00
20	2683	1.15	20	2733	1.18
40	2955	1.42	40	3090	1.50
60	3387	1.97	60	3590	2.12

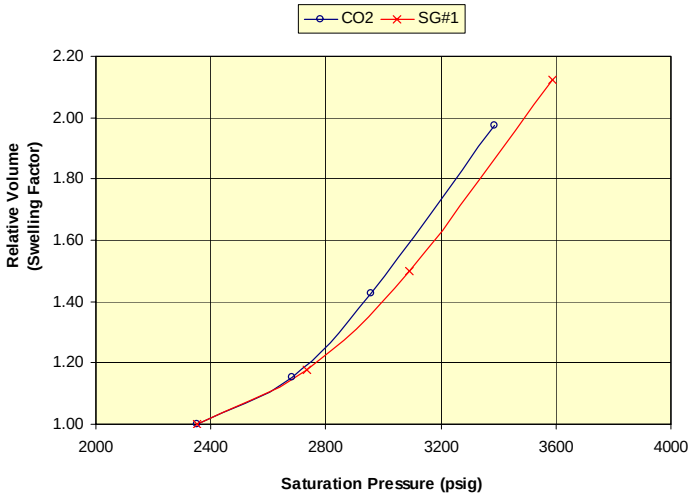

Figure 5-10: Solubility-Swelling Test for Oil A with CO_2 and SG#1 – Increase in Swelling Factor with respect to the increase in Saturation Pressure

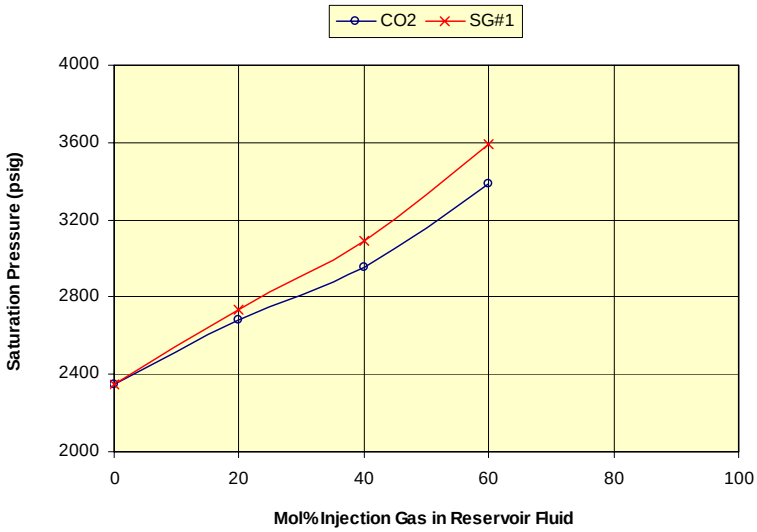

Figure 5-11: Solubility-Swelling Test for Oil A with CO_2 SG#1 – Change in saturation pressure with addition of injection gas

5.2.6 High Pressure Viscosity

During a pressure depletion at the reservoir temperature of 279°F, the viscosity of the oil phase of the reservoir fluid was determined in a rolling ball viscometer. The viscosity of the fluid was found to vary from a minimum of 0.139cP at the bubble point to a maximum of 0.428cP at atmospheric pressure.

A viscosity study was performed with mixes of 20mol% and 40mol% injection gas using both the pure CO_2 and the synthetic gas mix. It was noticed that the injection gas lowered the viscosity of the reservoir fluid and that the synthetic gas mix lowered the viscosity more than the pure CO_2. **Figures 5-13** and **5-14** show the viscosity oil plots and illustrate the effect of addition of the injection gas.

As expected the single-phase viscosity decreased due to the addition of the injection gas. However, an interesting observation was made of the two-phase fluid. Taking one example from the resultant data, the viscosity of Oil A + 40% SG#1 at 2500 psig is higher than the viscosity of Oil A at 2500 psig. This same trend was consistently seen throughout the data. Hence, below 2500 psig the viscosity of Oil A is in fact increased by the addition of these injection gases. This is due to the liquid remaining flashed liquid corresponding to the Oil A – Injection gas mix being heavier at this pressure than that of Oil A.

In our experimental studies with Oil A and CO_2 we saw that the addition of the injection gas increased the bubble point pressure (as expected). The rolling ball viscometer measures the viscosity of the liquid remaining at each corresponding pressure. Oil A + 40% SG#1 at 2500 psig had already flashed into two phases having a bubble point pressure of 3090psig. When it flashed the lighter components of both the SG#1 and Oil A are removed from the liquid phase, leaving a heavier, more viscous fluid. As the pressure drops this continues, and even though Oil A then flashes at 2350psig, the liquid phase at corresponding pressures is consistently lower than the Oil A + Injection gas mixtures catching up only at the stock conditions. The light components in the gas help vaporise the light components in the liquid.

Table 5-12 shows the compositional output from flash calculations at 2500psia and 279°F. The results match the experimental work in that the remnant liquid phase with injection gas is more viscous than that of Oil A on its own.

Table 5-12: Flash Calculation by EOS at 2500psia and 279°F:
Composition and Properties of Liquid Phase

Calculated Composition of Liquid Phase Only						
Component		**Oil A**	**Oil A + 20% CO_2**	**Oil A + 40% CO_2**	**Oil A + 20% SG#1**	**Oil A + 40% SG#1**
Hydrogen Sulphide	H_2S	0.00	0.00	0.00	0.00	0.00
Carbon Dioxide	CO_2	15.57	27.74	34.38	24.46	29.20
Nitrogen	N_2	0.73	0.51	0.37	0.55	0.43
Methane	C_1	23.95	18.10	13.95	20.16	17.22
Ethane	C_2	8.71	7.08	5.90	7.44	6.50
Propane	C_3	8.63	7.31	6.39	7.51	6.73
i-butane	iC_4	2.30	1.99	1.79	2.04	1.88
n-butane	nC_4	4.16	3.63	3.31	3.69	3.40
i-pentane	iC_5	1.46	1.30	1.21	1.32	1.25
n-pentane	nC_5	1.63	1.46	1.37	1.48	1.41
Hexanes	C_6	3.70	3.36	3.24	3.41	3.31
Heptanes	C_7	7.54	6.95	6.84	7.05	6.98
Octanes	C_8	3.80	3.54	3.53	3.59	3.61
Nonanes	C_9	3.91	3.67	3.72	3.73	3.79
Decanes	C_{10}	2.84	2.69	2.75	2.73	2.81
Undecanes	C_{11}	1.79	1.70	1.76	1.73	1.79
Dodecanes plus	C_{12}+	9.28	8.96	9.49	9.11	9.70
Total		100.00	100.00	100.00	100.00	100.00
Calculated Properties of Liquid Phase						
Z-factor		0.6392	0.626	0.6247	0.6298	0.6306
Molar Volume	m3/kmol	0.12654	0.12392	0.12366	0.12468	0.12484
MW	g/mol	70.14	70.22	72.44	70.1	72.16
Density	g/cc	0.555	0.567	0.586	0.563	0.578
Viscosity	cP	0.136	0.138	0.147	0.137	0.146
Phase Volume	%	100	83.16	64.57	81.43	62.81
Phase Mole	%	100	85.56	68.31	84.12	66.92

This is seen because the reservoir fluid is very light and has a similar viscosity to that of the injection gas at the reservoir conditions. Were the fluid heavier it is likely this would not have been seen. Instead the expected would have been seen - the viscosity of the mix always being lower than that that of the reservoir fluid on its own. The heavy molecules of the reservoir fluid would have kept some of the lighter molecules in solution even after flashing into two-phases maintaining it lighter and less viscous than the original reservoir fluid catching up only at stock tank conditions.

Were this not the case it is likely this would not have been seen but rather the opposite being the case, as shown below in **Figure 5-12**. The heavy molecules of the reservoir fluid would have kept the some of the lighter molecules in solution even after flashing into two-phases and hence the two-phase fluid would remain lighter than the original reservoir fluid.

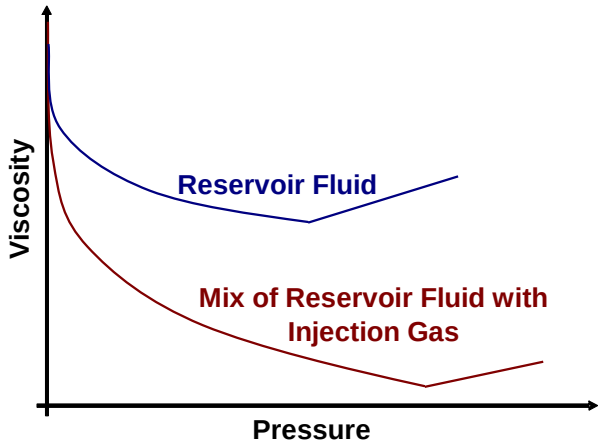

Figure 5-12: Typical viscosity relationship of a reservoir fluid compared to that of a reservoir fluid and injection gas mix

Table 5-13: Viscosity Study of Oil A with added CO_2 and SG#1

	Oil A	**CO_2**		**SG#1**	
Mol% Oil A	**100**	**80**	**60**	**80**	**60**
Mol% Inj. Fluid	**0**	**20**	**40**	**20**	**40**
Pressure (psig)	**Viscosity (cP)**	**Viscosity (cP)**	**Viscosity (cP)**	**Viscosity (cP)**	**Viscosity (cP)**
5000	0.194	0.185	0.157	0.177	0.146
4500	0.183	0.174	0.149	0.167	0.140
4000	0.173	0.164	0.140	0.156	0.133
3500	0.163	0.153	0.132	0.146	0.127
3000	0.152	0.142	0.122	0.136	0.125
2800	0.148	0.137	0.129	0.131	0.137
2600	0.143	0.138	0.142	0.137	0.150
2400	0.140	0.148	0.154	0.147	0.162
2200	0.147	0.158	0.166	0.157	0.172
2000	0.158	0.168	0.177	0.168	0.182
1800	0.169	0.178	0.189	0.178	0.192
1600	0.180	0.191	0.200	0.188	0.202
1400	0.192	0.203	0.210	0.198	0.213
1200	0.203	0.216	0.222	0.208	0.225
1000	0.214	0.229	0.235	0.220	0.238
800	0.228	0.244	0.249	0.234	0.252
600	0.244	0.259	0.266	0.249	0.268
400	0.264	0.279	0.285	0.268	0.286
200	0.291	0.306	0.312	0.296	0.309
100	0.322	0.330	0.343	0.325	0.333
0	0.428	0.428	0.428	0.428	0.428

From Extrapolation of Data :

	Pressure (psig)	Viscosity (cP)
Oil A :	2350	0.139
Oil A + 20mol% CO_2 :	2682	0.134
Oil A + 40mol% CO_2 :	2950	0.121
Oil A + 20mol% SG#1 :	2733	0.130
Oil A + 40mol% SG#1 :	3090	0.119

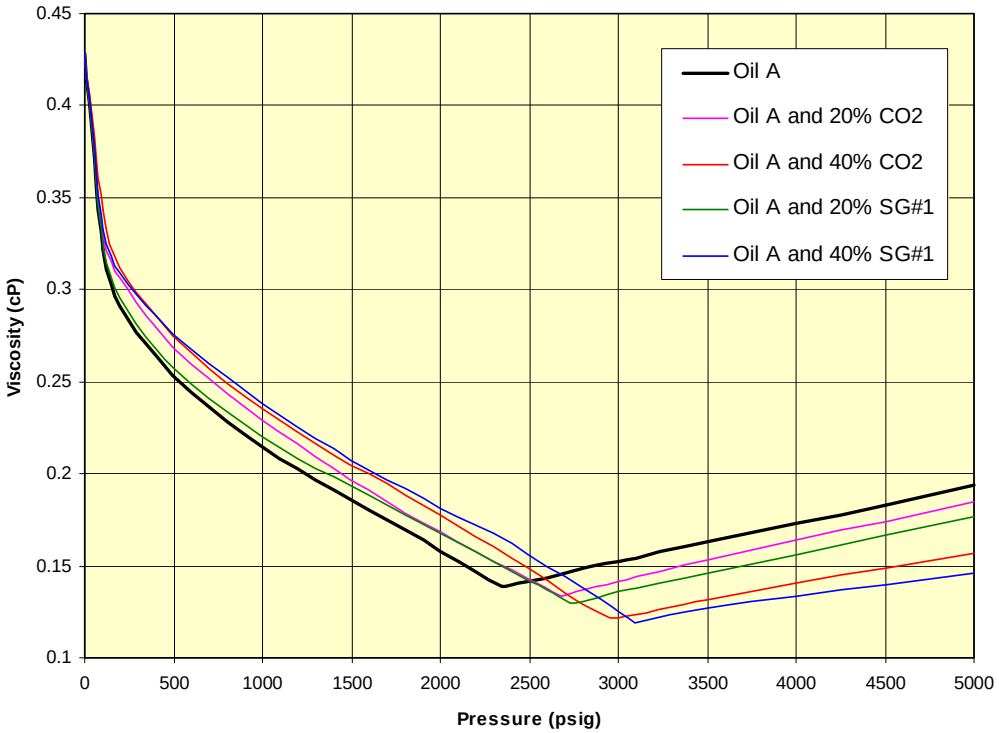

Figure 5-13: High pressure viscosity of Oil A and effect of injection gas on oil viscosity

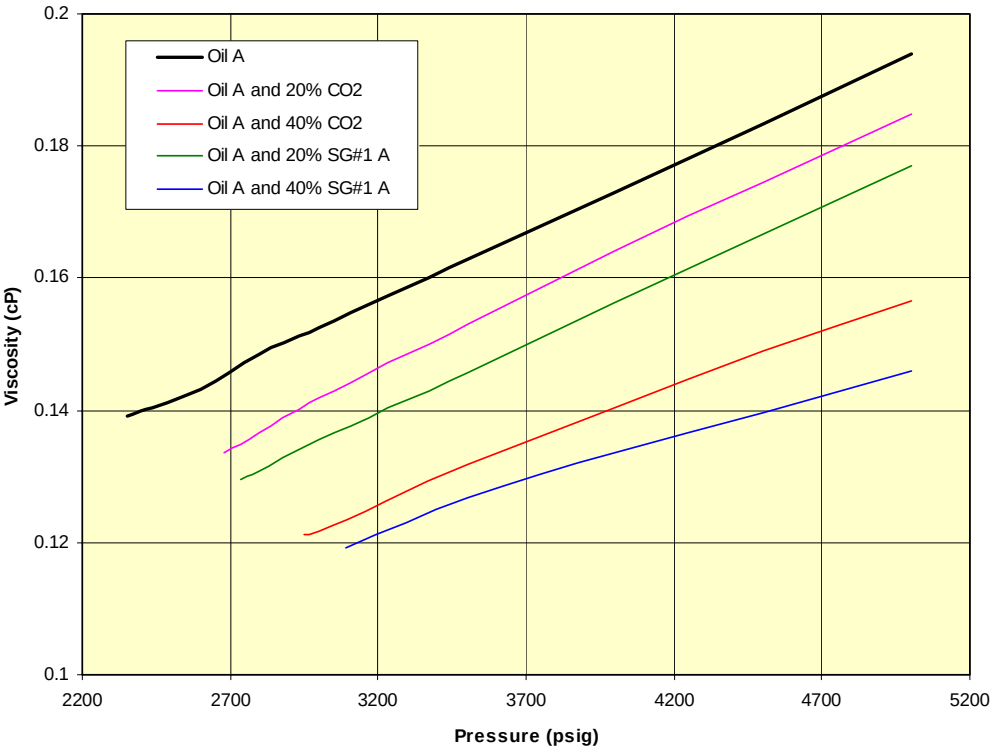

Figure 5-14: High pressure viscosity of Oil A and effect of injection gas on single-phase oil viscosity

5.3 Chapter Summary

- From the quality check of the separator gas and liquid samples, all samples checked are good and can be used to recreate representative reservoir fluid.

- The asphaltene analysis performed is indicative that asphaltenes are stable in solution with the reservoir fluid.

- The separator samples were recombined at a GOR that gave a fluid with a composition that is estimated for the time at which a possible gas injection project may commence. From pressure volume relationships established, this mix was found to have a bubble point of 2350psig at 279°F, a solution gas oil ratio of 1263 scf/stb and an oil formation volume factor of 1.998 rb/stb.

- The viscosity of the reservoir fluid as a function of pressure was determined with a minimum of 0.139cP at the bubble point pressure and a maximum of 0.428cP at atmospheric pressure.

- From the solubility-swelling study performed the saturation pressure was noticed to increase with the addition of the injection gases. The synthetic gas mix increased the saturation pressure more than pure CO_2. The pure CO_2 had caused slightly more swelling than the synthetic gas at corresponding pressures.

- From the viscosity study it was noted that the single phase viscosity was decreased by the addition of injection gas and that the synthetic gas decreased the viscosity further than pure CO_2.

6 TESTS WITH RESERVOIR CORES

The following tests were conducted using representative reservoir core plug samples from Field A:

- Porosity measurement by Liquid Saturation
- Absolute Liquid Permeability
- Core Flood at the reservoir temperature of 279°F and an injection pressure of 3,000 psig

Field A core plugs of 1.5” were taken from the 2/3 section of core. The plugs were then trimmed and cleaned in a Sohxlet extractor with a toluene:methanol mixture (50:50). Once cleaned and dried, the permeability and porosity was measured on the plugs. Two of the plugs were then selected for a reservoir condition core flood. Prior to the flood, the cores required ageing for 1000 hours in Oil A at reservoir temperature. After the ageing was complete the core pieces were charged with synthesised formation water, followed by Oil A and a reservoir condition core flood was conducted with SG#1 at 3,000 psig. **Figure 6-1** shows the Field A core plugs analysed.

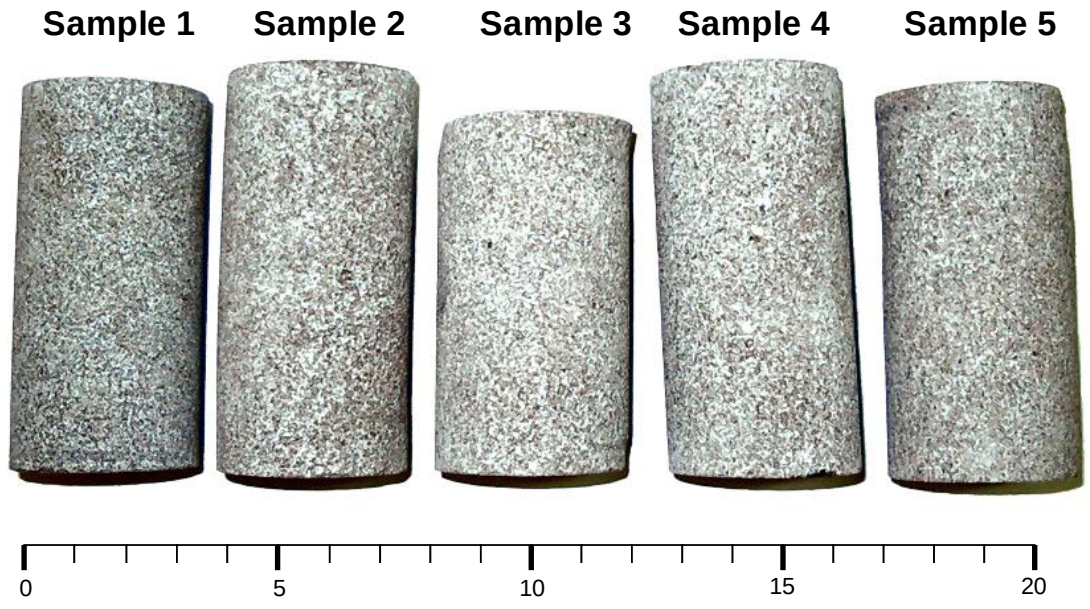

Figure 6-1: Field A core plug samples

6.1 Porosity Measurement by Liquid Saturation

The bulk volume of each sample was determined from measurements of the dimension of each plug, as from the equation below:

Eq. 6-1

$$V_B = \frac{\pi D^2}{4} * L$$

Where:

V_B = Bulk volume (cc)

D = plug diameter (cm)

L = plug length (cm)

The core plugs were then weighed dry and after saturating in distilled water.

The difference in weight was used to calculate the pore volume from the equation below:

Eq. 6-2

$$V_P = \frac{(W_{sat} - W_{dry})}{\rho_{water}}$$

Where:

V_P = pore volume (cc)

W_{dry} = Dry weight of core plug (gm)

W_{sat} = Saturated weight of core plug (gm)

ρ_{water} = Density of water (gm/cc)

The effective porosity was then calculated from the following equation:

Eq. 6-3

$$\phi_e = \frac{V_P}{V_B}$$

Where:

ϕ_e = effective porosity

6.2 Permeability

The permeability of the core plugs was determined by flowing water through the plug at a known temperature and measuring the pressure differential over the plug. The permeability was then determined from Darcy's equation:

Eq. 6-4

$$k = -\frac{q\mu}{A} * \frac{L}{\Delta P}$$

Where:

k = permeability (D)

q = flow rate (cc/sec)

μ = water viscosity (cP)

A = cross sectional area of plug (cm^2)

L = core plug length (cm)

ΔP = pressure differential over plug (atm)

Flow rate is known as it is fixed for the experiment. The viscosity of water was determined from empirical data. The cross sectional area and length of the plug is measured with a calliper and the pressure differential over the plug was measured during the test.

6.3 Reservoir Condition Core Flood

The core flood test measures the oil recovery factor from a flood by injecting a fluid into a core plug containing reservoir fluid. The test is done at reservoir pressure and temperature. The key parameters that are measured are initial and final reservoir fluid saturations. The core-flood test with additional equipment can also be used to measure relative permeabilities.

The schematic diagram of the core flood apparatus is shown in **Figure 6-2**. Prior to flooding the core plug, porosity and permeability were measured and the plug

must be cleaned and conditioned properly (Cuiec, 1975, Cuiec *et al.*, 1979, Gant, 1988). This involved cleaning the core plug in a Sohxlet extractor with a toluene:methanol mixture (50:50), saturating the dried plugs with synthetic formation water and ageing the core at reservoir temperature with the reservoir fluid for 1000 hours. The ageing process is performed to re-establish the wettability properties of the core plug. Once the core had been aged it was then completely saturated with synthetic formation water. The core was then flooded with reservoir fluid until the irreducible water saturation was attained. Once this was done the core sample was assumed to represent the original reservoir saturations.

When composite core is prepared by stacking small core plugs, the capillary continuity at the interface between two plugs is an important issue. The space between the two plugs acts as an open fracture with no permeability and the fluids which were flowing down a particular path suddenly meet a break in the path. A diaphragm is placed in between the core plugs and at the ends to ensure capillary contact. When placing in between core plugs the diaphragm aids in a fluid bridge forming across the gap between the plugs so that fluid flow can continue into the second plug with as little disturbance as possible to the saturation profile (Firoozabadi and Hague, 1990). Due to its availability, low cost and historical use for these purposes, a sheet of tissue paper was used to bridge the gap between the two core plugs and at the ends to ensure capillary contact (Oak, 1990, Ragazzini and Venturini, 1992).

The injection gas was then injected into the core and the incremental recovery of oil was measured. The fluids were flashed at the outlet and the composition of the gas stream at the outlet was measured.

By measuring the pressure differential over the core with respect to flow rate permeability alterations can be noted. A decrease in permeability can be a consequence of several problems, such as fines migration and asphaltene precipitation.

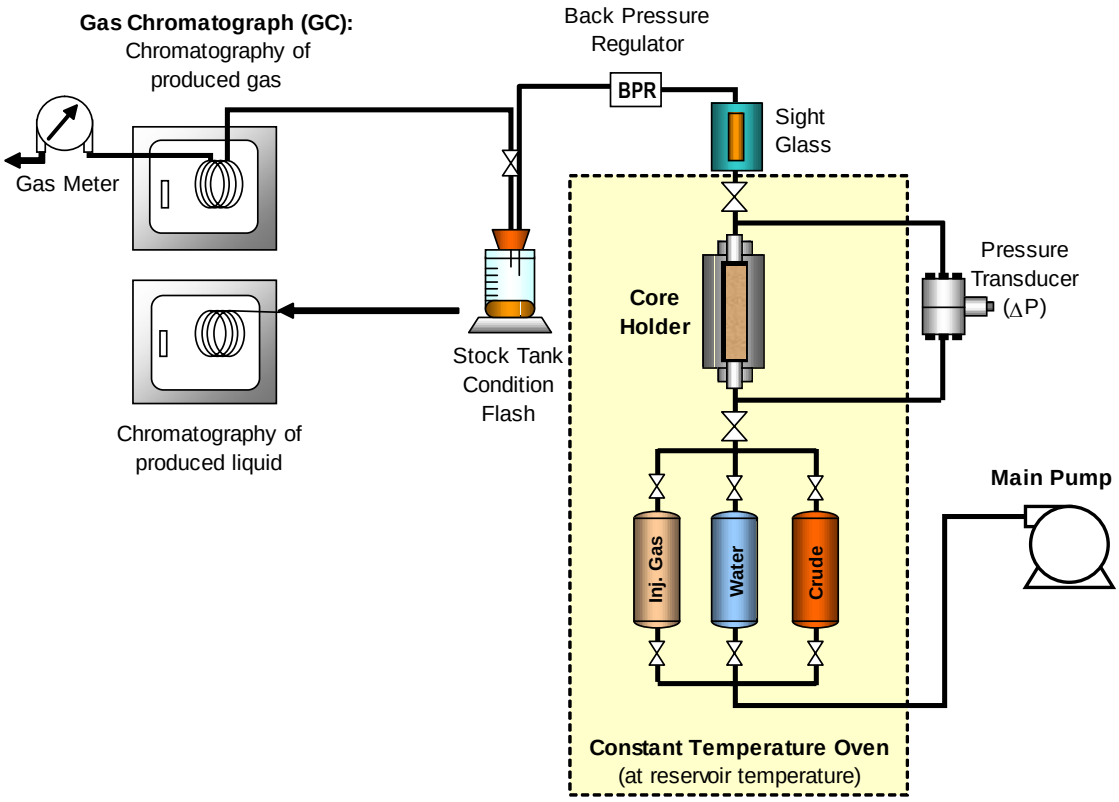

Figure 6-2: Schematic of Slim Tube experimental set-up

6.4 Discussion of Results

Five core plugs were sub sampled from core from the same well in Field A and one from a different well to compare. The well from which four plugs were taken from is the closest well from the well which fluid samples were taken from (within a kilometre). **Figure 6-1** is a photo of the 5 core plugs analysed.

Table 6-1 presents the core plug sample data including the porosity and permeability results. Porosity was measured ranging from 10% to 13% for the plugs. Very low permeability values were obtained ranging from 0.08mD to 0.16mD.

Table 6-1: Summary of basic core data

Sample No.	Diameter (cm)	Length (cm)	Porosity (%)	Permeability (mD)
1	3.801	7.678	12.95%	0.13
2*	3.802	7.931	12.62%	0.15
3*	3.800	4.775	11.19%	0.08
4	3.801	7.939	10.61%	0.16
5	3.809	6.347	11.05%	0.15

* Used in Core Flood

A reservoir condition core flood was then performed using two stacked plugs from Field A at 279°F and an injection pressure of 3000psig. After cleaning, the core plugs were saturated with synthetic formation water based on Field A formation water analysis. The core plugs were then aged in the Oil A for 40 days at reservoir temperature.

After ageing, the core plugs were charged with live reservoir fluid and the initial oil saturation (S_{oi}) of 54% was established (measured from the material balance of the oil and porosity measurements), hence, an initial water saturation (S_{wi}) was 46%. This matched well with the log derived water saturation. Once charged, the synthetic gas was injected at 3000psig. An ultimate oil recovery of 74% OOIP was measured after 0.9 PV of gas injected. This value did not increase any further with subsequent measurements.

Table 6-2 shows the test data with the volume of gas injected converted to fractions of the pore volume and the oil volume recovered as a recovery percentage. The GOR corresponding to each data point is also calculated based on stock tank oil and gas recovered and the methane to carbon dioxide ratio (C_1:CO_2) measured in the produced gas stream by gas chromatography is also shown. At breakthrough C_1:CO_2 dropped from 1.6 to 0.2, the C_1:CO_2 for the synthetic gas mix. Also the GOR increased as less oil was produced and injection gas reached the outlet. Further to this, the oil recovery steadily increased until breakthrough, after which it increased less with further gas injection and eventually reached a maximum of 74% after 0.9 PV of gas injected, leaving a residual oil saturation (S_{or}) of 14%. No formation water was measured to have been produced.

Table 6-2: Core Flood results

PV Gas Injected	Oil Recovery %	GOR (scf/stb)
0.00	0%	--
0.05	4%	1,743
0.29	26%	1,836
0.37	33%	1,816
0.43	39%	1,827
0.53	47%	1,828
0.65	58%	1,981
0.73	66%	2,540
0.85	73%	5,973
0.97	74%	24,039
1.24	74%	30,398

Results obtained from core floods can be difficult to interpret as the displacement as it occurs in the core flood test may or may not show the characteristics common to a reservoir displacement such as dispersion, mobile water, wettability, viscous fingering, gravity segregation, oil bypassing due to heterogeneity, and trapped oil saturation (Klins, 1984).

6.5 Chapter Summary

1. Porosity and permeability measurements were made on five core plug samples from two different wells of Field A. Porosities were measured in the range of 10-13% and permeabilities were all very low, measured at 0.08-0.16 mD.

2. From the core flood, an initial oil saturation (S_{oi}) of 54% was attained from measurement of oil produced and the plug porosity. This was consistent with well log data. Of this, 74% was produced after 0.9 PV of gas injection. No further oil was recovered in subsequent measurements. The residual oil saturation (S_{or}) was determined by material balance to be 14%.

7 SIMULATION STUDIES

Fully compositional models have the advantage that the composition of the fluids is modelled more accurately, however, as there is one equation per component per grid block per timestep, more equations need to be solved for the simulation. This results in either more computational time and memory required to run the simulation, or the model needs to be coarsened (fewer grid blocks and/or time steps). For modelling CO_2 floods, the difficulties in modelling the fluid are more accurately represented by a compositional model. For this reason a compositional model was chosen for modelling the core flood test. Furthermore, as the model represented only a small volume, the model created was small (30 grid cells) and as such, computational time was not an issue.

In simulating the core flood, a 3 x 1 x 10 radial model was chosen to simulate the volumetrics and the fluid flow through the core. **Figure 7-1** shows a 3D diagram of the model and a cross section of the core model.

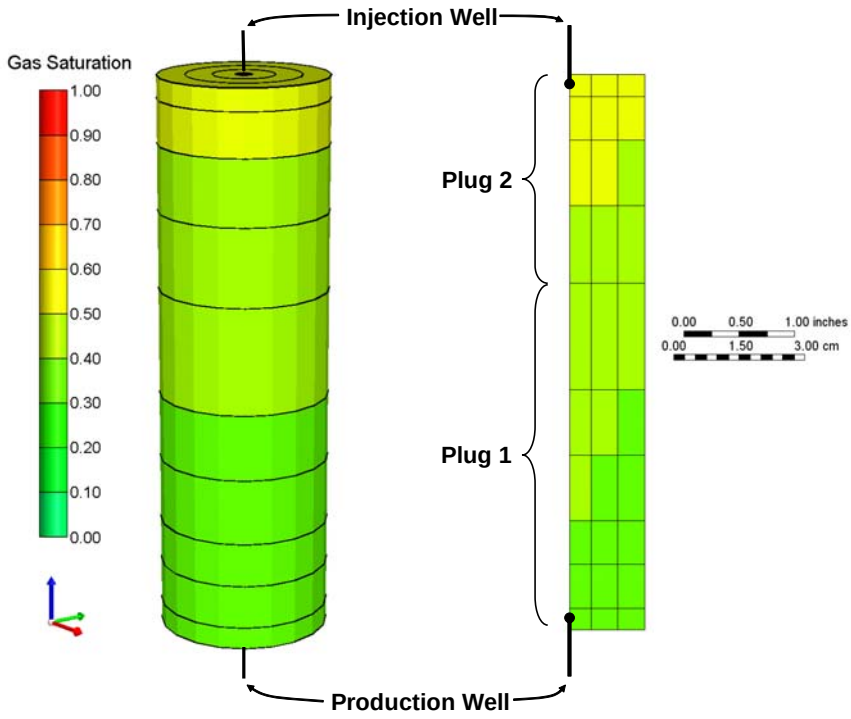

Figure 7-1: (left) 3D diagram of core flood model, (right) cross section of core flood model.

As can be seen in **Figure 7-1**, the producer was placed in grid cell 1, 1, 10 and the injector in grid cell 1, 1, 1. The grid sizing was chosen such that it represented the two core plugs used. A thin grid cell was used where the injector and producer wells are as the simulator places the well at the centre of the grid cell.

Wherever possible the true conditions observed during the experiment were adhered to, this includes:

- Well Placement
- Core placed vertically
- Dimensions (1.5” core plug, 5” total length)
- Connate water saturation of 46%
- Reservoir fluid model based on reservoir fluid composition and PVT analysis
- Porosity (12.62% for plug 1, 11.19% for plug 2)
- Absolute permeability (0.15mD for plug 1, 0.08mD for plug 2)
- Experimental temperature of 279°F

The gas-oil relative permeability was used as the main means of history matching once all other parameters were in place as no laboratory data was available upon which to base the curves.

The horizontal permeability was also altered in order to stabilise the gas front as it passed through the core.

The flow of fluids into the injection well was constrained by a maximum bottom hole pressure and bottom hole fluid rate. The flow of fluids out of the injection well was constrained by a minimum bottom hole pressure and bottom hole fluid rate.

First a parametric sensitivity was performed on a model that matched well the experimental data. After this an investigation into the effect of changing the injection gas and production regime was undertaken.

7.1 Comparison of Injection Gases

The second batch of simulation work had a more specific aim. Once the first batch of work giving the parametric sensitivities was completed the model was modified as follows:

- The fluid model was fine-tuned based on Oil A data from the laboratory work performed.
- The experimental core flood was history matched with the new fluid model.
- Permeability in i, j and k directions all equal.
- A thin grid block was placed at both ends so that the wells, which were placed in the centre of grid-block, is closer to the end of the plug.
- Permeability in the thin layer where wells were placed (cells 1,1,10 and 10,1,10) increased to 2000mD so injection and production fluids were spread evenly across the layer prior to reaching the next layer. This is to emulate the ends of the core holder which distribute the fluid across the face end of the plug.

The base case was run with SG#1 at 3000psig (3014.7psia) as per the core flood experiment. Once the model satisfactorily matched the experimental data, the simulation was run with the injection gases at the injection pressures shown on **Table 7-1**. Temperature of the model was always maintained constant.

Table 7-1: Simulation models to determine the effect of injection gas composition

Injection gases used and injection pressure at which model run

Injection Gas	**Injection Pressure (psia)**
Base Case (SG#1 at 3000psig)	3014.7
SG#1 1500psia	1500
SG#1 2200psia	2200
SG#1 3000psia	3000
SG#1 3200psia	3200
SG#1 3500psia	3500
SG#1 4000psia	4000
SG#2	3000
CO_2	3000
Gas#1	3000
Gas#2	3000
Gas#3	3000
Gas#4	3000
Methane	3000
Ray Gas	3000
Sam Gas	3000
Sam Gas at 2200psia	2200
Bob Gas	3000
Tim Gas	3000
Tim Gas 2200psia	2200
Ben Gas	3000

7.1.1 Injection Gas Compositions

The following tables, **Table 7-2**, **Table 7-3** and **Table 7-4** show the compositions of the gases used.

Table 7-2: Gas compositions – CO_2, Ray Gas, SG#1 and SG#2

Component		CO_2 Mol %	Ray Gas Mol %	SG#1 Mol %	SG#2 Mol %
Hydrogen Sulphide	H_2S	0.00	0.00	0.00	0.00
Carbon Dioxide	CO_2	100.00	45.53	80.20	79.61
Nitrogen	N_2	0.00	0.96	0.35	0.16
Methane	C_1	0.00	41.48	15.31	15.45
Ethane	C_2	0.00	6.80	2.34	1.89
Propane	C_3	0.00	2.87	1.10	0.97
Iso-Butane	iC_4	0.00	0.55	0.22	0.19
N-Butane	nC_4	0.00	0.63	0.19	0.22
Iso-Pentane	iC_5	0.00	0.24	0.07	0.10
N-Pentane	nC_5	0.00	0.19	0.06	0.55
Hexanes	C_6	0.00	0.22	0.06	0.27
Heptanes	C_7	0.00	0.23	0.06	0.46
Octanes	C_8	0.00	0.12	0.03	0.08
Nonanes	C_9	0.00	0.07	0.01	0.04
Decanes	C_{10}	0.00	0.07	0.00	0.01
Undecanes	C_{11}	0.00	0.04	0.00	0.00
Dodecanes Plus	C_{12}+	0.00	0.00	0.00	0.00
TOTAL		100.00	100.00	100.00	100.00
Mol Weight		44.01	32.04	39.52	40.08
Gas Gravity		1.526	1.111	1.370	1.39
P_c (psia)		1071	845.9	989.5	984.6
T_c (R)		547.9	470.4	518.7	523.2

Table 7-3: Gas compositions – Gas#1 to Gas#4

Component		Gas#1 Mol %	Gas#2 Mol %	Gas#3 Mol %	Gas#4 Mol %
Hydrogen Sulphide	H_2S	0.00	0.00	0.00	0.00
Carbon Dioxide	CO_2	91.75	90.84	89.08	87.38
Nitrogen	N_2	0.20	0.20	0.19	0.19
Methane	C_1	8.05	7.97	7.82	7.67
N-Pentane	nC_5	0.00	0.99	2.91	4.76
TOTAL		100.00	100.00	100.00	100.00
Mol Weight		41.73	42.03	42.61	43.17
Gas Gravity		1.446	1.457	1.478	1.498
P_c (psia)		1037.3	1031.8	1021.3	1011.1
T_c (R)		530.8	533.9	540.0	545.8

Table 7-4: Gas compositions – Sam Gas, Bob Gas, Tim Gas and Ben Gas

Component		Sam Mol %	Bob Mol %	Tim Mol %	Ben Mol %
Hydrogen Sulphide	H_2S	0.00	0.00	0.00	0.00
Carbon Dioxide	CO_2	1.83	20.56	26.83	99.06
Nitrogen	N_2	1.38	0.63	0.85	0.00
Methane	C_1	92.41	69.18	50.70	0.93
Ethane	C_2	3.87	6.09	13.98	0.01
Propane	C_3	0.33	2.15	4.41	0.00
Iso-Butane	iC_4	0.03	0.29	0.68	0.00
N-Butane	nC_4	0.05	0.45	1.20	0.00
Iso-Pentane	iC_5	0.03	0.15	0.36	0.00
N-Pentane	nC_5	0.07	0.15	0.39	0.00
Hexanes	C_6	0.00	0.17	0.34	0.00
Heptanes	C_7	0.00	0.13	0.20	0.00
Octanes	C_8	0.00	0.05	0.06	0.00
Nonanes	C_9	0.00	0.00	0.00	0.00
Decanes	C_{10}	0.00	0.00	0.00	0.00
Undecanes	C_{11}	0.00	0.00	0.00	0.00
Dodecanes Plus	C_{12}+	0.00	0.00	0.00	0.00
TOTAL		100.00	100.00	100.00	100.00
Mol Weight		17.45	24.07	28.5	43.75
Gas Gravity		0.604	0.834	0.988	1.517
P_c (psia)		672.5	747.5	771.8	1067.2
T_c (R)		355.4	410.8	455.4	546

7.1.2 Fluid Model

A fluid model was created using CMG's WinProp. This was based on the following data from the measured analyses on Oil A:

- Composition of Oil A
- Relative volume plot
- Gas compressibility (Z-factor)
- Percent liquid from CVD
- Oil viscosity

The model was created using the Peng-Robinson equation of state (Peng and Robinson, 1976). The fluid model matched the experimental data very well except for the Z-factor. This is likely to be due to the large amount of CO_2 in Oil A. The comparison of simulated (Sim.) and experimental (Exp.) data is shown in the following four diagrams. **Figure 8-2** shows the oil formation volume factor and

produced gas from CVD test, **Figure 8-3** shows the relative oil volume plot, **Figure 8-4** shows the gas compressibility (Z) factor and **Figure 8-5** shows the oil and gas viscosity as a function of pressure.

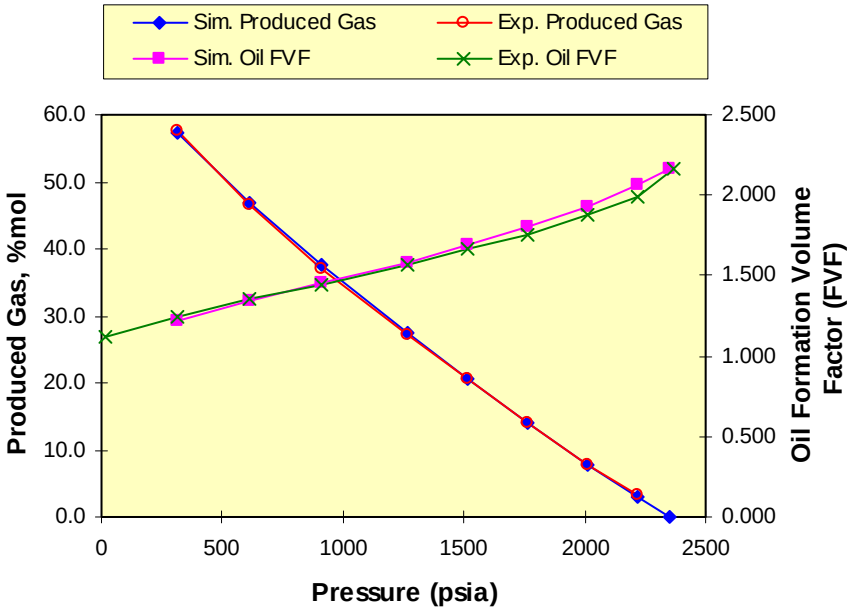

Figure 7-2: Comparison of simulated and measured formation volume factor and produced gas from CVD test.

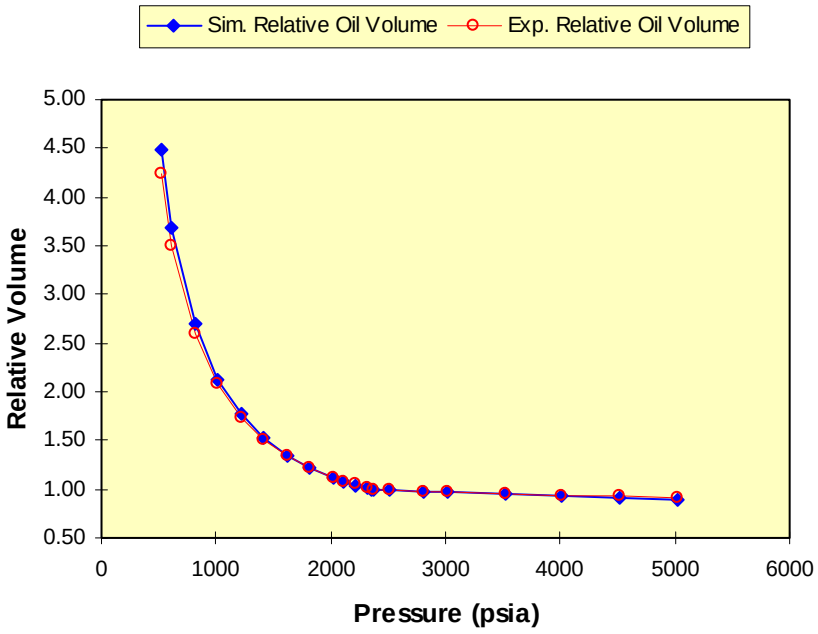

Figure 7-3: Comparison of simulated and measured relative oil volume plot.

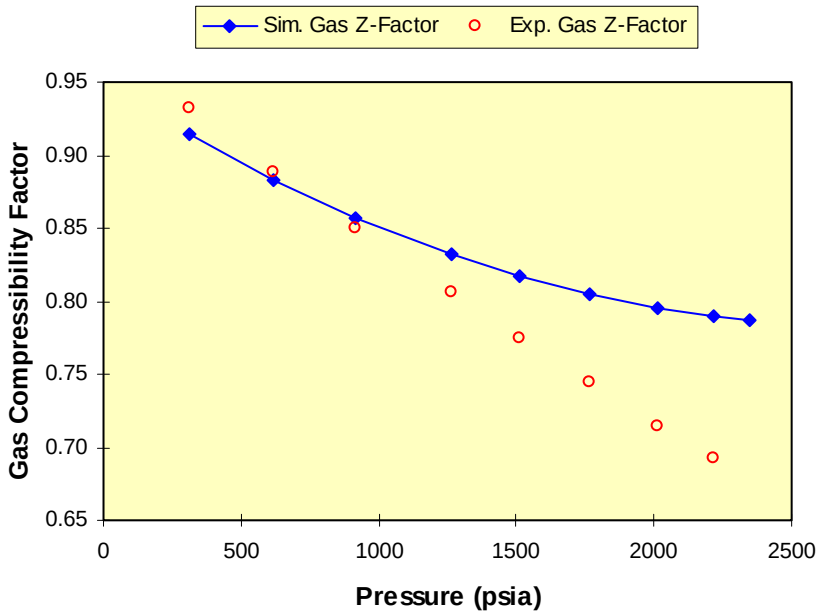

Figure 7-4: Comparison of simulated and measured gas compressibility (Z) factor.

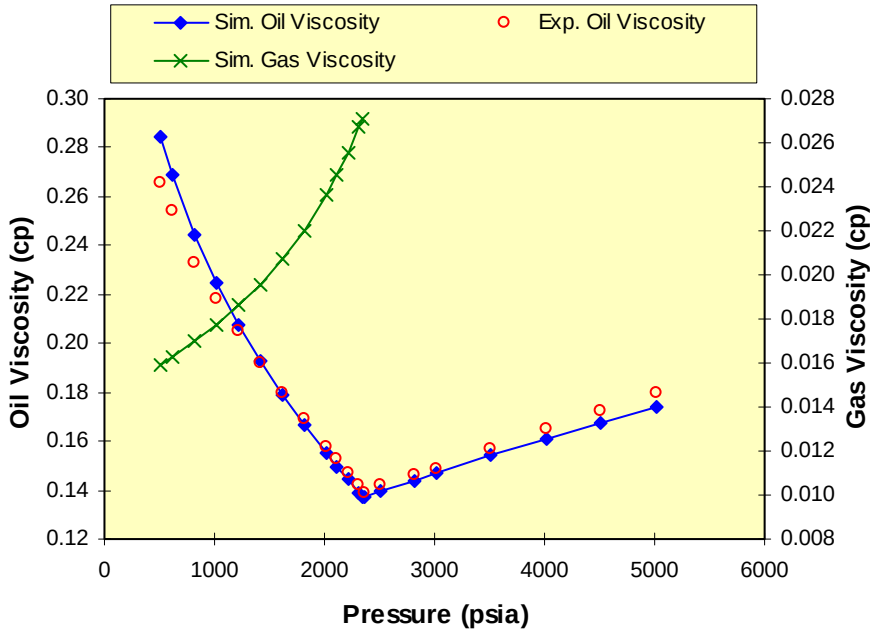

Figure 7-5: Comparison of simulated to measured oil viscosity as a function of pressure. Simulated gas viscosity is also shown.

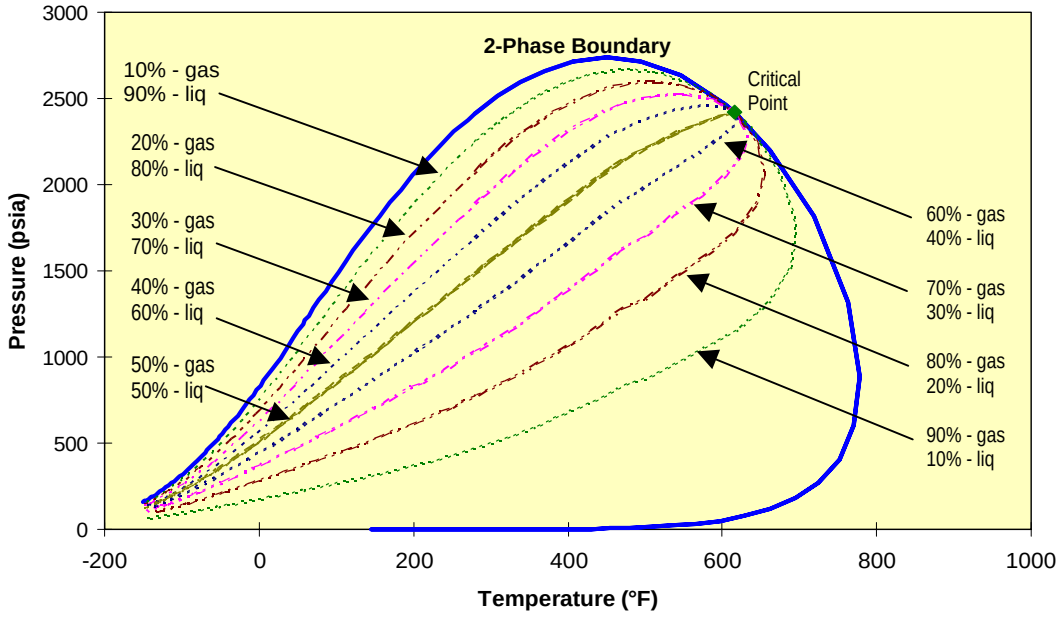

Figure 7-6: Oil A phase diagram produced from fluid model with gas-liquid ratios curves.

7.2 Comparison of Base Case to Experimental Core Flood

The reservoir condition oil recovery was used as the basis of the match of simulated data to the experimental data. This was to ensure that the residual oil saturation matched that of the experimental data. The experimental core flood data can be found on **Table 7-5** and the simulated core flood data can be found on **Table 7-6**. The comparison of the two can be found in **Figure 7-7**.

Table 7-5: Experimental Core Flood Data

PV Gas Injected	Oil Recovery %	GOR (scf/stb)
0.00	0%	--
0.05	4%	1,743
0.29	26%	1,836
0.37	33%	1,816
0.43	39%	1,827
0.53	47%	1,828
0.65	58%	1,981
0.73	66%	2,540
0.85	73%	5,973
0.97	74%	24,039
1.24	74%	30,398

Table 7-6: Simulated Flood Data

PV Gas Injected	Oil Recovery %	GOR (scf/stb)
0.01	0.0%	
0.01	0.9%	1,892
0.02	1.5%	1,892
0.03	2.0%	1,892
0.04	3.1%	1,892
0.07	5.7%	1,892
0.10	8.4%	1,892
0.17	13.8%	1,894
0.21	17.9%	1,897
0.26	21.9%	1,903
0.32	27.5%	1,925
0.39	33.2%	1,967
0.44	38.6%	2,031
0.51	44.4%	2,141
0.57	50.3%	2,327
0.63	55.2%	2,551
0.68	60.2%	2,882
0.73	65.2%	3,537
0.76	67.3%	4,025
0.80	69.4%	5,698
0.87	70.7%	8,828
0.89	71.0%	10,148
0.95	71.4%	12,308
1.02	71.6%	13,755
1.08	71.7%	14,815
1.15	71.7%	15,599
1.21	71.7%	16,364
1.27	71.7%	17,086

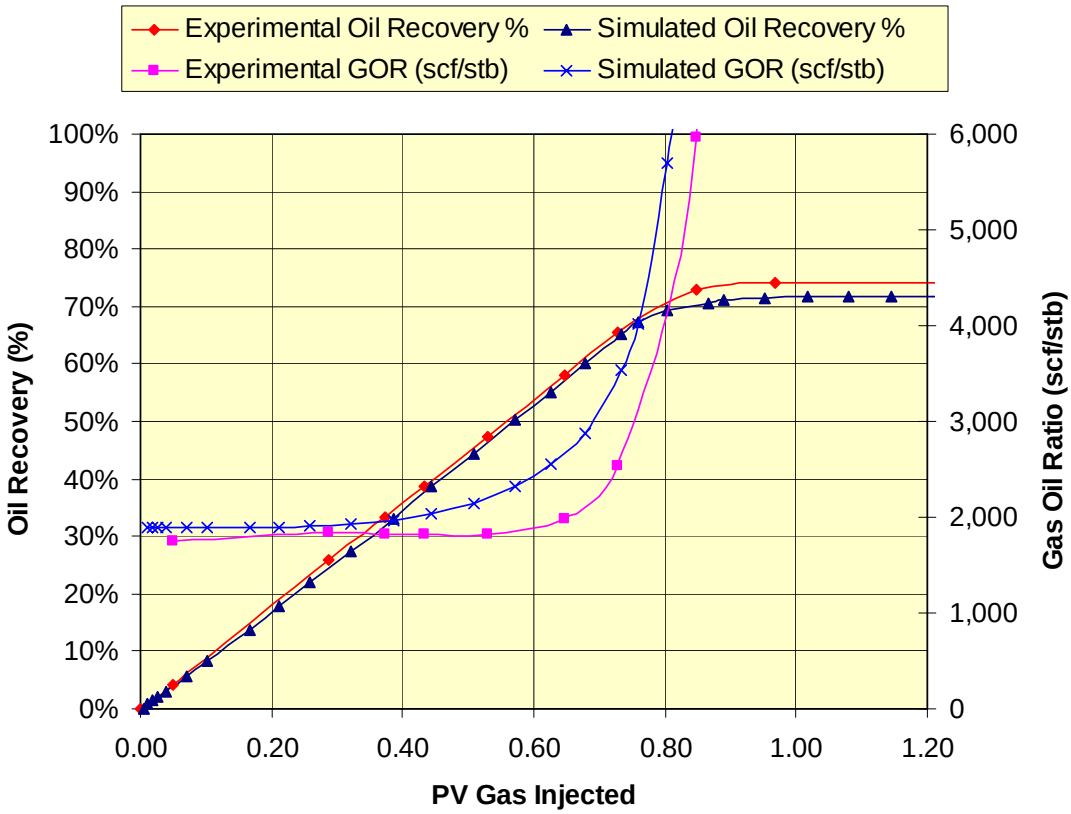

Figure 7-7: Comparison of simulated and experimental core flood of Oil A with Field A plugs using SG#1 as the injection gas at 3000psig and 279°F

7.3 Comparison of Different Injection Gases

Once the base case model was created and satisfactorily matched the experimental data, the injection gas composition was modified to see the subsequent effect on oil recovery due to change in injection gas composition.

As expected, the gases primarily made up of CO_2 had higher recoveries and those with higher methane contents. This is illustrated in the recovery plots shown in **Figure 7.8** and **Figure 7.9** and in the summary of comparison of injection gases shown in **Figure 7.12**. It was noticed that the oil recovery of methane-rich gases that were also rich in C_3+ components was quite high and comparable to the recoveries obtained from flooding with pure CO_2.

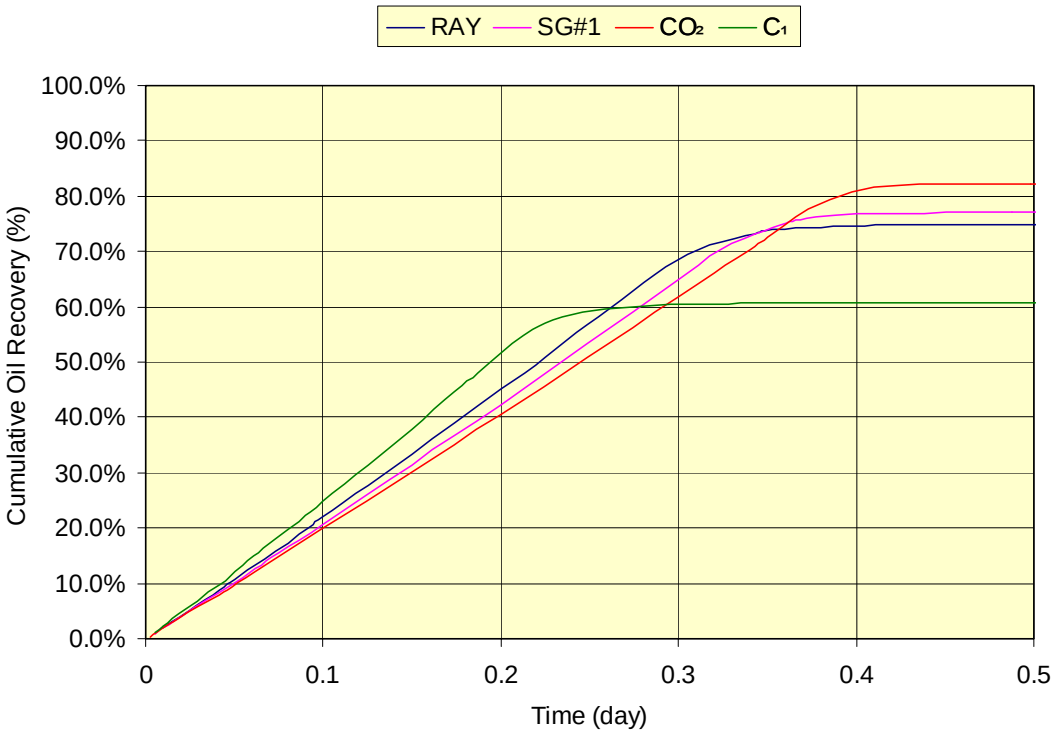

Figure 7-8: Cumulative oil recovery of Ray Gas, SG#1, CO_2 and C_1

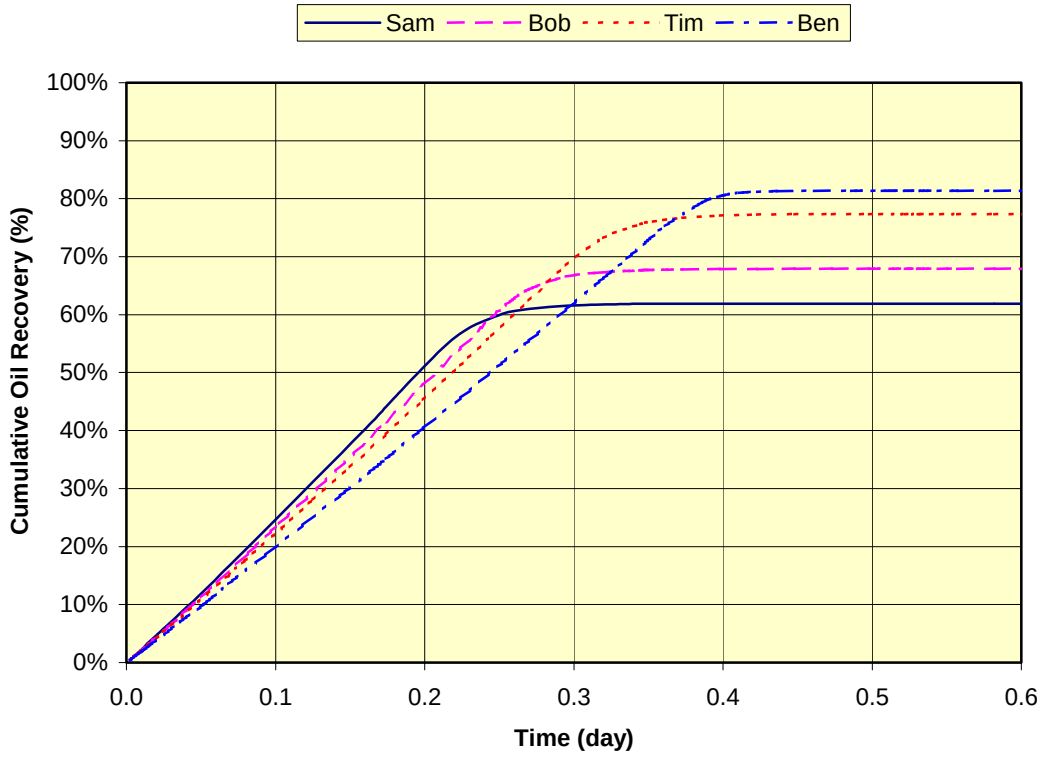

Figure 7-9: Cumulative oil recovery of Sam Gas, Bob Gas, Tim Gas and Ben Gas

Figure 7-10 shows the recovery plot of some of three of the gases with a different injection regime. In these scenarios, the reservoir pressure initiated at 3200 psia, it was then depleted to 2200 psia, injection then commenced (at 0.5day) for 1.5 PV at 0.004279m^3/day.

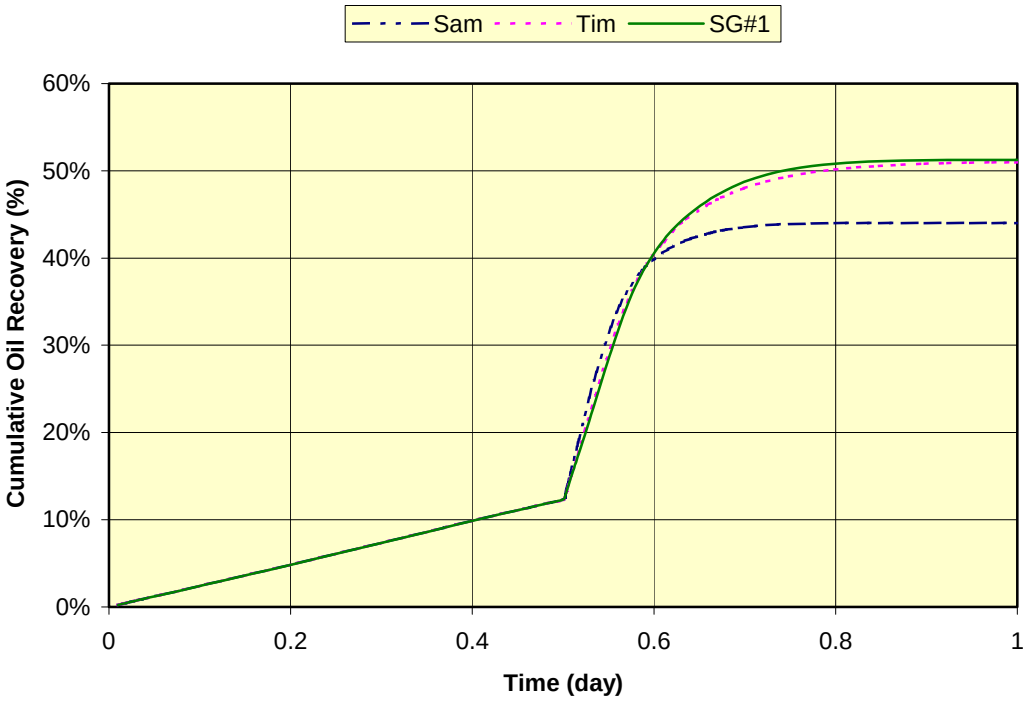

Figure 7-10: Cumulative oil recovery of Sam Gas, Tim gas and SG#1 with injection after depletion to 2200 psia

Figure 7-11 shows the recovery plots of Gas #1, Gas #2, Gas #3 and Gas #4. As expected the addition of nC_5 improved the recovery of oil. It was seen to improve from 78.6% for Gas #1 to 85.1% for Gas #4.

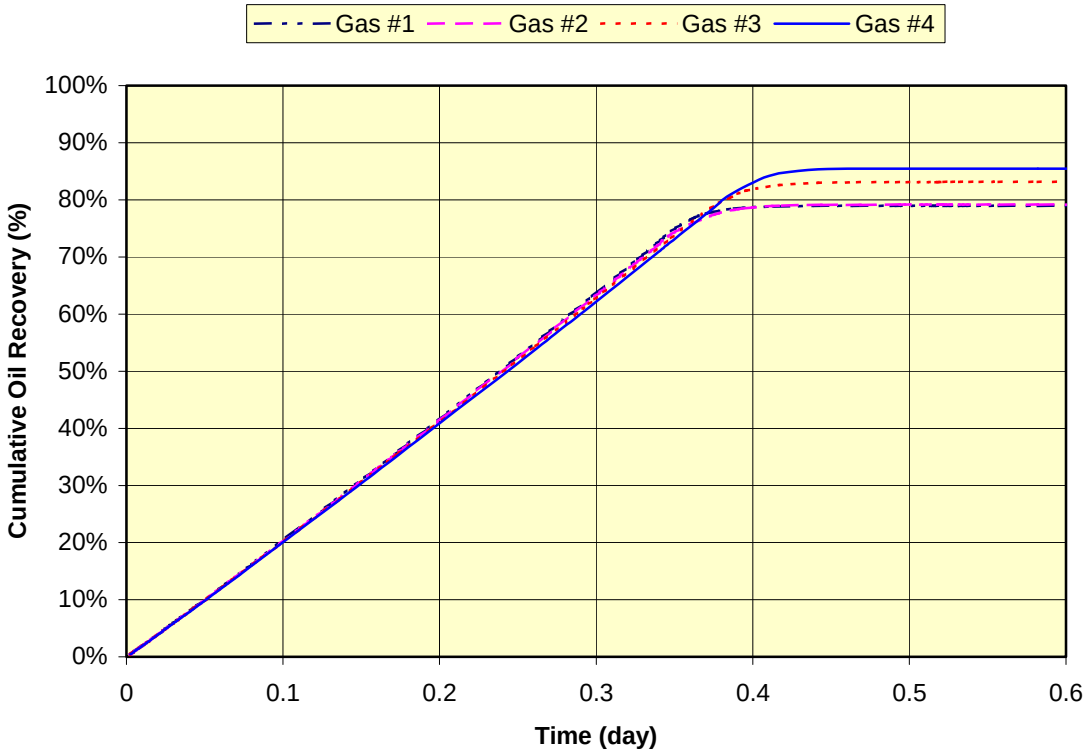

Figure 7-11: Cumulative oil recovery of Gas #1, Gas #2, Gas #3 and Gas #4

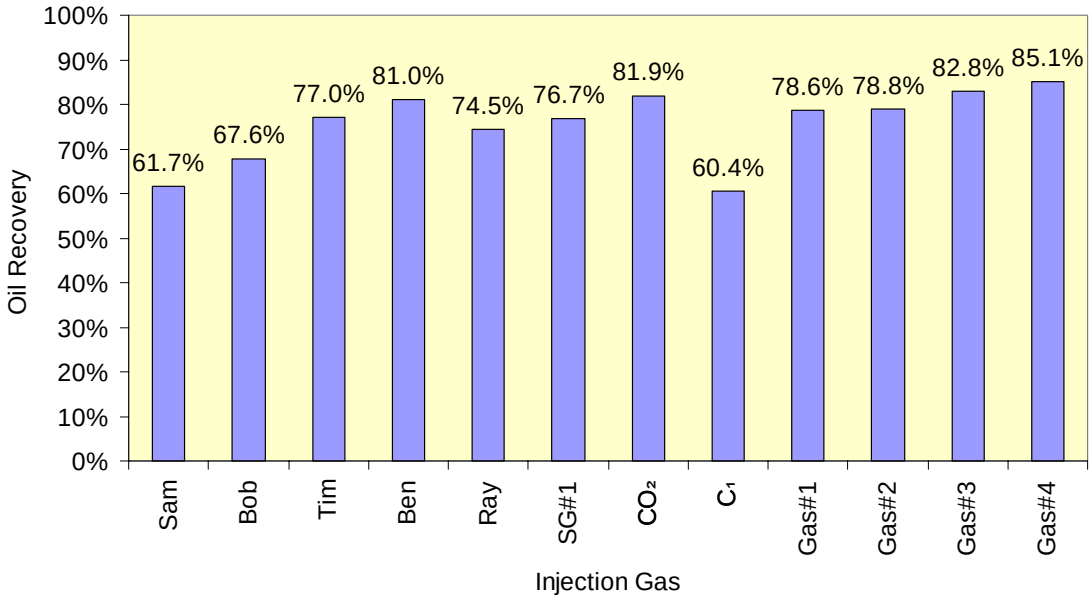

Figure 7-12: Comparison of cumulative oil recovery of all injection gases injected at 3000psia

7.4 Economic Benefit of Different Injection Gases

First and foremost, the work done in determining the economic benefit of each injection gas is not a complete economic evaluation. The value of the injected components was subtracted from the value of produced components and the plot generated over time was compared to that of the other injection gases. In implementing the injection project other costs are also involved such as pipelines, compression of the injection gas stream and surface facilities. However, due to the information either being not available or of confidential nature a complete economic evaluation was not performed. However, this analysis was performed with the aim of comparing the benefit of the different injection gases based on a dollar figure.

The assumptions made were as follows:

- Price of methane - ethane pseudocomponent of AU$3 per GJ
- Price of propane - butane pseudocomponent of AU$60 per boe
- Price of pentane plus pseudocomponent of AU$70 per boe
- 5.81608 GJe per boe
- CO_2 not considered to have a price due to its abundance and lack of market in the geographical area of interest

Based on this calculation, the methane rich Sam Gas showed the poorest results while pure CO_2 showed the best results. Sam Gas yielded approximately 85% of what of the “dollars profit” value for CO_2. While Tim Gas was not quite as good as CO_2 or the high CO_2 content gases, it was not much worse with an ultimate recovery of approximately 95% of what of the “dollars profit” value for CO_2. Out of the gases that were not rich in CO_2 (Sam Gas, Tim Gas and Bob Gas) Tim Gas yielded the best results. Pipeline costs are less for gases that are lower in CO_2 content as the gas is less corrosive. Due to this, a complete economic analysis may show that Sam Gas, Tim Gas or Bob Gas are better candidates than a CO_2 rich gas stream, with Tim Gas seeming to be the better option of the three. Other factors will include distance from the source of the gas stream to Field A as this will effect pipeline costs.

Analysing the results of Gas #1, Gas #2, Gas #3 and Gas #4 we find an interesting conclusion. The addition of nC_5 increases the oil recovery as expected, however when we look at the net dollars (price of components produced minus injected) all four gases give very similar results and in fact the results show a small deficit when nC_5 is added to the injection gas. This difference is greater if the net present value of the components is also taken into account since the produced components give you dollars later in time. Hence the conclusion that, although more oil will be produced, it is less feasible to add nC_5 to the injection gas.

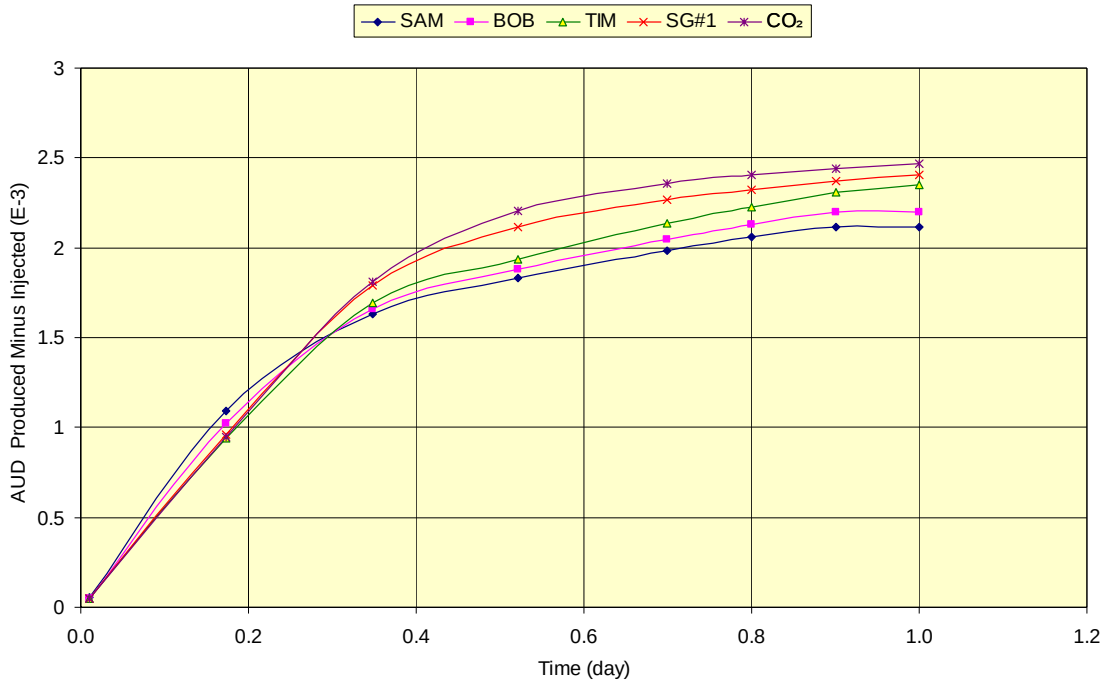

Figure 7-13: Comparison of AUD produced minus injected for Sam Gas, Bob Gas, Tim Gas, SG#1 and CO_2

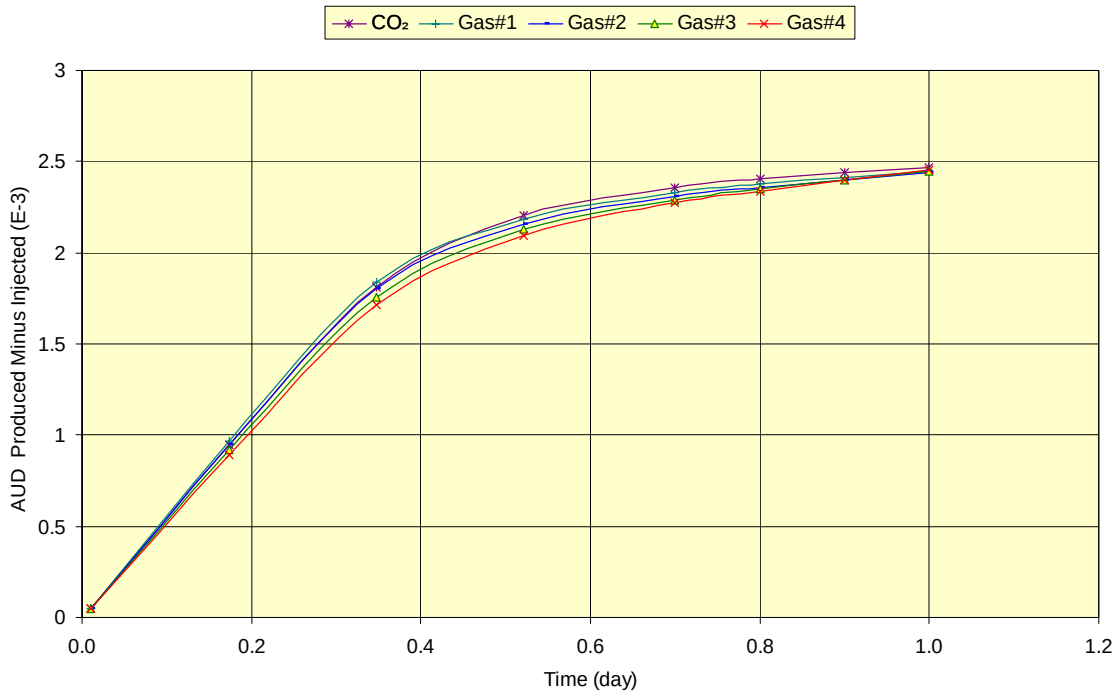

Figure 7-14: Comparison of AUD produced minus injected for CO_2, Gas #1, Gas #2, Gas #3 and Gas #4

7.5 Chapter Summary

- Excluding Gas #1, Gas #2, Gas #3 and Gas #4, pure CO_2 produced the best recoveries.
- Gases such as SG#1 and Tim gas, although high in methane, yield good oil recoveries due to the C_3+ fraction present in the gas stream.
- Although recoveries improved with addition of nC_5, the economic benefit of produced components to cost of injected components was only slightly worse when nC_5 was added. However, this does not account for Net Present Value (costs are incurred before benefit received) which would further decrease the benefit.

8 MISCIBILITY STUDIES

As mentioned in Chapter 2: Literature Review, several methods exist for determining the MMP, these include:

- Measurement by Slim Tube (industry standard)
- Measurement by RBA
- Calculation through Equation of State
- Estimation with a suitable correlation

In this project MMP was measured using both the Slim Tube and RBA. These results were compared to correlated results (Bon *et al.*, 2005).

A discussion of these methods, the benefits of each and the differences between the methods are presented below.

8.1 Slim Tube Method for Measuring MMP

From a Slim Tube test we determine the oil recovery as a function of injection pressure, observe miscibility and breakthrough time of the injection gas. Furthermore, the change in produced gas and oil properties can be monitored by placing a GC at the outlet. The recoveries determined are unrealistically high due to the idealized properties of the Slim Tube (ultra-high permeability, no water in pore volume). From measurements of several oil recoveries at a variety of pressures, the MMP can be determined. This is the key motive for the Slim Tube test.

The Slim Tube is first charged with the reservoir fluid in an oven at the reservoir temperature and at the operating pressure of the test. 1.2 pore volumes (PV) of CO_2 are then passed through and the volume of oil displaced by the CO_2 is measured. The test is repeated at several different pressures and at reservoir temperature so as to simulate the reservoir conditions as best as possible. By plotting the recovery at 1.2 PV at each injection pressure the plot shown in **Figure 8-1** can be generated. Once the injection fluid becomes miscible with the reservoir

fluid an inflection in the curve is noticed and the recovery will not improve as much above with a step change in pressure. The MMP is the intersection of the extrapolation of the miscible and immiscible parts of the curve.

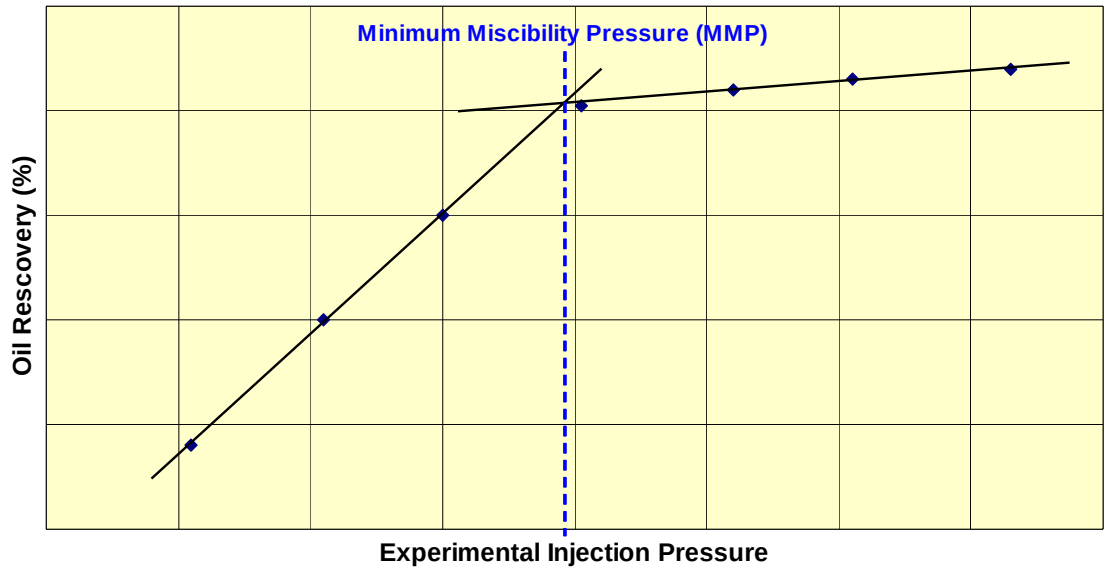

Figure 8-1: MMP determination from break-over point on recovery versus injection pressure plot

8.1.1 Slim Tube Design

The design of the Slim Tube is based on the following criteria (Wu and Batycky, 1990, Randall and Bennion, 1989, Flock and Nouar, 1984, Elsharkawy *et al.,* 1992, Thomas *et al.,* 1994, Novosad *et al.,* 1990):

- Length – the Slim Tube is made long to provide enough room for the development of a miscible bank and minimise the effect of the transition zone length. Typically a length between 20ft to 60ft is used, with 40ft being most common.
- Inner Diameter (ID) – the ID of the tubing is kept thin so that viscous fingering is eliminated. Usually ¼ in. stainless steel tubing is used.
- Packing Material – the Slim Tube is packed with either crushed silica grains or glass beads to create a porous media and mimic the reservoir conditions.
- Permeability – the permeability is high (above ~2.5 Darcy (Elsharkawy *et al.,* 1992)) so that the test can be carried out within a day and pressure drop across the Slim Tube is minimised. A lower permeability would imply a lower injection rate and the test would take longer to complete.

8.1.2 Miscibility Criteria for Slim Tube Tests

Various miscibility criteria exist for MMP determination by Slim Tube, such as the break-over point on pressure-recovery plot for recoveries at a fixed pore volume (PV) of gas injected (often 1.2 PV or 1.0 PV) or the pressure at which the oil recovery exceeds a certain amount (often 90% may be used). The break-over point on the pressure-recovery at 1.2 PV plot is commonly selected as the MMP as other aspects of the Slim Tube such as packing material and permeability influence the oil recovery. Further to this, experience has shown that generally after 1.2 PV very little additional oil will be recovered, therefore recoveries at different injection pressures can be compared to one another.

Four Slim Tube tests were conducted with each gas. Two of the tests were carried out with an injection pressure above the MMP, and two below. The break-over pressure on pressure-recovery plot for recoveries at 1.2 PV gas injected was taken to be the MMP.

Miscibility was also observed at each injection pressure through a sight glass placed at the outlet of the Slim Tube. A schematic diagram of the experimental setup is given in **Figure 8.2**.

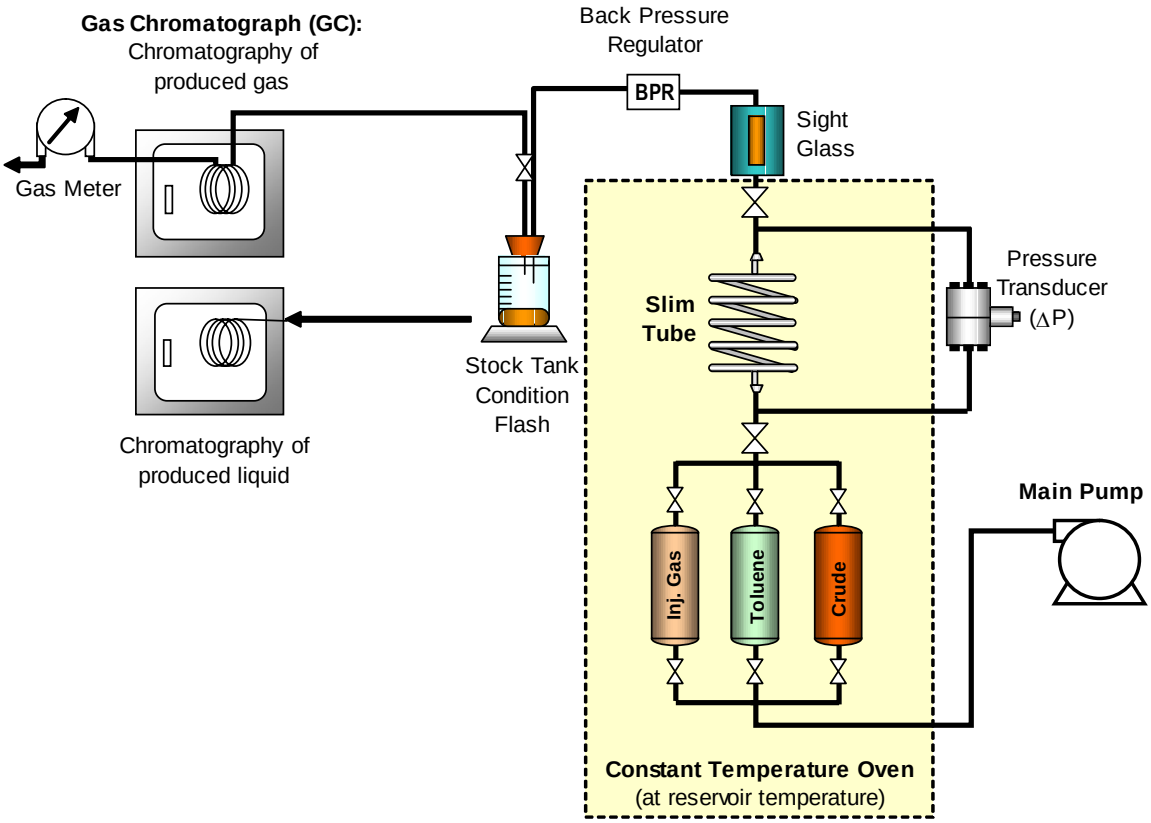

Figure 8-2: Slim tube experimental set-up.

A constant rate pump was used to maintain the gas injection flow rate at 15cc/hour through the 40ft (12.2m) Slim Tube. The injection gas was maintained inside the oven together with the Slim Tube at the reservoir temperature. A pressure transducer was tied into the system to measure pressure differential across the Slim Tube. A sight glass was placed at the outlet of the Slim Tube followed by a backpressure regulator. The fluids were flashed to stock tank conditions after the backpressure regulator. The stock tank oil was collected and its weight and density were measured. The stock tank gas was flowed through an on-line GC and then into a gas meter to measure its volume. An increase in GOR of the flashed fluids determined the breakthrough point. The GC was set up to monitor the change of light components in the produced gas to determine more accurately this breakthrough.

Toluene was used to wash the column after the test. The washes were collected and the oil volume in each wash was determined by capillary column chromatography to confirm our material balance.

Breakthrough of injection gas will be observed at some point during the test. At this point the GOR will increase drastically and the fluid composition will change (this can be seen from chromatography of the outlet gas). Also changes will be seen through the sight glass. Depending on whether the displacement is miscible or immiscible, different observations will be made. If miscible the fluid in the sight glass will gradually change colour from the brown of the reservoir fluid to completely clear. If immiscible, bubbles will be seen. Discrepancies will be noticed immediately around the MMP where some colour change and some bubbles may be seen. Regardless, sight glass observations should be taken for an indication of the state of miscibility/immiscibility however the MMP value reported should be produced from the 'break over' point on the oil recovery versus injection pressure plot.

8.2 Rising Bubble Apparatus for Measuring MMP

Almost fifty RBA tests were conducted as part of this project with several oils, injection gases and at a variety of operating temperatures. A schematic of the RBA setup is shown in **Figure 9-3**. Oil A within the RBA and the injection gas were maintained at the experimental temperature throughout each test.

The RBA consists of a high pressure visual cell tied into the reservoir fluid and the injection gas for analysis and a camera to record experimental observations (Christiansen and Haines, 1987, Elsharkawy *et al.,* 1992, Thomas *et al.,* 1994, Novosad *et al.,* 1990, Zhou and Orr, 1998).

Within the cell is a flat glass tube where the reservoir fluid is charged. The tube has the internal dimensions of 5mm wide by 1mm thick by 200mm long such that the rising bubble is visible in opaque and dark oils. The glass tube is inserted such that the inlet of the injection gas (a fine needle shaped inlet) is inside the tube. The cell is initially charged with distilled/demineralised water such that the glass tube is filled and surrounded with water, and thus, the pressure within and surrounding the tube is equal. The water inside the flat tube is then displaced by the reservoir fluid from the top of the tube such that the injection gas inlet is still submerged in distilled water. Once the cell and tube are charged at the experimental pressure and temperature, the bubble is released through the bottom of the tube. The

bubble travels through the water, crosses the oil/water interface and then travels through the oil.

8.2.1 Miscibility Criteria for RBA

The MMP can be determined using the RBA based on the change in the shape of the bubble as it crosses the oil/water interface and travels through the oil. At pressures well below the MMP the bubble will travel up to the interface and may get stuck at the interface due to the high interfacial tension between the oil and the CO_2 before crossing into the oil and travelling up the tube. The bubble will appear spherical at pressures well below the MMP. As it approaches the MMP the bubble shape will become more elliptical, then appear bullet shaped, then with an elliptical top and skirted bottom. Finally once the MMP is reached it will dissolve into the oil. Based on the observations of bubble shape and working pressure of the experiment the MMP can be determined. The schematic of the RBA is shown below in **Figure 8-3**.

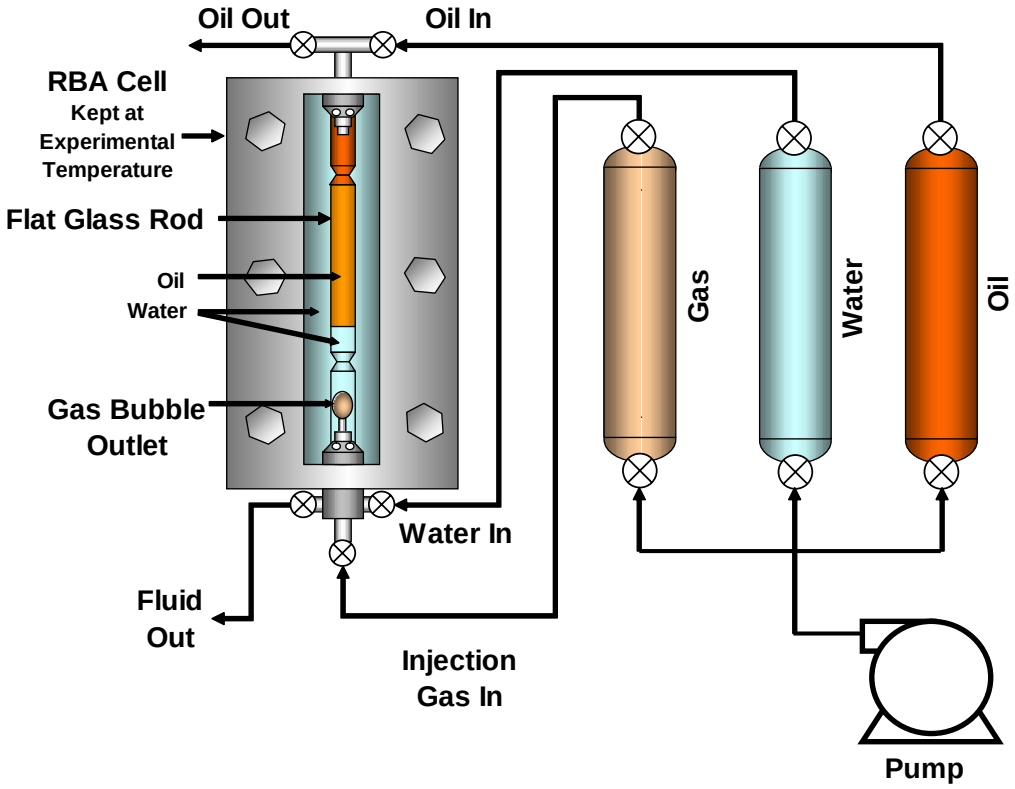

Figure 8-3: Schematic of RBA experimental set-up

The RBA is often believed to only be appropriate for measuring the MMP when the miscibility develops by vaporising gas drive, since it was for these purposes which it was designed (Christiansen, 1981). A pure CO_2 flood would be a vaporising mechanism. When impurities like nC_5 are present, the condensing gas drive mechanism may also become a significant contributing factor. However, the RBA can also be used to measure MMP when the condensing gas drive mechanism plays a significant role in miscibility as described by the discussion between Poettmann, *et al.* (1992) and Sibbald *et al.* (1992). As this discussion describes, when the condensing drive mechanism prevails the RBA can still be used to measure the MMP by passing multiple bubbles through. This enriches the fluid at the oil-water interface and then after approximately 6-8 bubbles the fresh bubble will dissolve with the enriched reservoir fluid (at the interface).

This occurs basically due to the difference in vaporizing and condensing drive. In a vaporizing drive miscibility is established at the leading edge of the solvent, perhaps not on first-contact but after multiple contacts. It results in light components from the reservoir fluid being vaporized into the solvent.

On the other hand for a miscible condensing drive mechanism, components from the solvent condense into the reservoir fluid eventually yielding a fluid which becomes miscible with the solvent.

In reality miscibility is always achieved through a combination condensing and vaporizing mechanism. The slim tube would likely However, many studies have been performed comparing results from the two methods all confirming good agreement between MMP values measured by RBA and Slim Tube. Generally what this results in is, when proposing required analyses for an investigation for miscible flooding, is RBA data to measure the MMP (speed and cost effectiveness) together with one or two slim tube tests to back up the MMP measurements and give recovery data which can then be modelled.

8.3 Comparison of Slim Tube and RBA

The Slim Tube test is the industry standard for measuring the MMP. As well as measuring the MMP, the Slim Tube test can also be used to measure oil recovery,

determine breakthrough time, change in produced gas and liquid compositions and change in liquid density throughout the flood.

A key disadvantage of the Slim Tube test is that there is no standard design for the experimental set-up or operation. Therefore, differences in the experimental set-up or operation may exist from one laboratory to the next. The tube is generally made from 20ft to 60ft long, ¼ inch packed tubing, 40ft is the most commonly used length. The packing material is made up of either glass beads or crushed silica grains. The permeability is kept high (above ~2.5 Darcy (Elsharkawy *et al.,* 1992)). Densitometers and sight glasses may or may not be part of the experimental setup. These differences may result in slight differences in measured data. However, the Slim Tube still provides an accurate measurement of the MMP and comparisons between laboratories result in differences within an acceptable margin, and hence for these reasons it is considered the industry standard.

The RBA was designed after the Slim Tube. Several comparisons between RBA and Slim Tube data have been made and the RBA has been found to also give accurate MMP measurements (Elsharkawy *et al.,* 1992, Thomas *et al.,* 1994, Novosad *et al.,* 1990). However, the RBA only gives MMP data. The key advantage of the RBA is that it is much quicker to determine an MMP (roughly a tenth of the time).

8.4 Results of MMP Measured by Slim Tube Tests

Eight Slim Tube tests were conducted at reservoir temperature and a range of pressures. Four were conducted with SG#1 and four with the pure CO_2 as injection fluid. Injection pressures were picked to have data above and below the MMP. The MMP was attained from the 'break-over' point on the recovery versus injection pressure plot that gave MMP for pure CO_2 of 2795psig and 2865psig for SG#1.

The composition of Oil A as used in this study can be found on **Table 8-1**. Compositions and properties of CO_2, Field B gas, SG#1 and SG#2 can be found on **Table 8-2**. And **Table 8-3** contains the compositions and properties of Gas #1, Gas #2, Gas #3 and Gas #4 used in the RBA analysis.

Tables and **Figures 8-4** to **8-8** refer to the results from Slim Tube floods with pure CO_2 at varying pressures. **Tables** and **Figures 8-9** to **8-13** refer to the results from Slim Tube floods with the SG#1 at varying pressures.

Tables 8-4 to **8-7** and **Tables 8-9** to **8-12** show the percent oil recovery, solution gas oil ratio of produced fluids and the methane to carbon dioxide ratio of the produced gas stream measured at progressive pore volumes of gas injected. It can be noticed in **Figures 8-4** to **8-7** and **Figures 8-9** to **8-12** that after breakthrough the increase in oil recovery with additional injection plateaus, the solution gas oil ratio increases sharply and the ratio of methane to carbon dioxide changes from the of the solution gas of the reservoir fluid to that of the injection gas.

Table 8-8 shows the percent oil recovery at 1.2 PV of gas injected for each test at its corresponding injection pressure for the CO_2 Slim Tube floods. **Table 8-13** shows the percent oil recovery at 1.2 PV of gas injected for each test at its corresponding injection pressure for the synthetic gas Slim Tube floods. **Figure 8-8** is the MMP plot for the CO_2 Slim Tube floods and shows the MMP to be 2795psig at the interception of the extrapolation of the miscible and immiscible parts of the curve. Likewise for synthetic gas, **Figure 8-13** shows the MMP to be 2865psig.

All Slim Tube tests used in determining the MMP provided very high recoveries in the range of 90-93%. It would have been desirable to have at least one more test at a lower pressure in each set to stretch the lower end of the break-over curve. However, the lowest MMP measurements were made only 150 psi and 200 psi above saturation pressure for SG#1 and CO_2 respectively. At pressures below this, we would be approaching the saturation pressure making it very difficult to handle the fluid and accurately analyse the MMP by Slim Tube. It was therefore not possible to make measurements at lower pressures. The first test of each batch were run at these low pressures and when the flood was found to be immiscible based on sight glass observations it was only logical to re-run the test at higher pressures to seek the MMP. The fact that MMP recoveries were still so high at these lower pressures (89.9% and 90.1% for SG#1 and CO_2 respectively)

is due to the volatile nature of the reservoir fluid and confirms the highly miscible nature of Field A reservoir fluid with CO_2 or SG#1.

Table 8-1: Compositions of oils used in miscibility studies

Component		**Oil A Mol %**	**Oil B Mol %**	**Oil C Mol %**
Hydrogen Sulphide	H_2S	0.00	0.00	0.00
Carbon Dioxide	CO_2	15.57	3.98	0.65
Nitrogen	N_2	0.73	0.13	0.27
Methane	C_1	23.95	13.40	11.88
Ethane	C_2	8.71	6.61	1.06
Propane	C_3	8.63	8.57	0.58
Iso-Butane	iC_4	2.30	2.77	0.19
N-Butane	nC_4	4.16	4.83	0.15
Iso-Pentane	iC_5	1.46	1.92	0.31
N-Pentane	nC_5	1.63	1.92	0.20
Hexanes	C_6	3.70	7.35	3.96
Heptanes	C_7	7.54	12.28	12.28
Octanes	C_8	3.80	7.00	9.28
Nonanes	C_9	3.91	6.31	8.63
Decanes	C_{10}	2.84	4.32	8.18
Undecanes	C_{11}	1.79	2.78	6.31
Dodecanes Plus	C_{12}+	9.28	15.83	36.07
TOTAL		100.00	100.00	100.00
		Stream Properties		
Molecular Weight		70.03	96.7	144.1
API Gravity		50.7	51.8	44.1
GOR (scf/stb)		1273	455	105
		Dodecanes Plus Properties		
Mol %		9.28	15.83	36.07
Molecular Weight		228.2	232.7	235.5
Density (gm/cc @ 60 °F)		0.8433	0.8459	0.8473
Gravity (°API @ 60 °F)		36.1	35.6	35.3

Table 8-2: Gas compositions: CO_2, Field B gas, SG#1 and SG#2

Component		CO_2 Mol %	Field B Mol %	SG#1 Mol %	SG#2 Mol %
Hydrogen Sulphide	H_2S	0.00	0.00	0.00	0.00
Carbon Dioxide	CO_2	100.00	45.53	80.20	79.61
Nitrogen	N_2	0.00	0.96	0.35	0.16
Methane	C_1	0.00	41.48	15.31	15.45
Ethane	C_2	0.00	6.80	2.34	1.89
Propane	C_3	0.00	2.87	1.10	0.97
Iso-Butane	iC_4	0.00	0.55	0.22	0.19
N-Butane	nC_4	0.00	0.63	0.19	0.22
Iso-Pentane	iC_5	0.00	0.24	0.07	0.10
N-Pentane	nC_5	0.00	0.19	0.06	0.55
Hexanes	C_6	0.00	0.22	0.06	0.27
Heptanes	C_7	0.00	0.23	0.06	0.46
Octanes	C_8	0.00	0.12	0.03	0.08
Nonanes	C_9	0.00	0.07	0.01	0.04
Decanes	C_{10}	0.00	0.07	0.00	0.01
Undecanes	C_{11}	0.00	0.04	0.00	0.00
Dodecanes Plus	C_{12}+	0.00	0.00	0.00	0.00
TOTAL		100.00	100.00	100.00	100.00
Mol Weight		44.01	32.04	39.52	40.08
Gas Gravity		1.526	1.111	1.370	1.39
P_c (psia)		1071	845.9	989.5	984.6
T_c (R)		547.9	470.4	518.7	523.2

Table 8-3: Gas compositions – Gas#1 to Gas#4

Component		Gas#1 Mol %	Gas#2 Mol %	Gas#3 Mol %	Gas#4 Mol %
Hydrogen Sulphide	H_2S	0.00	0.00	0.00	0.00
Carbon Dioxide	CO_2	91.75	90.84	89.08	87.38
Nitrogen	N_2	0.20	0.20	0.19	0.19
Methane	C_1	8.05	7.97	7.82	7.67
N-Pentane	nC_5	0.00	0.99	2.91	4.76
TOTAL		100.00	100.00	100.00	100.00
Mol Weight		41.73	42.03	42.61	43.17
Gas Gravity		1.446	1.457	1.478	1.498
P_c (psia)		1037.3	1031.8	1021.3	1011.1
T_c (R)		530.8	533.9	540.0	545.8

Table 8-4: Slim tube results – CO_2 at 3000psig

PV	%Rec	GOR	C_1/CO_2 Ratio
0.00	0.0%	--	1.30
0.09	8.4%	1572	1.30
0.19	17.7%	1709	1.29
0.33	30.1%	1692	1.30
0.59	54.3%	1476	1.28
0.86	78.0%	1693	1.28
1.02	88.7%	2628	1.10
1.13	92.3%	5829	0.35
1.20	93.1%	11795	0.11
1.25	93.7%	16401	0.02
1.38	94.3%	55508	0.01

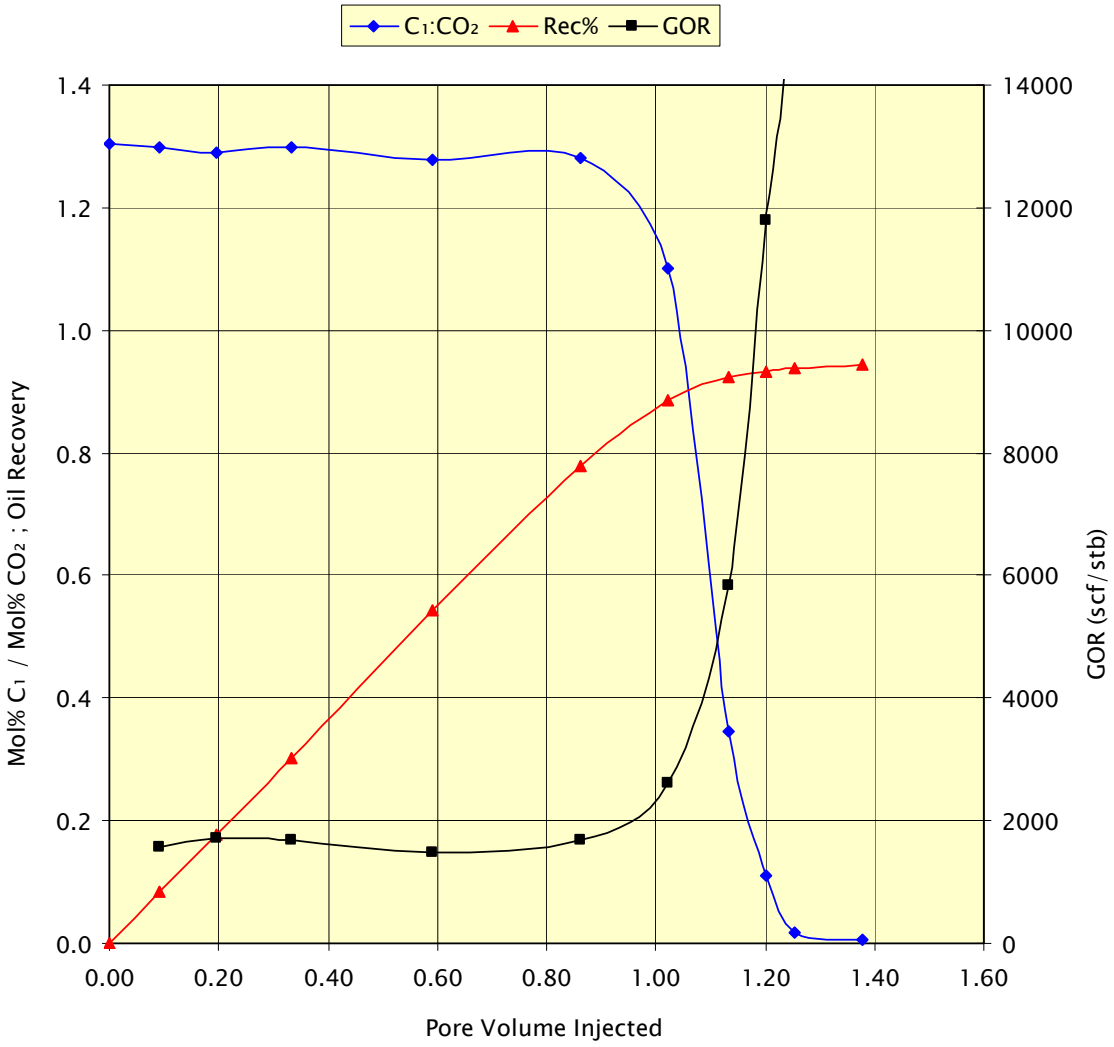

Figure 8-4: Slim tube results – CO_2 at 3000psig

Table 8-5: Slim tube results – CO_2 at 2850psig

PV	%Rec	GOR	C_1/CO_2 Ratio
0.00	0.0%	--	1.27
0.19	17.0%	1396	1.24
0.39	33.9%	1338	1.21
0.58	51.6%	1391	1.24
0.71	62.9%	1381	1.25
0.79	70.1%	1425	1.23
0.86	75.8%	1365	1.22
0.97	85.7%	1376	1.06
1.05	91.0%	2059	0.26
1.15	92.6%	8384	0.02
1.22	92.9%	52005	0.00

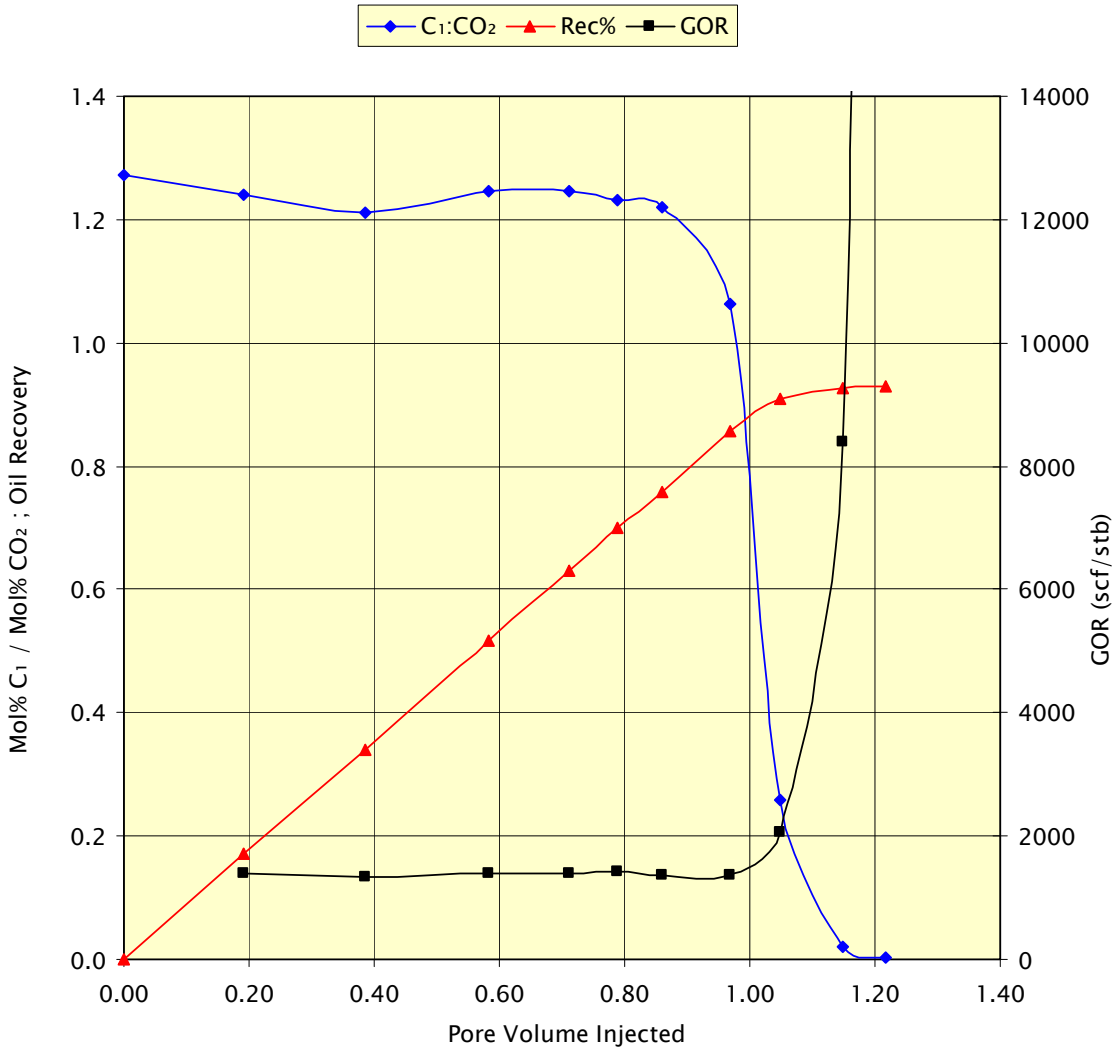

Figure 8-5: Slim tube results – CO_2 at 2850psig

Table 8-6: Slim tube results – CO_2 at 2700psig

PV	%Rec	GOR	C_1/CO_2 Ratio
0.00	0.0%	--	1.29
0.07	4.5%	1403	1.31
0.22	18.6%	1435	1.29
0.40	34.7%	1441	1.30
0.67	57.9%	1374	1.30
0.80	70.9%	1441	1.28
0.98	84.8%	1446	1.28
1.03	88.6%	1792	1.10
1.10	90.7%	3907	0.35
1.19	91.7%	22196	0.01
1.25	91.9%	56932	0.00

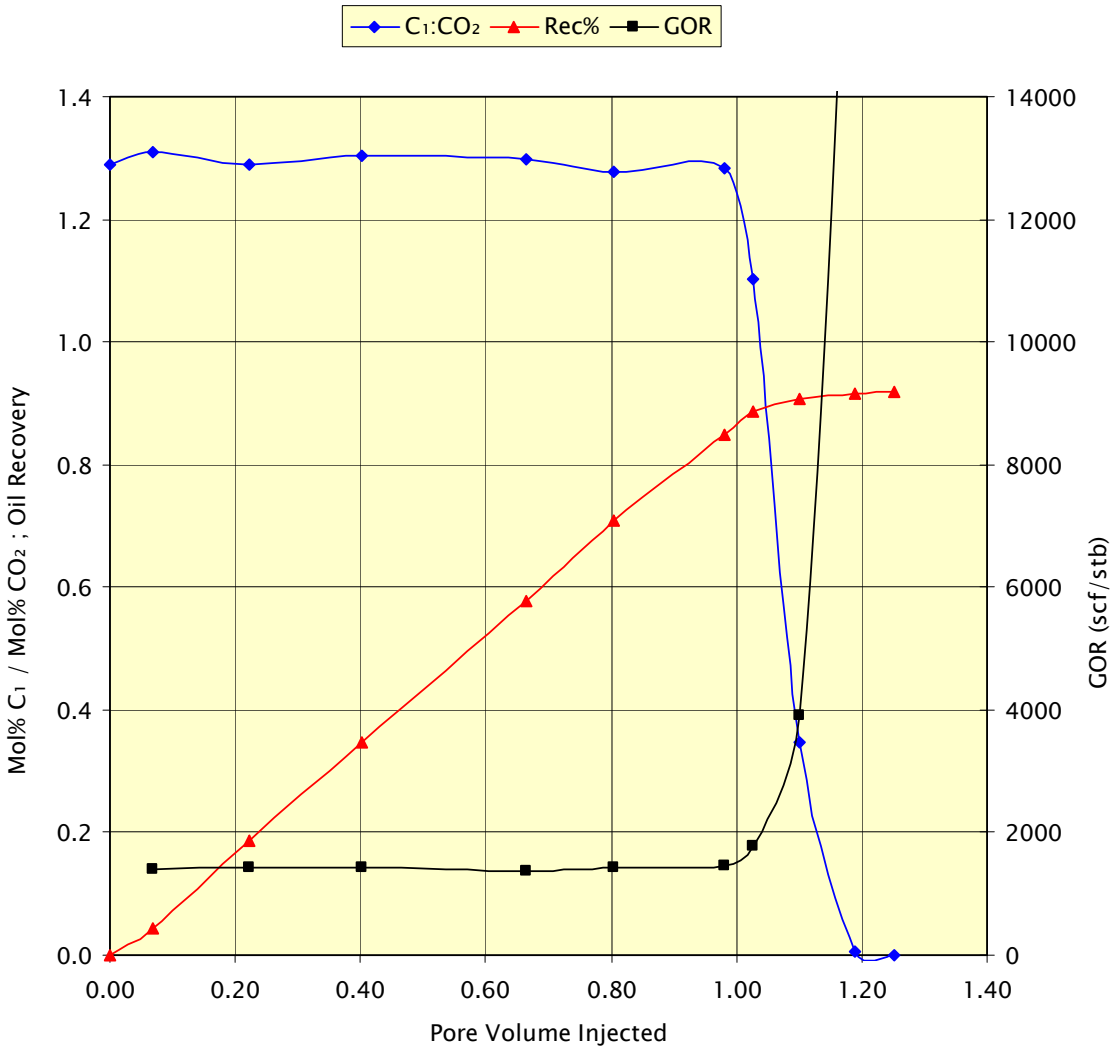

Figure 8-6: Slim tube results – CO_2 at 2700psig

Table 8-7: Slim tube results – CO_2 at 2550psig

PV	%Rec	GOR	C_1/CO_2 Ratio
0.00	0.0%	--	1.30
0.08	4.4%	1249	1.28
0.13	8.6%	1538	1.28
0.30	21.8%	1251	1.27
0.47	37.0%	1408	1.26
0.66	53.8%	1385	1.30
0.84	70.2%	1425	1.29
0.99	83.9%	1496	1.26
1.06	87.7%	2192	0.30
1.19	90.0%	11350	0.01
1.24	90.4%	23502	0.00

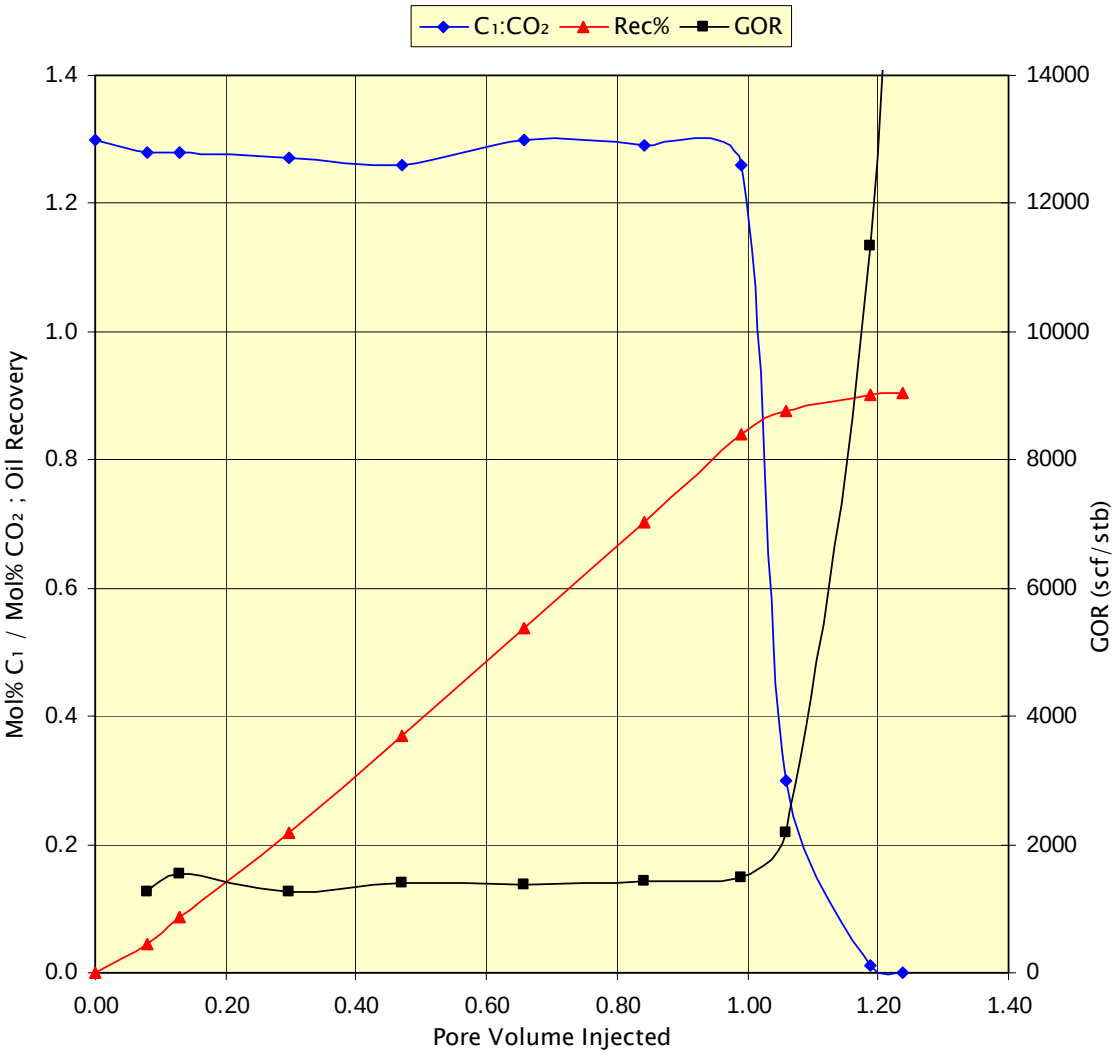

Figure 8-7: Slim tube results – CO_2 at 2550psig

Table 8-8: Oil recovery at 1.2PV of CO_2 injected at injection pressure of test

Injection Pressure (psig)	Oil Recovery at 1.2PV Gas Injected
2550	90.1%
2700	91.7%
2850	92.8%
3000	93.1%

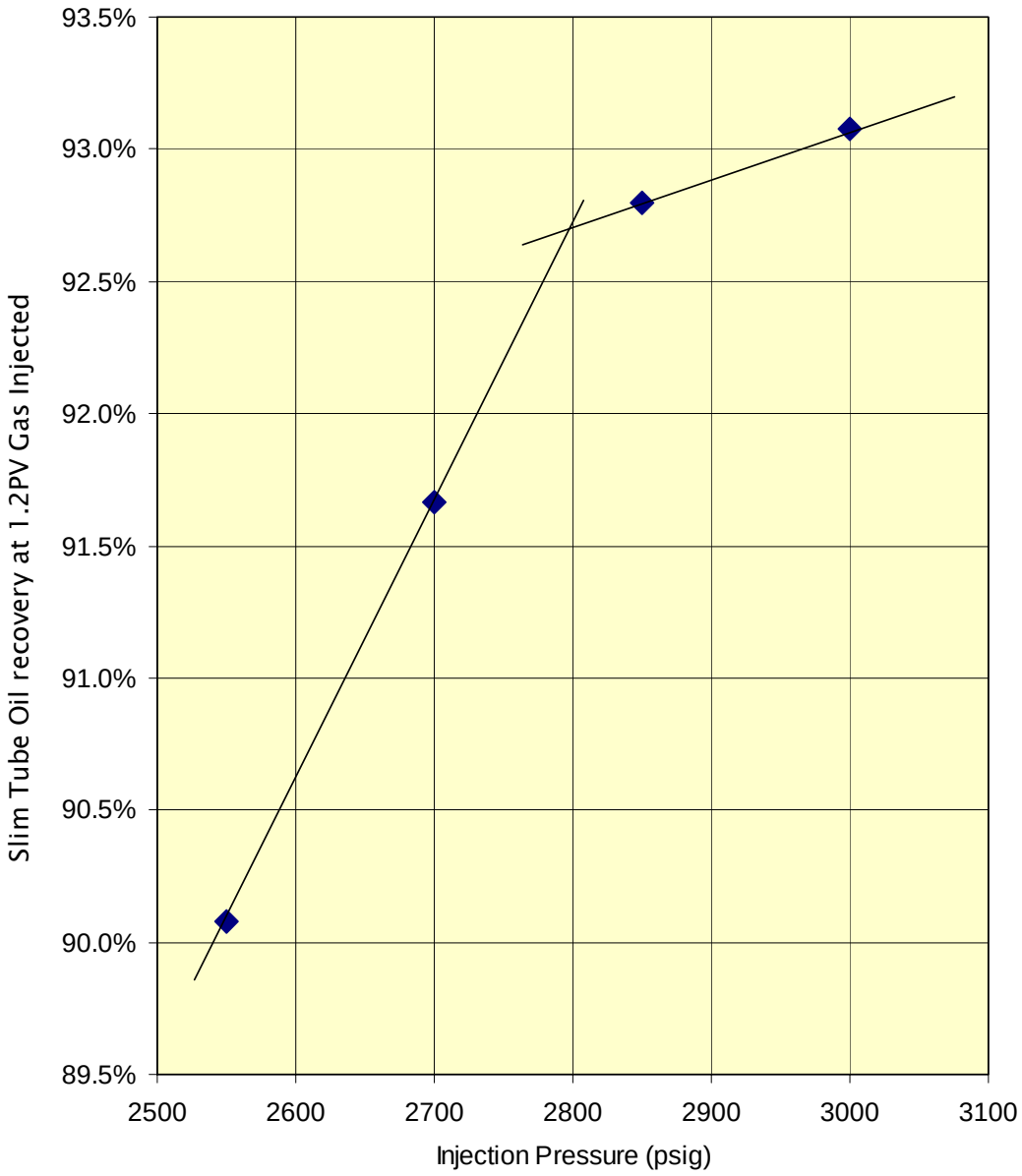

Figure 8-8: MMP plot for CO_2

Table 8-9: Slim tube results – SG#1 at 3200psig

PV	%Rec	GOR	C_1/CO_2 Ratio
0.00	0.0%	--	1.30
0.12	11.0%	2301	1.33
0.32	29.8%	2330	1.31
0.49	44.4%	2528	1.34
0.64	58.5%	2240	1.30
0.81	73.2%	2334	1.28
0.92	83.1%	2459	1.31
1.03	90.3%	3018	0.94
1.06	91.5%	8391	0.44
1.11	92.1%	26701	0.18
1.20	92.5%	54631	0.17

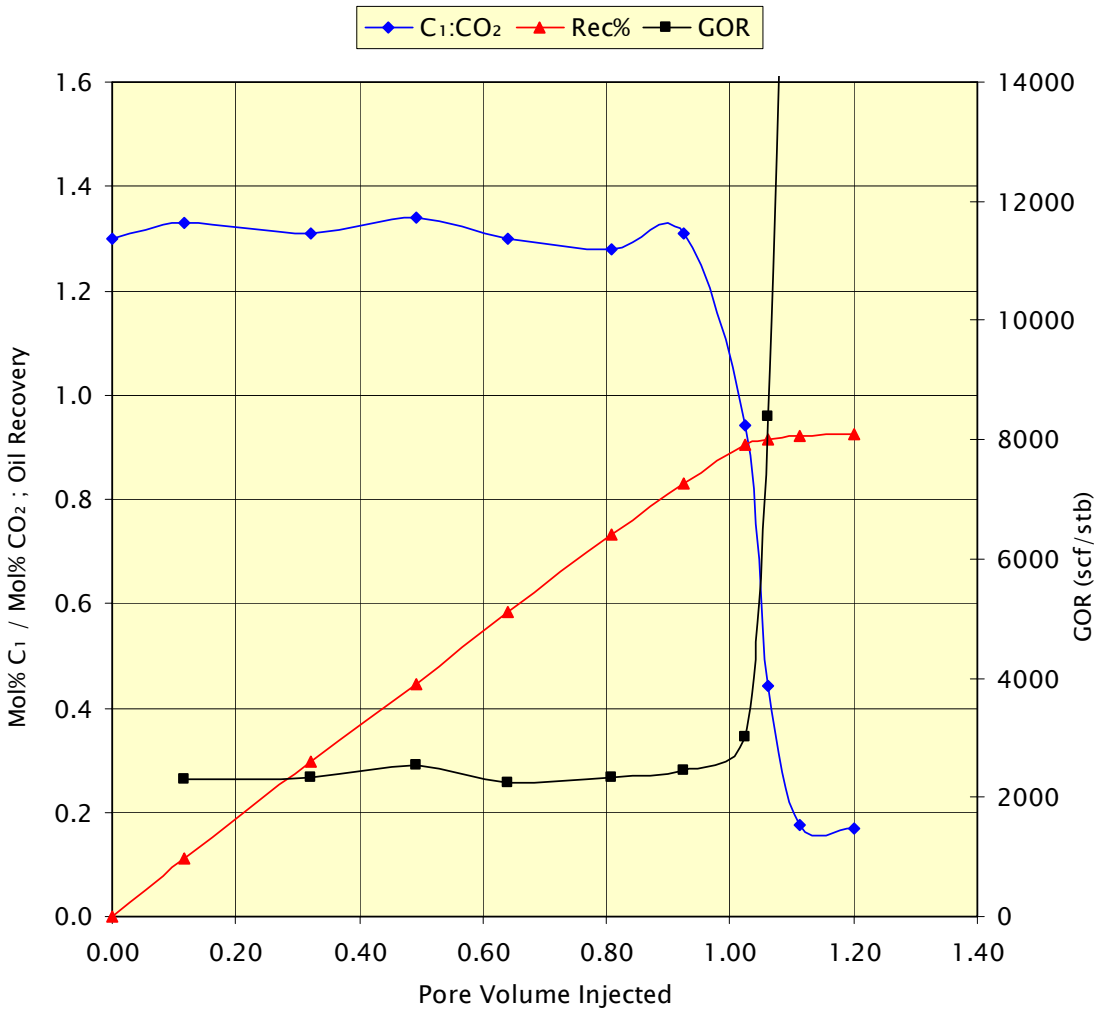

Figure 8-9: Slim tube results – SG#1 at 3200psig

Table 8-10: Slim tube results – SG#1 at 3000psig

PV	%Rec	GOR	C_1/CO_2 Ratio
0.00	0.0%	--	1.30
0.16	13.1%	1345	1.30
0.37	29.5%	1299	1.30
0.53	44.0%	1286	1.29
0.78	63.8%	1308	1.30
0.94	76.5%	1339	1.30
1.09	86.5%	1381	1.10
1.20	92.3%	2361	0.17
1.36	93.6%	17751	0.17

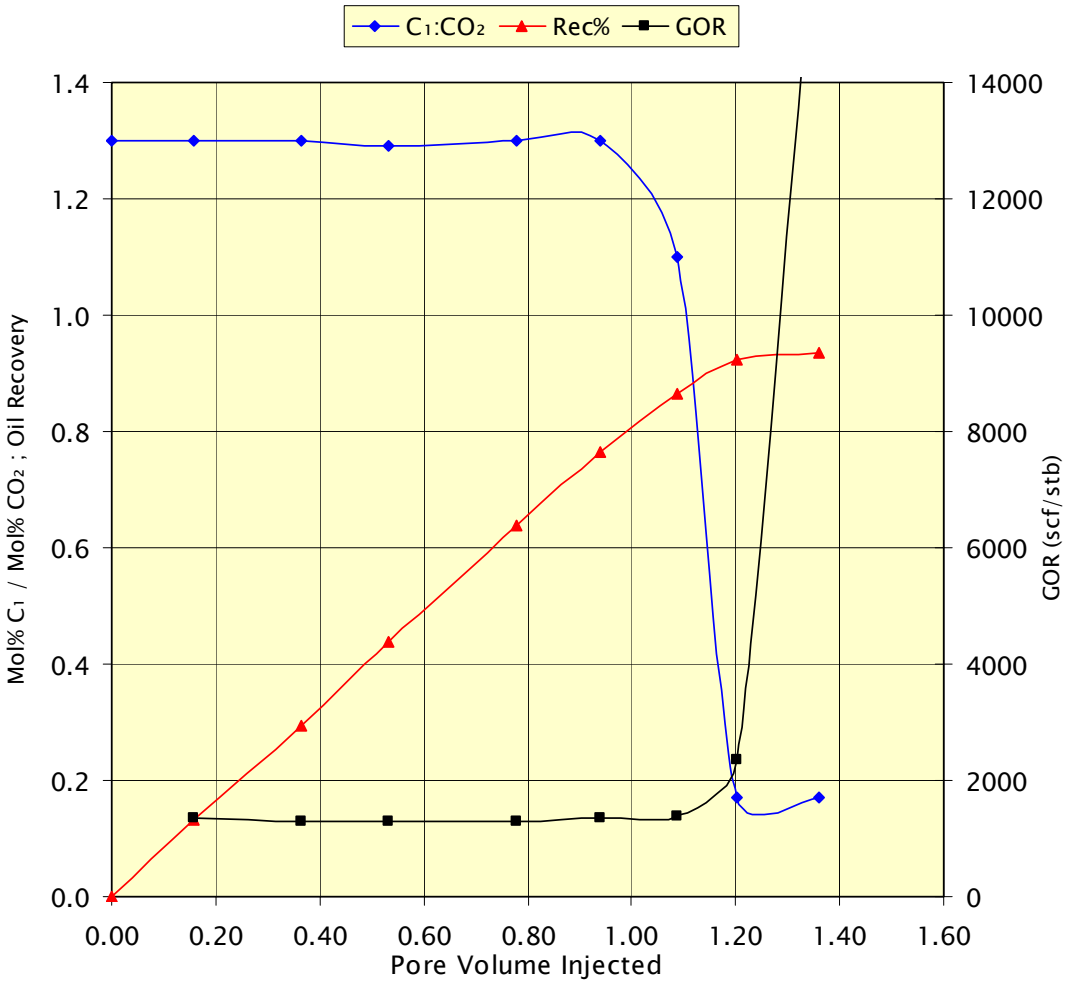

Figure 8-10: Slim tube results – SG#1 at 3000psig

Table 8-11: Slim tube results – SG#1 at 2700psig

PV	%Rec	GOR	C_1/CO_2 Ratio
0.00	0.0%	--	1.32
0.16	14.3%	1784	1.30
0.32	28.4%	1859	1.32
0.53	45.9%	1911	1.30
0.74	64.0%	1830	1.32
0.83	72.7%	1862	1.31
0.98	84.4%	1752	1.33
1.06	89.5%	2573	1.07
1.16	91.1%	4526	0.33
1.25	91.3%	9091	0.16
1.32	91.6%	52103	0.16

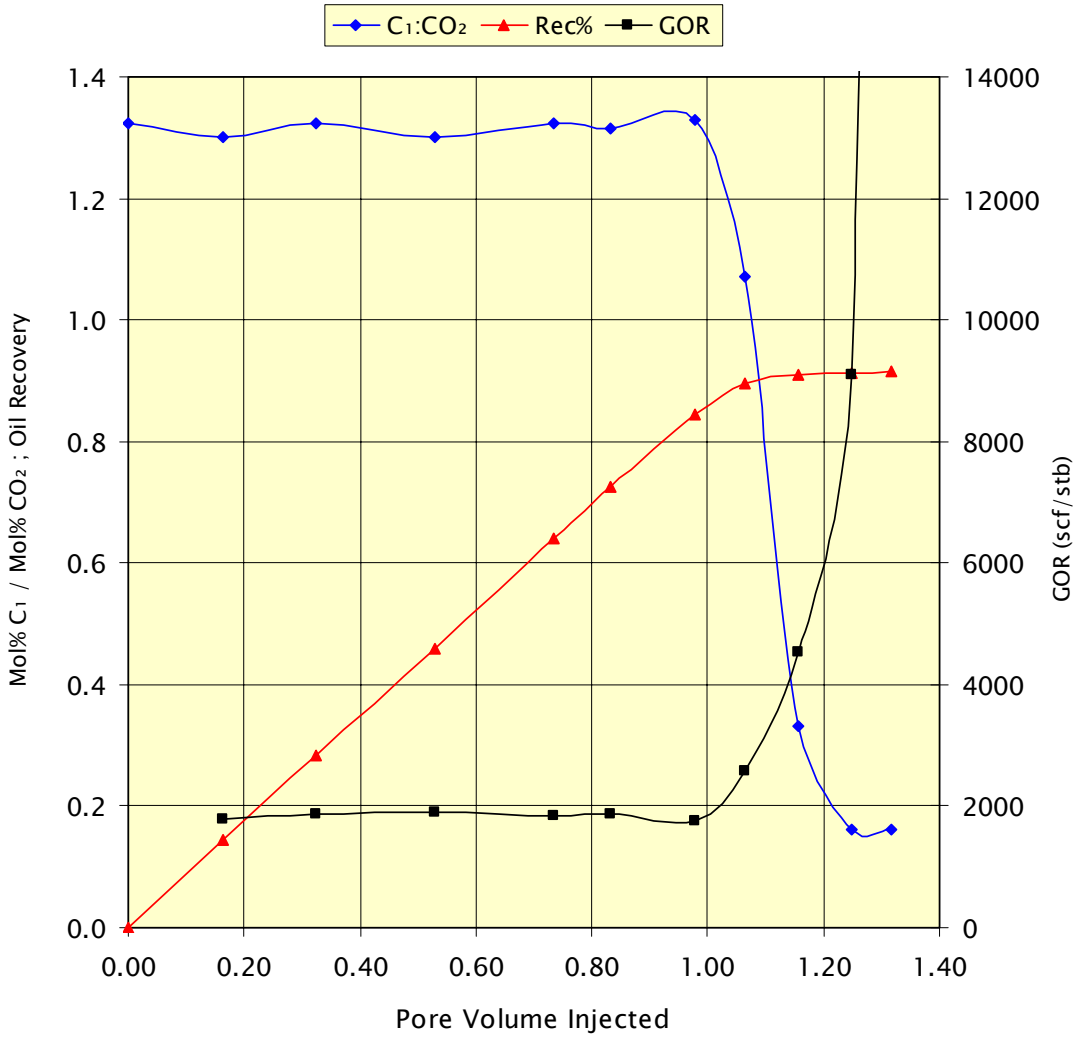

Figure 8-11: Slim tube results – SG#1 at 2700psig

Table 8-12: Slim tube results – SG#1 at 2500psig

PV	%Rec	GOR	C_1/CO_2 Ratio
0.00	0.0%	--	1.31
0.05	4.5%	2447	1.30
0.26	23.6%	2388	1.32
0.44	40.4%	2518	1.31
0.53	48.2%	2631	1.31
0.68	61.8%	2542	1.30
0.87	78.0%	2884	1.31
0.98	85.4%	3519	1.25
1.08	88.7%	7302	0.54
1.20	89.9%	28024	0.16
1.27	90.4%	45775	0.16

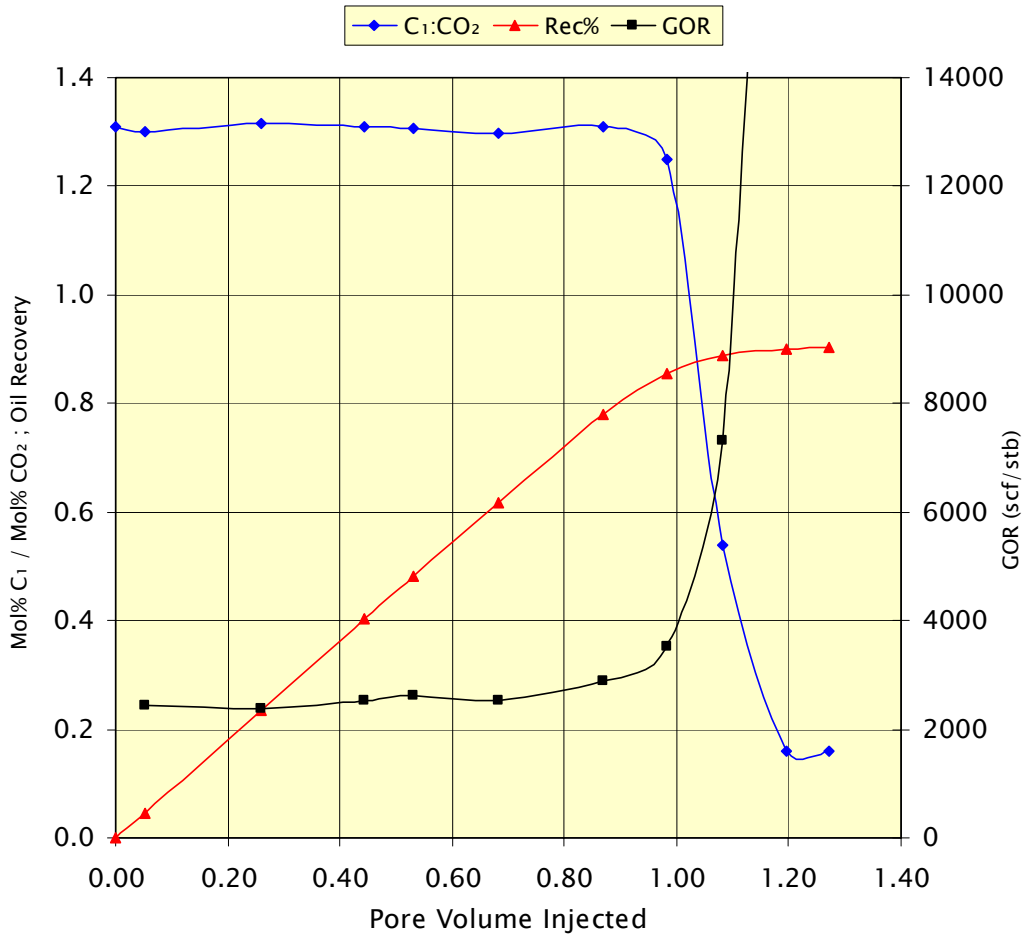

Figure 8-12: Slim tube results – SG#1 at 2500psig

Table 8-13: Oil recovery at 1.2PV of SG#1 injected at injection pressure of test

Injection Pressure (psig)	Oil Recovery at 1.2PV Gas Injected
2500	89.9%
2700	91.2%
3000	92.3%
3200	92.5%

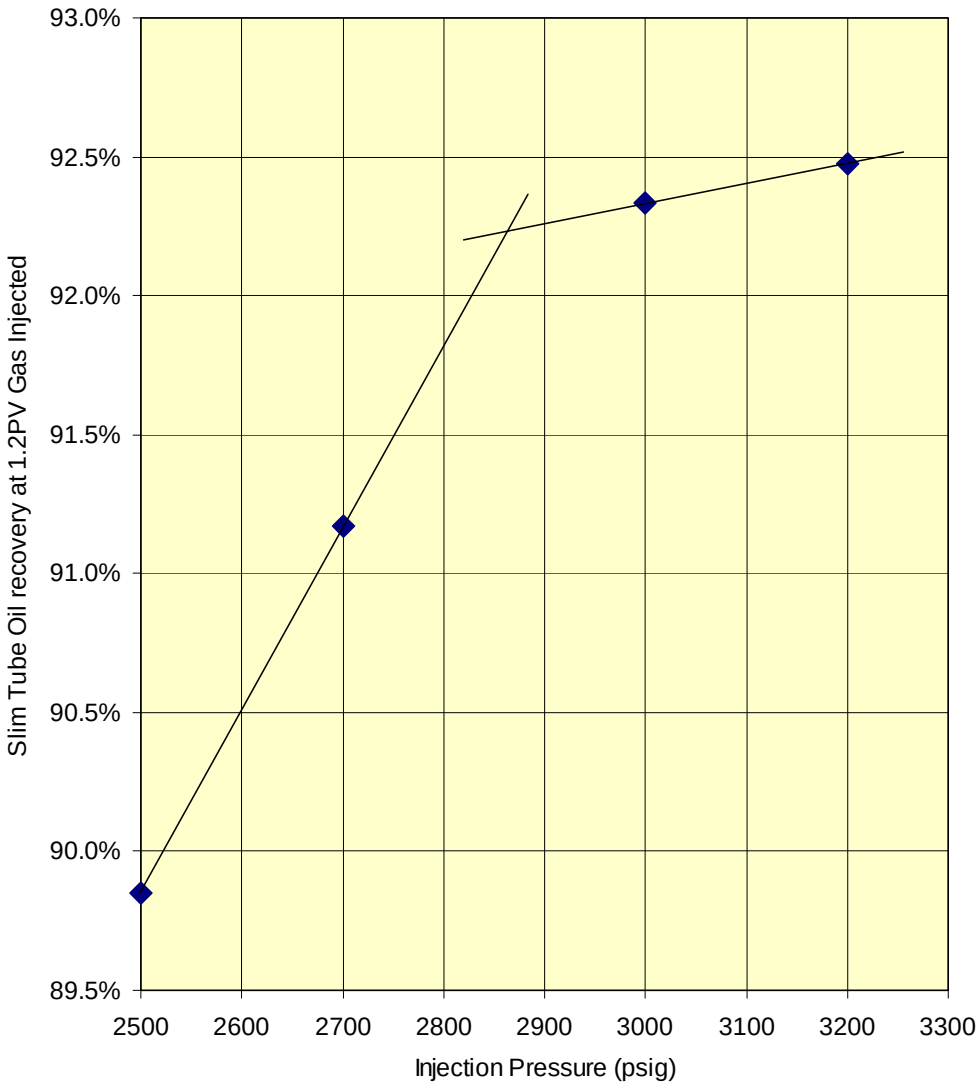

Figure 8-13: MMP plot for SG#1

8.5 MMP Measured by Rising Bubble Apparatus

Two separate groups of MMP measurements by RBA were made. The first program of RBA MMP measurements was designed to obtain the following data:

- Differentiate CO_2 and SG#1
- Re-measure the Slim Tube MMP measurements
- MMP measurements using gas SG#2 in an attempt to determine the effect of the C_5+ found in SG#1.

The second program of RBA MMP measurements was designed to investigate the effect of nC_5 on impure CO_2. This is further discussed in "8.5.2 Second Program of MMP Measurements by RBA".

8.5.1 MMP Measurements by RBA and comparison to MMP Measurements by Slim Tube

The pure CO_2 MMP at 279°F was determined both by Slim Tube and RBA. The Slim Tube gave an MMP at 279°F of 2810psia while RBA gave an MMP of 2690psia. Correlations predicted the MMP to be in the range 2028-3492psia, with most falling between 2500-3000psia. This agreed well with the measured data.

For SG#1, the Slim Tube gave an MMP at 279°F of 2880psia while RBA gave an MMP of 2775psia. Correlations predicted the MMP to be above 3433psia. As the results were well below the correlated results, the effect of C_5+ was further investigated by creating SG#2 and measuring the MMP. As can be seen, the results determined by Slim Tube and RBA were in good agreement.

SG#2 was created by dissolving additional C_5-C_{11} into SG#1 in the same ratio as found in Field B gas. This constituted a gas with 80mol% CO_2, 15mol% C_1 and 1.5mol% C_5+. At 279°F, the MMP was measured to be 2790psia.

Further to measuring RBA MMP values at 279°F for CO_2, SG#1 and SG#2, the RBA tests were also conducted at 176°F and 212°F. **Table 8-14** and **Figure 8-14** summarises the laboratory measured MMP data, and **Table 8-15**, **Table 8-16** and **Table 8-17** summarise correlated and experimental data at the three temperatures with the three injection gases. For pure CO_2, the MMP at 176°F and 212°F was

measured to be 2135psia and 2340psia, respectively. For SG#1, it was measured to be 2511psia and 2641psia, respectively and for SG#2 it was measured to be 2468psia and 2662psia, respectively. The MMP was observed to increase with an increase in temperature and decrease with the addition of C_5+ components. The RBA measured data for SG#1 confirmed a low MMP value, and at 279°F, far lower than correlated data. However, the increase in C_5+ fraction in SG#2 compared to SG#1 seemed to have little impact.

An increase in MMP with an increase in temperature was observed – a well documented finding for the CO_2-oil MMP. The gradient of the MMP-temperature plot for Oil A with pure CO_2 was determined to be approximately 5psi/°F. Examining **Figure 8-15**, **Figure 8-16** and **Figure 8-17** it can be seen that the RBA results have a much lower gradient than that of the correlations. This is likely to be due to the volatile nature of the reservoir fluid and the high temperatures the tests were operated at.

Comparing **Figure 8-16** and **Figure 8-17** we can see that some correlations are greatly affected by the change in injection gas (Emera and Sarma, 2005, Alston *et al.,* 1985) while others are affected only slightly or not at all (Dong, 1999, Yuan *et al.,* 2005). This is due to the differences in each correlation as well as applicability of each correlation. Most can tolerate any injection gas but have been designed and tested only with data of injection gases with no C_5+, while others are specifically developed for a particular impurity. Yuan *et al.,* 2005, has been plotted to demonstrate this. It is designed only for CO_2 with C_1 impurity, up to 20mol%. The assumption could be made that since SG#1 and SG#2 are both approximately 80mol% CO_2 and 15mol% C1, it may be reasonably well correlated by the Yuan *et al.,* 2005, correlation. However, as can be seen in **Figure 8-16** and **Figure 8-17** it correlates with the data very poorly. This does not mean that the correlation has performed poorly but rather that it has been used inadequately and illustrates the importance of using correlations with constraints that match that of the reservoir fluid and injection gas being correlated.

The MMP study conducted by RBA confirmed the low MMP of SG#1. A low MMP was also observed for SG#2. However, the added enrichment of C_5+ in SG#2

seemed to have little effect on the MMP. More data, with a larger range of C_5+ fractions and with different oils are required to further analyse and study its effects.

Table 8-14: Laboratory measured MMP (psia) data by Slim Tube (ST) and RBA for CO_2, SG#1 and SG#2

Lab Data	**Temperature (°F)**		
Gas	**176**	**212**	**279**
CO_2 - RBA	2135	2340	2690
CO_2 - ST	--	--	2810
SG#1 - RBA	2526	2651	2775
SG#1 - ST	--	--	2880
SG#2 - RBA	2483	2677	2790

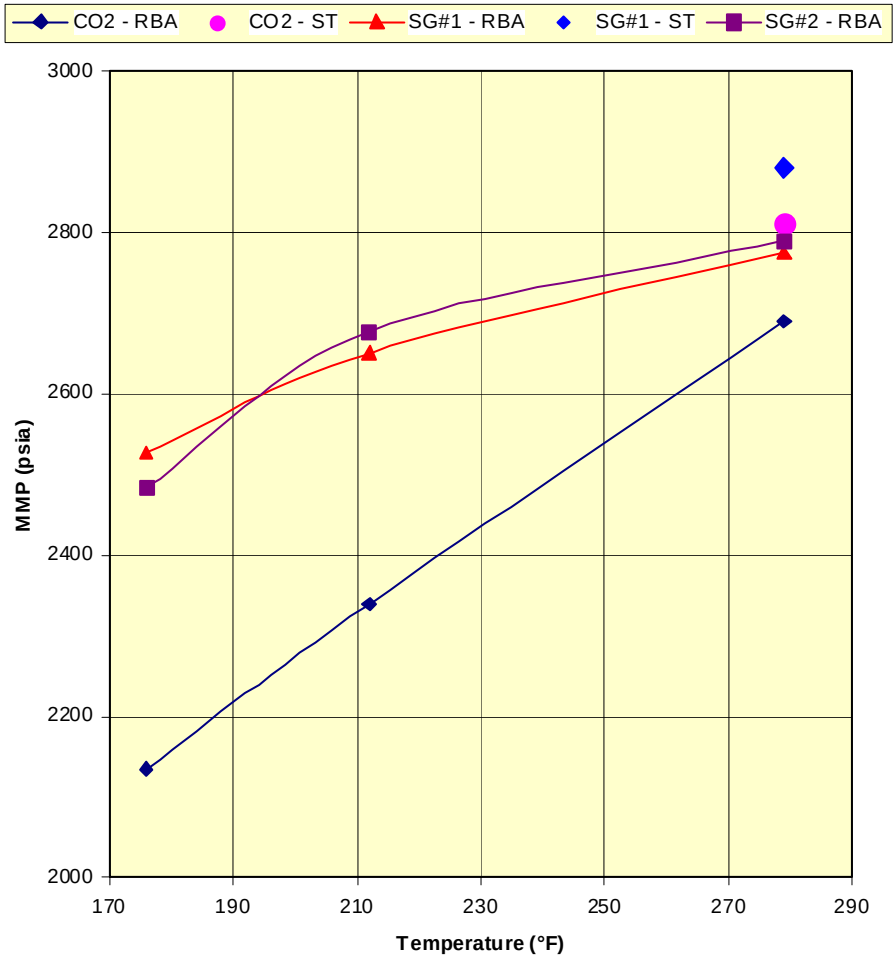

Figure 8-14: MMP – Temperature relation of laboratory measured MMP data.

Table 8-15: Correlated and measured results for MMP (psia) of Oil A with CO_2.

Pure CO_2	**Temperature °F**		
Correlation	**176**	**212**	**279**
Johnson and Pollin (1981)	1458	1836	2540
Alston *et al.* (1985)	1244	1515	2028
Cronquist (1978)	1970	2343	3026
Glasø (1985)	2281	2686	3440
Yellig and Metcalfe (1980)	2198	2631	3492
Yuan *et al.* (2005)	2078	2514	2995
Emera and Sarma (2005)	1563	1942	2676
RBA	2135	2340	2690
Slim Tube	--	--	2810

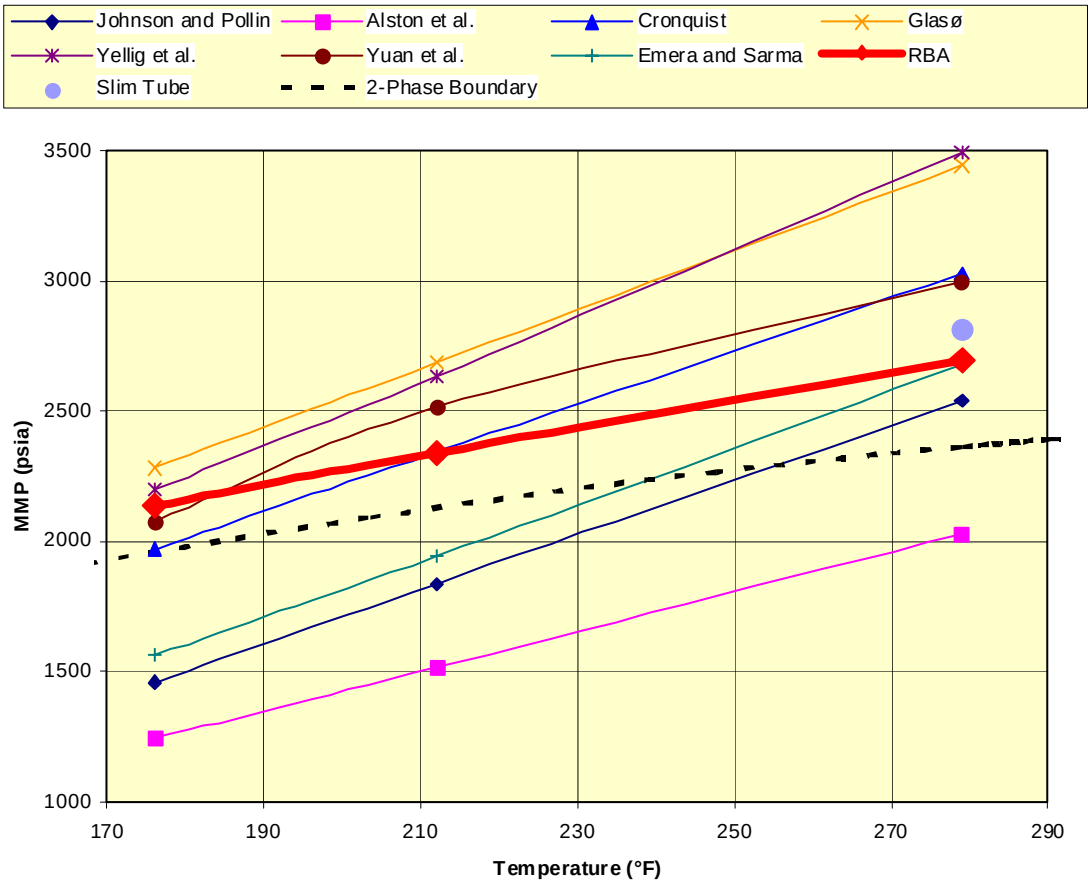

Figure 8-15: MMP – Temperature relation of Oil A and CO_2.

Table 8-16: Correlated and measured results for MMP (psia) of Oil A with SG#1.

SG#1	Temperature (°F)		
Correlation	**176**	**212**	**279**
Alston *et al.* (1985)	2608	2859	3433
Sebastian *et al.* (1985)	3067	3298	3795
Yuan *et al.* (2005)	2281	2869	4243
Dong (1999)	3132	3435	3952
Kovarik (1985)	3344	3549	3899
Emera and Sarma (2005)	2693	2951	3544
RBA	2526	2651	2775
Slim Tube	--	--	2880

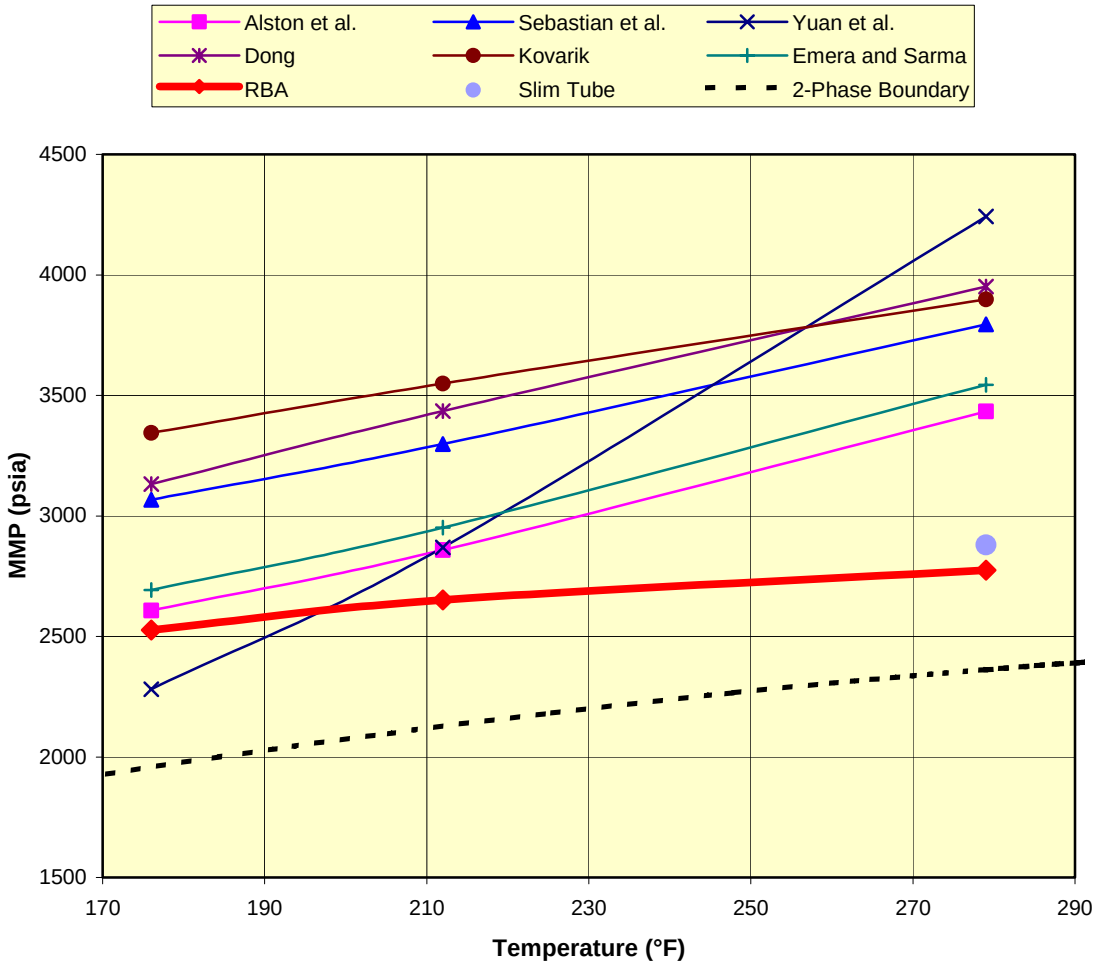

Figure 8-16: MMP – Temperature relation of Oil A and SG#1.

Table 8-17: Correlated and measured results for MMP (psia) of Oil A with SG#2.

SG#2	**Temperature (°F)**		
Correlation	**176**	**212**	**279**
Alston *et al.* (1985)	2037	2233	2682
Sebastian *et al.* (1985)	2829	3103	3507
Yuan *et al.* (2005)	2281	2869	4243
Dong (1999)	3162	3468	3990
Kovarik (1985)	3132	3337	3687
Emera and Sarma (2005)	2071	2270	2727
RBA	2483	2677	2790

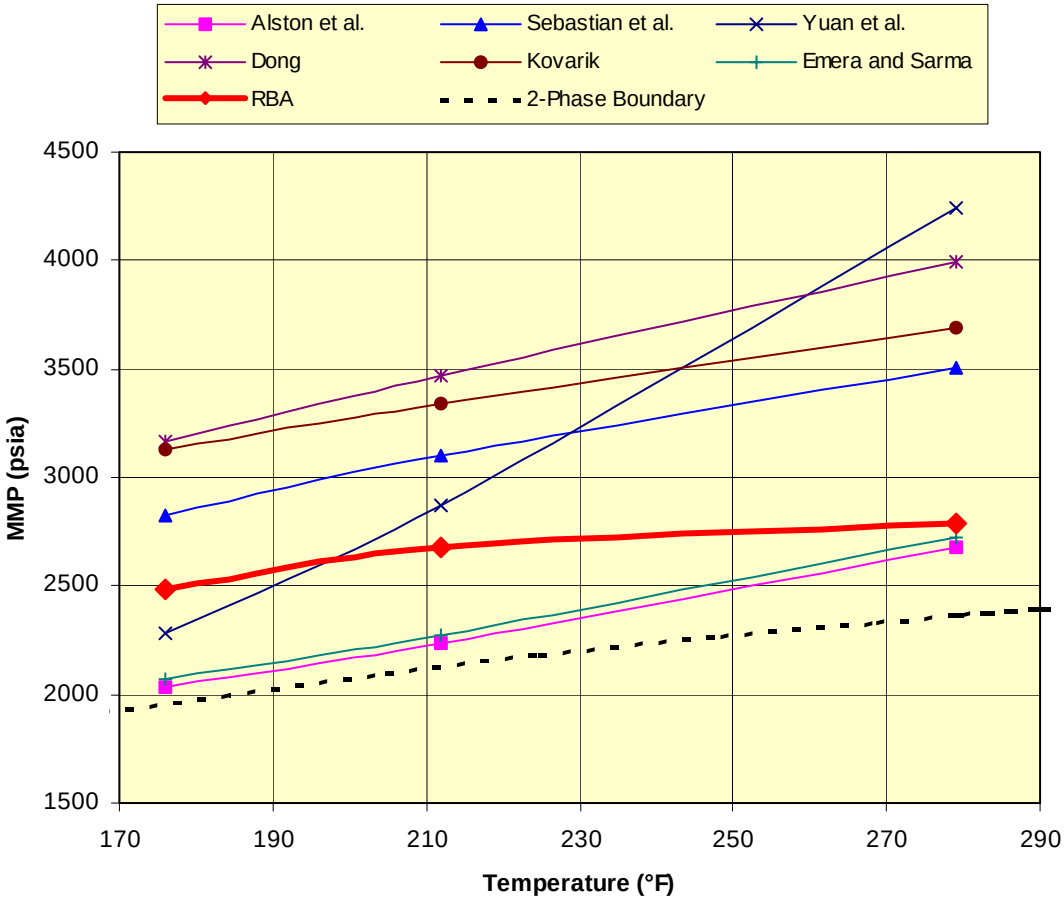

Figure 8-17: MMP – Temperature relation of Oil A and SG#2.

8.5.2 Second Program of MMP Measurements by RBA

After the conclusions made from the first program of RBA MMP measurements, a second program was designed. This was designed to continue on the path of determining the effect of the heavier components in the injection gas stream. One key flaw in the first program was that it used the C_5+ fraction found Field B gas. This made the results field specific but shed little light into anything with a broader application since C_5+ properties can vary significantly. As a result the second program was designed as such:

- The base injection gas was simplified to only two components, CO_2 and C_1
- The C_5+ fraction was simplified to target only the effect of n-pentane. A review of literature found no results using nC_5 or any hydrocarbon heavier, only butane and lighter.
- Three different reservoir fluids were used

Based on the above points four injection gases were made (Gas #1, Gas #2, Gas #3 and Gas #4) as well as two reservoir fluids (Oil B and Oil C) with the intention of evaluating the effect due to nC_5 but also to generalise and develop a data set upon which to base a correlation.

A total of 36 MMP measurements were made using the following combinations:

- Gas#1, Gas#2, Gas#3 and Gas#4 with
- Oil A, Oil B and Oil C at
- 60°C, 80°C and 100°C

The base gas, Gas#1, was created by mixing CO_2 (92mol%) and methane (8mol%). To this, 1mol%, 3mol% and 5mol% n-pentane (nC_5) was added to make Gas#2, Gas#3 and Gas#4 respectively. Compositions of Oil A, Oil B and Oil C previously reported in **Table 8-1**. Compositions and properties of Gas #1, Gas #2, Gas #3 and Gas #4 can be found on **Table 8-3**. The reservoir fluids were all relatively light, with gravities in the range of 44-52°API, however they ranged in the solution gas-oil ratio (GOR) from 100-1300scf/stb.

As expected with and increase in nC_5 content in the injection gas, the MMP decreased. A strong trend was found that was correlated (refer to "Chapter 9: Development of the Correlation for the Effect of nC_5 on Impure CO_2 MMP").

Table 8-18: Measured RBA MMP values for Gas#1 – Gas#4.

Gas	Reservoir Fluid*	Temp. °C	%nC_5 in Gas stream	Measured MMP
Gas #0	Oil A	60	0.00	2195
Gas #0	Oil A	80	0.00	2487
Gas #0	Oil A	100	0.00	2705
Gas #0	Oil B	60	0.00	1600
Gas #0	Oil B	80	0.00	1841
Gas #0	Oil B	100	0.00	2122
Gas #0	Oil C	60	0.00	2351
Gas #0	Oil C	80	0.00	2500
Gas #0	Oil C	100	0.00	2681
Gas #1	Oil A	60	0.99	2046
Gas #1	Oil A	80	0.99	2362
Gas #1	Oil A	100	0.99	2577
Gas #1	Oil B	60	0.99	1429
Gas #1	Oil B	80	0.99	1663
Gas #1	Oil B	100	0.99	1951
Gas #1	Oil C	60	0.99	2201
Gas #1	Oil C	80	0.99	2339
Gas #1	Oil C	100	0.99	2448
Gas #2	Oil A	60	2.91	1887
Gas #2	Oil A	80	2.91	2131
Gas #2	Oil A	100	2.91	2331
Gas #2	Oil B	60	2.91	1329
Gas #2	Oil B	80	2.91	1502
Gas #2	Oil B	100	2.91	1687
Gas #2	Oil C	60	2.91	1830
Gas #2	Oil C	80	2.91	1990
Gas #2	Oil C	100	2.91	2141
Gas #3	Oil A	60	4.76	1844
Gas #3	Oil A	80	4.76	2039
Gas #3	Oil A	100	4.76	2245
Gas #3	Oil B	60	4.76	1283
Gas #3	Oil B	80	4.76	1405
Gas #3	Oil B	100	4.76	1552
Gas #3	Oil C	60	4.76	1739
Gas #3	Oil C	80	4.76	1894
Gas #3	Oil C	100	4.76	2011

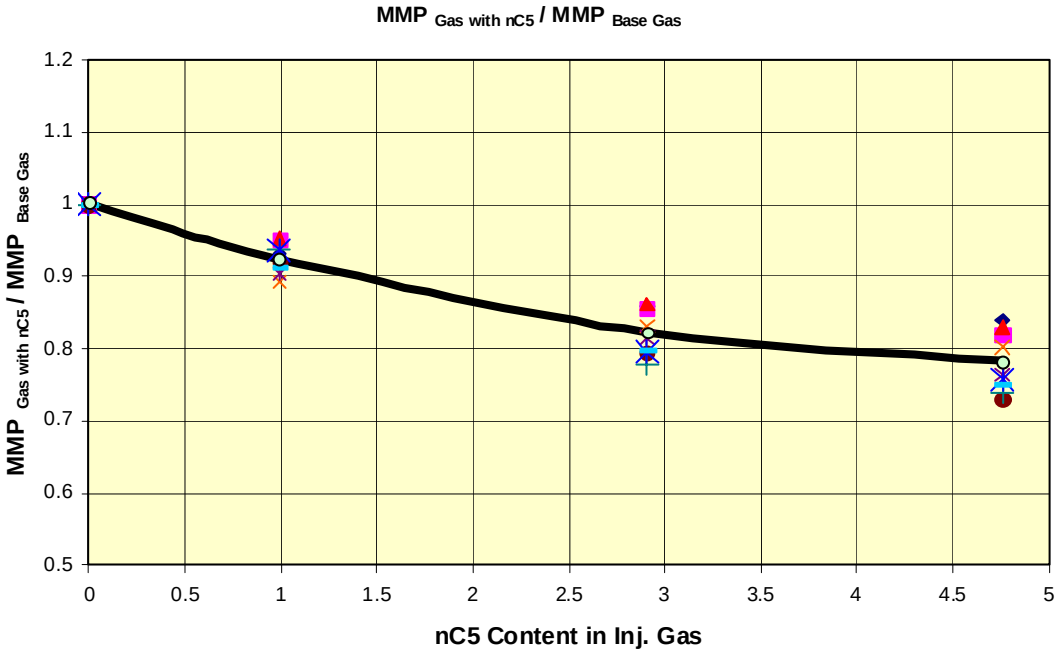

Figure 8-18: RBA generated data. Shows results of RBA MMP values from Gas#2-Gas#4 as a fraction of MMP of Gas #1 with each reservoir fluid at each temperature. Black line represents correlation generated based on regression.

8.6 Chapter Summary

From the work performed in this chapter the following conclusions can be made:

- MMP measurements made using the Rising Bubble Apparatus give comparable results to those from the Slim Tube
- The error from the correlations increased as the injection gas deviated from pure CO_2 and was enriched with more C_5+ components
- A strong trend was found in the reduction in MMP due to the addition of nC_5 to a CO_2 rich injection gas

9 DEVELOPMENT OF CORRELATION FOR THE EFFECT OF nC_5 ON IMPURE CO_2 MMP

Correlations were developed as part of this project to determine the effect of nC_5 on impure MMP. All developed correlations determine the same variable – MMP of an nC_5 enriched gas based on the MMP of a base gas (no nC_5) and the nC_5 content expected to be in the enriched gas. The differences between the correlations will be discussed and recommendations of the applicability of each. Furthermore, these correlations are compared to other already published CO_2 MMP correlations.

The correlations developed are as follows:

- A Genetic Algorithm based correlation
- Two linear regression based correlations
  - An exponential based relationship
  - A quadratic based relationship with an added oil characterisation factor

9.1 Genetic Algorithm

The correlation developed by Genetic Algorithm (GA) was developed together with colleagues (Bon *et al.,* 2006).

9.1.1 Assumptions and Basis for GA-Correlation for MMP of CO_2-Rich Injection Gas with nC_5 Enrichment

The Genetic Algorithm (GA) correlation was developed together with colleagues (Bon *et al.,* 2006) using the GA procedure developed by Emera and Sarma (2005). For further detail it is recommended to go through the procedure of the original authors (Emera and Sarma, 2005, Emera, 2006). This procedure is summarized as follows:

Creation of Initial Population

First the correlation coefficients are defined to incorporate input parameters that affect the result. In this case the input parameters for the correlation were the following:

- *Base gas MMP (MMP_{base})*: This is a measured value for the corresponding reservoir fluid at the corresponding temperature, hence it takes into account the oil composition and temperature of the MMP measurement.
- *Critical pressure ratio (F_{Pc})*: This is equal to the critical pressure of the base gas over the critical pressure of the nC_5 enriched gas.
- *Critical temperature ratio (F_{Tc})*: This is equal to the weight averaged critical temperature of the nC_5 enriched gas over the weight averaged critical temperature of the base gas. Note this is based on the weight percent average, not the mole percent average. Furthermore, correction factors have been applied.

An initial population of 100 real-coded genetic algorithms to calculate MMP based on the correlation coefficients was chosen. Each correlation coefficient then took a random value to build an initial random population of 100 different chromosomes, where each algorithm represents a “chromosome” comprised of different correlation coefficients or “genes”.

Creation of the Next Generation

The next generation of chromosomes was based on a combination of crossover, mutation and elite selection techniques.

Using the Roulette Wheel Parent Selection, two parents were selected from which two offspring chromosomes were obtained using the crossover technique, where the offspring contains traits from both parents.

The resulting MMP value produced by each chromosome of the population is compared to the measured MMP. This evaluation gives the fitness of the chromosome which is in effect a measure of the error from the measured data. The fitness was calculated as follows:

Eq. 9-1

$$PFit(i,j) = C_g \Big/ \left[C_g + \left(\left| MMP_{cal(i,j)} - MMP_{exp(i,j)} \right| \right) \right]$$

Where:

PFit(i,j) = Fitness function of data number j of chromosome i (fraction)

i = 1, n (population size)

j = 1,nn (number of available data)

MMP_{cal} = Calculated MMP

MMP_{exp} = Experimental MMP

C_g = an arbitrary constant value. Taken to be 5000 to not permit the fitness value to be too small.

Eq. 9-2

$$Fit(i) = \left(\sum_{j=1}^{nn} PFit(i,j) \right) \Big/ nn$$

Where:

Fit(i) = Average fitness of chromosome i, where the chromosome has many fitness values based on the number of data available (j)

If a variable has a fitness outside of these limits, the fitness value will be reduced using a penalty function defined as follows:

Eq. 9-3

$$PFit(i,j)_{new} = PFit(i,j)_{old} \times (1 - pen)$$

Where:

pen = Penalty function (a value between 0 and 1, in our case equal to 0.001)

Mutated offspring were also produced after the crossover process, where one of the traits is mutated. For mutation, the new value is determined as follows:

Eq. 9-4

$$\text{New Value} = \lambda_{GA} * \text{old value} + \beta_{GA} * \text{random value}$$

Where λ_{GA} and β_{GA} are between 0 and 1. In this work we used λ_{GA} = 0.35 and β_{GA} = 0.95. A one-point crossover probability ($P_{(c)}$) of 100% and a mutation probability ($P_{(m)}$) of 100% was used.

The measured MMP data used as input and for testing can be found in **Table 9-3**. The fitness factor was based on comparing the solutions from the chromosome to the measured values. Out of the parents and children chromosomes, the two chromosomes that had the best fitness factors went to the next generation. Hence, if parents had higher fitness factors than their offspring they were retained for the next generation of chromosomes rather than the offspring.

Stopping Criterion

The stopping criterion used in development of our correlation was when the difference between the fitness of the best chromosome and the average fitness of the population is less than or equal to 10^{-5}. Once this is met, the best chromosome will yield the final correlation.

9.1.2 GA Correlation for MMP of CO_2-Rich Injection Gas with nC_5 Enrichment

The GA produced the following correlation:

Eq. 9-5

$$MMP_{GA-nC_5.enriched} = MMP_{base} \times F_{Pc}[3.406 + 5.786 \times F_{Tc} - 23 \times F_{Tc}^2 + 20.48 \times F_{Tc}^3 - 5.7 \times F_{Tc}^4]$$

Where:

$MMP_{GA\text{-}nC5.enriched}$	= GA-based MMP for nC_5 enriched gas, psia
MMP_{base}	= MMP for base injection gas (no nC_5), psia
F_{Pc}	= $P_{cw\text{-}base}$ / $P_{cw\text{-}nC5}$
F_{Tc}	= $T_{cw\text{-}base}$ / $T_{cw\text{-}nC5}$
$P_{cw\text{-}base}$	= weight averaged pseudo-critical pressure of the base gas (no nC_5), psia
$P_{cw\text{-}nC5}$	= weight averaged pseudo-critical pressure of the injected nC_5 enriched gas, psia
$T_{cw\text{-}base}$	= weight averaged pseudo-critical temperature of the base gas (no nC_5), °F
$T_{cw\text{-}nC5}$	= weight average pseudo-critical of the injected nC_5 enriched gas, °F
$T_{cw\text{-}nC5}$	= $\sum_i^n w_i \times MF_i \times T_{ci}$
w_i	= weight fraction,
MF_i	= critical temperature modification factor (CO_2=1, C_1=1.6, N_2 =1.9, nC_5=0.67),
T_{ci}	= critical temperature of the gas component i, °F.

The GA-based correlation gave an absolute error of 3.39% and a standard deviation of 3.92%.

Figure 9-1 is a flow diagram illustrating the procedure followed in developing the GA correlation.

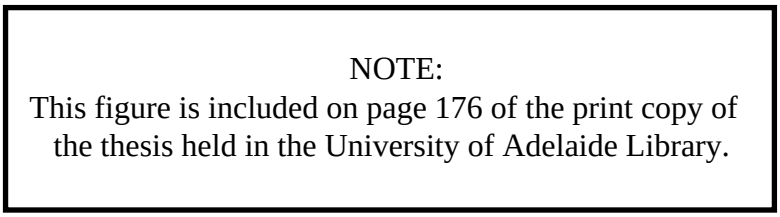

Figure 9-1: Flow diagram for procedure used in developing GA based MMP correlation (Emera and Sarma, 2005).

9.2 Linear Regression Correlations

Using linear regression three models were created. Two of the models were designed to fit a quadratic equation while the third was designed to fit an exponential equation. All three correlations relate the change in MMP from the base MMP to the nC_5 content I the injection gas stream.

9.2.1 Linear Regression Model 1 (LRM1)

A simple correlation was developed to fit the data with an exponential equation using linear regression. This model uses the base gas MMP and the percent of nC_5 in the injection gas to be modelled. The correlation was then tested against the same set of data as there was a limited amount of data. The correlation is as follows:

Eq. 9-6

$$MMP_{LRM1-nC_5.enriched} = MMP_{base}\left[0.7032 + 8.05\times10^{-16}e^{33.541\left(1-M_{nC_5}/100\right)}\right]$$

Where:

$MMP_{LRM1-nC_5.enriched}$ = The MMP for the nC_5 enriched gas correlated with LRM1

M_{nC_5} = The Mol% nC_5 in the injection gas stream

This correlation gave an error of 3.19% and a standard deviation of 4.19%.

9.2.2 Testing of the Correlations

The idea behind this work was to provide information that had not previously been presented. This poses the problem that since there had been little work previously preformed on this topic there is no literature data available to test the correlations against.

In order to test the correlated data, three other correlations were developed by the same method as LRM1 (linear regression to a quadratic equation) as follows:

- Using data from Oil A and Oil B
- Using data from Oil A and Oil C
- Using data from Oil B and Oil C

These were tested against Oil C Data, Oil B Data and Oil A Data respectively.

The results are as follows:

Table 9-1: Testing of correlated data

Correlation Based On	Tested Against	Absolute Error	Standard Deviation
Oil A and Oil B	Oil C	4.52%	5.14%
Oil A and Oil C	Oil B	2.77%	3.62%
Oil B and Oil C	Oil A	6.17%	6.85%

Having the data from the three oils available it could be seen that it was likely that using data from Oil A and Oil C and testing it against Oil B would give the best results as the results of Oil B lie between those of Oil A and Oil C.

This highlights what is apparent from looking at **Figure 9-2**. Although the oil characteristics are taken into account in the base MMP, it is still influencing the data. Looking only at the properties of each oil (GOR, MW_{C5+}), Oil A's properties differ most from Oil B and Oil C. Oil B's properties lie between those of Oil A and Oil C. This indicates that there should be a way of characterising these oils and improving the correlation. The following section goes through the development of a correlation with an oil characterisation factor; however it only uses the three oils used in this study. More data is required to improve on the correlation presented in Eq. 9-8, Eq. 9-9 and Eq. 9-10 and ultimately it is envisaged that using the same or a similar technique and data measured with more oils an improved correlation can be created.

9.2.3 Linear Regression Model 2 (LRM2)

Even though LRM1 predicted the data with a good accuracy, it was noticed that the oil composition still influenced the scatter of data. LRM2 was designed to

incorporate an extra variable to lessen the spread of data. Since there are only three oils there are only three data points upon which to base the correction factor on, which is far from sufficient. Regardless, the correlation is being presented in order to illustrate the added effect due to the oil composition, that a trend was found and correlated, the factor itself and to bring to awareness that the oil composition is still influencing the data even though it has been incorporated already in the base MMP.

In **Figure 9-2** we can clearly see segregation from Oil A data to Oil B and Oil C. The next step required finding a parameter which modelled the oil data well, this was based upon looking at what differed from Oil A to Oil B and Oil C. A trend can be noticed from Oil A to Oil B to Oil C in the overall molecular weight (Oil A is the lightest, Oil C is the heaviest).

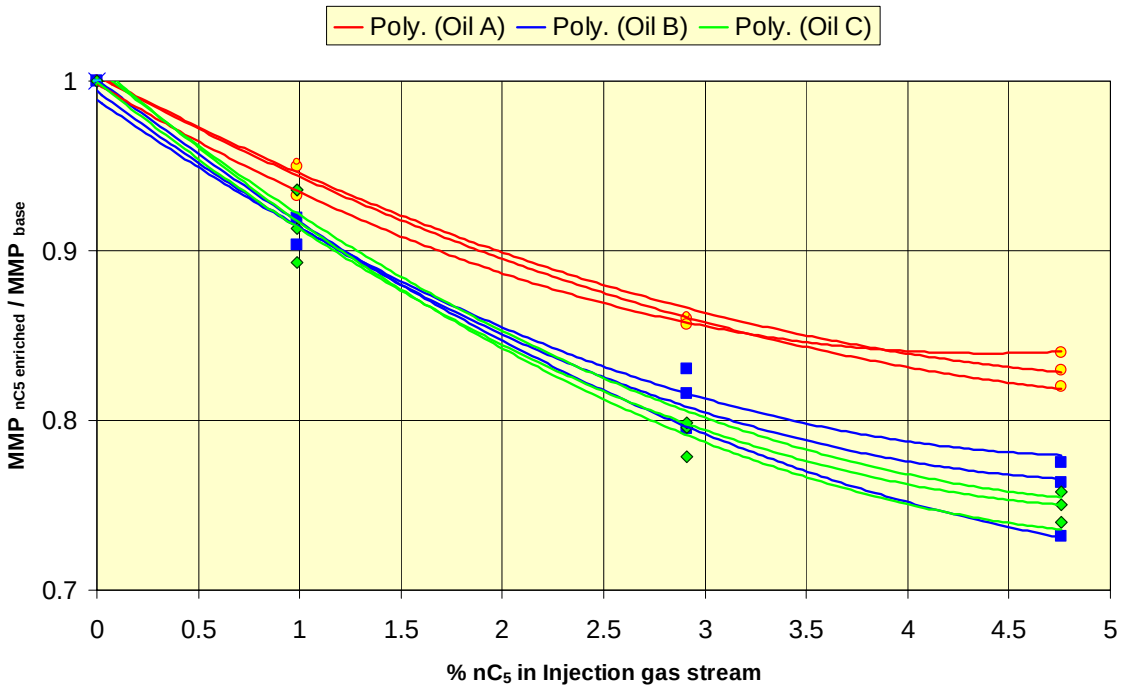

Figure 9-2: Experimental data illustrating segregation in the data due to the oil composition.

Many correlations use the molecular weight of the C_5+ or C_7+ fraction to characterise the oil. However, this neglects the C_2-C_4 fraction of the fluid. For example, in the Taranaki Basin, New Zealand gas condensate reservoirs have been found with a waxy and heavy condensate fraction. These fluids present a

small but heavy C_5+ fraction. Therefore, looking only at the molecular weight of C_5+ will tend to give misleading results.

It was found that the best way to characterise an oil for correlations such as this is to incorporate both the composition and volumetrics of the oil with a general factor. One good example of this is the Alston *et al.* (1985) correlation which uses the MW_{C5+} and a Volatile to Intermediate ratio incorporating the volume of light components (volumetric and compositional factor), volume of intermediate components (volumetric and compositional factor) and the composition of the heavy components with the MW_{C5+} (compositional factor, volumetrics implied because it is the only remaining pseudo-component).

The mole percent of C_5+ in the oil ($M_{C5+.oil}$) over the molecular weight of C_5+ in the oil ($MW_{C5+.oil}$) was chosen as the oil characterisation factor for our data set as it fit the data well and will tolerate changes in oil composition aside from these three oils. It incorporates the volume with the $M_{C5+.oil}$, this factor also takes into account the light fraction (1- $M_{C5+.oil}$) and the composition of the heavy fraction with $MW_{C5+.oil}$.

The correlation was developed as follows:

- The data for each of the oils was correlated individually to produce the ratio between $MMP_{nC5\text{-}enriched}$ and MMP_{base} at each nC_5 concentration in the injection gas stream.
- The relationship for $MMP_{nC5\text{-}enriched}$ / MMP_{base} vs $M_{C5+.oil}$ / $MW_{C5+.oil}$ was developed.
- The trend in this line was found to fit a straight line with slope (α) and intercept (β). This line was extrapolated to 0, the minimum of the value for $M_{C5+.oil}$ / $MW_{C5+.oil}$. This was done to normalise the oil composition data. Hence a relationship of the following form was found:

Eq. 9-7

$$MMP_{nC5\text{-}enriched} / MMP_{base} = \alpha \,.\, (M_{C5+\ oil} / MW_{C5+\ oil}) + \beta$$

Where α and β are both functions of nC_5 content in the gas

- The slope (α) and intercept (β) of the relationship between $MMP_{nC5\text{-}enriched}$ / MMP_{base} vs $M_{C5+.oil}$ / $MW_{C5+.oil}$ relationship were plotted individually against the nC_5 content in the gas. This was done to determine influence of nC_5 on the normalisation factor.
- Using the nC_5 content of the gas stream, and the relationships found above, α and β can be determined and thus the MMP for the nC_5 enriched gas.

Expanding the correlation out, we obtain the following:

Eq. 9-8

$$MMP_{LRM2-nC_5.enriched} = MMP_{base} * \left(\alpha * \frac{M_{C_{5oil}^+}}{MW_{C_{5oil}^+}} + \beta \right)$$

Eq. 9-9

$$\alpha = 0.024 * M_{nC_5}^2 - 0.183 * M_{nC_5}$$

Eq. 9-10

$$\beta = 1 - 0.017 * M_{nC_5}$$

Where:

$MMP_{LRM2-nC_5.enriched}$ = The MMP for the nC_5 enriched gas correlated with LRM2

$M_{C_{5oil}^+}$ = Mol % of C_5+ in the oil

$MW_{C_{5oil}^+}$ = The molecular weight of C_5+ in the oil

This correlation yielded an error of only 1.56% and a standard deviation of 1.98%. LRM2 is only applicable for M_{nC5} less than 5%. Although LRM2 gives the best results in error and standard deviation, it is reiterated that this correlation is only

based on three oils and hence may give large errors with oils that differ greatly from those used to develop the correlation. However, it illustrates that a trend relating to the oil composition was found, it was correlated and improved the results of LRM1 and the GA developed correlation.

9.3 Chapter Summary

The MMP data set used for developing all correlations had already been reported in the previous chapter in **Table 8-18**.

Figure 9-3 shows the results of all correlations. The y-axis is the measured values and the x-axis represents the correlated values. A perfectly matching correlation would see the points lining up along the diagonal line, any deviation from this represents the error. As can be seen all correlations fit the data very well. Also, **Figure 9-3** shows that LRM2 predicts with the best accuracy and that the GA-based, LRM1 and LRM3 all predict very similarly. This is not surprise as they are all based on the same data set.

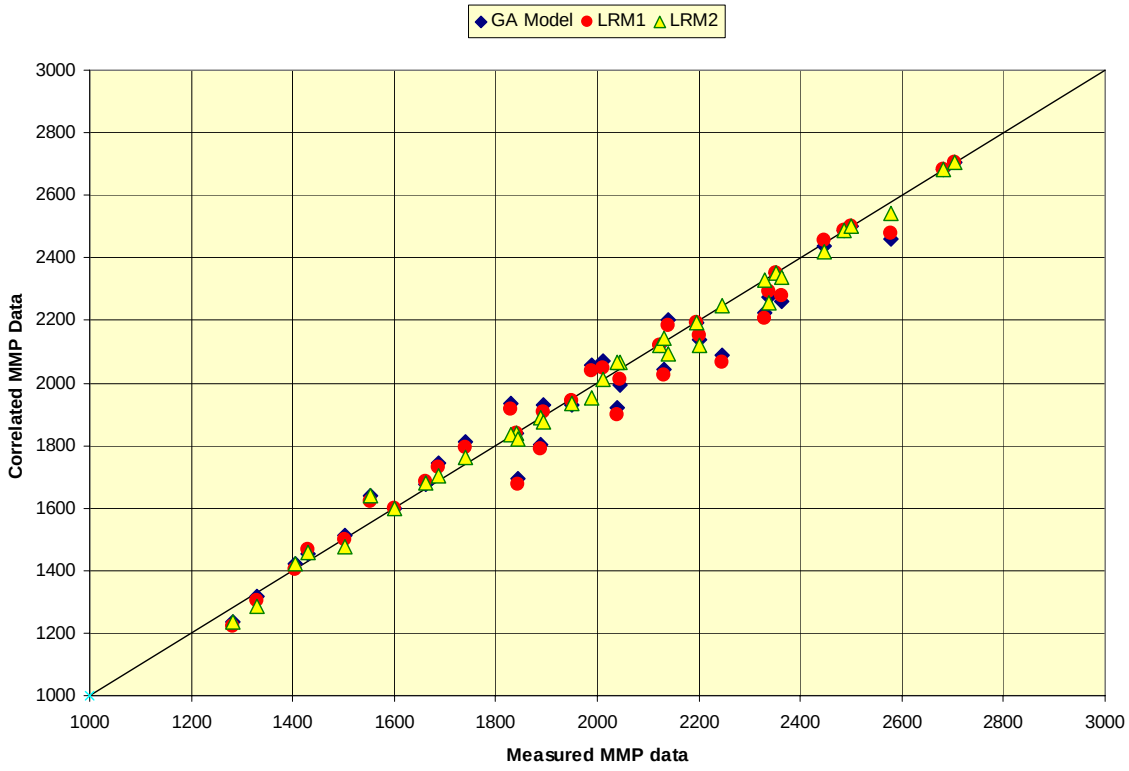

Figure 9-3: Comparison of developed correlations

To test the performance of the developed correlations, the predicted MMP values were compared against the experimental MMP values, the results of which are presented in **Figure 9-3**. As a reference, the literature correlations are compared to LRM3 in **Figure 9-4**.

Furthermore, the developed correlations were compared to Alston *et al.,* (1985) and Sebastian *et al.,* (1985) correlations. The developed correlations all predicted with better accuracy than the correlations from literature. A comparison cross-plot is presented in **Figure 9-4**.

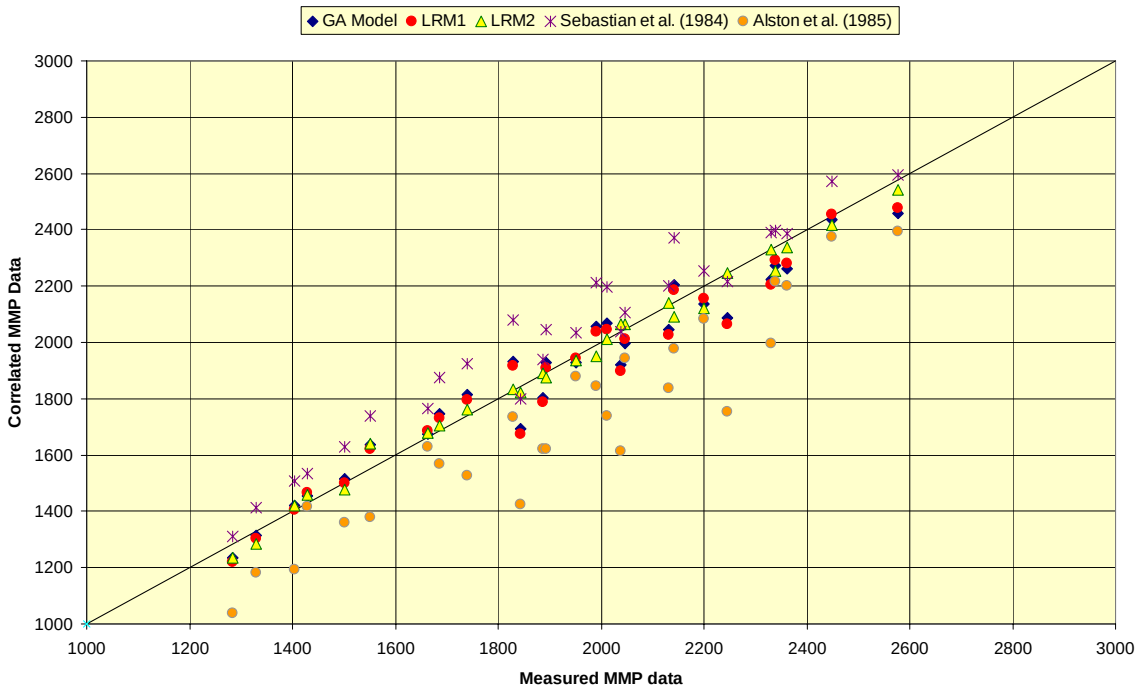

Figure 9-4: Comparison of correlations from literature to developed correlations from this work

From the correlations found in literature, the Alston *et al.,* (1985) and Sebastian *et al.,* (1985) correlations were found as adequate for comparison due to the following:

- They tolerate an impure CO_2 gas stream whose impurities are methane and n-pentane, and
- They tolerate an impure gas stream as the base gas for comparison

Both these points needed to be met for comparison to the correlation developed. Other correlations either required an MMP from a pure CO_2 base gas or were not designed to meet changes in nC_5 concentration.

Emera and Sarma in 2005 provided an excellent summary of existing MMP correlations from literature for both pure and impure CO_2 injection gases illustrating the above points.

The error and standard deviation for each are presented in **Table 9-2**. The measured and correlated results are presented in **Table 9-3**. The average absolute error for the correlations developed as part of this thesis excludes the data for 0mol% nC_5. However, the data has been included in **Table 9-3** to demonstrate that the correlations correctly predict no change at 0%.

Table 9-2: Comparison of developed correlations to correlations from literature

Correlation	Absolute Error	Standard Deviation
GA-based (Eq.9-5)	3.39%	3.92%
LRM1 (Eq. 9-6)	3.19%	4.19%
LRM2 (Eq. 9-8)	1.56%	1.98%
Alston *et al.,* 1985	10.37%	12.22%
Sebastian *et al.,* 1985	5.76%	7.11%

Table 9-3: Measured and Correlated MMP values

Gas	Reservoir Fluid	Temp. °C	Measured MMP	GA Model Eq. 9-5	LRM1 Eq. 9-6	LRM2 Eq. 9-8	Sebastian *et al.* (1985)	Alston *et al.* (1985)
Gas #1	Oil A	60	2195	--	2195	2195	--	--
Gas #1	Oil A	80	2487	--	2487	2487	--	--
Gas #1	Oil A	100	2705	--	2705	2705	--	--
Gas #1	Oil B	60	1600	--	1600	1600	--	--
Gas #1	Oil B	80	1841	--	1841	1841	--	--
Gas #1	Oil B	100	2122	--	2122	2122	--	--
Gas #1	Oil C	60	2351	--	2351	2351	--	--
Gas #1	Oil C	80	2500	--	2500	2500	--	--
Gas #1	Oil C	100	2681	--	2681	2681	--	--
Gas #2	Oil A	60	2046	1995	2011	2064	2105	1944
Gas #2	Oil A	80	2362	2261	2278	2339	2385	2203
Gas #2	Oil A	100	2577	2459	2478	2544	2594	2396
Gas #2	Oil B	60	1429	1455	1466	1460	1534	1417
Gas #2	Oil B	80	1663	1674	1687	1680	1765	1631
Gas #2	Oil B	100	1951	1929	1944	1936	2035	1879
Gas #2	Oil C	60	2201	2137	2154	2120	2254	2082
Gas #2	Oil C	80	2339	2273	2290	2254	2397	2214
Gas #2	Oil C	100	2448	2437	2456	2417	2571	2374
Gas #3	Oil A	60	1887	1804	1789	1890	1941	1620
Gas #3	Oil A	80	2131	2045	2027	2141	2199	1836
Gas #3	Oil A	100	2331	2224	2205	2329	2392	1997
Gas #3	Oil B	60	1329	1315	1304	1285	1415	1181
Gas #3	Oil B	80	1502	1513	1500	1478	1628	1359
Gas #3	Oil B	100	1687	1744	1730	1704	1876	1566
Gas #3	Oil C	60	1830	1933	1916	1835	2079	1735
Gas #3	Oil C	80	1990	2055	2038	1951	2211	1845
Gas #3	Oil C	100	2141	2204	2185	2092	2371	1979
Gas #4	Oil A	60	1844	1694	1676	1822	1797	1424
Gas #4	Oil A	80	2039	1919	1898	2064	2036	1614
Gas #4	Oil A	100	2245	2087	2065	2245	2215	1755
Gas #4	Oil B	60	1283	1235	1221	1236	1310	1038
Gas #4	Oil B	80	1405	1420	1405	1422	1507	1195
Gas #4	Oil B	100	1552	1637	1620	1639	1738	1377
Gas #4	Oil C	60	1739	1814	1795	1763	1925	1526
Gas #4	Oil C	80	1894	1929	1908	1875	2047	1622
Gas #4	Oil C	100	2011	2069	2046	2011	2195	1740

Note: All MMP values are in psia

9.4 Recommendations for Use of Correlations

- The GA-based correlation predicts the data well. It could be applied to data with nC_5 greater than 4.76% as it correctly predicts a continued decrease in MMP with further addition of nC_5 to the injection gas. However, as it has only been tested to 4.76%, the error is unknown beyond this value.
- LRM1 predicts the best error out of LRM1, the GA-based and the correlations from literature. Since it is based on an exponential equation it correctly predicts a continued decrease in MMP with further addition of nC_5 to the injection gas. The standard deviation is slightly worse than that of the GA-correlated data.
- LRM2 predicts the best error overall, however the correction factor that improves the correlation from LRM1 is based only on three oils. Due to this its use is recommended only for oils similar to the three tested. However, it illustrates that the oil composition still has an effect on the MMP even though it has been taken into account with the base gas MMP. If further data is attained to create a large enough data base, this trend should be sought and corrected for. Also, we present the use of $M_{C5+.oil}/MW_{C5+.oil}$ as a characterisation factor for the oils. As it is based on a quadratic equation and therefore the curve has a minimum after which it increases. This means that beyond an nC_5 content of 5 mol% the correlation will erroneously predict an increase in MMP with further addition of nC_5 to the injection gas. Hence, it should only be used for nC_5 content less than 5 mol%.
- Both linear regression models (LRM1 and LRM2) have been anchored to an $MMP_{nc5\text{-}enriched}/MMP_{base}$ value of 1, thus, they predict with 0% error when there is no nC_5 present in the injection gas. These values have not been used in the error calculation. The GA-based correlation is not anchored at 1, but instead uses the data at that point as it does the rest of the data to improve accuracy over the whole range of data. Because of this the GA-based correlation will predict with an error of 2.8% when there is no nC_5 present in the injection gas. Therefore, for values of nC_5 mol% near 0 the LRM correlations will predict better.

- The correlations predict that addition of approximately 1.5mol% of nC_5 to the injected gas causes a decrease in the MMP value of approximately 10% of its base value (no nC_5 enrichment).
- In the presence of other components, or a different base gas than Gas #1, it is expected that the effect of nC_5 will not be quite the same due to intermolecular interactions. It is expected that having other components that would help achieve miscibility (say ethane through butane) would result in a less pronounced effect on reducing the MMP due to nC_5 addition since the other components are already having an effect. Conversely, having more methane or nitrogen present would likely display a more pronounced effect as these components reduce the miscibility and therefore the effect due to the nC_5 fraction would be relatively larger. It is expected that this effect has a strong correlation to the change in critical properties and molecular weight of the overall gas. More research in this area would shed more light on how exactly other components will affect the change due to nC_5 in a CO_2-rich injection gas stream.

10 CONCLUSIONS AND RECOMMENDATIONS

The reservoir fluid studies performed show that the reservoir fluid of Field A is suitable for miscible flooding with CO_2 at the reservoir conditions of pressure and temperature.

The results of the analyses show that at pressures in the range of 2800 psig to 3500 psig miscibility will be attained with CO_2 or CO_2-rich gases. In order to have a reasonable flow of fluids into the reservoir the injection pressure will need to be above these pressures, hence injection of CO_2 or a CO_2-rich gas for miscible EOR is a viable option.

It is expected that the oil recovery factor improve from the current 3-4% and expected 10% to some 25%. A full field scale reservoir simulation model for the EOR process is expected to improve this estimate.

The simulation studies showed that that retaining a small fraction of C_5+ components can balance the effect of retaining methane in the injection gas on oil recovery and miscibility. This is exemplified from the results of Tim Gas which had relatively little CO_2 (26.83 mol%) but a range of hydrocarbon components including 50.70 mol% methane and 1.35% pentanes plus. Tim Gas yielded recovery factors just under those of pure CO_2.

It is recommended that a miscible gas flood project at Field A should be seriously considered with CO_2, Tim Gas or SG#1 with the key factors to be considered being the economic differences between the different gas streams, cost of compression, piping the gas to site and distance from source to destination. To better assess this it is recommended that a full field scale model be created and the proposed EOR project be run with CO_2, Tim Gas and SG#1. An economic analysis should then be used to decide which is gas will give the best results to the company and if economically viable.

A viscosity study was performed with mixes of 20mol% and 40mol% injection gas using both the pure CO_2 and the synthetic gas mix. It was noticed that the injection gas lowered the viscosity of the single-phase reservoir fluid and that the synthetic gas mix lowered the viscosity more than the pure CO_2. However, an interesting observation was made of the two-phase fluid. The viscosity of Oil A with injection gas at pressures below 2500 psig is higher than the viscosity of Oil A at 2500 psig. This trend was consistently seen throughout the data. This is due to the remaining flashed liquid corresponding to the Oil A and injection gas mix being heavier at this pressure than that of Oil A.

The recovery factors of injection gases with an nC_5 component showed a definite improvement, however, a simple economic evaluation based solely on the sale value of the components showed that there is no economic benefit in retaining or adding nC_5 to the injection gas. This excluded the costs of transportation, processing of the gas stream and benefit of requiring less compression of the gas, however these effects are expected to further decrease the economic viability of retaining / adding nC_5 in the gas stream. While this conclusion was perhaps to be expected, until now it had not been studied in such detail. However, the results of benefit due to increased recovery against cost of the components in the injection gas stream were quite close and perhaps if for whatever reason future prices of the components were to change (chiefly, a lowering in the price of pentane relative to the other sale components of the produced reservoir fluid) then the results of this study could be re-assessed and perhaps show a benefit in the addition of pentane into injection gas streams.

The effect of nC_5 on CO_2 MMP was evaluated based on RBA measured MMP data. The study showed a strong trend relating the reduction of CO_2 MMP with the addition of nC_5. Two types of correlations were developed to model the trend, one based on the genetic algorithm and the other based on linear regression.

The error of the correlations were very low (less than 4%), however it must be kept in mind that due to the limitation in data and the need to develop our own data set, the correlations were tested upon the same data set which they were based on. If further data were to come about for MMP of CO_2-rich gases with nC_5 impurity then

the correlations could be tested against this data as well to gain a better feel for the error over a larger range of data.

Even though oil composition is taken into account in the base gas MMP, it still influences the correlation correcting for the effect of nC5. An oil characterisation factor was developed to account for this effect and it significantly improved the results reducing the error of the correlation to just 1.6%. Again, it must be kept in mind that due to the limitation in data and the need to develop our own data set, the correlations were tested upon the same data set which they were based on.

The RBA measured MMP values were in good agreement with the Slim Tube measured values.

In summary, the key original contributions made from this work are:

- Extensive data set of MMP values. A total of 45 MMP measurements by RBA and 2 MMP measurements by Slim Tube are reported in this thesis
- Fluid study and miscibility study using a Cooper Basin reservoir fluid
- Comparison of oil recovery due to different potential injection gases
- MMP Correlation for the effect of nC_5 on CO_2-rich gas streams
- Oil characterization factor for improving the MMP correlation for the effect of nC_5 on CO_2 rich gas streams

10.1 Recommendations for Use of Correlations to Predict nC_5 Effect on CO_2-rich MMP

The recommendations for use and application of each of the correlations are as follows:

The genetic algorithm presented very good however it has two key limitations, at 0% nC_5 impurity the correlation predicts with a small error. The correlation cannot be used above the values used to develop it as the curve has a minimum at approximately 10% and wrongly predicts an increase (when it should predict a decrease) in MMP with additions of nC_5 above this minimum. While these values are outside the range of the correlation it is still to be noted to stress the point of the range of use.

The linear regression correlations were all anchored to the measured MMP at 0 mol% nC_5 in the gas stream. Hence, at 0 mol% nC_5 they will correctly predict no deviation from the measured point. For this reason, the linear regression correlation based on an exponential relationship (LRM1) is most recommended for widespread use as it is more stable when extrapolated to values of nC_5 impurity above 5 mol% and still presents a good error.

If the reservoir fluid to be used has similar properties to those used in the study then LRM2 should present an improvement. However, since it is based on a quadratic equation it has a minimum and will, at a point outside the range of application of the correlation, wrongly predict an increase in MMP with additions of nC_5 above approximately 5 mol%. Hence LRM2 should only be used for nC_5 concentrations between 0 mol% and 5 mol%.

The limitations of the correlations are within the base conditions used of:

- Temperature from 60°F to 200°F
- Volatile reservoir fluids of °API from 40-51
- nC_5 composition from 0-5%

The following recommendations are for future research on this topic:

- More CO_2 MMP data with nC_5 impurity required for further study on the topic of the effect of nC_5 on CO_2 MMP.
- Create another bigger database of MMP measured values using pure CO_2 as a basis rather than the CO_2-rich blend used in this case. For this project, a CO_2-rich blend was used to better represent the most likely injection gas at Field A. While these results are still very generic and used only 3 pure components, it is recommended for future research to use pure CO_2 with no methane to eliminate any relative effect due to the methane.
- The importance of relative permeability values is to be stressed when comparing the results of different injection gases. It is recommended that this data be obtained or available prior to a similar study evaluating the effect of different injection gases.

- The RBA proved to be an efficient way of obtaining a large volume of MMP values quickly. The values compared to those from Slim Tube studies were found to be within an acceptable error margin. Its use for obtaining a large amount of MMP values in a reasonable amount of time is recommended.
- In the presence of other components, or a different base gas than Gas #1, it is expected that the effect of nC_5 will not be quite the same due to intermolecular interactions. This effect will likely have a strong correlation to the change in critical properties and molecular weight of the overall gas. More research in this area would shed more light on how exactly other components will affect the change due to nC_5 in a CO_2-rich injection gas stream. By changing the base gas composition and comparing the change due to 1, 3 and 5 mol% additions to those with a different base gas to the one used in this research (Gas #1) the results can be compared to those presented in this thesis.

REFERENCES

Achourov, V., Khamitov, I. and Yatsenko, V.: "A Technique for Measuring Permeability Anisotropy and Recovering PVT Samples in a Heavy Oil Reservoir in North West Siberia", paper SPE 102460 presented at the SPE Russian Oil and Gas Technical Conference and Exhibition, Moscow, 3-6 October 2006

Ahmed, T.H.: *Hydrocarbon Phase Behaviour*, Gulf Publishing Co., (1989) 120, 379-385

Alston, R.B., Kokolis, G.P. and James, C.F.: "CO_2 Minimum Miscibility Pressure: A Correlation for Impure CO_2 Streams and Live Oil Systems", paper SPE 11959, Society of Petroleum Engineer, *SPE Journal*, April, 1985, pp 268-274

Amroun, H. and Tiab, D.: "Alteration of Reservoir Wettability Due to Asphaltene Deposition in Rhourd-Nouss Sud Est Field, Algeria", paper SPE 71060 prepared for presentation at SPE Rocky Mountain Petroleum Technology Conference, Keystone, Colorado, USA, 21-23 May 2001

Amyx, J.W., Bass, D.M. and Whiting, R.L.: *Petroleum Reservoir Engineering*, McGraw-Hill Book Company, New York, (1960) 360

Ayan, C., Douglas, A. and Kuchuk, F.: "A Revolution in Reservoir Charaterization", Schlumberger Middle East Well Evaluation Review No. 16 (1996) 44-55

Bingham, M.D.: "Field Detection and Implications of mercury in Natural Gas, Paper SPE 19357-PA, *SPE Production Engineering* Vol. 5 No. 2 (1990) 120-124

Bon, J., Emera, M.K and Sarma, H.K.: "An Experimental Study and Genetic Algorithm (GA) Correlation to Explore the Effect of nC_5 on Impure CO_2 Minimum Miscibility Pressure (MMP)", paper SPE 101036 presented at the SPE Asia Pacific Oil & Gas Conference and Exhibition (APOGCE), Adelaide, Australia, 11–13 September 2006

Bon, J. and Sarma, H.K.: "A Technical Evaluation of a CO_2 flood for EOR Benefits in the Cooper Basin, South Australia, paper SPE 88451 presented at the SPE Asia Pacific Oil and Gas Conference and Exhibition (APOGCE), Perth, Australia, October 18-20, 2004

Bon, J., Sarma, H.K., Rodrigues, T. and Bon, J.G.: "Reservoir Fluid Sampling Revisited - A Practical Perspective", paper SPE 101037-PA, *SPE Reservoir Evaluation & Engineering*, Vol. 10, No. 6 (December 2007) 589-596

Bon, J., Sarma, H.K. and Theophilos, A. M.: "An Investigation of Minimum Miscibility Pressure for CO_2 - Rich Injection Gases with Pentanes-Plus Fraction", paper SPE 97536 presented at the International Improved Oil Recovery Conference (IIORC) in Asia Pacific, Kuala Lumpur, Malaysia, December 5-6, 2005

Bradley, H.B., *Petroleum Engineering Handbook*, Society of Petroleum Engineers, (1987) 45-1 - 45-7

Brush, R. M., Davitt, H. J., Aimar, O. B., Arguello, J. and Whiteside, J.M.: "Immiscible CO_2 Flooding for Increased Recovery and Reduced Emissions", paper SPE 59328 prepared for presentation at Improved Oil Recovery Symposium, Tulsa, Oklahoma, USA, 3-5 April 2000

Carcoana, A.: "Enhanced Oil Recovery in Romania" Proceedings Third Joint SPE/DOE Symposium on Enhanced Oil Recovery, SPE of AIME, Dallas, TX, (1982) 367-379.

Chang, R., *Chemistry*, McGraw-Hill Inc., 5^{th} Edition (1994) 458

Christian, L.D., Shirer, J.A., Kimbel, E.L. and Blackwell, R.J.: “Planning a Tertiary Oil-Recovery Project for Jay/LEC Fields Unit", paper SPE 9805-PA, *Journal of Petroleum Technology*, Vol. 33, No. 8 (August 1981) 1535-1544

Christiansen, R.L. and Haines, H.K.: “Rapid Measurement of Minimum Miscibility Pressure with the Rising-Bubble Apparatus”, paper SPE 13114-PA, *SPE Reservoir Engineering*, Vol. 2 No. 4 (November 1987) 523-527

Cobenas, R.H. and Crotti, M.A.: “Volatile Oil. Determination of Reservoir Fluid Composition From a Non-Representative Fluid Sample” paper SPE 54005 prepared for presentation at the 1999 SPE Latin American and Caribbean Petroleum Engineering Conference held in Caracas, Venezuela, 21–23 April 1999

Cronquist, C., “Carbon Dioxide Dynamic Miscibility with Light Reservoir Oils”, Proceedings of the Fourth Annual US DOE Symposium, Tulsa, Oklahoma, USA, 1978

Cuiec, L.E.: "Restoration of the Natural State of Core Samples", paper SPE 5634 prepared for presentation at the Fall Meeting of the Society of Petroleum Engineers of AIME, Dallas, Texas, 28 September - 1 October, 1975

Cuiec, L.E., Longeron, D. and Pacsirszky, J.: "On the Necessity of Respecting Reservoir Conditions in Laboratory Displacement Studies" paper SPE 7785-MS prepared for presentation at the Middle East Technical Conference and Exhibition, Bahrain, 25-28 February 1979

Dake, L. P.: *Fundamentals of Reservoir Engineering*, Elselvier Science B.V., Amsterdam, (1978) 80, 116, 127-129

Dake, L.P.: *The Practice of Reservoir Engineering*, Elsevier Science B.V., Amsterdam, (1994) 33

Danesh, A.: *PVT and Phase behaviour of Petroleum Reservoir Fluids,* Elsevier Science B.V. (1998) 260-265

Danesh, A., Krinis, D., Henderson, G.D. and Peden, J.M.: “Asphaltene Deposition in Miscible Gas Flooding of Oil Reservoirs”, Institute of Chemical Engineers, *Chem Eng Res Des*, Vol. 66, (July 1988)

de Boer, R.B., Leerlooyer, K., Eigner, M.R.P. and van Bergen, A.R.D.: “Screening of Crude Oils for Apshalt Precipitation: Theory, Practice and the Selection of Inhibitors”, paper SPE 24987, *SPE Production & Facilities*, Vol. 10, No. 1 (February 1995) 55-61

Donaldson, E. C., Chilingarian, G. V. and Yen, T. F.: *Enhanced Oil Recovery, I Fundamentals and Analyses*, Elselvier Science Publishers B.V. (1985) 63-67, 193

Dranchuk, P. M. and Abou-Kassem, J. H.: “Calculation of Z-Factors for Natural Gases Using Equations of State,” *The Journal of Canadian Petroleum Technology*, Vol. 14, No. 3 (July-September 1975) 34-36

Dybdahl, B.: “A Systematic Approach to Sampling During Well Testing”, paper prepared for presentation at the ENI E&P Division and ENI Technology Conference, 23 February 2006

Dyer, S. B. and Farouq Ali, S. M.: “The Potential of the Immiscible Carbon Dioxide Flooding Process for the Recovery of Heavy Oil”, presented at the third technical meeting of the South Saskatchewan section, The Petroleum Society of CIM, Regina, September 1989

El-Banbi, A.H. and McCain Jr., W.D.: “Sampling Volatile Oil Wells” paper SPE 67232 was prepared for presentation at the SPE Production and Operations Symposium held in Oklahoma City, Oklahoma, 24–27 March 2001

Elshahawi, H. and Hashem M.: “Accurate Measurement of the Hydrogen Sulfide Content in Formation Fluid Samples – Case Studies” paper SPE 94707 prepared for presentation at the 2005 SPE Annual Technical Conference and Exhibition held in Dallas, Texas, U.S.A., 9-12 October 2005

Elsharkawy, A.M., Poettman, F.H. and Christiansen, R.L.: “Measuring Minimum Miscibility Pressure: Slim Tube or Rising-Bubble Method?”, paper SPE/DOE 24114 presented at the SPE/DOE Eighth Symposium on Enhanced Oil Recovery held in Tulsa, Oklahoma, USA, April 1992

Emera, M.K.: *Modelling of CO_2 and Green-House Gases (GHG) Miscibility and Interactions with Oil to Enhance the Oil Recovery in Gas Flooding Processes*, Ph.D. Thesis, University of Adelaide, Australian School of Petroleum (March 2006)

Emera, M.K. and Sarma, H.K.: “Genetic Algorithm (GA)–based Correlations Offer More Reliable Prediction of Minimum Miscibility Pressures (MMP) between the Reservoir Oil and CO_2 or Flue Gas”, CIPC Paper No. 2005-003, presented at the Canadian International Petroleum Conference (CIPC), 56th Annual Technical Meeting of Canadian Institute of Mining, Metallurgy & Petroleum, Calgary, Canada, June 6 – 9, 2005.

Fevang, Ø and Whitson, C.H.: “Accurate In-Situ Compositions in Petroleum Reservoirs”, paper SPE 28829 prepared for presentation at the European Petroleum Conference, London, U.K., 25-27 October 1994

Firoozabadi, A. and Aziz, K.: "Analysis and Correlation of Nitrogen and Lean-Gas Miscibility Pressure", paper SPE 13669-PA, *SPE Reservoir Engineering,* Vol. 1, No. 6 (November 1986) 575-582

Firoozabadi, A. and Hauge, J.: "Capillary Pressure in Fractured Porous Media", paper SPE 18747-PA, *Journal of Petroleum Technology*, Vol. 42, No. 6 (June 1990) 784-791

Gant, P.L.: "Core Cleaning for Restoration of Native Wettability", paper SPE 14875, *SPE Formation Evaluation*, Vol. 3, No. 1 (March 1988) 131-138

Glasø, Ø.: “Generalized Minimum Miscibility Pressure Correlation”, paper SPE 12893-PA, *SPE Journal*, Vol. 25, No. 6 (December 1985) 927-934

Gozalpour, F., Ren, S.R. and Tohidi, B.: "CO_2 EOR and Storage in Oil Reservoirs", *Oil & Gas Science and Technology – Rev. IFP*, Vol. 60, No. 3, (2005) pp. 537-546

Hammami, A., Ferworn K.A., Nighswander J.A., Over, S. and Stange, E.: “Asphaltenic Crude Oil Characterization: An Experimental Investigation on the Effects of Resins on Stability of Asphaltenes”, *Petroleum Science and Technology*, Volume 16, Issue 3 & 4 March 1998 (1998) 227 - 249

Hammami, A., Phelps, C. H., Monger-McClure, T. and Little, T. M.: “Asphaltene Precipitation from Live Oils; An Experimental Investigation of Onset Conditions and Reversibility”, *Energy and Fuels*, Vol. 14, (2000) 14-20

Hirschberg, A., de Jong, L. N. J., Schipper, B. A. and Meijer, J. G.: “Influence of Temperature and Pressure on Asphaltene Flocculation”, paper SPE 11202-PA, *SPE Journal*, Vol. 24, No. 3 (June 1984) 283-293

Holm, L.W. and Josendal, V.A.: “Mechanisms of Oil Displacement by Carbon Dioxide”, *Journal of Petroleum Technology*, (December 1974) 1427-1438

Jacoby, R.H., Berry Jr., V.J., “A Method for Predicting Depletion Performance of a Reservoir Producing Volatile Crude Oil”, *Petroleum Transactions*, AIME, Vol. 210, (1957) 27-33

Jamaluddin, A.K.M., Creek, J., Kabir, C.S., McFadden, J.D., D'Cruz, D., Joseph, M.T., Joshi, N. and Ross, B.: "A Comparison of Various Laboratory Techniques to Measure Thermodynamic Asphaltene Instability", paper SPE 72154 prepared for presentation at the SPE Asia Pacific Improved Oil Recovery Conference held in Kuala Lumpur, Malaysia, 8–9 October 2001

Johnson, J.P. and Pollin, J.S.: "Measurement and Correlation of CO_2 Miscibility Pressures", paper SPE 9790, presented at the SPE/DOE Enhanced Oil Recovery Symposium, Tulsa, OK, April 5-8, 1981

Kapel, A. J.: "The Coopers Creek Basin" *Australian Petroleum Exploration Journal*, v. 6 (1966) 71-75.

Klins, M.A.: *Carbon Dioxide Flooding: Basic Mechanisms and Project Design*, International Human Resources Development Corp. Boston, Massachusets, (1984) 267-275

Mattax, C.C., Dalton R.L., *Reservoir Simulation*, Society of Petroleum Engineers, Monograph vol. 13, (1990) 6-12, 115-116

McCain Jr., W.D. and Alexander R.A.: "Sampling Gas-Condensate Wells" paper SPE 19729, SPE Reservoir Engineering, (August 1992) 358

Michaels, J., Moody, M., and Shwe, T.: "Wireline Fluid Sampling" paper SPE 30610 prepared for the SPE Annual Technical Conference & Exhibition, Dallas, Texas, USA, 22-25 October 1995

Morton, K.L., Osman, M.S. and Kew, S.A.: Heavy-Oil Uncertainties Facing Operators in the North Sea", Paper SPE 97898 presented at the SPE/PS-CIM/CHOA International Thermal Operation and Heavy Oil Symposium, Calgary, 1-3 November 2005

Mungan, N.: "Carbon Dioxide Flooding Fundamentals" *Journal of Canadian Petroleum Technology*, Vol. 20, (January–March 1981) 87

Nagarajan, N.R., Honarpour, M.M. and Sampath, K.: "Reservoir Fluid Sampling and Characterization - Key to Efficient Reservoir Management", Paper SPE 101517 presented at the Abu Dhabi International Petroleum Exhibition and Conference, Abu Dhabi, UAE, 5-8 November 2006

Neubauer, M.: *Feasibility of Time-Lapse Seismic Methods in Monitoring CO_2 Injection in the Fly Lake Field, Cooper Basin*, Honours Thesis, The Unviersity of Adelaide, Australia (2003)

Novosad, Z.: "Exploring the Fascinating World of Reservoir Fluid Phase Behaviour", *The Journal of Canadian Petroleum Technology*, Distinguished Author Series, (1996) 10-12

Novosad, Z., Sibbald, L.R. and Costain, T.G.: "Design of Miscible Solvents for a Rich Gas Drive - Comparison of Slim Tube and Rising Bubble tests", *Journal of Canadian petroleum Technology*, Volume 29, No. 1, January-February (1990) 37-42

Oak, M.J.: "Three-Phase Relative Permeability of Water-Wet Berea", paper SPE 20183-MS presented at the SPE Enhanced Oil Recovery Symposium, Tulsa, Oklahoma, 22-25 April 1990

Pecanek, H.T. and Paton, I.M.: "The Development of the Tirrawarra Oil and Gas Field", *The APEA Journal*, Vol. 24, Part 1 (1984) 278-288

Peng, D.Y. and Robinson, D.B.: "A New Two-Constant Equation of State", *Industrial and Engineering Chemistry: Fundamentals,* Vol. 15 (1976) 59–64

Pitt, G.M.: “Geothermal gradients, geothermal histories and the timing of thermal maturation in the Eromanga-Cooper Basins” Geological Society of Australia, Special Publication 12 (1986) 323-351

Poettmann, F.H., Christiansen, R.L. and Mihcakan, I.M.: "Discussion of Methodology for the Specification of Solvent Blends for Miscible Enriched-Gas Drives", paper SPE 23836, *SPE Reservoir Engineering* (February 1992) 154-156

Poettmann, F.H., Christiansen, R.L. and Mihcakan, I.M.: "Further Discussion of Methodology for the Specification of Solvent Blends for Miscible Enriched-Gas Drives", paper SPE 24471, *SPE Reservoir Engineering* (May 1992)

Ragazzini, G. and Venturini, C.: "A New Technique to Obtain the Real Capillary Pressure-Saturation Curve Directly from Centrifuge Experiments", The Society of Core Analysts, Conference Proceedings (1992) 65-89

Reudelhuber, F.O.: “Sampling Procedures for Oil reservoir Fluids” paper SPE 816-G, Journal of Petroleum Technology, (December 1957) 15

Rezaee, M. R. and N. M. Lemon: “Influence of Depositional Environment on Diagenesis and Reservoir Quality: Tirrawarra Sandstone Reservoir Southern Cooper Basin, Australia” *Petroleum Geology*, Vol. 19, (1996) 369-391.

Riley, M. D., Walters, R. P., Cramer, S. D. and McCawley, F. X.: “Isokinetic Technique for Sampling Geothermal Fluid In Two-Phase Flow”, Unsolicited paper SPE 7885 (1979)

Sahin, S., Kalfa, U. and Celebioglu, D.: "Bati Raman Field Immiscible CO_2 Application--Status Quo and Future Plans", paper SPE 106575-PA, *SPE Reservoir Evaluation & Engineering Journal*, Vol. 11, No. 4 (August 2008) 778-791

Schulz-Rojahn, J.P. and Phillips, S.E.: “Diagenetic Alteration of Permian Reservoir Sandstones in the Nappamerri Trough and Adjacent Areas, Southern Cooper Basin”. *In:* O’Neil, B.J., (ed.), *The Cooper and Eromanga Basins, Australia* Proceedings of Petroleum Exploration Society of Australia, Society of

Petroleum Engineers, Australian Society of Exploration Geophysicists (SA Branches), Adelaide, Australia (1989) 629-645

Sebastian, H.M. and Lawrence, D.D.: "Nitrogen Minimum Miscibility Pressures", paper SPE 24134 prepared for presentation at SPE/DOE Enhanced Oil Recovery Symposium, Tulsa, Oklahoma, 22-24 April 1992

Sebastian, H.M., Wenger, R.S. and Renner, T.A.: “Correlation of Minimum Miscibility Pressures for Impure CO_2 Streams”, paper SPE 12648-PA, Journal of Petroleum Technology, Vol. 37, No. 11 (November 1985) 2076-2082

Sibbald, L.R., Novosad, Z. and Costain, T.G: "Methodology for the Specification of Solvent Blends for Miscible Enriched-Gas Drives", paper SPE 20205, *SPE Reservoir Engineering*, Vol. 6 No. 3 (August 1991) 373-378

Sibbald, L.R., Novosad, Z. and Costain, T.G: "Authors' Reply to Discussion of Methodology for the Specification of Solvent Blends for Miscible Enriched-Gas Drives", paper SPE 24319, *SPE Reservoir Engineering* (February 1992) 156

Sibbald, L.R., Novosad, Z. and Costain, T.G: "Authors' Reply to Further Discussion of Methodology for the Specification of Solvent Blends for Miscible Enriched-Gas Drives", paper SPE 24548, *SPE Reservoir Engineering* (May 1992)

Spivak, A., Karaoguz, D., Issever, K. and Nolen, J.S.: "Simulation of Immiscible CO_2 Injection in a Fractured Carbonate Reservoir, Bati Raman Field, Turkey", paper SPE 18765 prepared for presentation at SPE California Regional Meeting, Bakersfield, California, 5-7 April 1989

Stalkup Jr., F. I.: *Miscible Displacement*, Society of Petroleum Engineers, AIME, Monograph, Vol. 8, (1984) 1-3, 6, 17, 139

Standing, M.B.: *Volumetric and Phase Behavior of Oil Field Hydrocarbon Systems*, Society of Petroleum Engineers of AIME, Dallas (1977) 74-78

Standing, M.B. and Katz, D.L.: “Density of Natural Gases”, *Trans.*, AIME (1942) *146*, 140-149

Stankiewicz, B.A., Broze, G., Couch, J., Dubey, S., Flannery, M., Fuex, N., Iyer, S.D., Leitko, A.D., Nimmons, J., Ratulowsk, J. and Westrich, J.: “Prediction of Asphaltene Deposition Risk in E&P Operations”, Paper 47C AIChe 3rd International Symposium on Mechanics and Mitigation of Fouling in Petroleum and Natural Gas Production, New Orleans, USA, March 10-14, 2002

Strong, J., Thomas, F.B. and Bennion, D.B.: “Reservoir Fluid Sampling and Recombination Techniques for Laboratory Experiments” paper No. CIM 93-54 prepared for presentation at the CIM 1993 Annual Technical Conference in Calgary, May 9-12, 1993

Taber, J.J. and Martin, F.D.: “Technical Screening Guides for the Enhanced Recovery of Oil”, paper SPE 12069 presented at the SPE Annual Technical Conference and Exhibition, San Francisco, CA, 5-8 October 1983

Taber, J.J., Martin, F.D. and Seright, R.S.: “EOR Screening Criteria Revised-Part 1: Introduction to Screening Criteria and Enhanced Recovery Field Projects”, paper SPE 35385-PA, *SPE Reservoir Engineering*, Vol. 12, No. 3 (August 1997) 189-198

Towler, B.F.: “Reservoir Engineering Aspects of Bottom Hole Sampling of Saturated Oils for PVT Analysis”, Unsolicited paper from the University of Wyoming. SPE 19438 (1989)

Willhelm, S.M. and McArthur, A.: "Removal and Treatment of Mercury Contamination at Gas processing Facilities", paper SPE 29721 presented at

the SPE/EPA Exploration and Production Environmental Conference, Houston, 27-29 March 1995

Williams, J.M., “Getting the Best Out of Fluid Samples”, paper SPE 29227*, Journal of Petroleum Technology*, Vol. 46, No. 9 (September 1994) 752

Williams, C. A., Zana, E. N. and Humphrys, G. E.: "Use of the Peng-Robinson Equation of State to Predict Hydrocarbon Phase Behavior and Miscibility for Fluid Displacement", Paper Number 8817-MS presented at the SPE/DOE Enhanced Oil Recovery Symposium, Tulsa, Oklahoma, USA, 20-23 April 1980

Wolcott, J.M., Monger, T.G., Sassen, R. and Chinn, E.W.: “The Effects of CO_2 Flooding on Reservoir Mineral Properties”, Society of Petroleum Engineers, 1989, paper SPE 18467 prepared for presentation at the SPE International Symposium on Oilfield Chemistry in Houston, Texas, USA, February, 1989

Yellig, W. F. and Metcalfe, R. S.: “Determination and Prediction of CO_2 Minimum Miscibility Pressures”, *Journal of Petroleum Technology*, (January 1980) 160-168

Yuan, H., Johns, R.T. and Egwuenu, A.M.: "Improved MMP Correlations for CO_2 Floods Using Analytical Gasflooding Theory", SPE 89359-PA, *SPE Reservoir Evaluation & Engineering*, Vol. 8, No. 5 (October 2005) 418-425